CALIBRATION AND TESTING OF A WIRELESS SUSPENDED SEDIMENT SENSOR

by

DANIEL BIGHAM

B.S., KANSAS STATE UNIVERSITY, 2011

A THESIS

Submitted in partial fulfillment of the requirements for the degree

MASTER OF SCIENCE

Department of Biological and Agricultural Engineering
College of Engineering

KANSAS STATE UNIVERSITY
Manhattan, Kansas

2012

Approved by:

Major Professor
Dr. Naiqian Zhang

Abstract

A real time wireless, optical sensor network was tested for long-term, remote monitoring of suspended sediment concentrations (SSC) in streams. The sensor and control board assembly was calibrated using a two-stage calibration procedure, including a pre-calibration conducted in the laboratory to adjust the sensitivity of the sensor and a field calibration using grab samples to establish an effective statistical model to predict SSC from the sensor signals. The assembly was installed in three military bases around the United States. These bases were Fort Riley, Kansas; Fort Benning, GA; and Aberdeen Proving Ground, MD. The types of water bodies and watersheds varied greatly among the sites, which allowed the sensor to be tested under versatile conditions for potential widespread use.

The results show that the sensor was capable of measuring SSC at each watershed independently. The calibration model developed for each sensor can be used to predict SSC from real-time sensor data. A data processing algorithm was developed to lessen the effect of fouling and clogging on sensor signals, along with eliminating anomalies in the data gathered. The results of this study displayed meaningful prediction data that can be used to estimate SSC in a stream over a long period of time. Information obtained in this study can be used as a launching point for future work and understanding of stream processes.

Table of Contents

List of Figures

List of Tables

Acknowledgements

I would like to express my sincere thanks to my major professor, Dr. Naiqian Zhang for his continual advice and guidance throughout my time at Kansas State. Dr. Zhang taught me a lot over my years as research assistant and then graduate student.

I would also like to thank my graduate committee members, Dr. Stacy Hutchinson and Dr. Phil Barnes, for agreeing to serve on my committee and for their guidance and teaching during my time at Kansas State. I would like to also thank the entire BAE department at for pushing me and giving me the education to complete this research effectively.

I would like to thank Mr. Carl Johnson for his help with this research project and gathering samples for me in Maryland along with all of his help installing and maintaining the sensor sites.

I would also like to thank my co-workers and friends, Joe Dvorak, Xu Wang, Wei Han, and Yali Zhang for their extensive help and cooperation on this project. The teamwork of this group is a major reason this project has been successful. I would also like to thank Brent Ware and Spencer Kepley for their help and assistance with this project.

I would like to thank Mr. Darrell Oard for his assistance and advice with the physical components of this system and extensive help with the installation and testing of this sensor network.

Finally, I would like to extend a sincere thank you to my Mom, Dad, and sisters for their support and love throughout this process and working with me to accomplish this goal. I would also like to thank my girlfriend, Kari, for her support and advice throughout my studies.

1. **Introduction**

Prevention of sediment pollution in surface water bodies has been an area of emphasis for some time and has increased greatly in recent years. Sediment is defined as an non-point source (NPS) pollution and can be caused by various methods including construction sites, agricultural land use, military training areas, and natural soil erosion (Stoll, 2004). Suspended sediments have the ability to have various environmental impacts on water bodies. The sediment can carry with it various pollutants and trace elements that have been absorbed into the soil particles (Tessier, 1992).

Erosion of soil is a major threat to the productivity and sustainability of agricultural, in turn a threat to the sustainability of the life on Earth. It is estimated that more than 10 million hectares of the world's arable land is lost by erosion every year with an economic impact in the billions of dollars annually (Pimentel, et al., 1995).This type of erosion attributes to an increase in suspended sediment concentration (SSC) in surface water bodies. Fluvial sediment is the single most prevalent pollutant in American rivers and streams. Increased sediment decreased the ability for light to penetrate the water column, thus reducing photosynthesis (Kirk, 1994). This sediment can also affect drinking water treatment, aquatic ecology and habitats, and recreational use of rivers, lakes and other surface water bodies (Glysson & Gray, 2002).

The measurement and monitoring of SSC has been a key area of environmental study with the overall goal of having a real-time, accurate sediment monitoring system. The ability to quantify the amount of sediment moving through hydrologic bodies over time could lead to the development and implementation of management practices that help to reduce overall sediment load (Jastram, Zipper, Zelazny, & Hyer, 2010).

The most accurate method for measuring SSC is field sampling. However, this method is very time consuming and labor intensive. The majority of suspended sediment is transported during periods of high flow; usually storm events are the cause of these periods (Wolman & Miller, 1960). During high flow in a particular reach it can also be dangerous to acquire these samples. As streamflow increases, the energy potential of that stream also increases, thus increasing the size and amount of particles the stream can carry (Gordon, McMahon, Finlayson, Gippel, & Nathan, 2004).

A real-time, optical, in-situ sensor was developed previously by Stoll (2004) and Zhang (2009) at Kansas State University and will be used in this study. This sensor uses a combination of light-emitting diodes and phototransistors to measure light diffraction and transmission in water. These signals change with SSC and can be used to predict concentration of suspended sediment in a particular reach. In order for this sensor to be accurate and effective, it must be calibrated and tested in each particular watershed it is installed in, because each watershed has different soil types, organic matter, and microorganisms that cause different readings from the sensor at the same SSC.

With these factors in mind, some objectives were created to help study and improve the effectiveness of this particular sensor. These objectives are to (i) calibrate and test this wireless sediment sensor under both laboratory and field conditions; (ii) take grab samples during normal and high flow periods to gather a range of suspended sediment concentrations; (iii) derive correlations between sensor readings and actual sediment concentrations in order to develop prediction models for SSC; (iv) develop an algorithm to correct the effect of fouling on the sensor over time. The overall objective is to bring this particular sensor one step closer to implementation and possible widespread application in helping monitor and analyzing SSC in water bodies for various applications.

2. **Literature Review**

2.1 Turbidity

Turbidity is defined by the EPA as "a principal physical characteristic of water and is an expression of the optical property that causes light to be scattered and absorbed by particles and molecules rather than transmitted in straight lines through a water sample" (EPA, 1999). Turbidity is usually measured in Nephelometric Turbidity Units (NTU). NTU can be defined as the intensity of light at a specified wavelength scattered or attenuated by suspended particles or absorbed at a specified angle, from the path of incident light in comparison to a chemically prepared standard (Ziegler, 2002). Turbidity and NTU have been used for some time as a method for measuring total suspended solids in water bodies for use as an assessment of water quality (Sadar, 2002). However, turbidity is not a true measure of SSC because it is an optical property rather than a physical quantity (Zhang, 2009).

The use of turbidity as a surrogate for SSC requires manual sampling and development of a site-specific SSC estimation model that is calibrated using manual sampling data (Jastram, Zipper, Zelazny, & Hyer, 2010). The development of turbidity based relationships between continuous water-quality measurements and periodic collection of samples can lead to a more accurate estimation of actual daily loads (Christensen, Rasmussen, & Ziegler, 2000). Christensen et. al further explains that due to the continuous nature of stream data, estimated loads may be more reflective as they can be measured more frequently than manually collected samples. As peak concentrations are more likely to be documented because of the increased feasibility of more frequent data collection.

Some factors can affect the relationship between SSC and turbidity, thus creating some challenges using this technique. Sediment particle size distribution, shape, and composition can alter the turbidity of a water sample and can cause different output readings in the same sediment concentration (Davies-Colley & Smith, 2001). (Gippel, 1995) further states that particle size variation can affect turbidity by a factor of four under the same sediment concentration, this is due to turbidity being a function of surface area of the suspended particles and their light scattering characteristics, while SSC is a function of particle mass. Other factors affecting the turbidity of a water sample include organic matter, mineral composition, season, color of

sediment particles, density, and other aquatic organisms (Davies-Colley & Smith, 2001; Gippel, 1995; Sutherland, et. al, 2000).

2.2 Current SSC Methods

The SSC has been measured or estimated in many different ways over the years. The methods vary widely in both accuracy and feasibility. This section will discuss these methods and the benefits and drawbacks of each.

2.2.1 Field Sampling

This type of measurement involves field collection of water samples using bottles or automatic samplers. The water samples must then be taken back to the laboratory to be weighed, filtered, dried, and weighed again in order to find the SSC. The method takes a period of at least two days to obtain results for concentration. However, this technique is the most accurate way to measure the total amount of suspended material in a water sample collected from flow in open channel at an instantaneous point in time (Glysson & Gray, 2002). The drawback to this method is that it is very time consuming and labor intensive. Moreover, the peak sediment concentrations which are responsible for the vast majority of sediment transport are usually not recorded with this method. Water sampling also usually leads to an underestimation of loads and an unrealistically high sampling frequency is required to accurately predict sediment loads and trends over time (Gippel, 1995).

2.2.2 Optical Measurement

Optical sensors have been used for some time for the measurement of SSC and have been proven as a reliable method. These types of sensors have been used for a variety of scientific, engineering, and environmental-monitoring applications (Downing, 2006). Optical sensors work by emitting a light source at one point and measuring either the transmittance of light or the backscattered light (OBS) through the water using a photodetector. These two types of optical measurement have proven to be successful, especially in applications with fine-grained sediments (Hoitink & Hoekstra, 2005). The relationship between SSC and sensor signal is almost linear over many sediment types (Downing, 2006). However, measurement with optical methods can vary greatly with a variety of parameters such as particle size, composition, shape, and environmental characteristics (Bunt, Larcombea, & Jagob, 1999).

One of the difficulties in measuring SSC with an optical sensor is that it must be calibrated in a site-by-site basis, thus the sensor signal is not transferable between different watersheds (Marquis, 2005). In order to properly calibrate these types of sensors a calibration curve must be established for each sediment type because different materials scatter and absorb light differently (Pratt & Parchure, 2003). Grab sampling must be done over a range of different concentrations in order to accurately predict the SSC.

After deployment of sensor in the water body, the effects of fouling can begin to have an effect on the perceived turbidity of a fluid. Fouling or biological fouling is the growth or deposition on the surface of an object by organisms or materials of biological origin. This may include items such as microorganisms, algae, diatoms, plankton (Kent, 1988). These organisms will grow to form a film on the fouled surface causing a deviation in the reading of the optical sensor. This change in sensor signal can either amplify or reduce the actual amount depending on the type of fouling that is occurring (Campbell Scientific, 2008). Steps can be taken to correct the effects of fouling using data processing techniques in order to get a more accurate prediction of SSC (Zhang, 2009).

2.2.3 Acoustic Measurement

Acoustic measurement of SSC is a method that involves using high frequency sound waves directed into the stream. This method is much less prone to biological fouling than optical measurements and is non-intrusive to the stream (Gartner, 2002). The sound wave is backscattered to the transducer that emits the sound wave; the strength of that signal is then measured and can be used to determine SSC from a pre-calibrated model (Zhang, 2009). In recent years the use of acoustic backscatter (ABS) intensity has gained popularity for its use in determining SSC. One advantage of ABS is that it measures the entire water column rather than specific point in the stream (Perkey, Pratt, & Ganesh, 2010).

A disadvantage of acoustic measurement is that this sensor cannot differentiate between SSC and particle size. Thus, if the particle size distribution of the sediment changes in a stream but the concentration of sediment remains the same, the sensor will read it as a change is SSC unless independent particle size measurements are taken and accounted for (Gartner, 2002). Acoustic measurement devices most often take a measurement of the vertical profile of the stream which can cause the effective measurement depth to decrease during periods of high

concentrations (Wren & Kuhnle, 2002). Since this type of sensor measures a column of water, limitations can occur in shallow rivers where the depth of water to be measured is small (Meral, Smerdon, Merdun, & Demirkiran, 2010).

2.2.4 Laser Diffraction

Laser diffraction is another technology used for SSC measurement. This type of measurement uses Mie scattering properties from light scattering physics. When a laser beam comes in contact with a particle, some of the light rays are absorbed or diffracted at large angles from the original beam, while others are diffracted around the particle at small angles. This small angle diffraction is the area important to this type of technology and is measured using a series of ring-shaped detectors (Agrawal & Pottsmith). To use this method, the known particle density must be used along with volume of the sediment to determine SSC (Gray & Gartner, 2010).

The current leader in development of this type of SSC measurement is Sequoia Scientific, Inc. They have developed an instrument called Laser In-Situ Scattering and Transmissometry (LISST) (Zhang, 2009). This instrument is not subject to inaccuracies due to changes in particle size because of known properties of the diffraction signals (Agrawal & Pottsmith, 2000). This instrument also uses a pump to withdraw a filament of water and route it through the laser beam at the ambient current velocity, giving it the ability to measure velocity as well. (Gray & Gartner, 2010).

Some of the disadvantages of a laser diffraction sensor can be its large size and cost. This technology can cost 2-6 times that of a fully equipped in-situ turbidimeter, partly because it is only available from one manufacturer (Gray & Gartner, 2010). This instrument's large size can also cause flow obstruction and would not be ideal for shallow stream because the instrument would be out of the water it is sampling (Zhang, 2009).

2.2.5 Pressure Difference Instruments

The pressure-difference technique for SSC measurement relies on two precision pressure-transducers taking simultaneous measurements at different elevations in the water column. The difference in pressure is then converted to a water-density value, from which SSC is inferred after water temperature is accounted for (Gray & Gartner, 2010). This technology is not widely accepted as there have been some complications to date in the accuracy of the results. One advantage of this system is that it is similar in cost to a fully equipped turbidimeter and these

types of sensors are widely available from a number of sources (Gray & Gartner, 2010). The accuracy of this system seems to improve with increasing SSC. It also provides a large range of SSC measurement (Kuhnle & Wren, 2005).

A disadvantage of this system is that it has very poor accuracy in low SSC (<1000 mg/L) (Kuhnle & Wren, 2005). This greatly limits its application. It is also susceptible to temperature fluctuations, turbulence, and large dissolved solids concentrations (Gray & Gartner, 2010). These factors have limited the use of this technology in non-laboratory settings.

2.2.6 Remote Sensing

Satellite images have been analyzed to determine the SSC of a water body. Variations of SSC alter the optical properties of the water column, causing changes in reflectivity (Pavelsky & Smith, 2009). An advantage of this method in comparison to other methods is that a researcher would be able to measure SSC in a large area quickly (Zhang, 2009). The images can be taken using hand held equipment, or equipment mounted in aircraft or satellite. This method is best suited for marine environments where large areas of water present (Wren & Kuhnle, 2002).

One of the main disadvantages of this system is its low resolution. The resolution of an image depends on the camera resolution and the height at which the image is taken. During periods of high SSC, this technology is also limited in its ability to measure the entire water column as the imaging equipment cannot penetrate the entire water column (Wren & Kuhnle, 2002). As image capturing and processing technology improves the use of this type of method could increase.

3. **Wireless Suspended Sediment Sensor**

In partial fulfillment of a water quality research project an optical sediment sensor was developed to measure SSC in the Instrumentation and Control Laboratory at Kansas State University (Stoll, 2004). This sensor was designed to be insensitive to a variety of in-stream parameters such as suspended and dissolved objects, particle size, organic matter, non-soil particles, along with color of the water (Stoll, 2004).

3.1 Structure

The structural design of this particular sensor was derived from testing different soil types, water types, and different angles of the optical components in the optical sensor (Stoll, 2004; Zhang, 2009). From this testing, it was determined that an upside down U-Shaped sensor was the most effective design. The advantage of the U-shape over a circular tube is that the U-shape helps to prevent clogging of the sensing area. Figure 1 shows the structural design of the optical sensor. The outer shell is made of polyethylene; the sensor also has an aluminum bracket attached to the frame for mounting of the sensor in the stream.

Figure 1. Optical sensor frame and housing

3.2 Optical Components

Based on testing in three different water types – distilled water, lake water, and stream water, Stoll (2004) was able to determine which "feature wavelengths" were ideal. He identified three wavelengths where spectral responses peaked (Zhang, 2009). These three wavelengths were 505nm, 610nm, 880nm, which were referred to by Stoll as blue-green (BG), orange (OR), and infra-red (IR), respectively. From these wavelengths three LEDs were selected as the light sources and three phototransistors were placed at various angles from the LEDs (180^0, 90^0, and 45^0) to measure the amount of light transmitted, scattered, and backscattered across the sensor, respectively (Zhang, 2009). Of the various combinations of LEDs and phototransistor angles, three were determined to be the most effective for measuring suspended sediment concentration and were used in calibration and testing. These combinations were a phototransistor placed 45° from the axis of an LED with a peak spectral response within the IR region (IR45), and two phototransistors, one placed 45° and another at 180^0 from the axis of another LED with a peak response in the orange region of the visible light spectrum (OR45 and OR180). These combinations were chosen to prevent over-fitting of prediction models and prevents redundancy of data.

A second set of orange LED and phototransistors were equipped on the sensor as well. The two sets were located 4 cm apart and placed along the U-shaped tube on the sensor structure. The goal of this arrangement was to observe the readings of these two phototransistors over time in order to determine the velocity of the stream. This was achieved by injecting dye into the U-shaped area of the sensor and analyzing the readings over a time period to determine the lag time of the phototransistor readings, in turn finding the velocity of the stream. The measured flow velocity can be used along with known stream cross-section to find overall volume of sediment flowing through a particular reach. Figure 2 shows the location of the LEDs and phototransistors on the optical sensor.

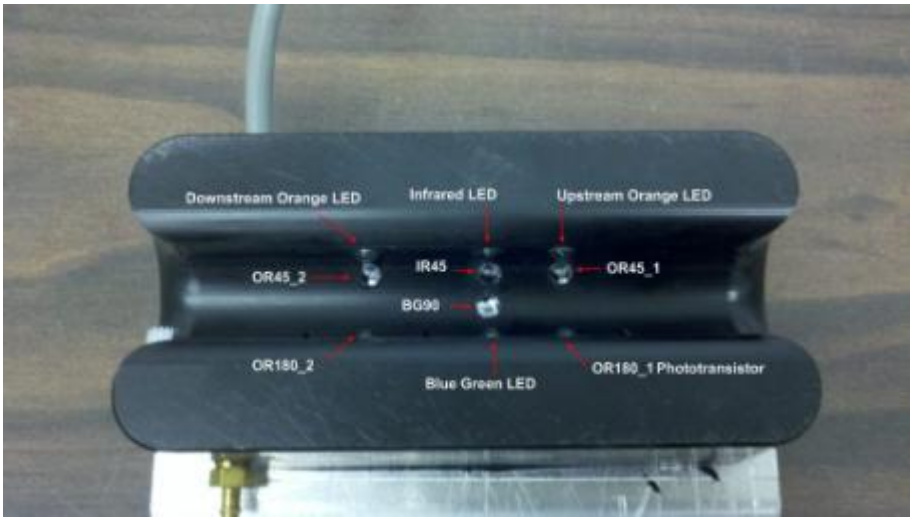

Figure 2. Sensor LED Arrangement

3.3 Air Cleaning

Fouling has been a large area of study for optical in-situ sensors. Once an object is placed in a stream the microbial activities in the stream can begin to create a film on the surface of the sensing element. This fouling effect causes the need for a cleaning system which can be expensive and impractical. The goal for this system is to provide a virtually labor free method so that there is no need to go into the stream to physically clean the sensor. The effects of fouling can be seen in the sensor readings over time and while a corrective program can be applied to reduce the effect, an unfouled sensor is still the best solution.

The solution to this problem for this research project is to utilize an air-cleaning system that is built into the sensor structure. This system uses compressed air to blast the sensor to remove dirt, algae, and other foreign material from the LEDs, phototransistors, and the sensor body. Compressed air is delivered from an air compressor placed in a waterproof box on the stream bank that is powered by a battery and solar-power. The air is delivered through a 1/4 inch air hose that is attached to the optical sensor. The air is then sprayed to the U-shape area to clean the sensor. This air-blast cleaning method can be programmed to run at different time intervals.

3.4 Installation

The sensors installed in the stream were attached to a T-Post usually driven into the thalweg of the stream. This was to help ensure that the sensor will always be submerged in water as long as the stream is flowing. Once the post was driven into the streambed it was then cut off

at water level to reduce the possibility of catching debris during high flow periods. The sensor was then attached to the post with the U-Shape of the sensor parallel with the flow of the stream. Another post was driven 3-6 feet upstream from the sensor to act as a safety device to catch or divert large pieces of debris around the sensor.

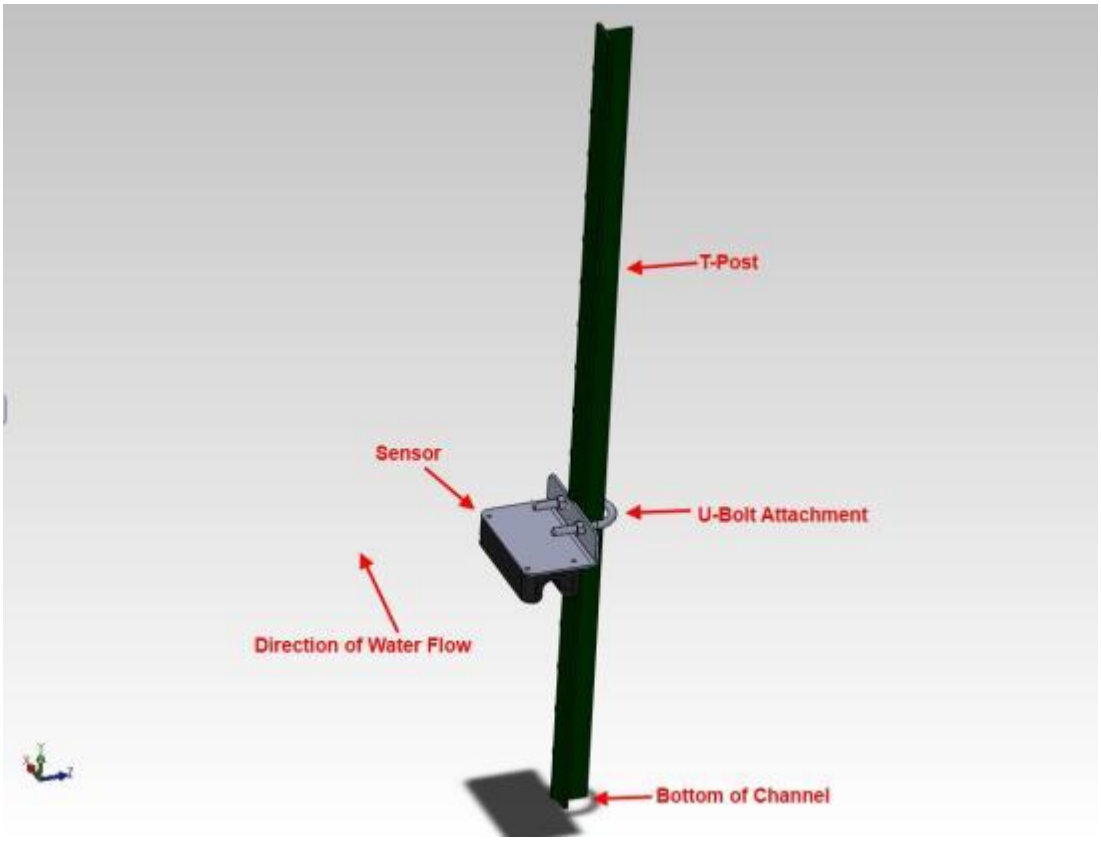

Figure 3. Installation of sensor in stream attached to T-Post. (source: Joseph Dvorak, edited by author)

3.5 Sensor Covers

The optical SSC sensor has been found to be most accurate and have the least interference when placed in complete darkness (Zhang, 2009). This finding created the need to block the sensing area from ambient light. The upside-down U-shape of the sensor helps to block some, but not all light, causing skewed readings of the sensor during certain times in a day. This was improved by installing an aluminum cover plate on the T-post above the sensor itself.

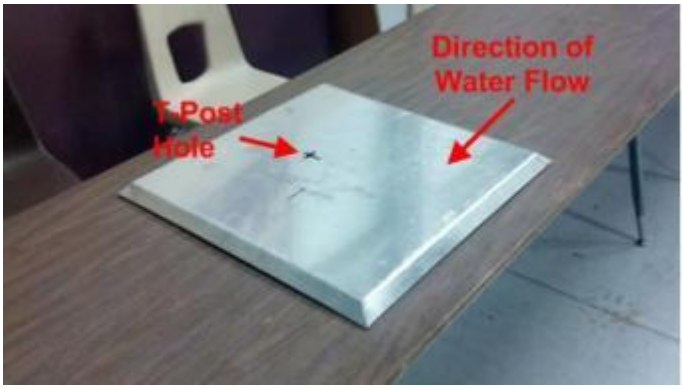

Figure 4. Initial sensor cover design

Initial designs utilized a large, flat square plate (Figure 4). Through testing and real-world application, it was determined that these large plates catch a large amount of debris and cause a damming effect in the stream. A new pyramid type design was created that provided adequate light cover while protecting and diverting debris flowing down the stream. This cover system had the front corner of the pyramid facing upstream to act as diversion plate to move debris such as limbs, leaves away from the sensor area. The cover was attached to a T-post that went through a hole in the cover and was attached using a U-bolt. This cover was also placed above the sensor as to not affect the sediment or velocity readings.

Figure 5. Top and bottom views of final sensor cover design.

4. Locations

The overall goal of this project was to provide a versatile suspended sediment sensor that can be used in a variety of soil types, ecological regions, and climates. Another goal of the project was for the sensor to be used on military bases to monitor streams near tank crossings to observe the effects military vehicles have on sediment runoff. With this in mind, the locations of the sensor installation was studied and determined by Dr. Zhang and his colleagues.

4.1 Fort Riley, Kansas

Fort Riley was selected as a desirable location for this project because of its close proximity to Kansas State University. This site can be classified under the Flint Hills Eco region, which is characterized by large rolling hills composed of shale and limestone. The average annual precipitation of the region is between 28-35 inches (Castle, 2007).The region is dominated by tallgrass prairie and remains mostly undeveloped in the study sites chosen. Three streams and four sensor sites where selected for this location. All of the streams used in this study are part of the Wildcat Creek basin.

4.1.1 Little Kitten Creek

Little Kitten Creek is a stable, perennial stream that drains a 1,900 acre watershed on located on the western edge of Manhattan, KS (Castle, 2007). Little Kitten Creek is not located on the grounds of Fort Riley military training area, but for the purposes of this research it will be included in the Fort Riley sensor location sites for easier referencing. The watershed and stream are highlighted in Figure 6 below:

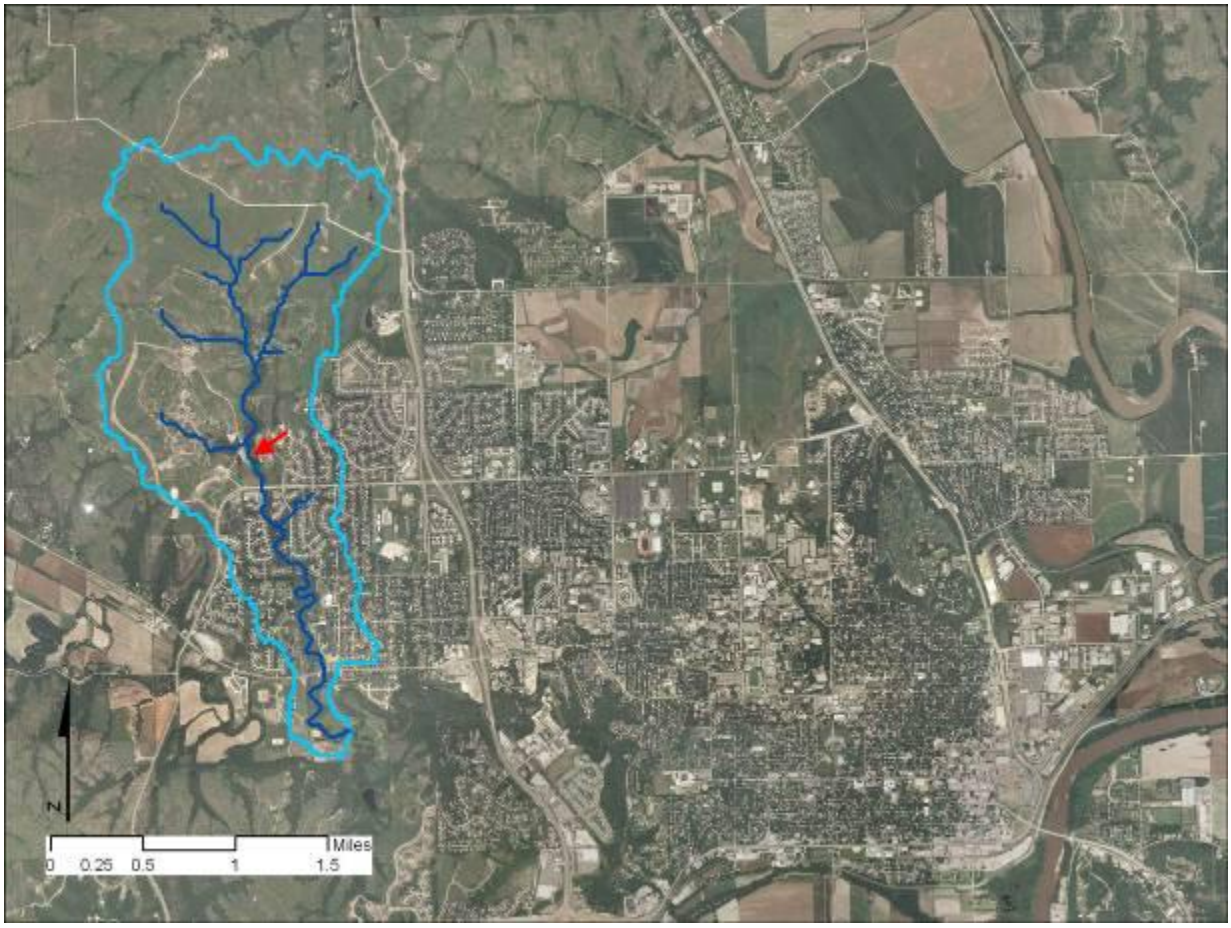

Figure 6. Little Kitten Creek Watershed. Sensor location denoted by red arrow. (Source: (Castle, 2007), edited by author)

The portion of the stream that is upstream from the sensor location is mostly undeveloped and is mostly dominated by groundwater seepage from the Flint Hills with stormwater runoff being added during storm events.

Usually the sensor is placed 6-12 inches from the bottom of the streambed. However at Little Kitten Creek the stream was not 6-8 inches deep at the site during normal flow so the sensor was placed 1-2 inches above the streambed but still submerged in the stream. Figure 7 displays the sensor placed in Little Kitten Creek.

Figure 7. Sensor installed in Little Kitten Creek, with velocity attachment and without cover.

4.1.2 Wildcat Creek

Wildcat Creek is a larger stream than Little Kitten Creek; this stream drains an 88 square mile area with its headwaters located 28 miles west of Manhattan, KS (Stutterheim, 1972). The portion of Wildcat Creek that was used in this study is directly south and southwest of the city of Keats, Kansas which is approximately 8 miles west of Manhattan. This study site is upstream from the entry of the Little Kitten Creek. This section of the stream also serves as the border between Fort Riley and private land.

Two sensors were installed in this stream approximately 1.3 miles apart from each other, measured on the stream channel. The names of these sensors/sites that will be used in this report are Wildcat Bridge and Wildcat Creek.

4.1.2.1 Wildcat Bridge

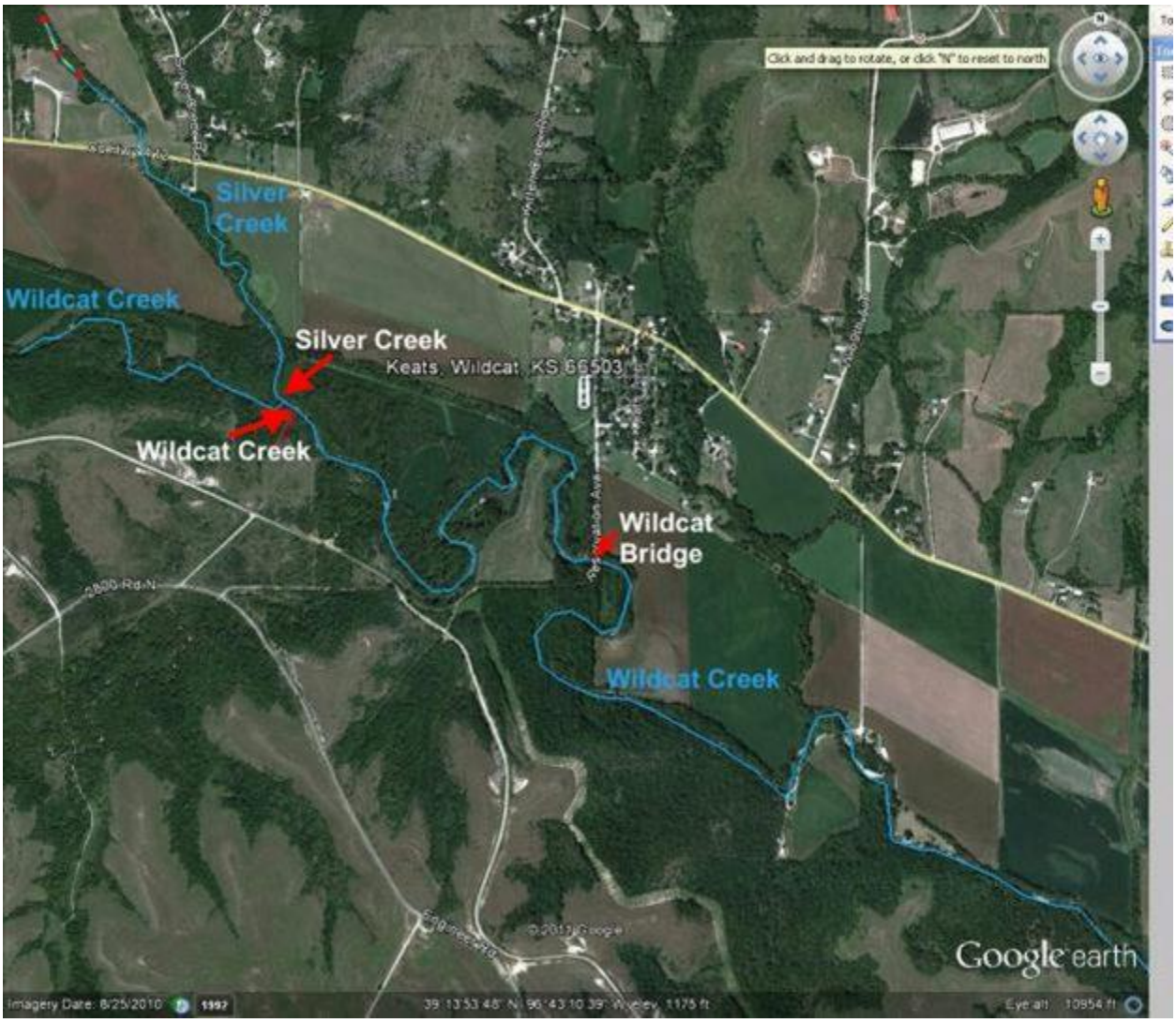

Figure 8. Wildcat Bridge, Wildcat Creek, and Silver Creek sensor sites. (Source: Google maps, edited by Author)

The Wildcat bridge sensor site was installed near an old military bridge that is directly south of Keats, KS. This can be seen in Figure 8 along with the other nearby sensor sites. The sensor was installed in a 3-6 foot deep portion of the stream. This depth created some difficulties for sensor calibrations. During periods of higher flow it was deemed unsafe to enter the middle of the stream channel. In order to properly gather calibration data the sensor was placed at the edge of the stream where it could be more easily accessed. After calibration was completed the sensor was then moved to the middle of the stream channel.

Figure 9. Wildcat Bridge sensor installed in stream with sensor name displayed.

4.1.2.2 Wildcat Creek

The Wildcat Creek site was located upstream from the Wildcat Bridge sensor. The sensor was initially placed in the riffle of the stream in a part of the channel that was between 2-8 inches deep in normal flow periods. During the summer of 2011 there was a very large rain event in the Wildcat Creek watershed causing considerable flooding for this stream. Because of the force of the flood event the streambed underwent some changes and the sensor site became a pool area of the stream, roughly 3-4 feet deep during normal flow periods.

During the flooding event some of the electronic components on the streambank also became damp and therefore needed to be replaced or fixed. After a period of troubleshooting it was determined to focus mainly on the Wildcat Bridge and Little Kitten sites. Although this site still transmits data back to our database, the data it is sending no longer carries sediment information.

4.1.3 Silver Creek

Silver Creek is also a tributary of Wildcat Creek; this stream is approximately 7 miles long and drains a mostly undeveloped tallgrass ecosystem (Gustafson, 1999). The site for our sensor study is located at the mouth of Silver Creek just upstream from the Wildcat Creek sensor site. Since this location was at the mouth of the stream, there was a large amount of streambed movement, burying the sensor in rocks on numerous occasions. This is because as the smaller, faster moving stream enters the larger slower moving Wildcat Creek, the velocity decreases, causing sediment and rocks to be deposited. This was especially true during periods of high flow. This is the same type of phenomena that happens when a stream enters a large pond or lake.

The sensor was moved from the newly formed rock bed to a new stream flow path several times. However, in the summer of 2011, there was a large rain event that buried the sensor once again, and the force of the water also broke the sensor cables and conduit, making the sensor dysfunctional. After this flood event the area went through a very dry period for the rest of the year and this stream stopped flowing altogether so this site was abandoned.

4.2 Fort Benning, Georgia

The second site that was chosen for this project was Fort Benning, Georgia. This military installation is located just south and east of Columbus, Georgia, near the Georgia-Alabama state line. This area is dominated by evergreen and deciduous forest and has rolling hill topography (Bourne & Graves, 2001). The average annual rainfall for this area is approximately 49 inches (U.S. Climate Data, 2011). This site has a different climate, soil type, and ecological makeup from the Fort Riley site and provides the study with data to improve versatility. Two different streams were chosen for this study site with two sensors installed in each stream.

4.2.1 Pine Knot Creek

Pine Knot Creek is located on the northeastern edge of Fort Benning; the sediment type is mostly sand so high sediment concentrations were seldom occurring. Pine Knot Creek is a tributary of the Upatoi River which will be discussed in the next section. There were two sensors installed at this site to measure the SSC. The sensors were installed approximately 15 feet apart from each other, with the northernmost sensor being installed near the bank of the stream and the southern sensor being installed in the middle and deepest part of the channel. Figure 10 displays both the Pine Knot and Upatoi River along with the location of the sensor sites.

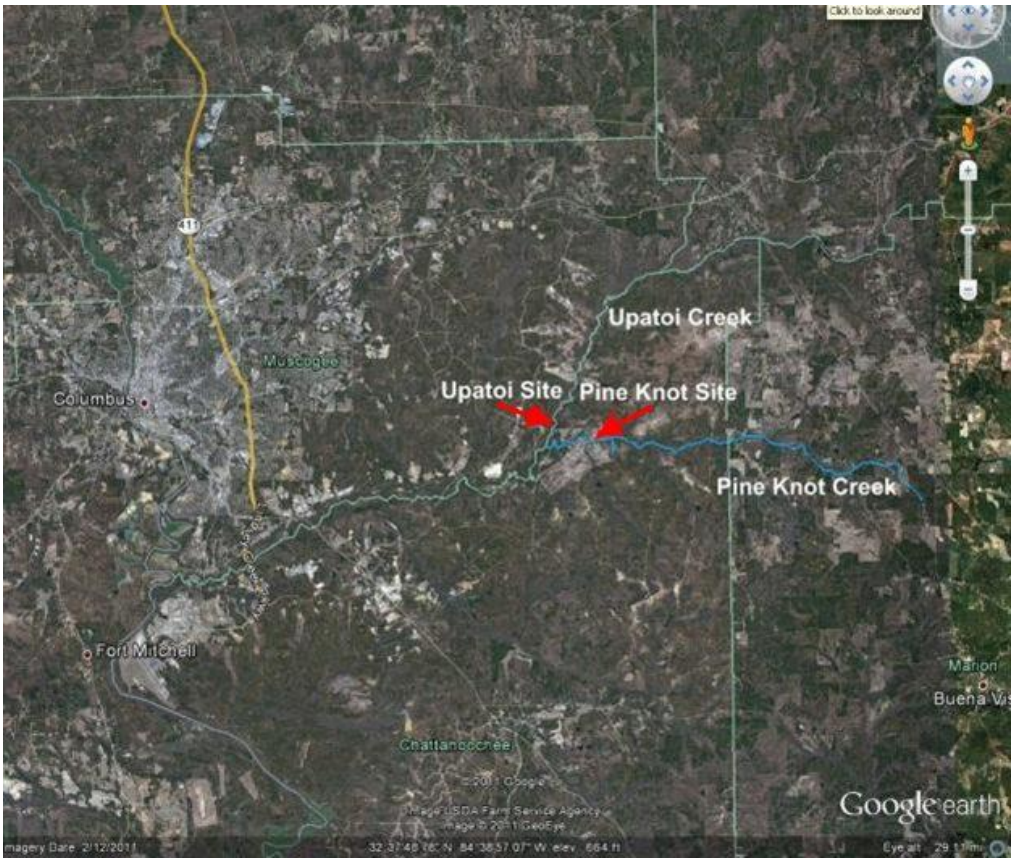

Figure 10. Ft. Benning stream sites with sensor location. (Source Google Earth, edited by Author)

The north sensor will be referred to as Pine Knot North (PKN) while the south sensor will be referred to as Pine Knot South (PKS) in this report. The PKS sensor had the capability of measuring velocity as well as SSC. Figure 11 displays the sensors installed in the stream.

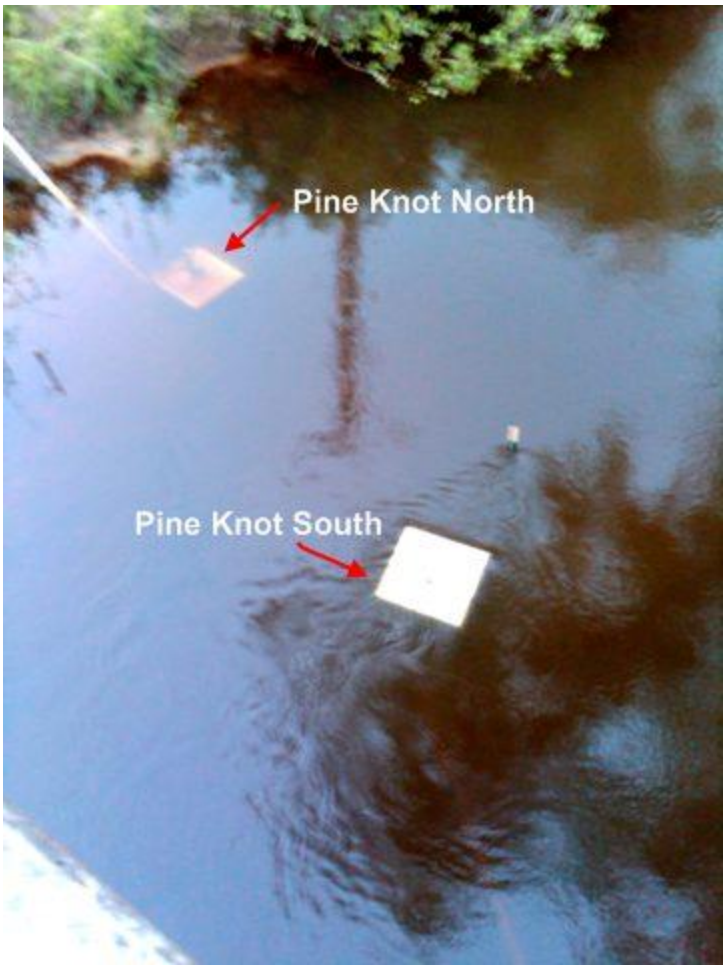

Figure 11. Pine Knot sensor site with labels displaying sensor names. Sensor covers are installed on both sensors.

4.2.2 Upatoi River

Upatoi Creek is a 35.5 mile long river that runs through Fort Benning before depositing in the Chattahoochee River (USGS, 2011).The section of this river where the sensors are installed are near the middle of the length of this river. The streambed of this river is mostly sand which tends to settle very quickly to the bottom of the stream. This caused some difficulty in obtaining high SSC samples. Both sensors at this site were installed approximately 15 feet apart from each other with one sensor being slightly north and east of the other sensor. In this report, the north sensor will be referred to as Upatoi North while the south sensor Upatoi South. Figure 12 displays the sensors installed in the river with the sensor covers.

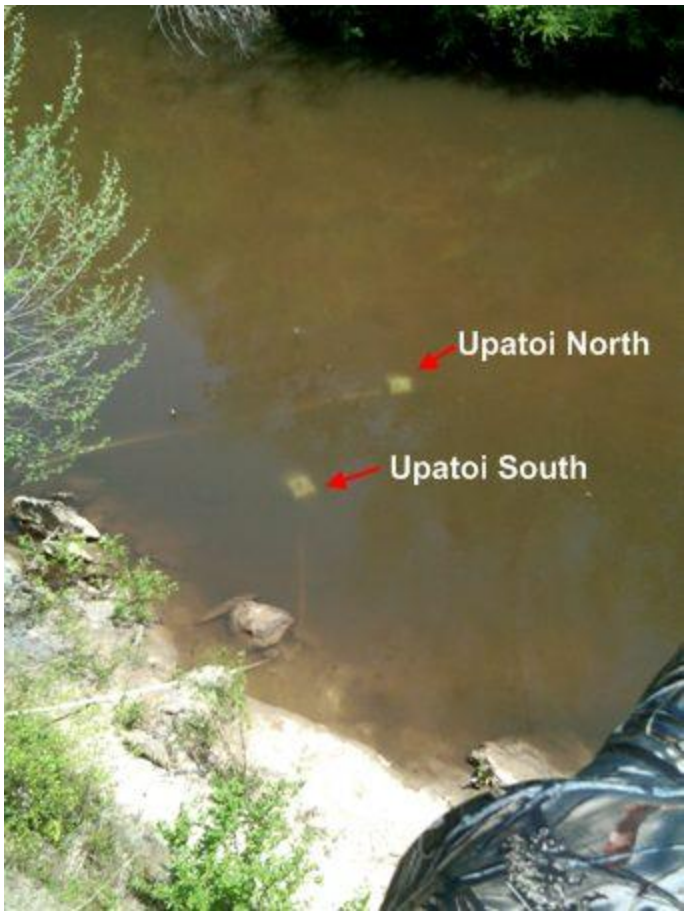

Figure 12. Upatoi sensor site displaying sensor name labels, sensor covers are installed on both sensors.

4.3 Aberdeen Proving Grounds, Maryland

Aberdeen Proving Grounds (APG) is located adjacent to the north end of Chesapeake Bay in Maryland. The ecological region of this area is defined as the outer coastal plain, mixed forest and is fairly developed (Doe III, Shaw, Bailey, Jones, & Marcia, 1999). The Eco region is characterized by mostly flat topography with oak-hickory-pine forests being the natural vegetation (McNab & Peter, 1994). The rivers in this area are mostly stagnant with their flow coming from tidal influence. Two sites were selected for this location with two sensors installed at each site.

4.3.1 Anita Leigh Estuary

Anita Leigh Estuary is part of a tidal cove that is part of the Chesapeake Bay. Fluctuations in SSC at this site are usually seen from tidal action and rain events. The area that

drains into this sensor site is mostly developed with a small nature preserve directly east of the sensor site. Figure 13 displays the sensor location.

Figure 13. Anita Leigh sensor site location. (Source: Google maps, edited by author)

Sensors at this site were attached to support posts of a boat dock. This type of set up was chosen because of the protection the dock offers along with the ease of access to the sensors. Sensor covers for this site where modified in a way that the sensors where attached to the covers and the covers were then attached to the dock using a bracket and lag bolts.

4.3.2 Gunpowder River

Much like the Anita Leigh site, the Gunpowder River site is also part of the Chesapeake Bay system. This site is on the APG base and also has tidal fluctuations. Much of the area that drains into this river system is developed. The sensors at this site were attached to a boat dock as well using the same method as described in the Anita Leigh section. Figure 14 displays the location of the Gunpowder sensor site.

Figure 14. Gunpowder River sensor site location (Source: Google Inc. edited by Author)

Initial calibration and testing of this sensor site was performed in the initial round of sensor deployment from 2009-2010. Some difficulty with data transmission was encountered during the test. Also one of the sensors at this site was hit by a boat and knocked off of its

attachment to the boat dock. It was determined that, for the second round of calibration, the sensors would only be attached at the Anita Leigh site for this location with the Gunpowder site only being used for data transmission testing.

5. **Control Board**

The printed circuit board (PCB) for sensors and controls is an essential part in the sensor assembly. Functions of the PCB board include (1) voltage regulation, (2) mote and data acquisition, (3) sensor control, (4) sensor gain adjustment, (5) relay control, (6) signal conditioning for temperature measurement, (7) interfaces. These components will be explained in greater depth in the Sections 5.1 - 5.7.

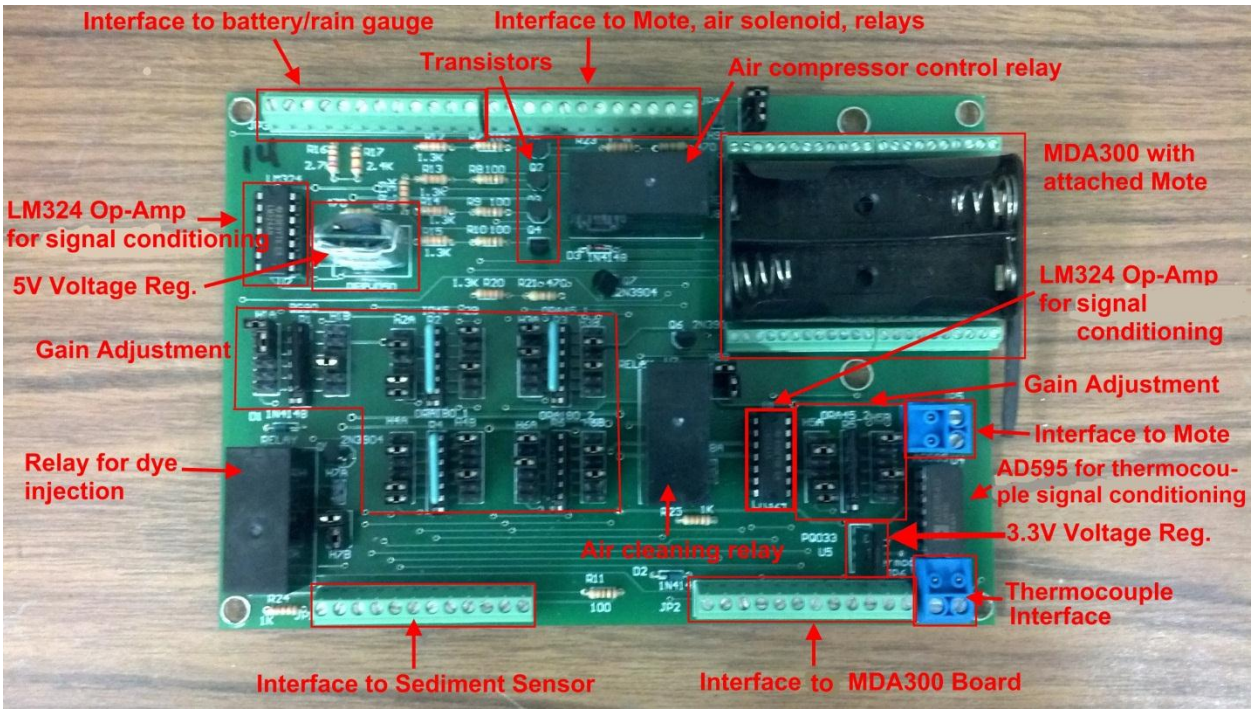

Figure 15. PCB control board

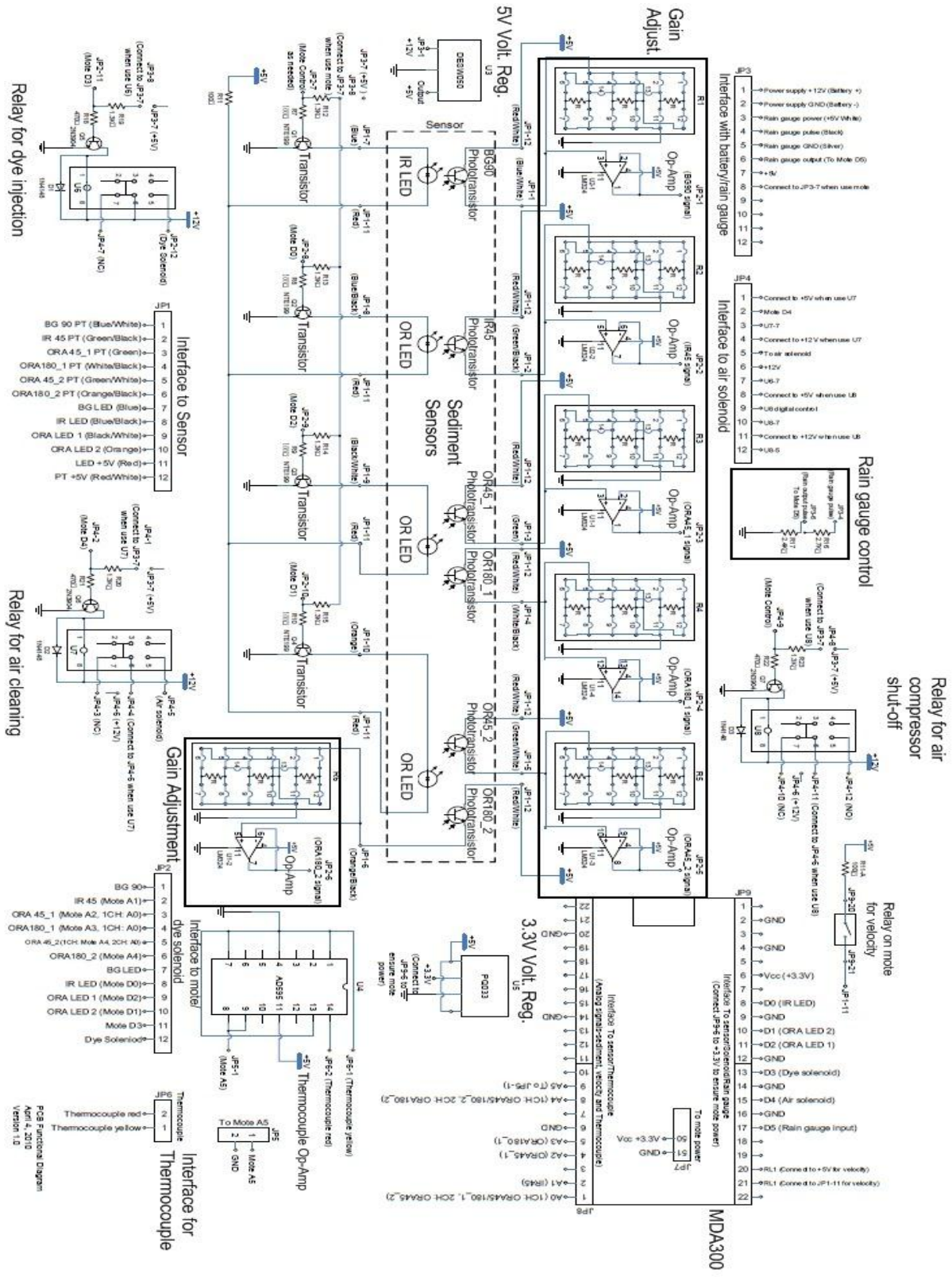

Figure 16. Functional Diagram of PCB board (source: Joseph Dvorak, edited by author)

5.1 Voltage Regulation

The PCB board provides 3.3V power to the wireless mote (Micaz, Crossbow Technology Inc.) and the data acquisition board (MDA300, Crossbow Technology Inc.), and 5V power to the remaining components of the system – sediment sensors, control relays, rain gauge and temperature measurement.

5.2 Mote and Data Acquisition Board

The PCB board provides a 50 pin connector slot for the data acquisition board MDA300 to plug in. A Micaz mote can then be plugged into the MDA300 to control the sensor and relays. The MDA300 is equipped with a 6 ADC channels, 6 digital I/O channels, high-speed counter, 2.5V, 3.3V, and 5V external sensor excitation, and 2 relay control.

5.3 Sensor Control

The PCB board serves as the bridge between the data acquisition system (MDA300) and the sediment sensors. It provides power to the LEDs in a controlled time sequence, converts current signals from the phototransistors in the sediment sensors to voltage signals, and sends the voltage signals to the data acquisition board MDA300 for processing.

5.4 Gain Adjustment

The PCB board provides a gain adjustment circuit to each sediment sensor so that the gains of the current-to-voltage converters can be adjusted during the pre-calibration stage to achieve similar gains under the laboratory conditions. The gain adjustment is achieved by adjusting the resistor and jumper combination in order to achieve a desired resistance. The gain adjustment circuit is shown in Figure 17.

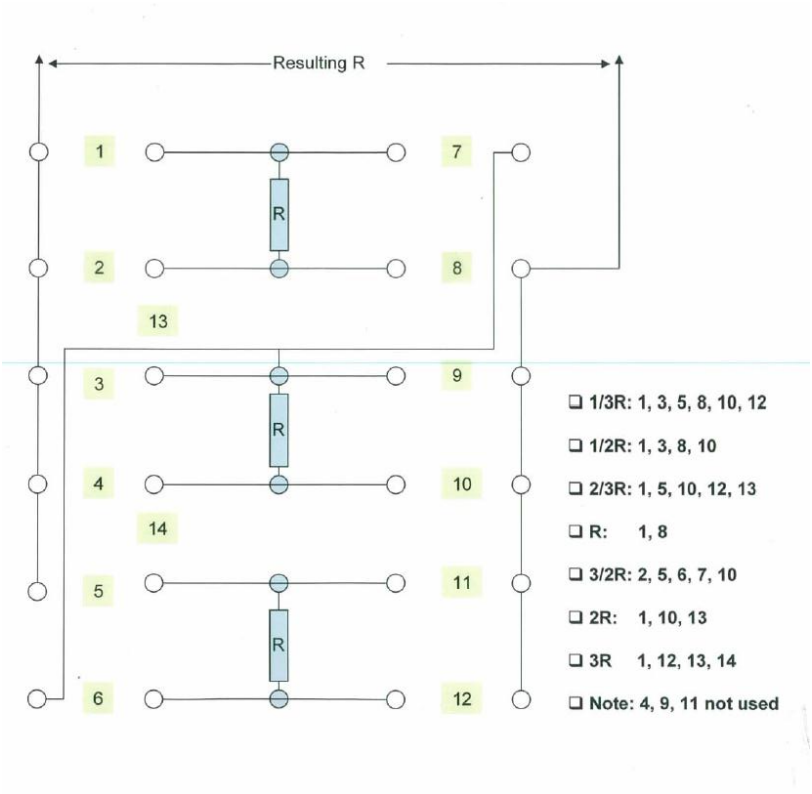

Figure 17. Gain adjustment diagram used to achieve desired resistance needed for calibration

After a six pin resistor array with resistance of R plugged in the resistor socket, by selecting 2-6 from the 14 possible jumper connectors, nine different resistances, from 1/3 R to 3R, can be achieved (Figure 17).

5.5 Relays

The circuit board provides three separate Omron G2R-24 Industrial relays to have the capability to control various relays. Two relays are used to control solenoid valves for air compressor and dye injection for velocity measurement. The third relay is used to prevent the air compressor from turning on when battery voltage is below 12V.

5.6 Temperature Measurement

The PCB board uses an AD595 type-K thermocouple amplifier with cold junction compensation to measure water temperature.

5.7 Interfaces

The PCB board serves as a general hub to provide interfaces between the mote/data acquisition system and several peripherals, including the sediment sensors, rain gauge, thermocouple, and solenoids to control air compressor and dye injector.

6. Sensor Pre-calibration

Calibration of the SSC sensors composes two stages – a pre-calibration conducted in laboratory using formazin stock suspensions and a final calibration conducted in stream using grab water samples. This section discusses the procedures for pre-calibration.

6.1 Test Stand

In order to properly measure the SSC in the streams the sensor/PCB board assembly needed to be pre-calibrated. This was performed using a test stand that would test the various functions of the sensor and the PCB board in the laboratory while mimicking real-world settings. The PCB boards and sensors could be attached to the stand quickly and the functionality of different field operations could be checked before being installed in an actual field setting.

Figure 18 displays a picture of the test stand with all components labeled.

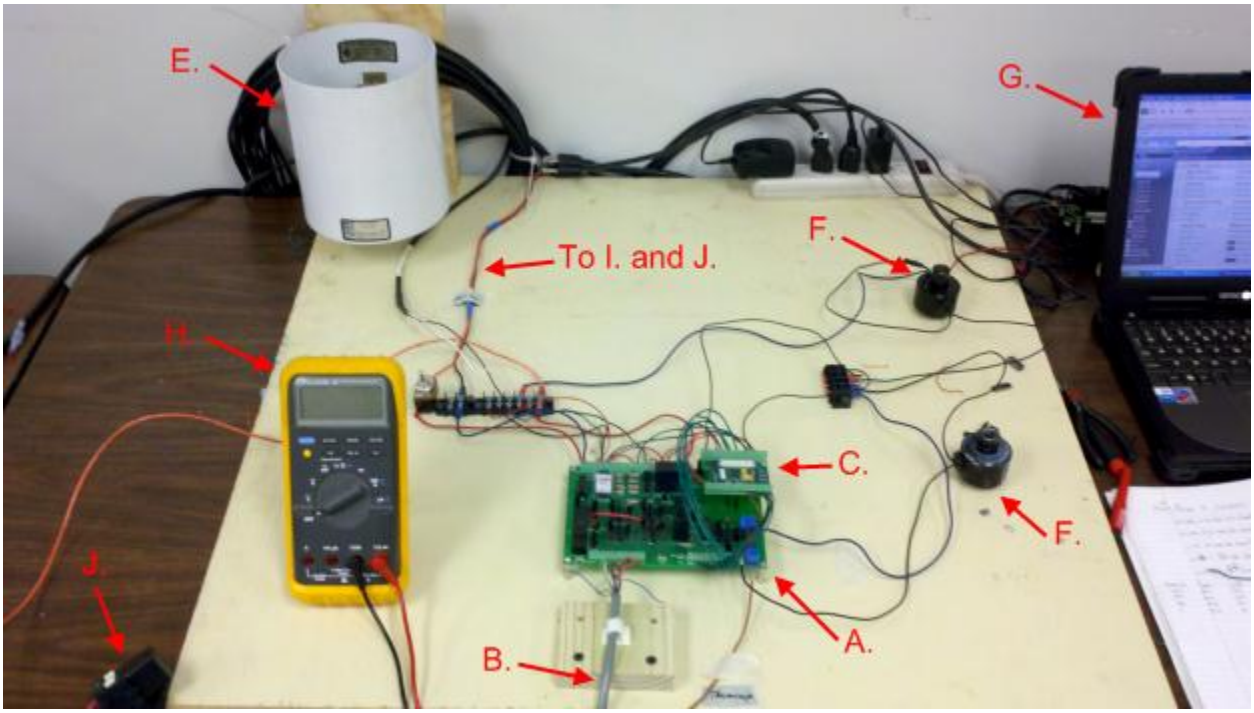

Figure 18. Test stand for testing PCB board and sensor assembly. The components are: A. PCB board; B. Suspended sediment sensor; C. MDA300; D. Crossbow mote (not in the picture); E. Rain gauge; F. Two solenoid valves; G. Laptop; H. Multimeter; I. 12V DC battery power (not in the picture); J. Voltage regulating relay.

6.2 Suspended Sediment Solution

In order for the sensor to be properly pre-calibrated it must be placed in solutions with known turbidities for all sensors. The goal of the pre-calibration was to make all sensors output the same signal level for the same turbidity. Although this sensor is used to estimate SSC, it is actually measuring the turbidity of the stream it is installed in. Turbidity is an optical property while SSC is a volumetric property. This type of pre-calibration was used to get the sensors within an appropriate range of sensitivity for each watershed based off of previous testing and background knowledge of each location. Fine tuning of sensor and estimation of SSC was performed later when a correlation could be established based off of field sampling taken at each particular sensor site.

Pre-calibration of the sensor was performed using formazin stock suspensions, following the EPA standard 2130B (EPA, 1999). The suspension was created using the following procedure:

- Dissolve 1.0 gram of hydrazine sulfate in filtered, de-ionized water and diluted to 100 milliliters
- Dissolve 10.0 grams of hexamethylenetramine in filtered, de-ionized water and diluted to 100 milliliters
- Mix the two resultant solutions and let the mixture stand for 24 hours after mixing at 24-26 °C to produce a 200 milliliter formazin suspension

This process was adjusted in order to create three separate 6000-milliliter formazin suspensions at various Nephelometric Turbidity Units (NTU), which were used in pre-calibration. Selection of the concentrations of these solutions was based on previously observed SSC and sensor readings at the location where the sensor is installed. Table 1 displays the concentrations of the stock formazin solutions used for calibration of the sediment sensors to be deployed at the three installations.

Table 1. Stock formazin concentrations used for calibration of suspended sediment sensor

Ft. Riley, Kansas	Ft. Benning, GA	Aberdeen, MD
1200 NTU	1200 NTU	400 NTU
800 NTU	800 NTU	0 NTU
400 NTU	400 NTU	
0 NTU	0 NTU	

The solutions were placed in black boxes with lids in order to eliminate ambient light. During pre-calibration, the black box was placed on a magnetic stirrer (Fisher Scientific) and was stirred at a constant rate in order to maintain particle suspension and to keep a uniform concentration throughout the solution. Figure 19 displays the sensor housed in the black box assembly atop the stirrer.

Figure 19. Sensor assembly placed in black box (without lid) for calibration in clean water.

6.3 Gain Adjustment

In order to adjust the signal levels of the sensors so that they can achieve a uniform level at the same stock formazin concentration, the gain of the current-to-voltage converters system must be adjusted.

Within a sensor, the phototransistors placed at different angles from their associated LEDs have different trends in signal variation when the NTU concentrations changes. Therefore, using more than one angle would allow the sensor to measure SSC over a wider range of sediment loads (Zhang, 2009). Based on sensor design and previous research it was determined that the OR180 signal should reach its maximum value in clean water. The reason for this is because the 180 degree phototransistor is measuring transmitted light through the U-shape of the sensor, so as the sediment concentration increases; the output signal for this sensor should decrease. The IR45 and OR45 signals should approach their minimum value in clean water because the 45 degree phototransistors are measuring backscattered light, so as the concentration increases, the signal from these phototransistors should also increase. The maximum value a signal was calibrated to was 1800 mV. This was determined based on previous sensor testing and knowledge of typical SSC of the area where the sensors were installed. Table 2 displays the average signal output for each location after calibration and Figure 20 demonstrates the signal variation trends

Table 2. Average signal output (mV) of sensor/PCB board assembly after calibration

	IR45	OR45	OR180
Ft. Riley			
0 NTU	160	62	1858
400 NTU	976	854	822
800 NTU	1450	1098	559
1200 NTU	1793	1790	435
Ft. Benning			
0 NTU	167	44	1810
400 NTU	1044	833	746
800 NTU	1522	1469	506
1200 NTU	1917	1870	372
Aberdeen			
0 NTU	242	97	1739
400 NTU	1786	1818	766

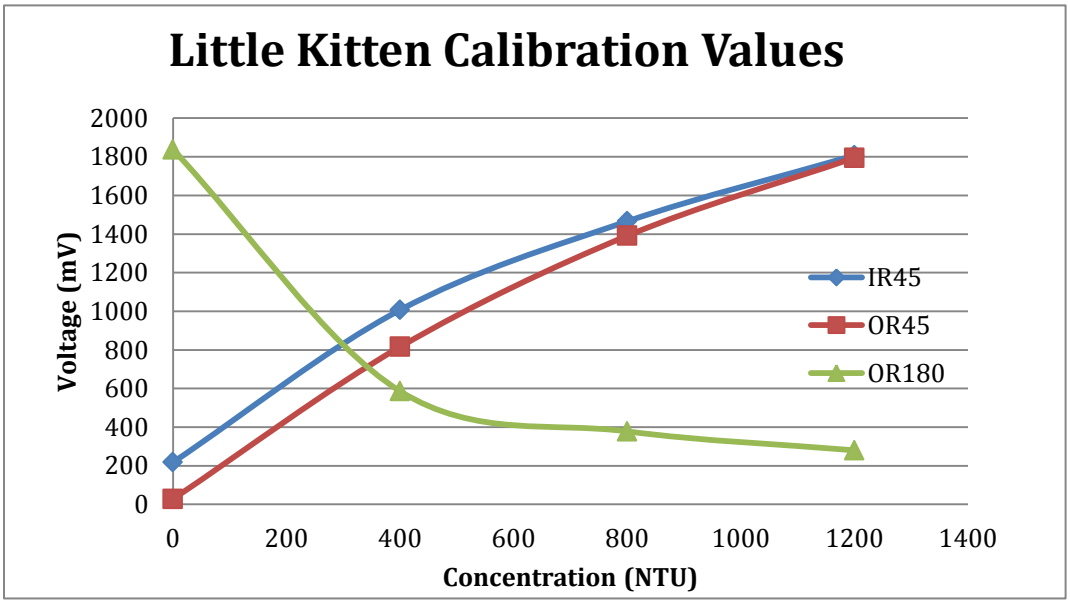

Figure 20. Calibration values of the sensor/PCB assembly for Little Kitten Creek

6.4 Pre-calibration Procedure

The first step of the pre-calibration procedure is to mount the PCB board to the test stand and attach the wires properly. All solenoid valves and other attachments were also wired to the PCB board to imitate a real-world environment. The sensor is attached to the JP_1 port of the PCB board in the orientation displayed in Figure 21.

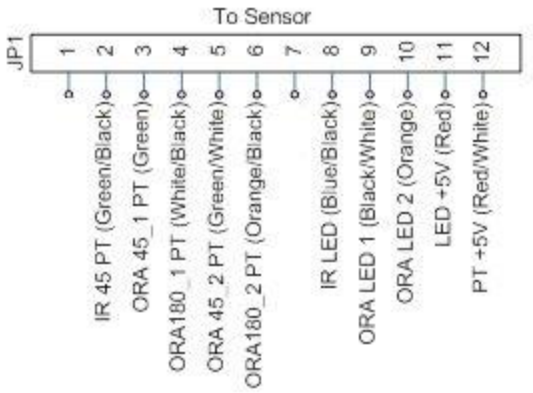

Figure 21. Jumper 1 of PCB board with sensor wire orientation

The sensor was then placed inside the first of suspended sediment solutions and the pre-calibration program was run on the attached mote. The output signals from the sensor channels were then read and from this data the needed resistance was calculated and the gain was adjusted by choosing different jumper combinations as mentioned in the previous section. This procedure was repeated until all channels were calibrated to their proper gain.

7. **Water Sampling**

As discussed in Section 6, water sampling provides the base for the second stage of sensor calibration – the final calibration. Water sampling is also the core action for sensor validation. At all sensor sites, water sampling has been conducted throughout the experiment to provide sufficient numbers of grab samples for SSC sensor calibration and validation.

7.1 Field Sampling

7.1.1 Sensor Cleaning

Prior to taking each grab sample the sensor was cleaned manually using a cotton cloth or paper towel. The sensor was not removed from the T-post during cleaning. Sometimes in order to reach the sensor in the stream the cover needed to be removed in order to clean the lens. Before the sample was taken the cover was reattached in order to obtain more accurate results and reduce the effect of ambient light.

7.1.2 Sampling Process

Grab sampling was done most often during or shortly after rain events, as these were the periods of time when highest SSCs were observed. Each grab sample was taken at the height of the sensor in the stream directly in front of the sensor. The lid of the sampling container was kept on the container until the container was at the same height as the sensor then it was removed until the container was filled and placed back on the container. The sampling container used was a 120 mL sampling cup, the date, time, and location of the sample were then recorded to be used later for correlation with sensor signals. Any water samples not processed immediately when returned to laboratory were refrigerated until the sampling processing took place, usually within a few days of sampling. Samples shipped from other locations such as Aberdeen were next-day shipped cold in coolers of ice to keep the samples as cold as possible and prevent bacterial growth.

7.2 Sediment Concentration Measurement

7.2.1 Equipment

Weighing of the water samples and filters were done using a Mettler HK 160 balance (Mettler Instrument Corp.) which has a resolution of 0.1 mg and a max weight of 160 g. Before beginning the analysis, calibration of the balance should be performed. The calibration procedure is as follows:

- Turn on balance and allow the balance to warm up. It is important that no air drafts or floor vibrations are present.
- Tare scale to all zeroes on the digital display, also should display a + symbol.
- Press the CAL button or lever. You must push the button gently so that the stability of the balance is not lost. CAL will appear on the digital display.
- Place calibration weight on weighing pan, dashes will be displayed on the output screen. The HK 160 uses an internal 100 gram weight for calibration.
- When the digital display shows a value of 100 g, calibration is complete.

The filters used for this study were GN-6 Gridded 0.45 µm 47 mm filters (Pall Corporation); the water was pumped through the filter using a vacuum pump. Figure 22 displays the experimental set-up for water sampling analysis.

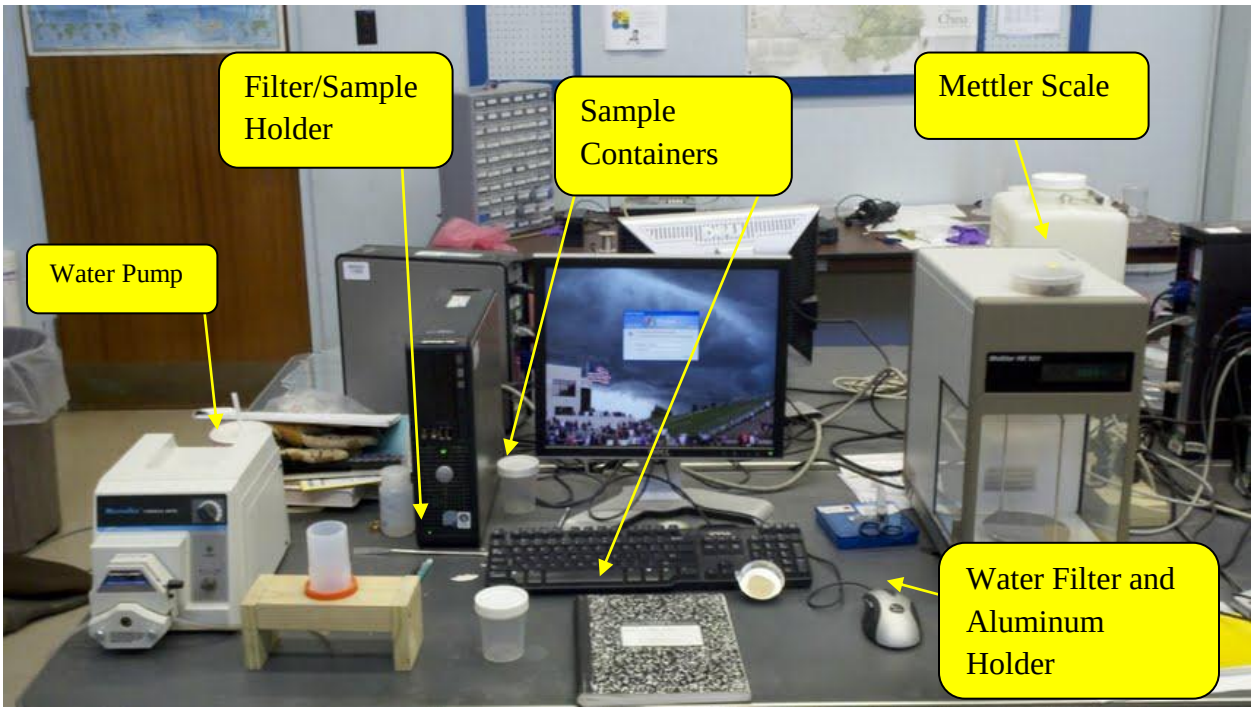

Figure 22. Water sampling analysis set-up

7.2.2 Procedure

Water samples were taken back to the laboratory where they were processed for SSC measurement by filtration. Analysis was typically done within 24 hours after the sample was taken; however samples that were not analyzed in this time frame were place in a refrigerator in accordance with the EPA guidelines for water sample measurement. SSC was calculated based on EPA method 160.2. The procedure used is as follows:

- Weigh the water sample together with its container and lid (M1); then weigh the dry, sterilized filter paper (S1).
- Place the filter paper in a holder and pour water sample in the container on top of the paper and turn on the vacuum pump.
- After filtration is complete remove the filter and place it on the aluminum weighing dish.

- Place this along with the empty water sample container and lid in an oven at 105°C for 24 hours.
- After drying, weigh the container and lid together (M2); then weigh the dried filter paper with sediment (S2).

The following calculations were then performed to find the SSC in mg/L:

$$SSC = \frac{1x10^6(S_2 - S_1)}{M_1 - M_2}$$

where

SSC = suspended sediment concentration in mg/L

S_1 = mass of clean, dry filter paper

S_2 = mass of dried filter paper with sediment

M_1 = mass of water sample with container and lid

M_2 = mass of dried container and lid

The data was then matched up with the sensor signals in the online database recorded at the same time in order to find a correlation between sensor signal and SSC. Sensor signal was then plotted against actual concentration to determine the relationship between the signal and SSC for the IR45, OR45, and OR180 signals used.

8. Results and Discussion

8.1 Calibration Models

In order to use the water sample data most effectively, statistical analysis was ran on the data on a site-by-site basis. This was done under the assumption that each sensor was unique and therefore requires its own unique calibration model. This was because opto-electronic components - LEDs and phototransistors - on each sensor have different characteristics; as a result, each sensor should be calibrated independently. Another reason was that each site has different soil type, water chemistry, and biological factors, causing variation in sensor readings.

Each site had a different amount of samples taken within different ranges of SSC. This was because different regions have different stream types, soil types, watershed management

practices, and storm events. These differences along with the need to travel to each site made calibration for some sites somewhat difficult. Travel to some of the sites is very costly and timing of traveling to these sites can determine whether a high sediment flow period can be observed. Table 3 displays the sites, time periods in which the water samples were taken along with the SSC ranges observed.

Table 3. Water sample data displaying number of grab samples taken at each site, period samples were taken, and range of concentration of water samples

Sensor Location		Number of grab samples taken	Time period the grab samples were taken	Range of sediment concentration (mg/L)
Fort Riley	Little Kitten	29	5/17/2011 – 11/08/2011	7.27 – 815.63
	Wildcat Bridge	20	5/20/2011 – 12/3/2011	2.67 – 4685.12
	Wildcat Creek	2	5/25/2011	106.73 – 116.29
	Silver Creek	2	5/25/2011	105.08 – 190.28
Total		53	5/17/2011 – 12/3/2011	2.67 – 4685.12
Fort Benning	Pine Knot North	14	4/1/2011 – 12/21/2011	1.52 – 27.85
	Pine Knot South	19	4/1/2011 – 12/21/2011	0.74 – 90.17
	Upatoi North	19	4/1/2011 – 12/21/2011	7.22 – 94.98
	Upatoi South	18	7/5/2011 – 12/21/2011	1.53 – 34.28
Total		70	4/1/2011 – 12/21/2011	0.74 – 94.98
APG	Anita Leigh Near	19	4/28/2011 – 12/20/2011	12.62 – 461.37
	Anita Leigh Far	16	4/28/2011 – 12/21/2011	11.2 – 729.1
Total		35	4/28/2011 – 12/21/2011	11.2 – 729.1
Grand Total		183		

The following sections display the calibration models obtained for each site. These models were used in the prediction of SSC. For each sensor, the signals (IR45, OR45, and OR180) were used to predict the SCC and statistical analyses were performed to determine the significance of each signal in predicting SSC. For each signal, the "on-off" value, which was the difference between the signals measured when the LED was turned on and that measured when it was turned off, was used as the predictor in the calibration model, because these values were not greatly affected by the ambient light intensity. Once completed, the three "on-off" signals were

entered into a stepwise regression procedure in which insignificant predictors were eliminated to produce the most effective and simple linear model for prediction of SSC.

Once the linear regression model for each site was determined, a second order polynomial regression model was tested to see if the model could be improved by adding some of the second-order terms. In the program, each signal was tested using a quadratic regression model and was compared to the linear model to determine the significance using the p-value. Once the signals had been tested and the significant models retained, a stepwise regression procedure was run using both linear and non-linear factors to determine the most effective second-order model. In some cases the linear model was more effective and a second-order model was not used. The full statistical analysis for each sensor is display in Appendices A-H, including the models, ANOVA table, PRESS value, R^2 values (real, pred, and adjusted), and unusual observations.

8.1.1 Fort Riley Calibration Models

The Little Kitten and Wildcat Bridge sites were the first sites modeled for sediment prediction. The Wildcat Bridge sensor site had water samples within a much larger range of SSC than any other site.

After running the statistical analysis it was determined that the IR45 and OR180 signals were the most significant for both sites and the best models were found to use both IR45 and OR180 signals as the predictors. Figure 23-Figure 26 shows the regression models using the IR45 and OR180 signals independently.

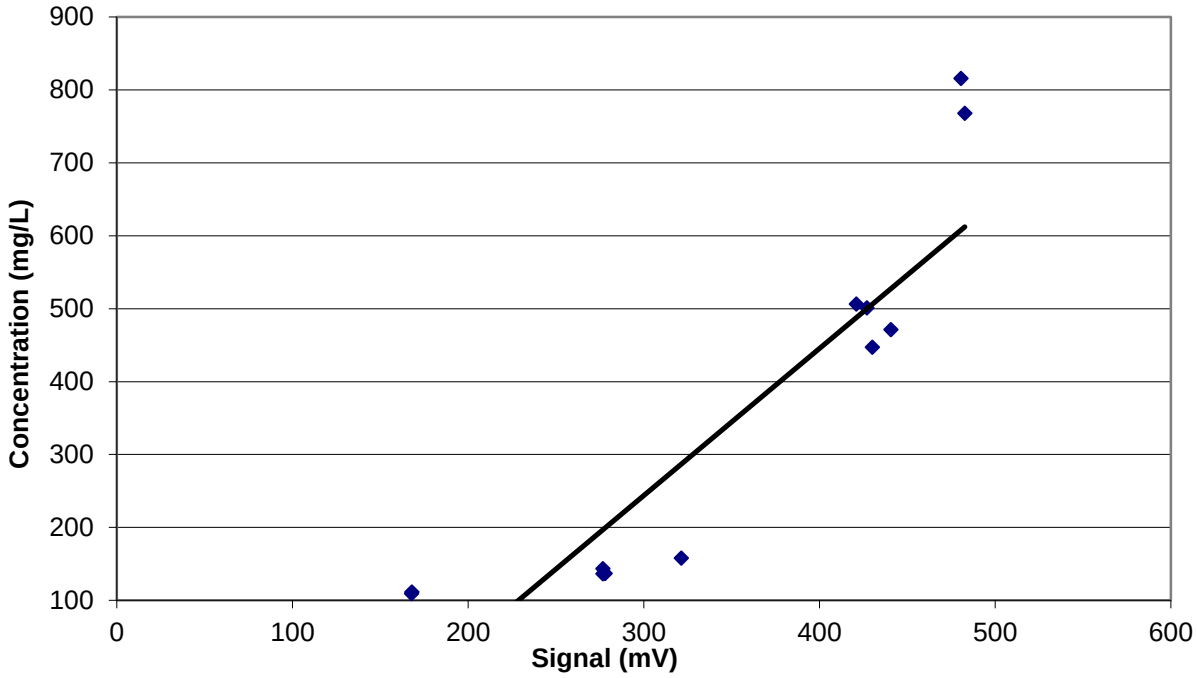

Figure 23. Regression model to predict the suspended sediment concentration using IR45 signal for Little Kitten Creek, Manhattan, KS

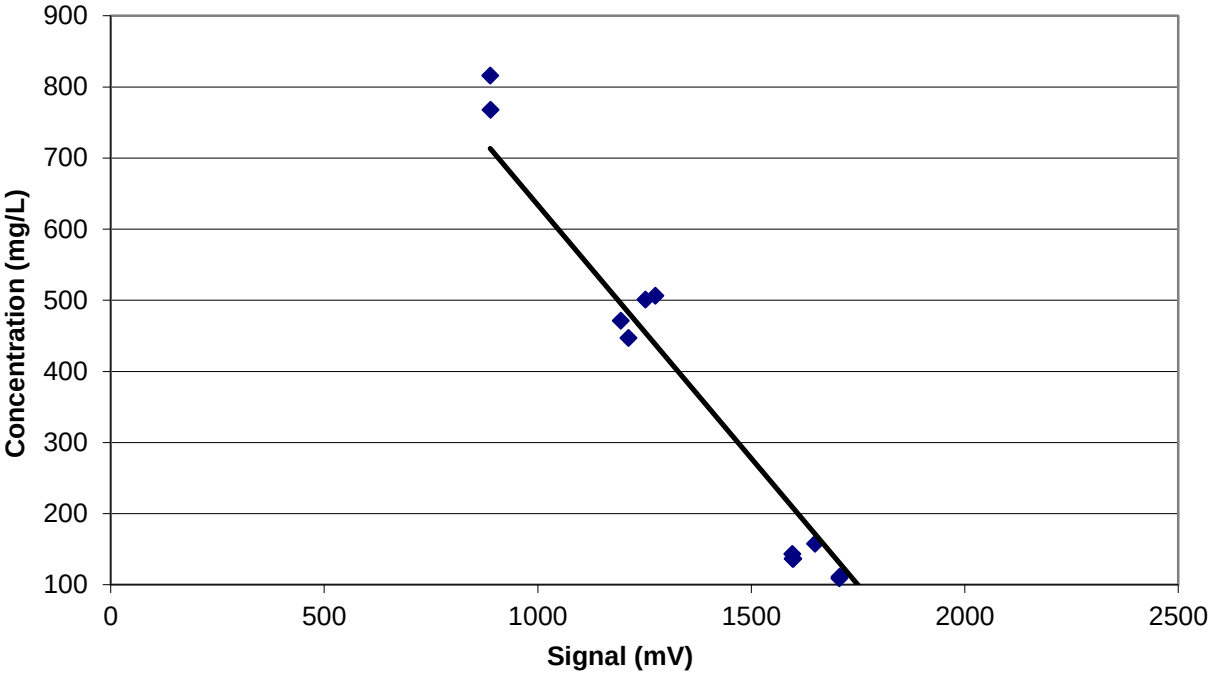

Figure 24. Regression model to predict the suspended sediment concentration using OR180 signal for Little Kitten Creek, Manhattan, KS

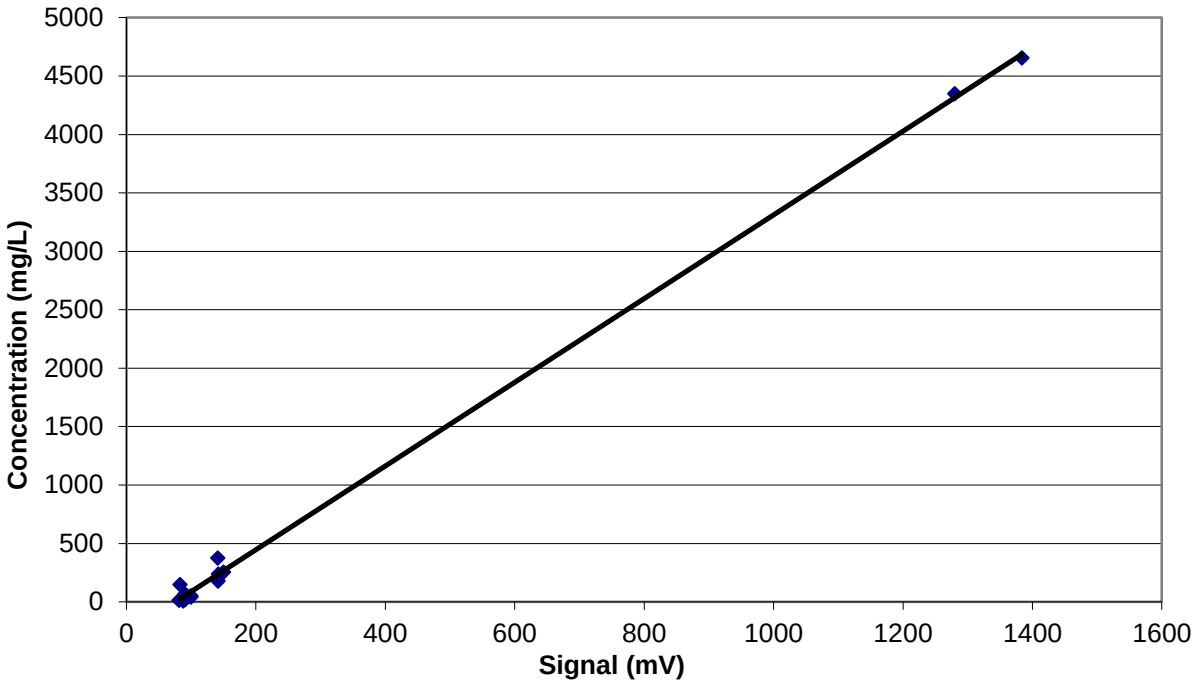

Figure 25. Regression model to predict the suspended sediment concentration using IR45 signal for Wildcat Bridge site location, Wildcat Creek, Ft. Riley, KS

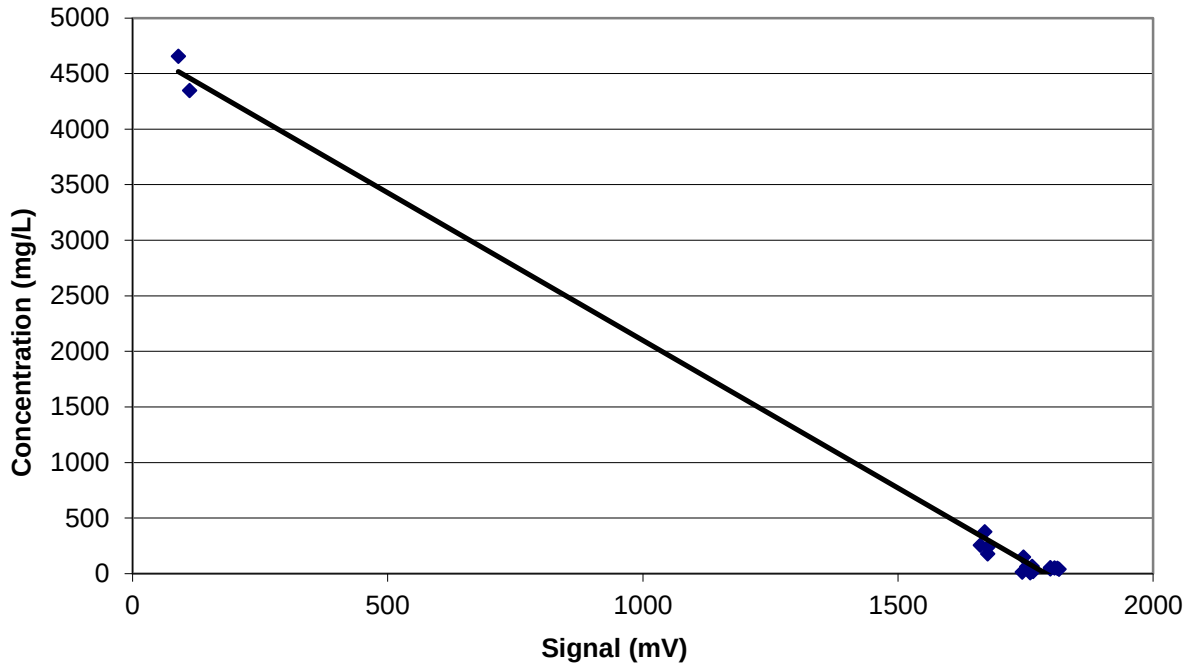

Figure 26. Regression model to predict the suspended sediment concentration using OR180 signal for Wildcat Bridge site location, Wildcat Creek, Ft. Riley, KS

The linear model with both IR45 and OR180 signals determined to be the best fit for the Little Kitten sensor site is:

Concentration (mg/L) = 844 + 0.625*IR45 Value (mV) – 0.509*OR180 Value (mV)

The linear model for sediment prediction for the Wildcat Bridge sensor site is:

Concentration (mg/L) = 984 – 0.664*OR180 signal (mV) + 2.69*IR45 signal (mV)

Figure 27- Figure 28 displays the residual plots created for the combined models for the Little Kitten and Wildcat Bridge sensors, respectively. These plots were generated by the Minitab software (Minitab Inc., 2012). The "normal probability plot" displays the sample data distribution against a theoretical normal distribution and is used to assess whether the sample data is normally distributed. A straight line indicates a good fit to a normal distribution. The next graph ("Versus Fits") plots the regression residuals against the model-fitted values. From this graph, trends of over- or under-prediction of the model within various SSC ranges (low, medium, and high) can be observed. The third graph ("Histogram") displays a histogram of residuals to show how the sample data fit the normal distribution assumption based on which the model was established. The final graph ("Versus order") displays the residuals plotted against time as the data was recorded. From this graph, temporal trend in prediction error of the model can be observed. From Figure 27, it can be seen that the sample data collected at the Little Kitten site was approximately normally distributed and the sampling time did not enter the model as a significant factor.

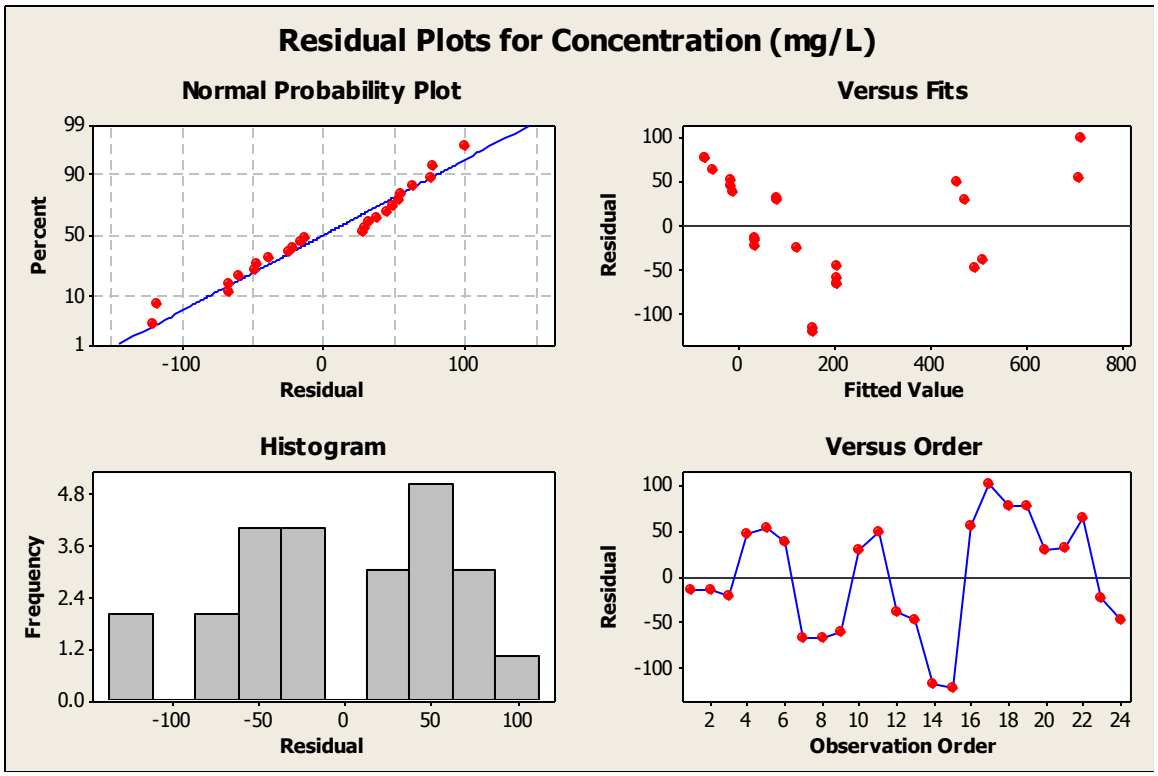

Figure 27. Residual plot of linear model for Little Kitten sensor site (source: Minitab)

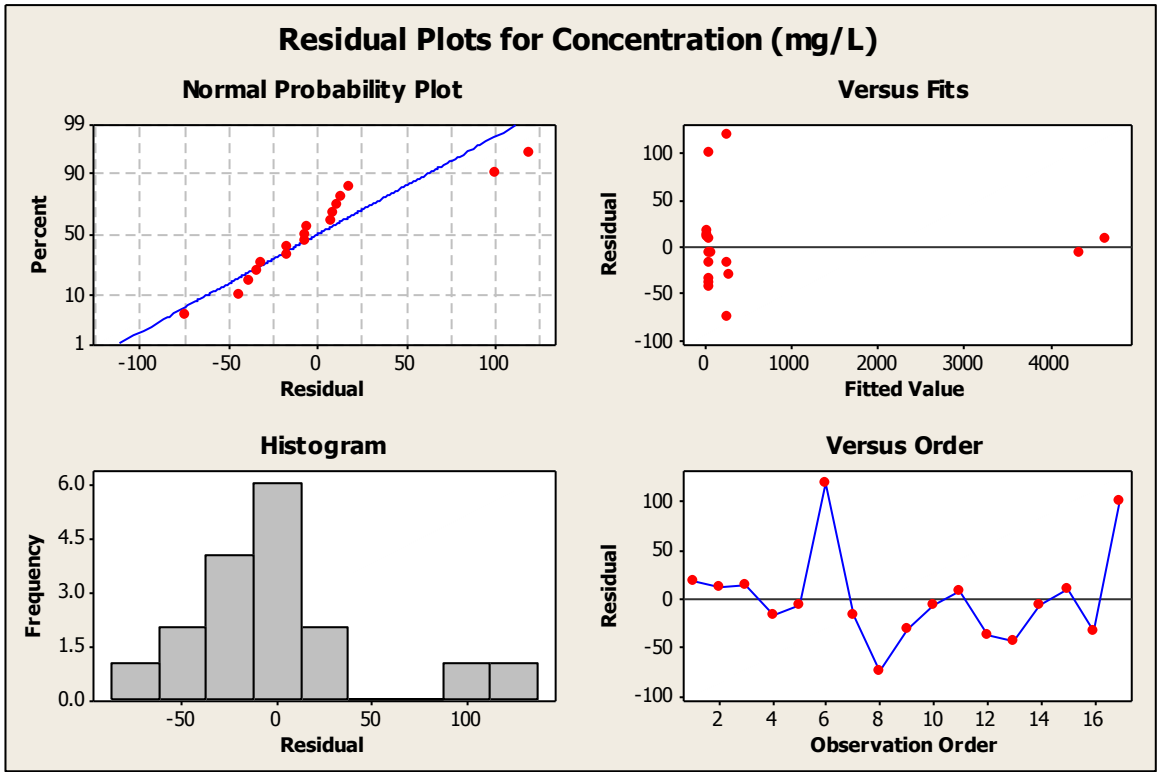

Figure 28. Residual plots of linear model for Wildcat Bridge sensor site (source: Minitab)

The “normal probability plot” follows the normal distribution line meaning that the samples taken are generally normally distributed, which is the ideal scenario in residual analysis. In addition, the “versus fits” graph for Little Kitten shows a parabolic pattern, indicating that a higher order model may provide a more accurate prediction.

The “normal probability plot” and “versus fit” for Wildcat Bridge shows skewness toward the right side of the graphs. This is because that not many data points were gathered during the high sediment flow periods. The “histogram” plot display roughly a normal distribution, with a slight variability in the right side of the graph.

After testing the second order calibration model for Little Kitten using the stepwise procedure it was found that adding a second order term for the IR45 signal improved the model prediction accuracy. However, it was also found that using a higher-order model for Wildcat Bridge did not significantly improve the prediction model. The most accurate model for prediction of SSC for the Little Kitten sensor site is:

Concentration (mg/L) = 702 + 0.00598*(IR45 Value (mV))^2 – 2.36*IR45 Value (mV) – 0.239*OR180 Value (mV)

The model was evaluated using Minitab. Figure 28 shows the result.

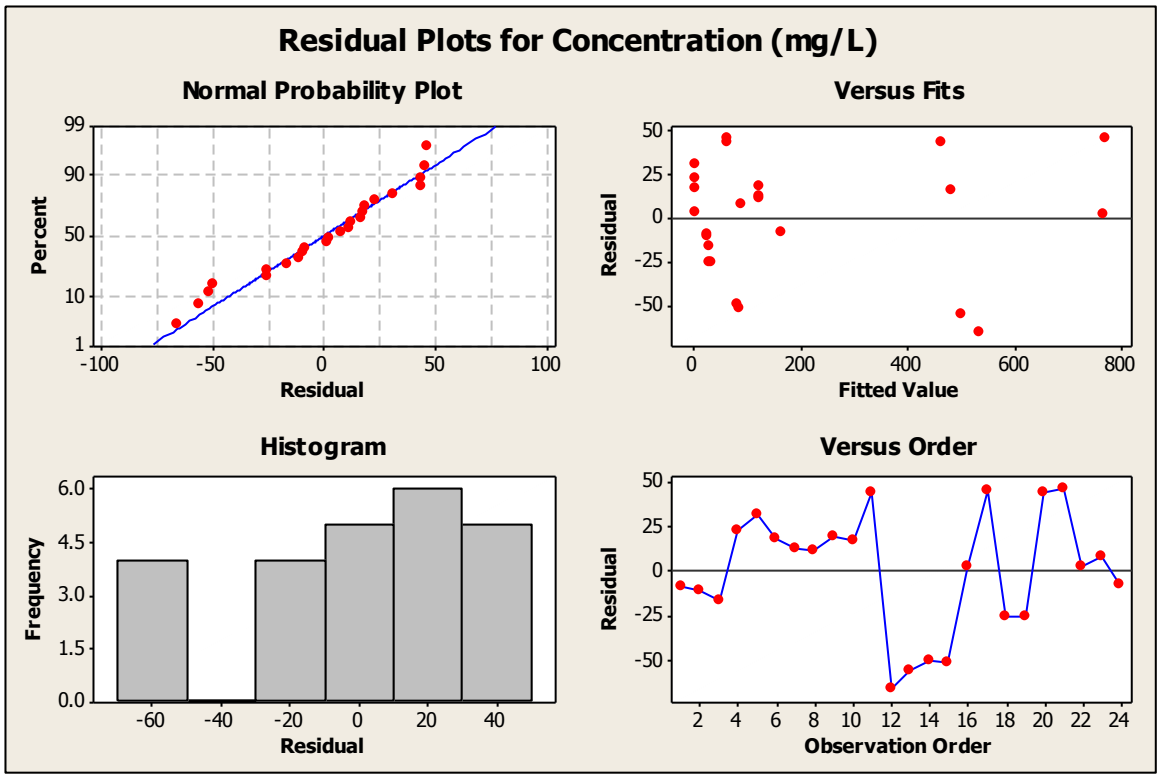

Figure 29. Residual plots of polynomial prediction model for Little Kitten sensor site (source: Minitab)

Statistical analyses showed that this model is an improvement over the linear model when the R^2 and PRESS values are considered. The "PRESS" stands for Predicted Residual Sum of Squares and can be used to evaluate the model. The PRESS value is calculated by leaving out one observation, fitting the rest of the data to a prediction model, and then using this model to predict the "left out" observation and calculate the square of the prediction error. After repeating this process for all observations in the data set, the squares of errors are summed to derive the PRESS. (Quan, 1988). Thus, the PRESS value is good indicator for the prediction power of the prediction model. A lower PRESS value is more desirable and is most useful in comparison between different models, rather than an arbitrary number. Table 4 displays the R^2 and PRESS values for the various models established for the Fort Riley sensors. Figure 30-32 show SSC predicted using these models vs. actual SSC.

Table 4. R^2 and PRESS values for calibration models used at Fort Riley sensor sites

Sensor Site	Model Type	Signal(s)	R^2 Value	PRESS Value
Little Kitten	Linear	IR45	0.854	261767
	Linear	OR180	0.923	129101
	Linear	IR45 and OR180	0.936	124326
	2^{nd} Order	IR45 and OR180	0.982	38615
Wildcat Bridge	Linear	IR45	0.999	59656
	Linear	OR180	0.996	233303
	Linear	IR45 and OR180	0.999	47198

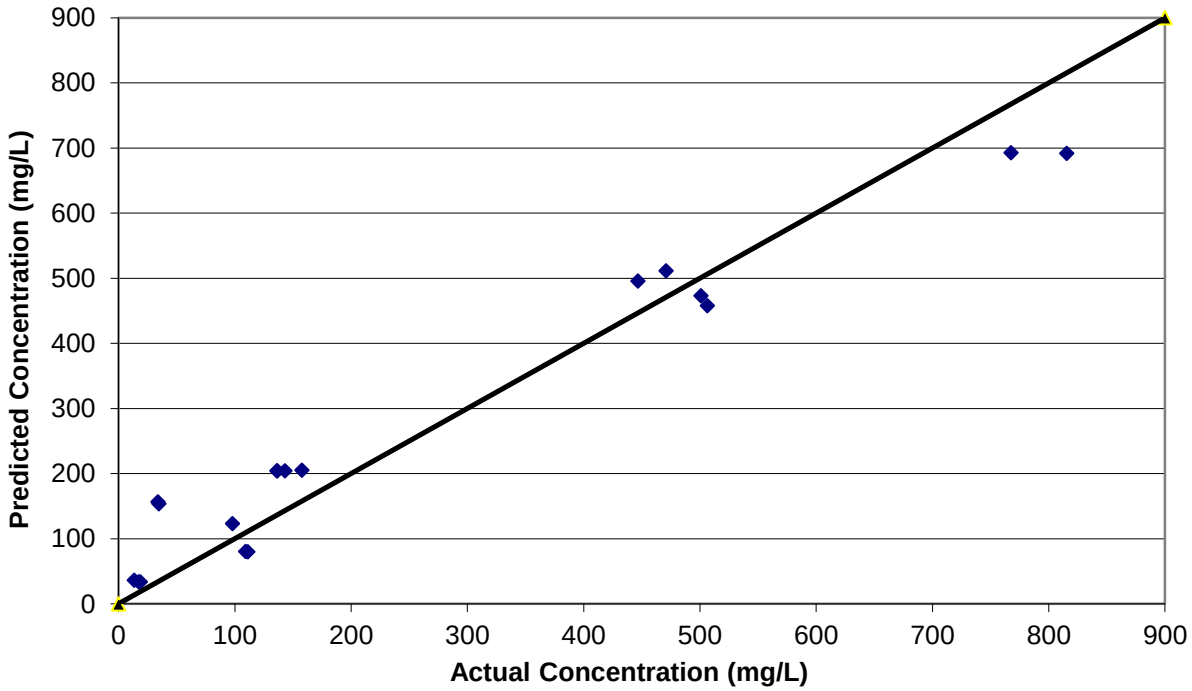

Figure 30. Predicted SSC vs. actual SSC for the Little Kitten sensor using a linear calibration model

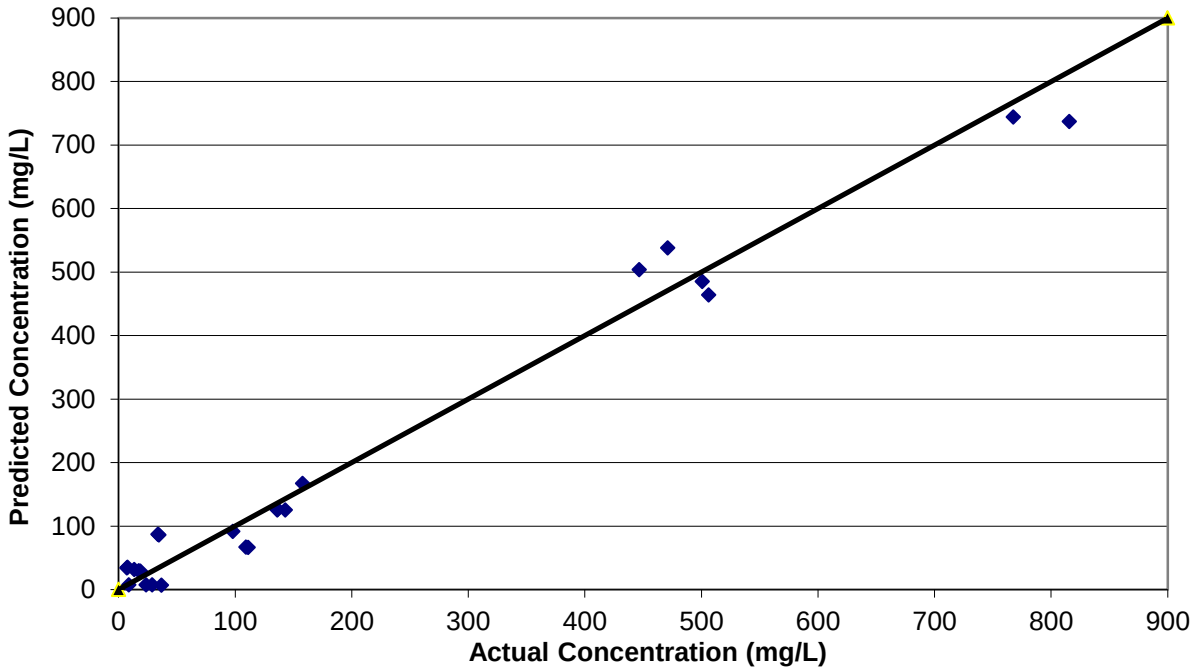

Figure 31. Predicted SSC vs. actual SSC for the Little Kitten sensor using a polynomial calibration model

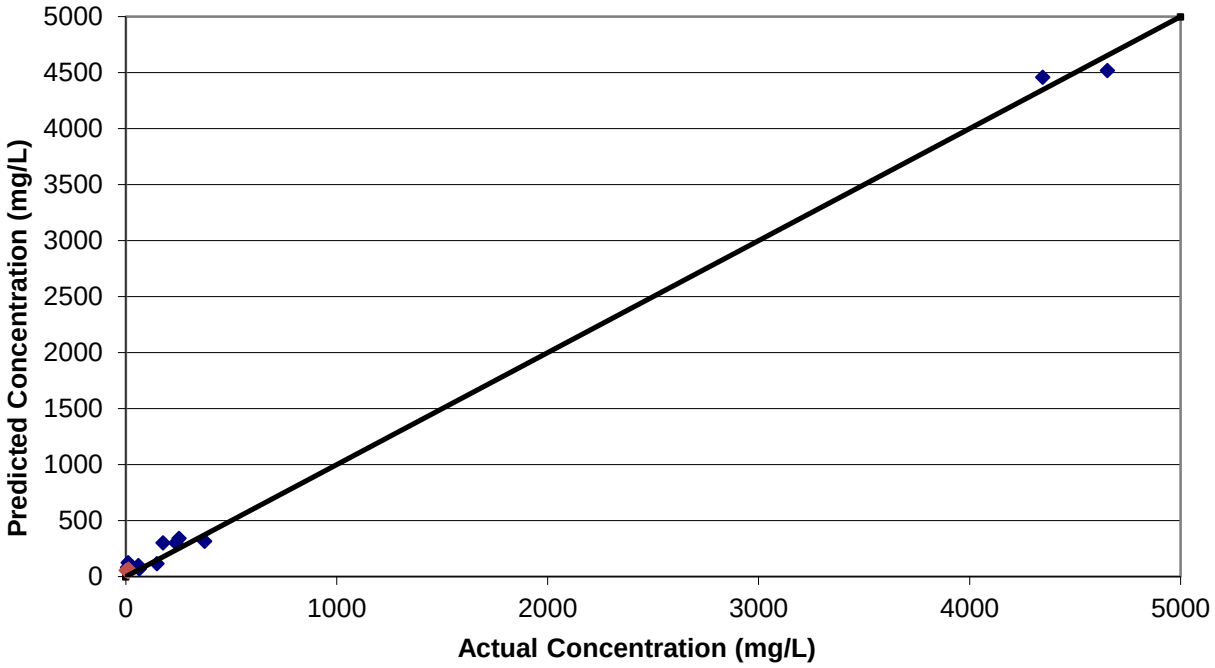

Figure 32. Predicted SSC vs. actual SSC for the Wildcat Bridge sensor using a linear calibration model

8.1.2 Fort Benning Calibration Models

For the Fort Benning sensor sites, prediction models were established for three of the four sensors. For the Upatoi South sensor, a prediction model was not successfully established mainly due to problems with the sensor control board that caused sporadic sensor readings.

After performing statistical analyses on data from the remaining three sensors and running the stepwise regression analysis for both linear and polynomial models, it was determined that a linear model was the most appropriate for all three sensors. It was also determined that, only one of the three signals was the most significant and adding multiple signals to the models did not significantly improve the prediction accuracy. Figure 33Figure 35 display the sample SSC against the signals measured at the sampling times for the three sensors at Fort Benning along with their lines of best fit and R^2 values.

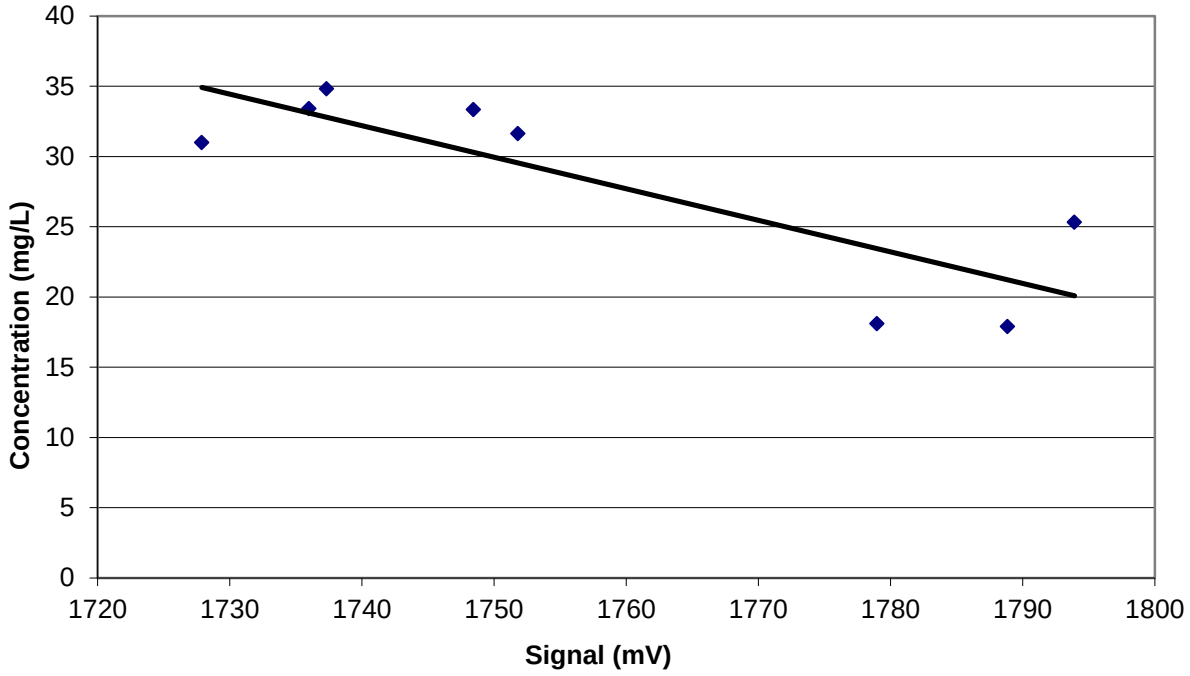

Figure 33. Regression model to predict the suspended sediment concentration using OR180 signal for Upatoi North site, Upatoi Creek, Ft. Benning, GA

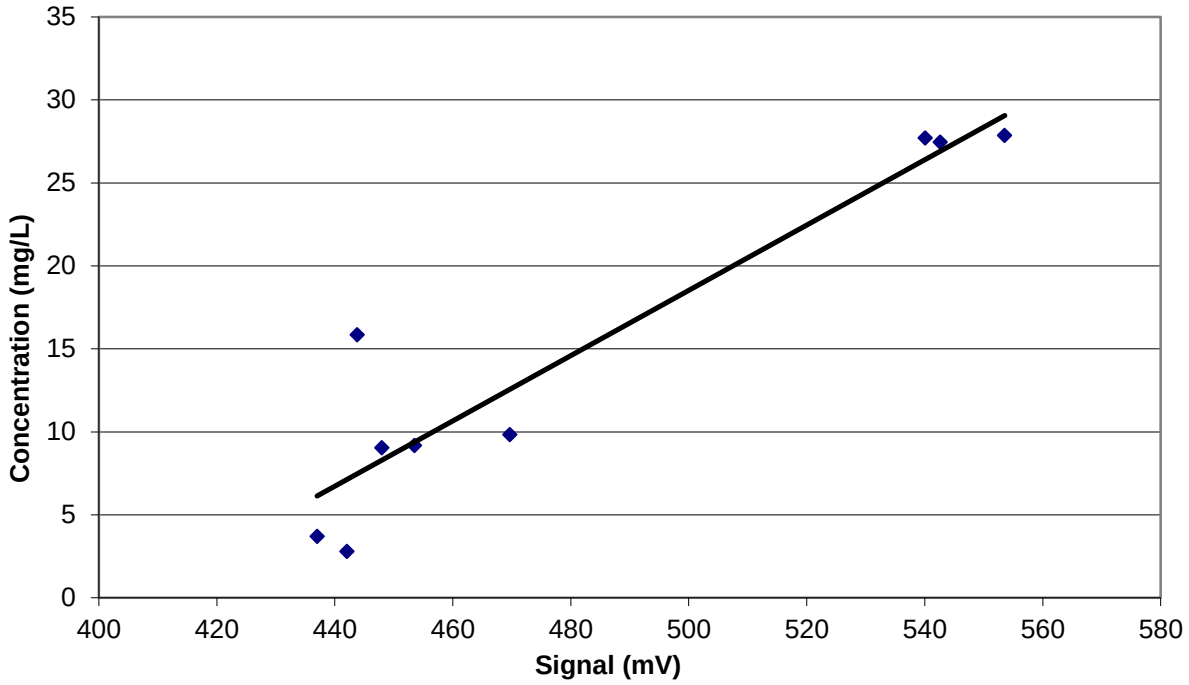

Figure 34. Regression model to predict the suspended sediment concentration using IR45 signal for Pine Knot North site, Pine Knot Creek, Ft. Benning, GA

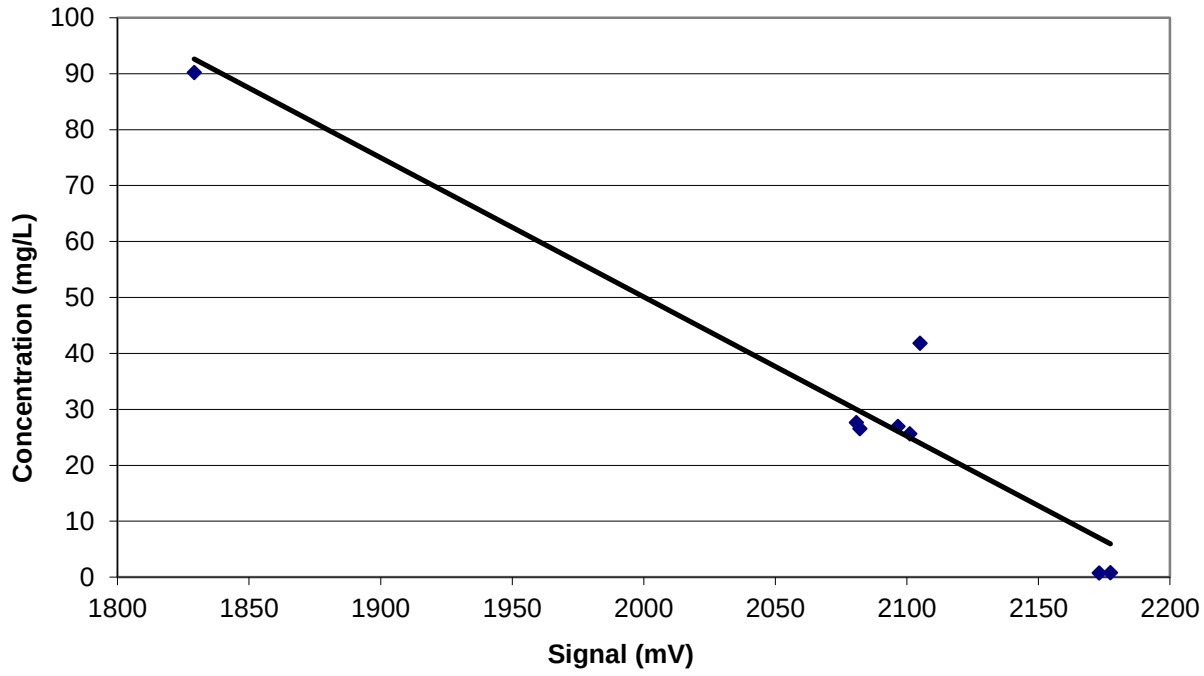

Figure 35. Regression model to predict the suspended sediment concentration using OR180 signal for Pine Knot South site, Pine Knot Creek, Ft. Benning, GA

The linear model determined to be the best fit for the Upatoi North sensor site is:

Concentration (mg/L) = 423 – 0.225*OR180 Signal (mV)

The linear model determined to be the best fit for the Pine Knot North sensor site is:

Concentration (mg/L) = -79.8 + 0.197*IR45 Signal (mV)

The linear model determined to be the best fit for the Pine Knot South sensor site is:

Concentration (mg/L) = 548 – 0.249*OR180 Signal (mV)

R-squared values for these models were in general lower than those for the Fort Riley sensor sites. This was mainly caused by the very narrow SSC range covered by the soil samples. The sandy soil type found in this area caused the SSC to be generally lower than 100 mg/L, which was only 8% of the expected maximum SSC, which was used in the pre-calibration in laboratory

Statistical analysis was run on all three sites and residual plots were developed using Minitab in order to determine how the samples fit the normal distribution and how the prediction models predict SSC within different SSC regions and at different sampling times. The graphs of the residual analysis are displayed in Figure 36Figure 38.

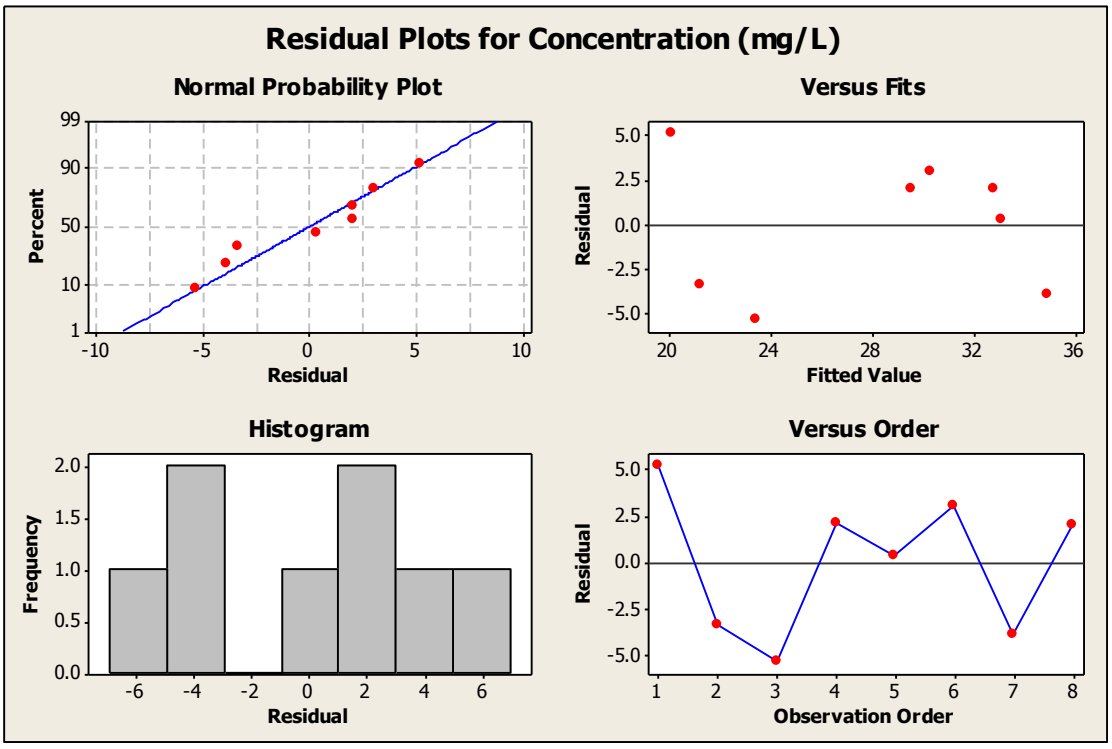

Figure 36. Residual plots of linear prediction model for Upatoi North sensor site (source: Minitab)

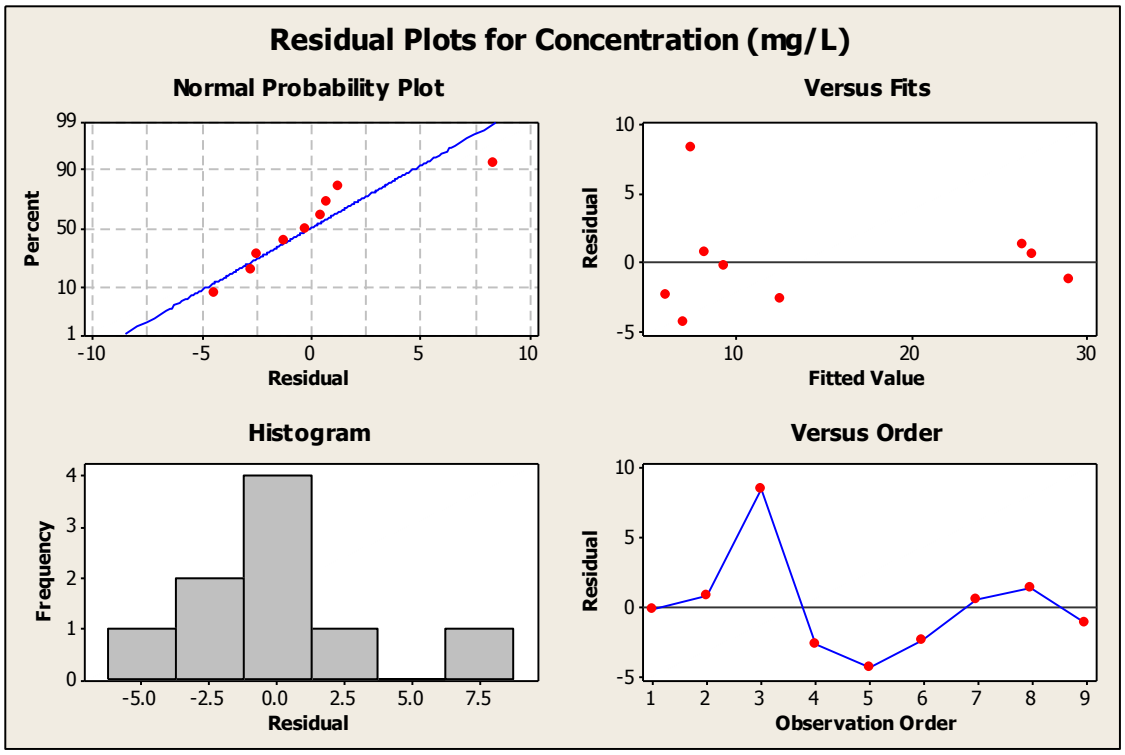

Figure 37. Residual plots of linear prediction model for Pine Knot North sensor site (source: Minitab)

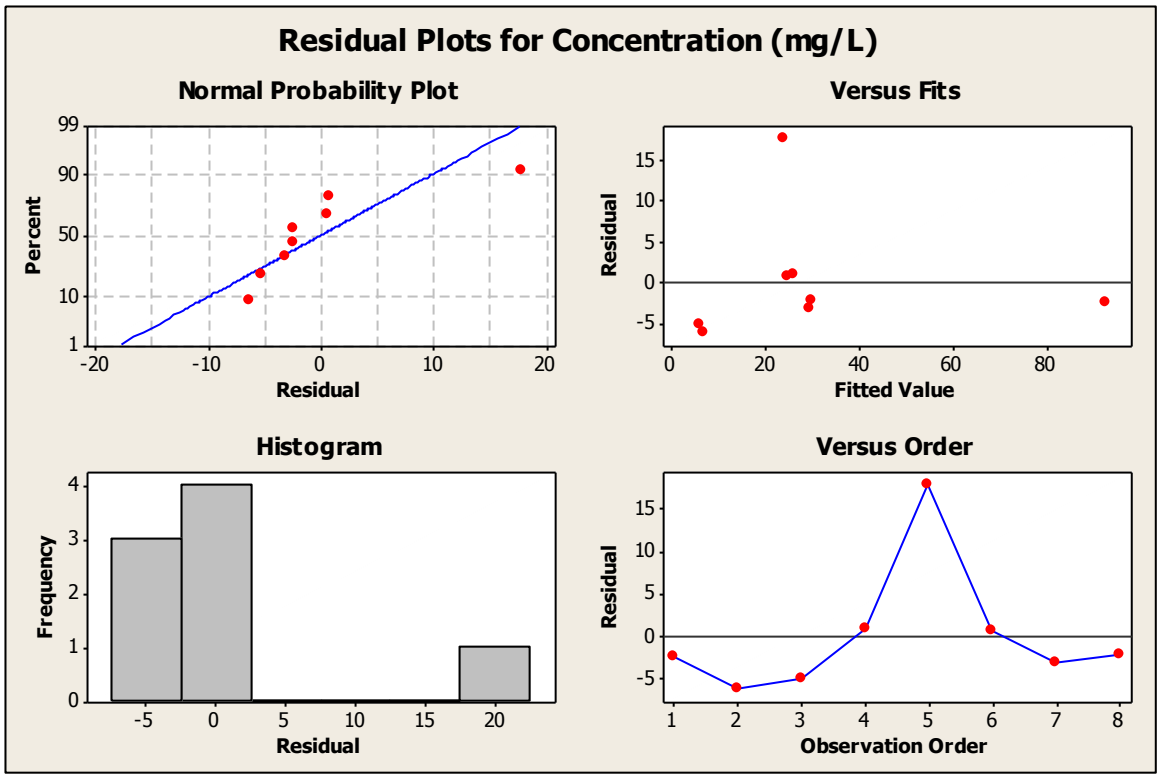

Figure 38. Residual plots of linear prediction model for Pine Knot South sensor site (source: Minitab)

From these graphs, it can be clearly seen that the smaller number of samples and narrower SSC range of the samples greatly affected the accuracy of these models. The normal probability plots for the PKN and PKS sensors show significant deviations from the straight lines. These deviations indicate the model has less normality, which is probably due to the small sample sizes.

The "versus fits" plot for the Pine Knot South sensor showed smaller prediction errors in the high and low ends of the measured SSC range. This trend, however, cannot be confirmed due to the small sample size. The SSC predicted using the regression models for the water samples are plotted against the SSC values measured through the filtering methods in Figure 39Figure 41 for the three sensor sites. The RMSE values for the Upatoi North, Pine Knot North, and Pine Knot South are 4.09, 3.90 and 8.23, respectively.

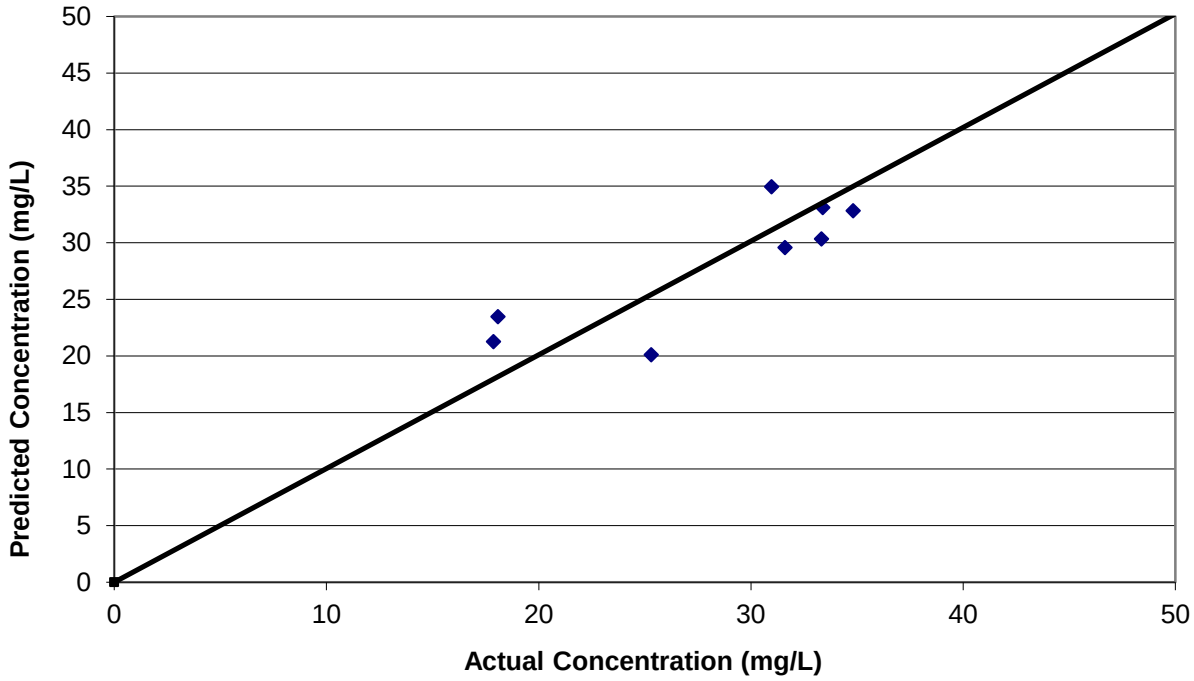

Figure 39. Predicted SSC vs. actual SSC for the Upatoi North sensor site using linear calibration model

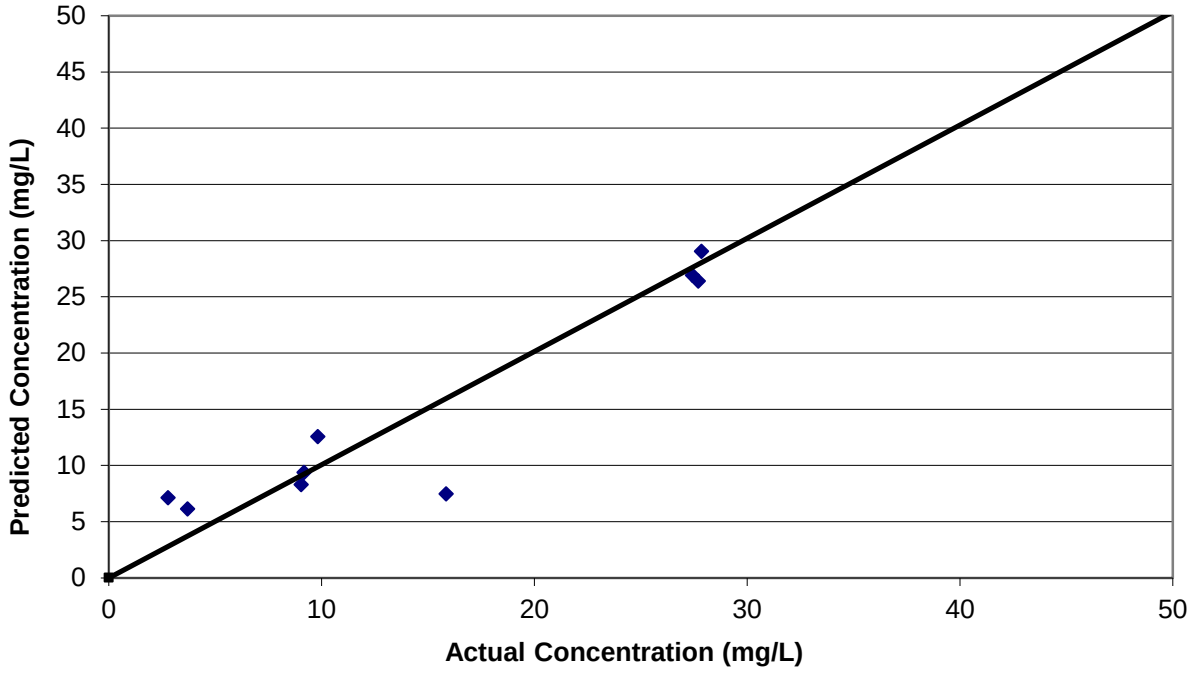

Figure 40. Predicted SSC vs. actual SSC for the Pine Knot North sensor site using linear calibration model

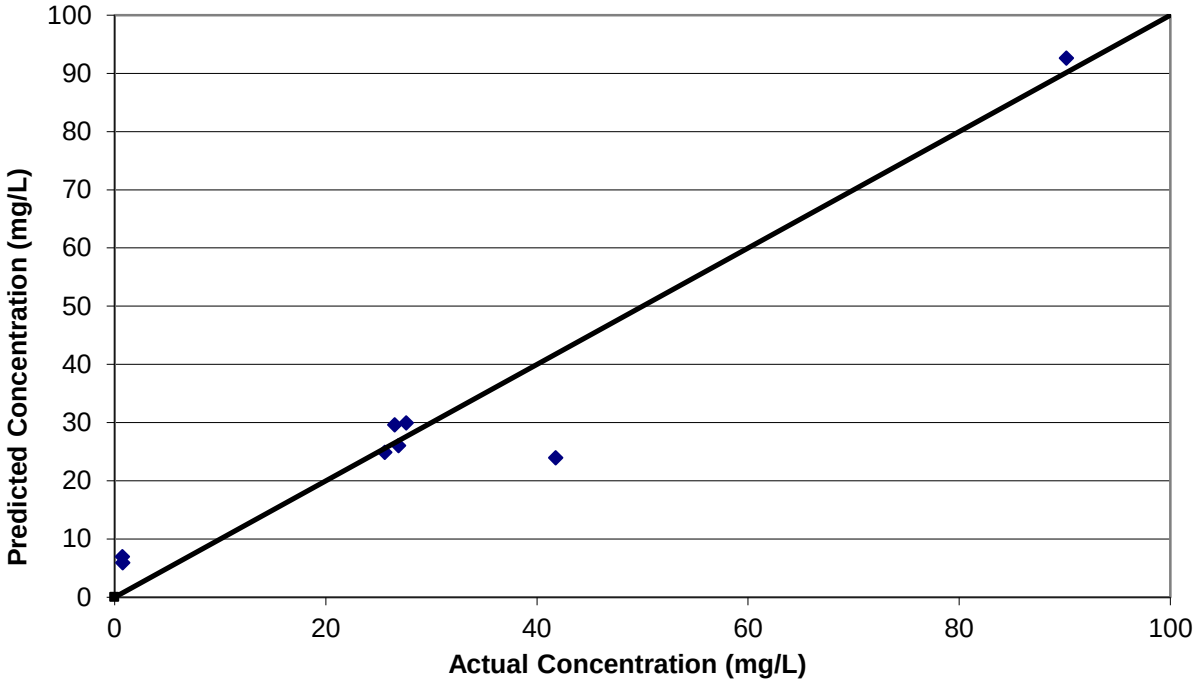

Figure 41. Predicted SSC vs. actual SSC for the Pine Knot South sensor site using linear calibration model

8.1.1 Aberdeen Proving Grounds Calibration Models

Water samples taken from both sensor sites at Anita Leigh Estuary covered a small range of SSC. Calibration models using only a single signal as the predictor had low R2 values (Figures 42 and 43).

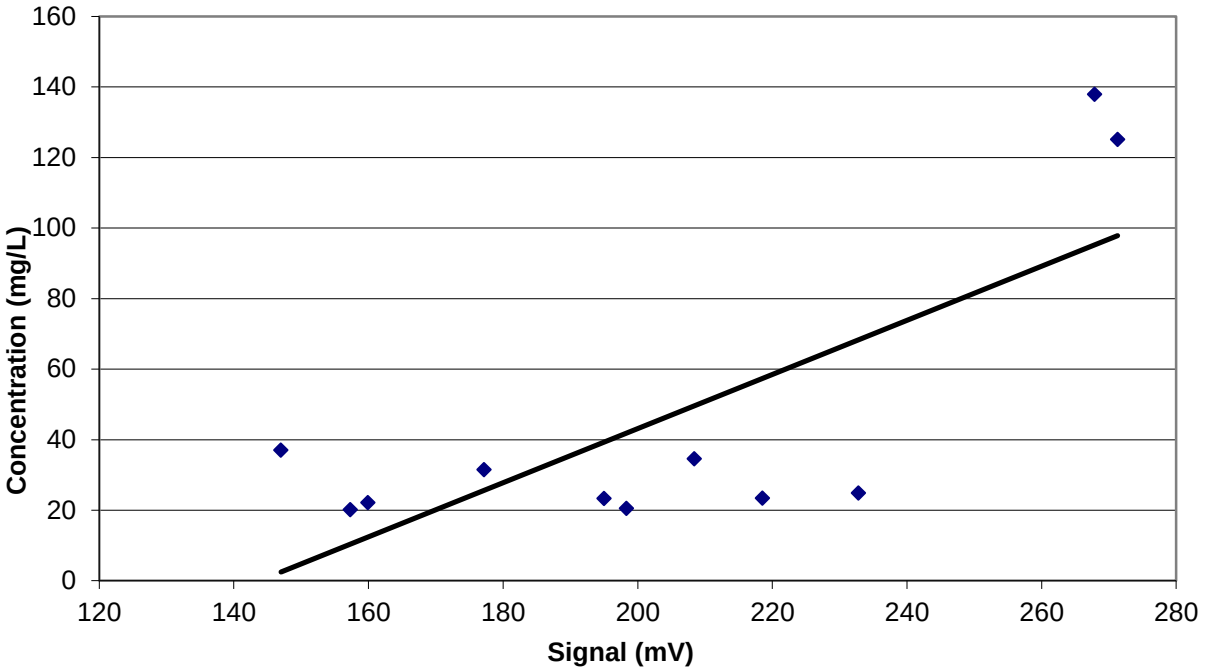

Figure 42. OR45 signal vs. suspended sediment concentration for the Anita Far site, Anita Leigh Estuary, Edgewood, MD

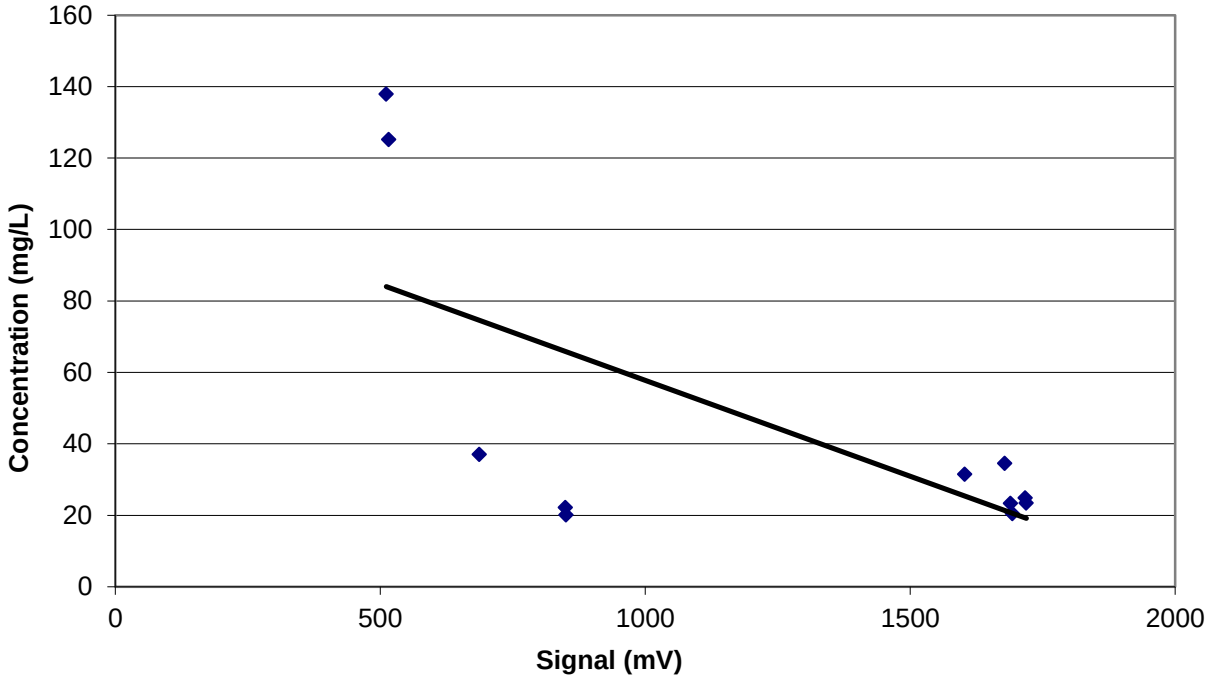

Figure 43. OR180 signal vs. suspended sediment concentration for the Anita Far site, Anita Leigh Estuary, Edgewood, MD

After running the stepwise regression analysis using all three signals, a linear calibration model was derived for each site. The model for the Anita Near sensor used all three signals, while the Anita Far sensor used the OR45 and OR180 signals to predict SSC. The linear model determined to be the best fit for the Anita Near sensor site is:

Concentration (mg/L) = - 116 + 0.0680*IR45 Signal (mV) + 2.12*OR45 Signal (mV) – 0.0610*OR180 Signal (mV)

The linear model determined to be the best fit for the Anita Far sensor site is:

Concentration (mg/L) = - 39.0 + 0.707*OR45 Signal (mV) – 0.0481*OR180 Signal (mV)

These models were analyzed using Minitab, as shown in Figure 44 and Figure 45.

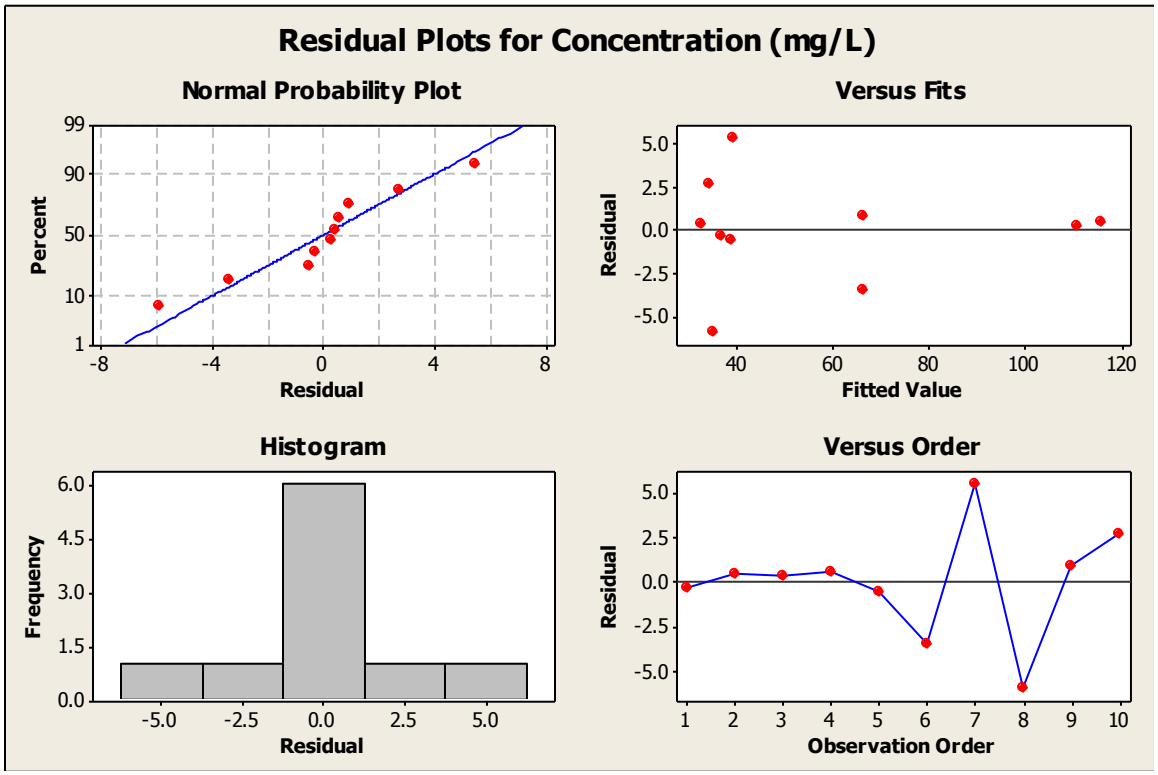

Figure 44. Residual plots of linear prediction model for Anita Near sensor site (source: Minitab)

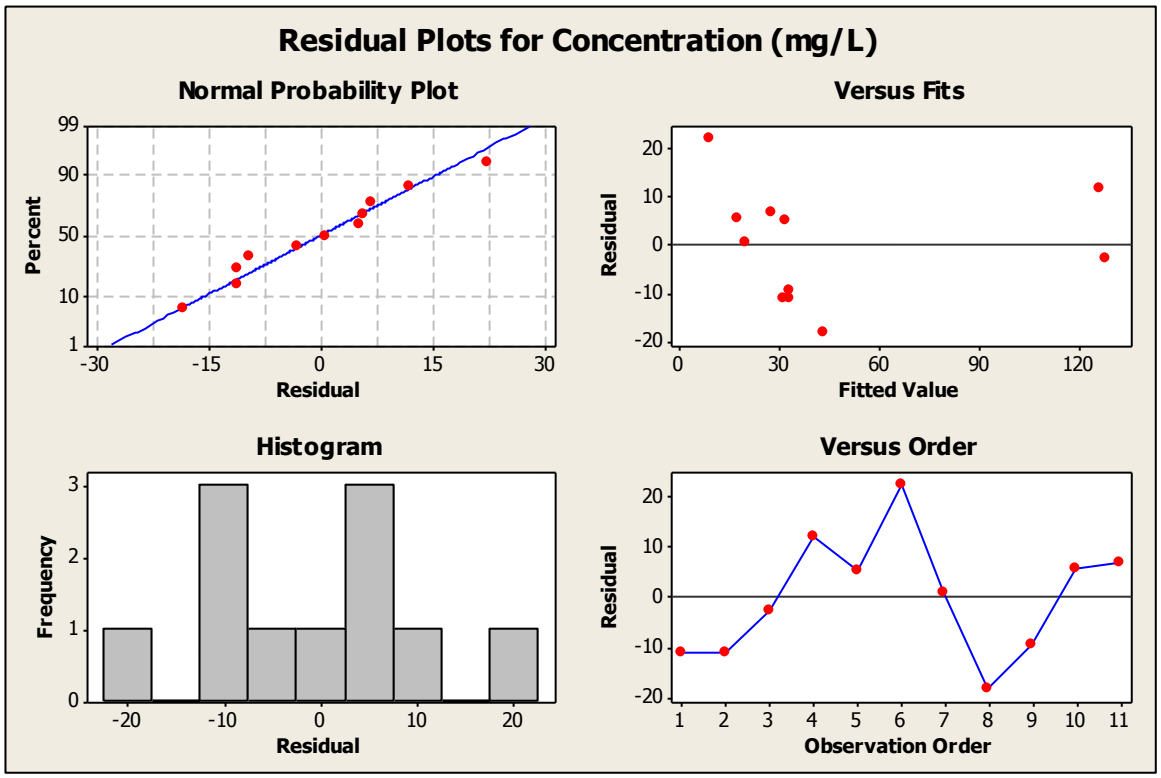

Figure 45. Residual plots of linear prediction model for Anita Far sensor site (source: Minitab)

From the "normal probability plots" in Figures 44 and 45, it can be seen that the sample data taken from both sites generally fit the normal distribution. From the "versus fits" graph, it can be seen that a majority of the water samples had SSC at the lower or higher region. This indicates that another model may be more effective as the samples are not randomly distributed.

The data was then analyzed to determine if a higher-order model was more appropriate for this data set. After adding the second-order terms, a stepwise regression analysis was performed. For both sites, adding second-order terms improved the model. The polynomial model used for the Anita Near sensor site to predict SSC is:

$$\textbf{Concentration (mg/L)} = -153 - 0.00611*(\text{OR45 Signal (mV)})^2 - 0.000058*(\text{OR180 Signal (mV)})^2 + 0.0735*\text{IR45 Signal (mV)} + 3.00*\text{OR45 Signal (mV)}$$

The polynomial model used for the Anita Far sensor site to predict SSC is:

Concentration (mg/L) = 25.6 + 0.00170*(OR45 Signal (mV))^2 – 0.0431*OR180 Signal (mV)

The models were then analyzed using Minitab to show the amount of improvement this model had over the linear model. The residual plots for the polynomial models are displayed in Figure 46 and Figure 47. From the "histogram" residual plot it can be seen that the model for Anita Near exhibits a normal distribution, while the "versus fits" plot shows a random distribution of samples with roughly the same amount of negative and positive residuals.

The "normal probability plot" for the Anita Far site shows that the residuals follow the standard blue line which indicates the model generally follows a normal distribution.

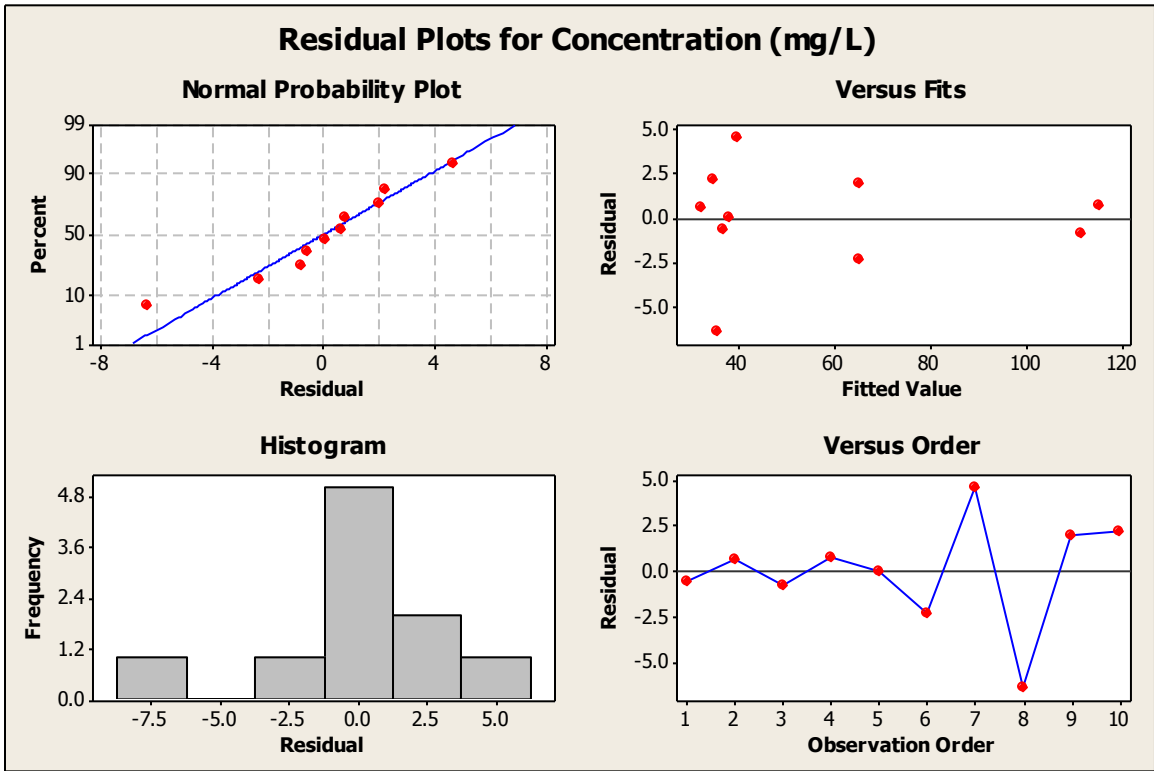

Figure 46. Residual plots of polynomial prediction model for Anita Near sensor site (source: Minitab)

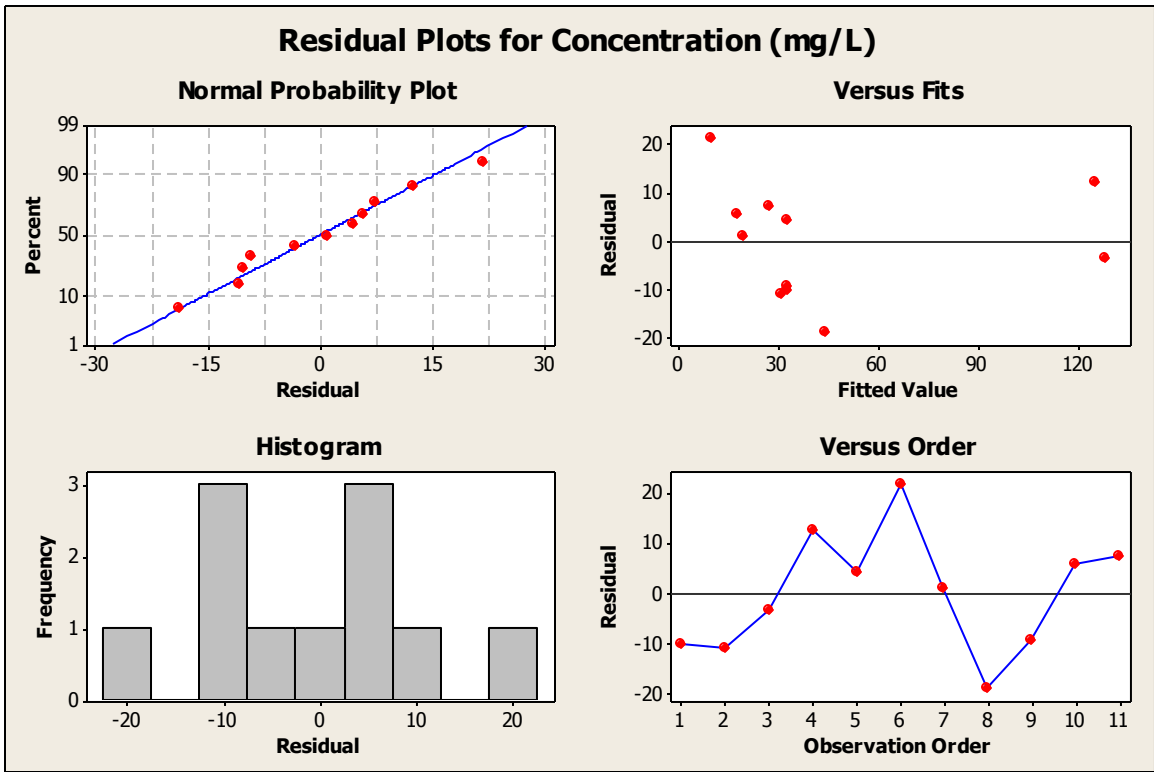

Figure 47. Residual plots of polynomial prediction model for Anita Far sensor site (source: Minitab)

Table 5 displays the R^2 and PRESS values for the calibration models at Aberdeen sites. From this table it can be observed that the R^2 and PRESS values for the linear and polynomial models are very similar, suggesting that adding the second-order terms did not significantly improve the model in predicting SSC.

Table 5. R2 and PRESS values for calibration models used at Aberdeen sensor sites

Sensor Site	Model Type	Signal(s)	R^2 Value	PRESS Value
Anita Near	Linear	IR45, OR45, & OR180	0.991	219.8
	2^{nd} Order	IR45, OR45, & OR180	0.991	494.7
Anita Far	Linear	OR45 and OR180	0.923	2632
	2^{nd} Order	OR45 and OR180	0.924	2614

The SSC predicted using these models are compared with the SSC measured using the filtering-weighing methods for the grab samples. The results of this comparison are displayed in Figures 48-51.

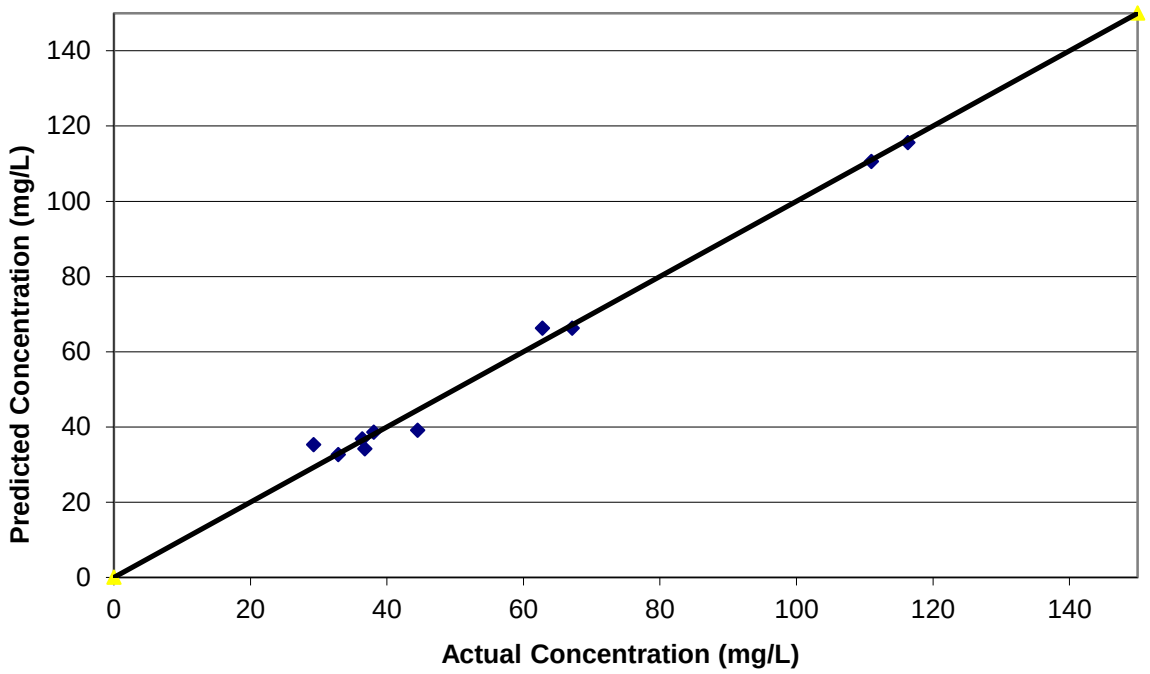

Figure 48. Predicted SSC vs. actual SSC for the Anita Near sensor site using linear calibration model

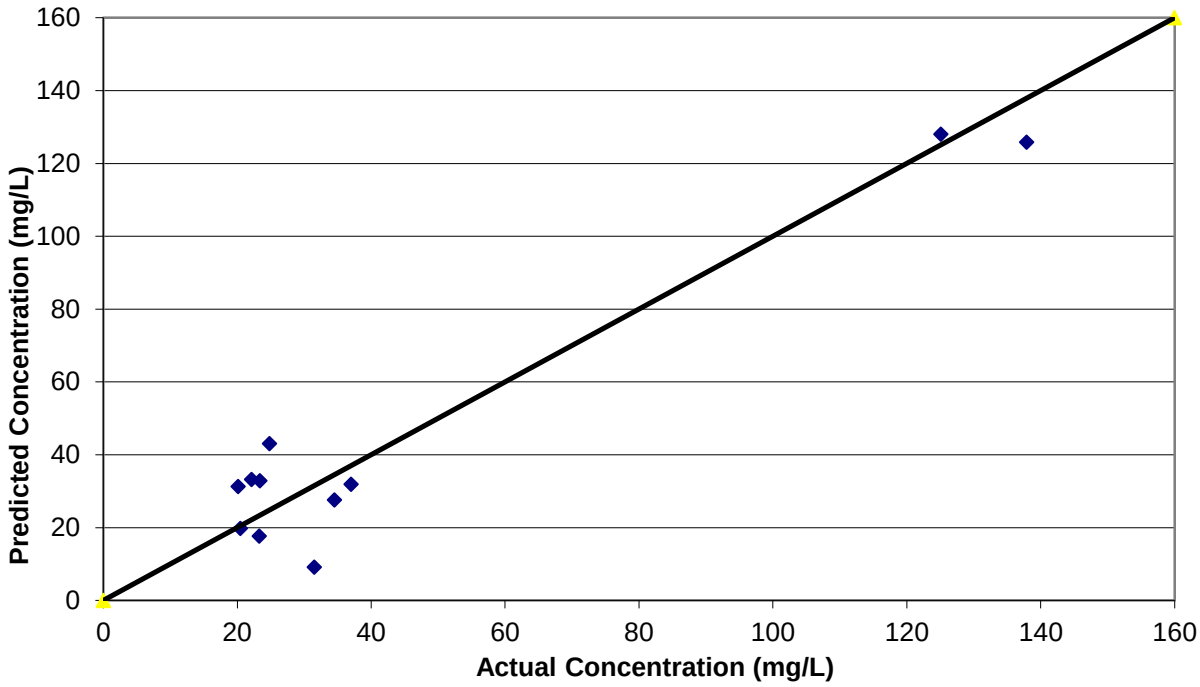

Figure 49. Predicted SSC vs. actual SSC for the Anita Far sensor site using linear calibration model

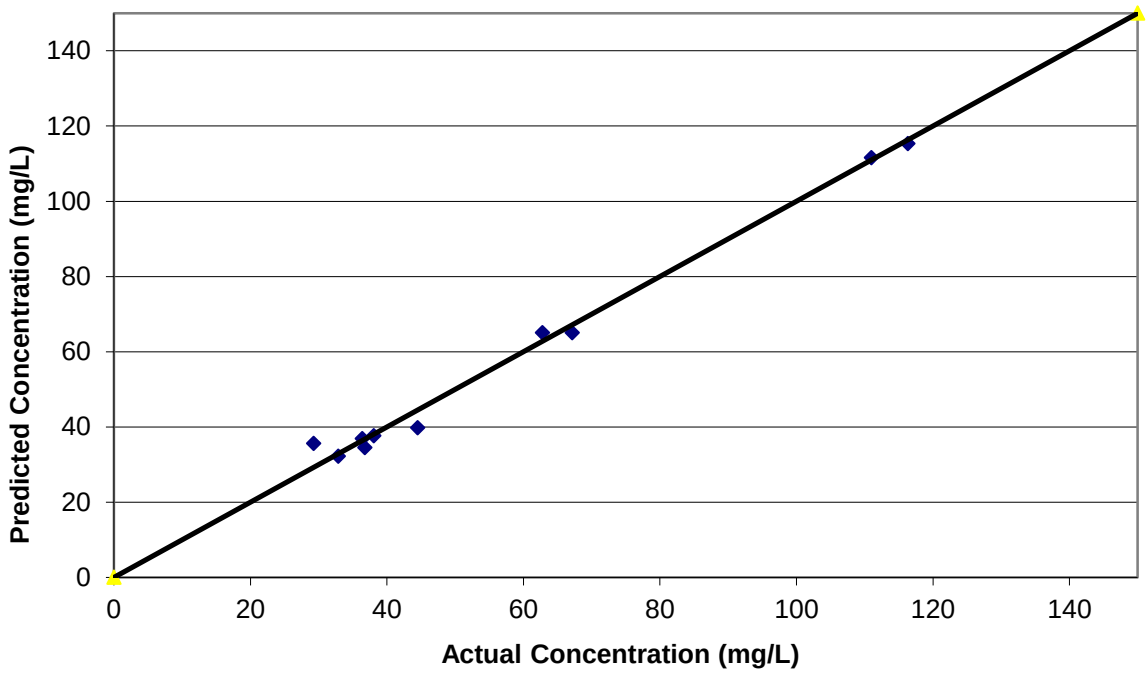

Figure 50. Predicted SSC vs. SSC for the Anita Near sensor site using polynomial calibration model

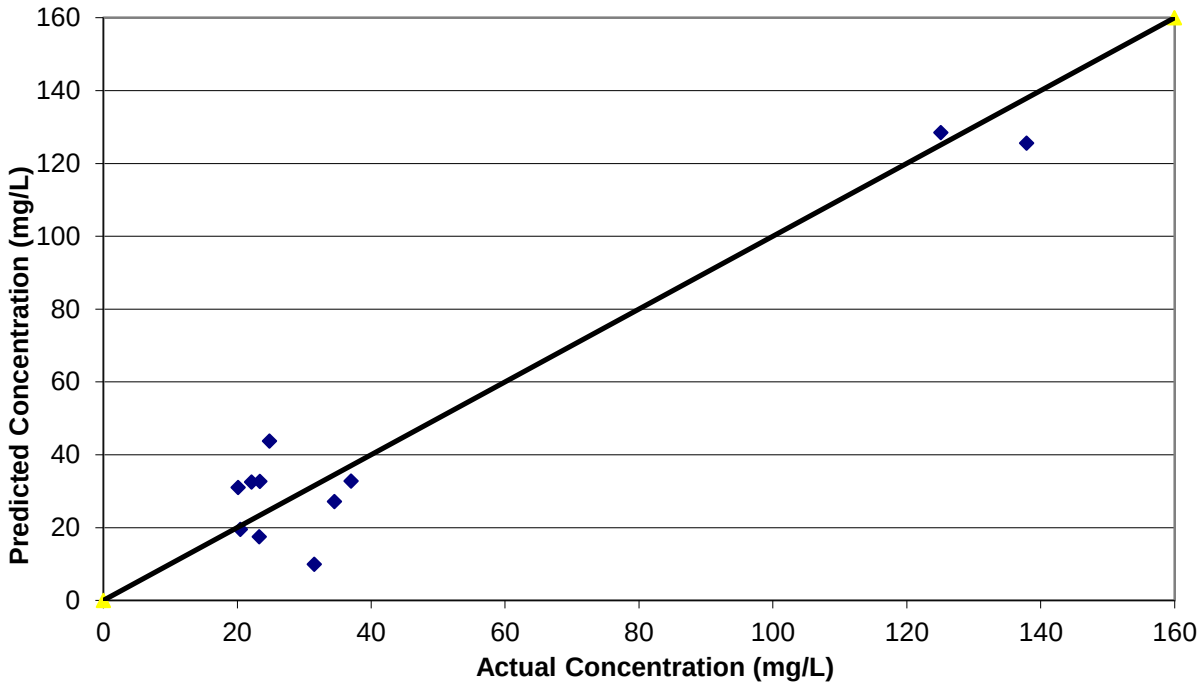

Figure 51. Predicted SSC vs. SSC for the Anita Far sensor site using polynomial calibration model

8.2 Model Validation

After the calibration models were developed, the models were validated. Validation analysis was only performed on the models for the Fort Riley sensor sites; this is because the number of samples taken at the other military installations was not sufficient to perform a meaningful analysis.

The validation process began with randomly selecting half of the water samples taken at a site using Minitab. The samples selected were classified as "calibration" data set while the remaining unselected data points were classified as "validation" data set. The calibration data set was entered into Minitab to establish a calibration model through regression. The validation data set was then entered into the calibration model to see how it fits in the calibration model. RMSE values were calculated for both calibration and validation data sets. Figure 52-54 show predicted SSC of both the calibration and validation data sets against the actual SSC.

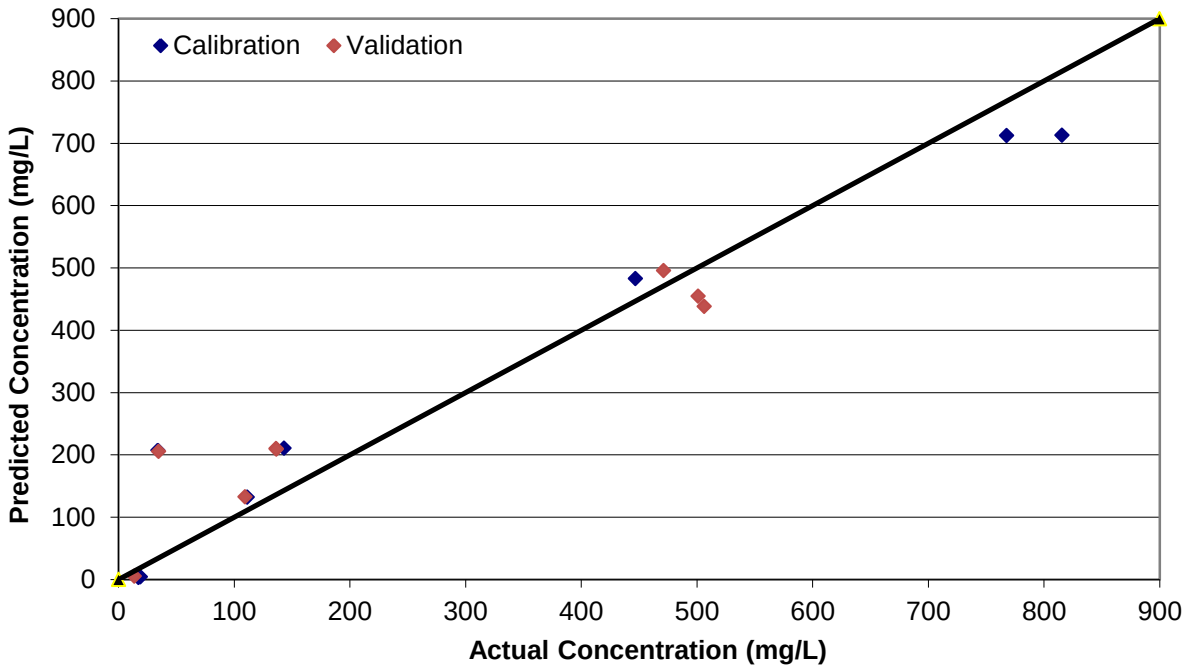

Figure 52. Predicted SSC vs. actual SSC of the calibration and validation data sets for the Little Kitten sensor site using linear calibration model

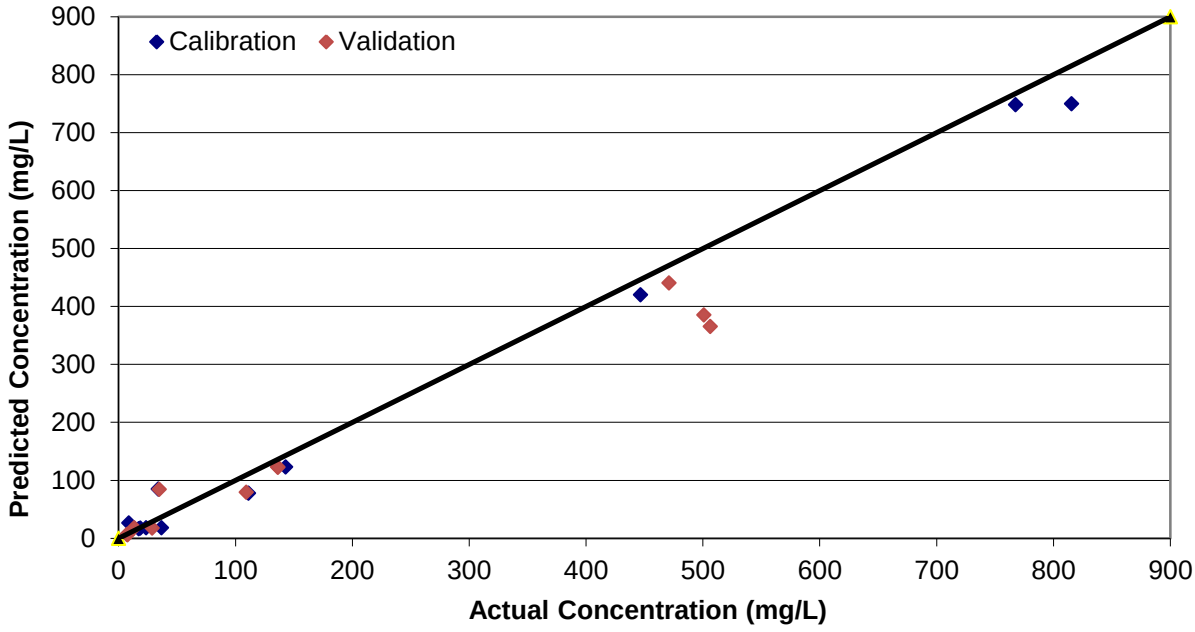

Figure 53. Predicted SSC vs. actual SSC of the calibration and validation data sets for the Little Kitten sensor site using polynomial calibration model

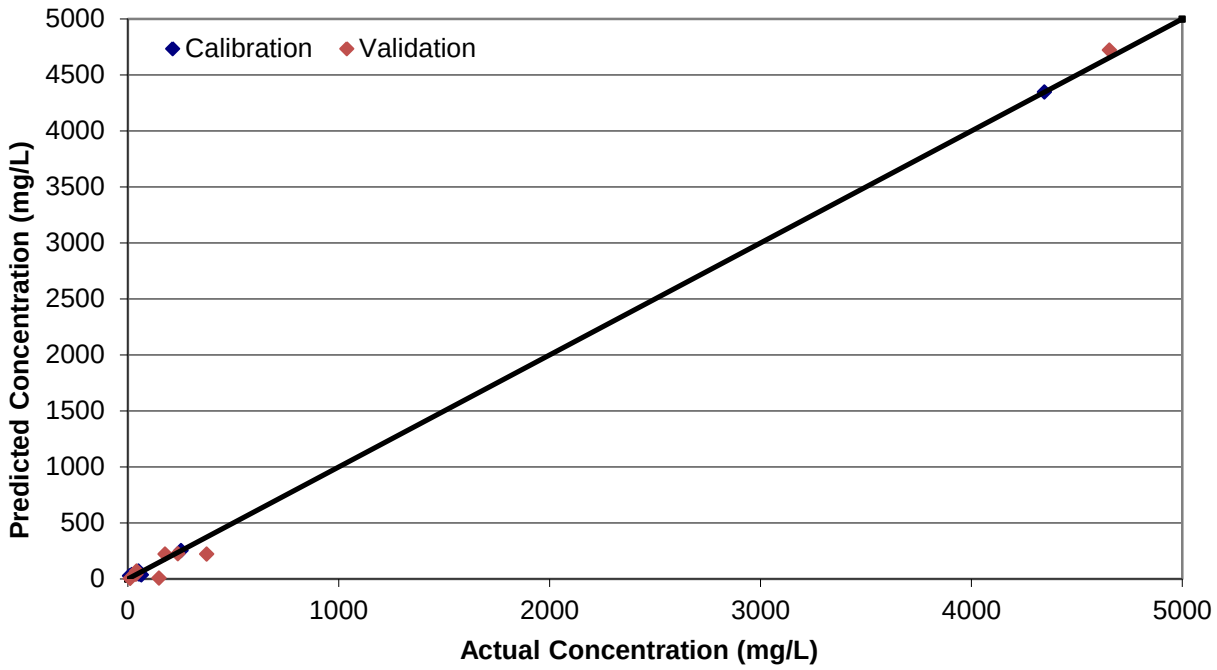

Figure 54. Predicted SSC vs. actual SSC of the calibration and validation data sets for the Wildcat Bridge sensor site using linear calibration model

Root-mean-square errors (RMSE) for both the calibration and validation data sets were calculated. It can be observed from Table 4 that a second-order polynomial model reduced the RMSE error.

Table 6. RMSE (mg/L) for the calibration and validation datasets based on the calibration model

RMSE Values	Calibration	Validation
Little Kitten (Linear Model)	78.32	74.45
Little Kitten (Second-order polynomial model)	33.19	61.91
Wildcat Bridge (Linear Model)	18.45	92.13

9. **Data Analysis**

9.1 SSC Sensor Data

SSC sensor signals were recorded for each sensor every 30 seconds from the time the sensor was installed. The data was wirelessly transmitted to an online database where the data could be observed and analyzed. The data can also be plotted to observe the changes in sensor signals over time. Precipitation data can be plotted with the signal to observe the effect of rain events on the signals. The times when the sensor was cleaned were also recorded and can be displayed in the same plot. Figure 55-56 display the unprocessed IR45 and OR180 signals from the Little Kitten Creek sensor, within a half-year period, from May 1 – October 31, 2011. Figures 57-76 display signals measured at other sensor sites.

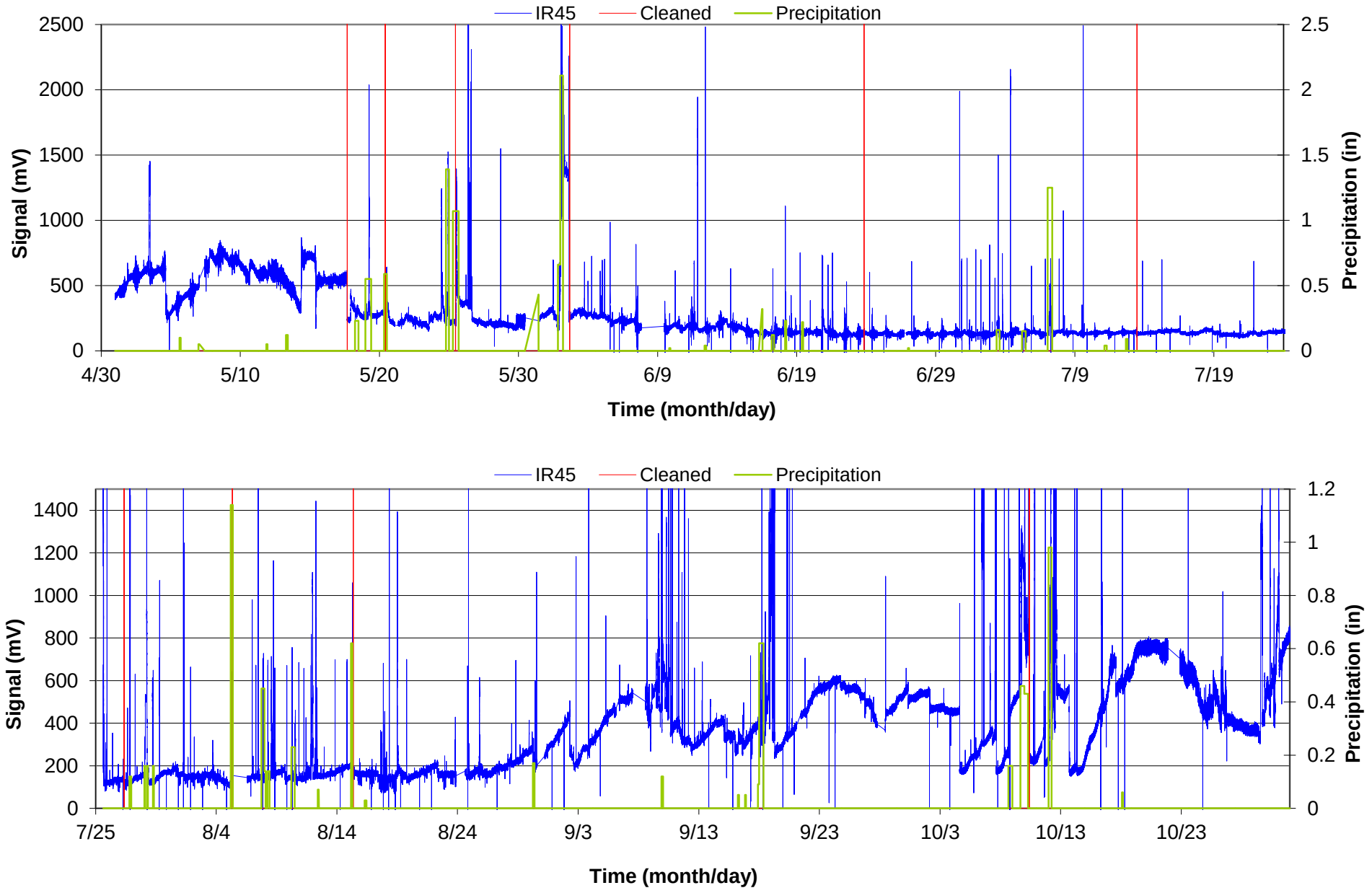

Figure 55. Unprocessed IR45 signals measured from May 1 – October 31, 2011 for Little Kitten Creek, Manhattan, KS. Precipitation data source: www.wunderground.com

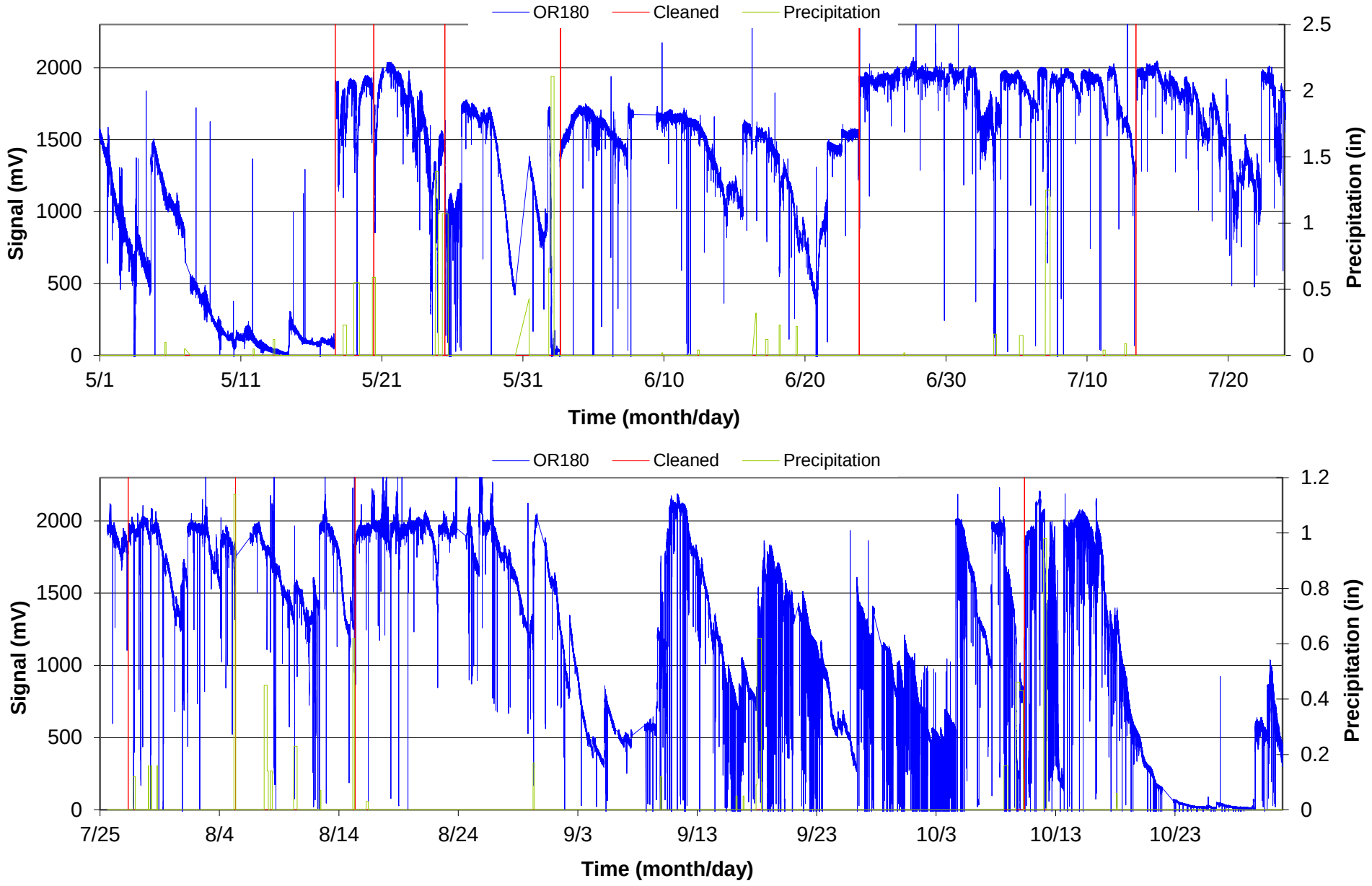

Figure 56. Unprocessed OR180 signals measured from May 1 – October 31, 2011 for Little Kitten Creek, Manhattan, KS. Precipitation data source: www.wunderground.com.

Occasional data loss is reflected in the figures as straight lines connecting sections of signals. This loss was mainly due to packet loss of the wireless transmission between motes on the PCB board and the gateway station. Within the half year period, the total time for data loss occurring for the Little Kitten Creek sensor was found to be 4 days, 19 hours and 53 minutes, resulting in a data-loss rate of 2.62%.

Air blasts cleaning was performed on these sensors twice an hour, but were sometimes sporadic in their functionality as time passed; this was the reason for some of the spikes and sudden changes in the sensor signals.

The effect of rain events on sensor signals can be clearly seen in these figures. A rain event can cause runoff which significantly increases the SSC in the streams. Usually, a rise in SSC causes an increase in the back scattered signal (IR45) and a decrease in the transmitted signal (ORA180). These trends can be clearly observed in Figures 58 and 59.

From August 15th to October 10th, 2011, the sensor was deliberately not cleaned to observe the effect of fouling on the sensor reading over time. During this period of time, the IR45 signal gradually increased and the OR180 signal decreased. After a month of non-cleaning the OR180 signal became much more sporadic from the fouling and the trend of the signal became harder to recognize. Part of the reason for this is that Little Kitten Creek is a very small stream and area of the cross section where the sensor was installed is very narrow so that nearly all of the water in the stream passes under the sensor. During the fall season, leaves from trees would get caught on the sensor and the cover, clogging the optical components and causing spikes in the readings. The clogging effect can be seen throughout the fall season from August through the end of October. The effects of clogging and fouling on the signals are different. Usually, clogging causes sporadic changes in the signals, while fouling causes steady signal changes over time.

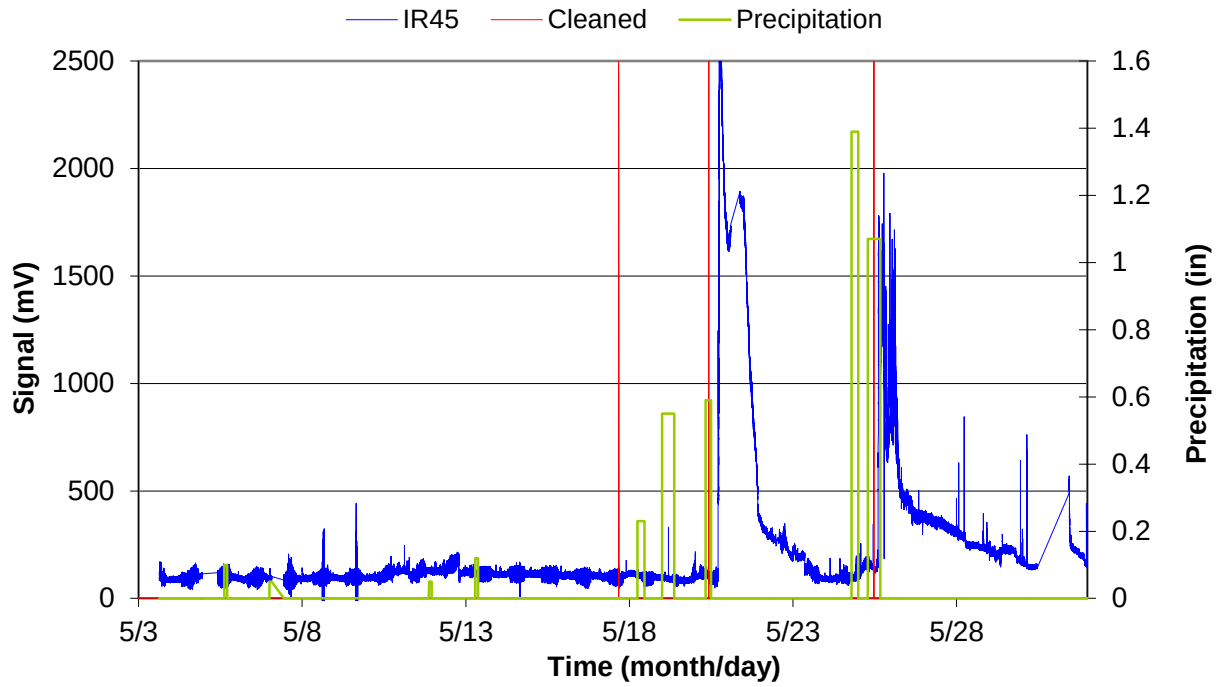

Figure 57. Unprocessed IR45 signals measured in May, 2011 for Wildcat Bridge, Manhattan, KS. Precipitation data source: www.wunderground.com.

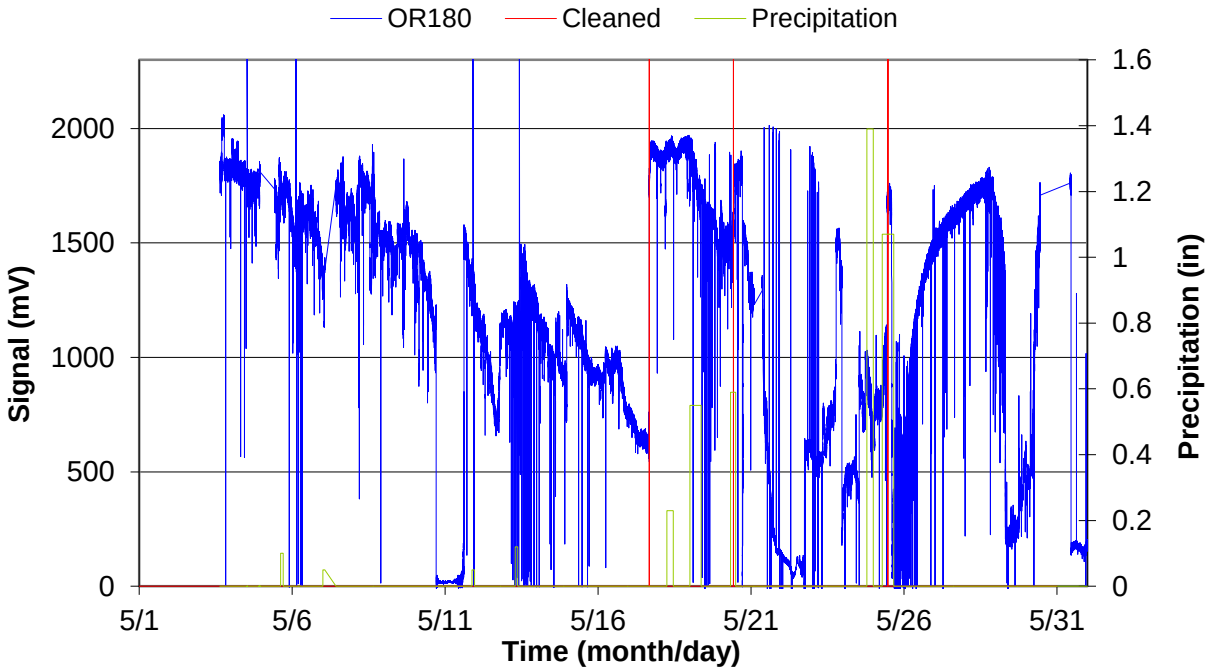

Figure 58. Unprocessed OR180 signals measured in May, 2011 for Wildcat Creek, Manhattan, KS. Precipitation data source: www.wunderground.com.

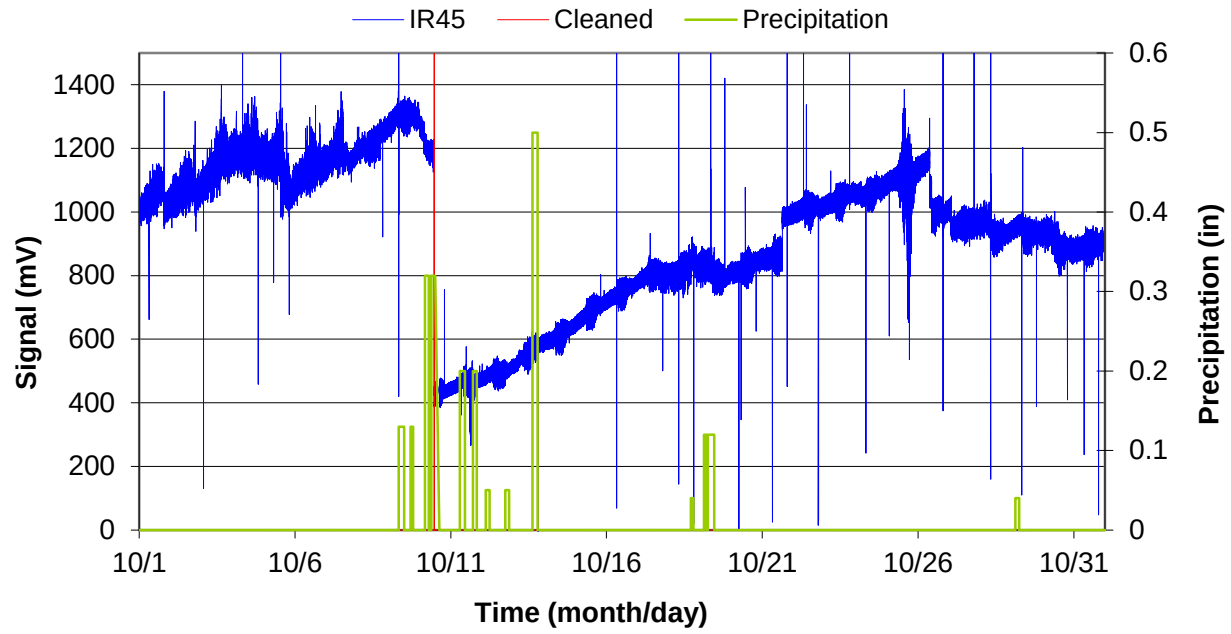

Figure 59. Unprocessed IR45 signals measured in October, 2011 for Pine Knot North site, Fort Benning, GA. Precipitation data source: www.wunderground.com.

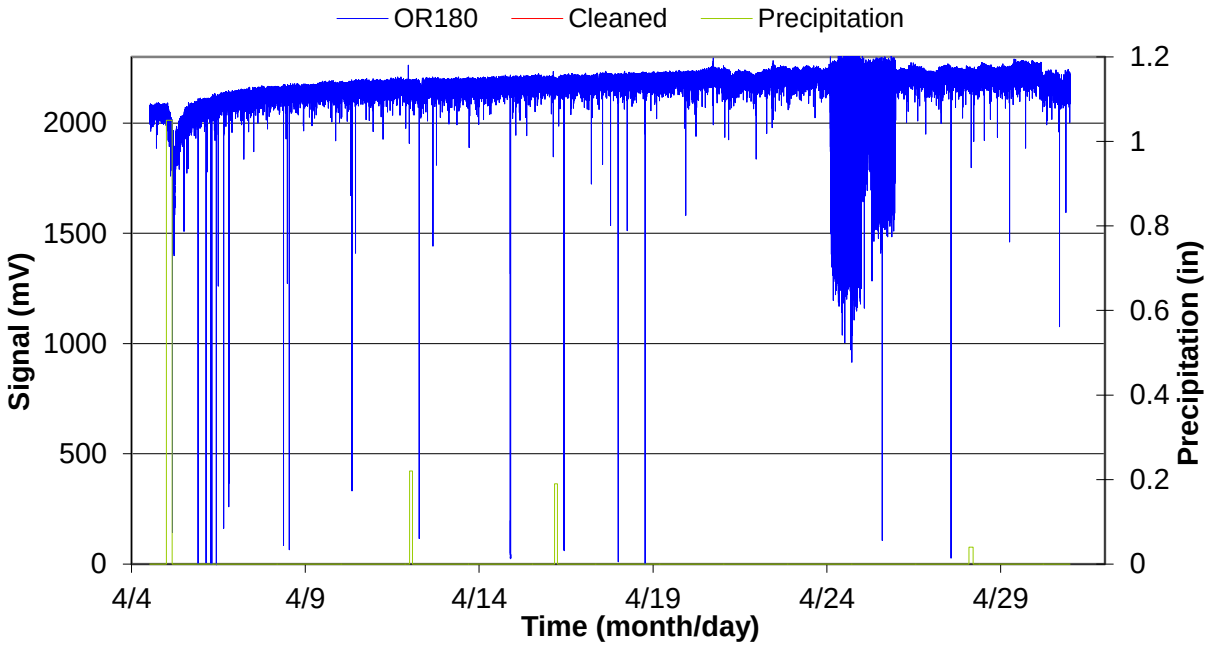

Figure 60. Unprocessed OR180 signals measured in October, 2011 for Pine Knot South site, Fort Benning, GA. Precipitation data source: www.wunderground.com.

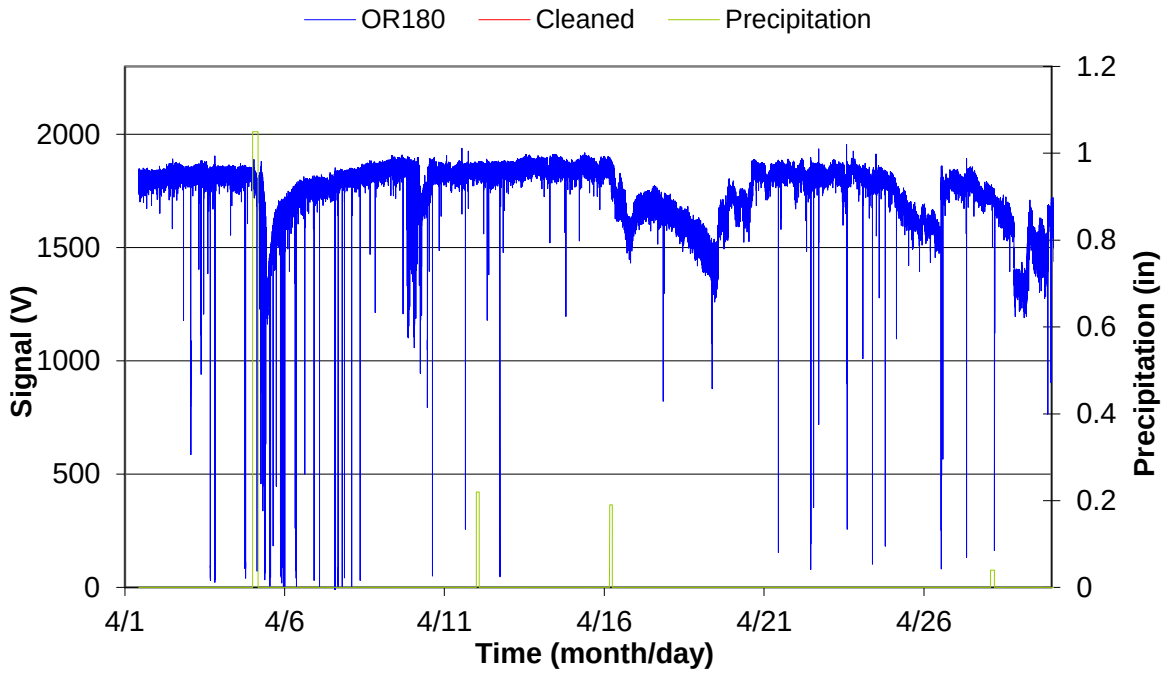

Figure 61. Unprocessed OR180 signals measured in April, 2011 for Upatoi North site, Fort Benning, GA. Precipitation data source: www.wunderground.com.

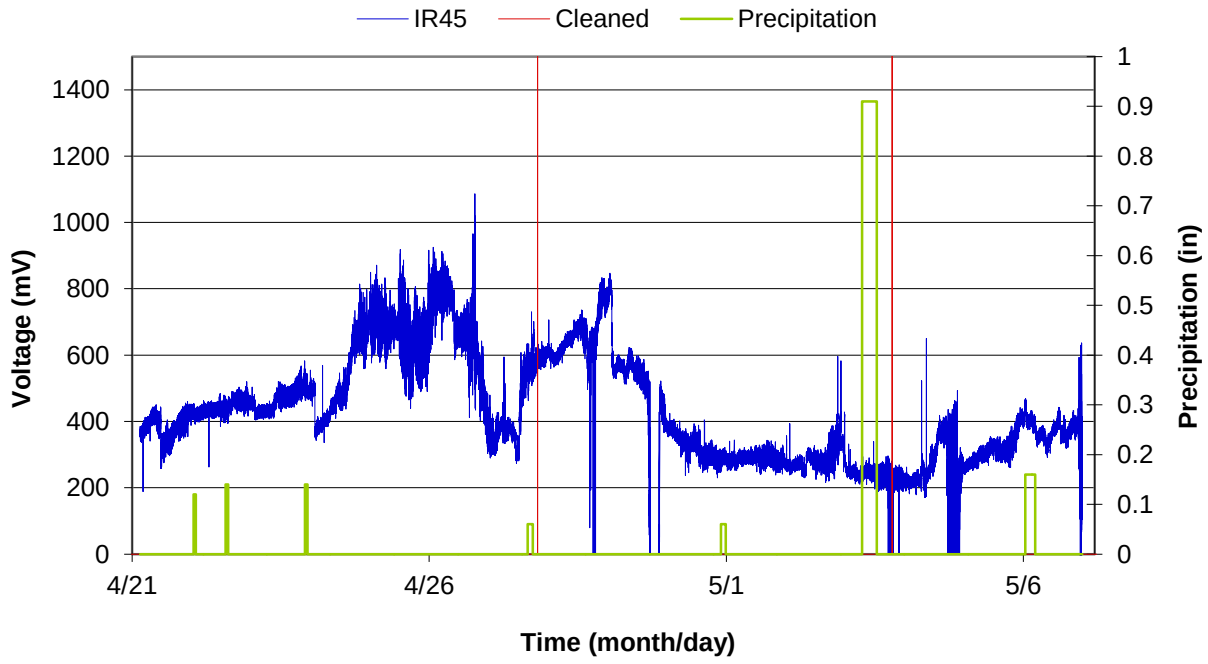

Figure 62. Unprocessed IR45 signals measured in April 21 – May 8, 2011 for Anita Near site, Edgewood, MD. Precipitation data source: www.wunderground.com.

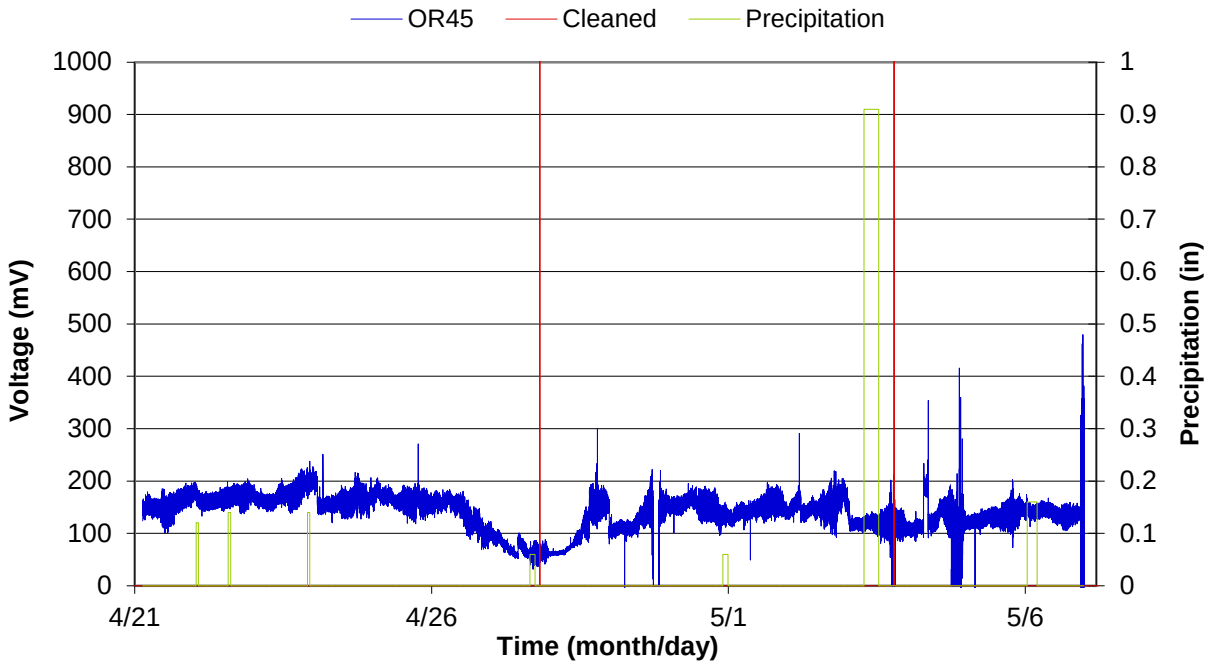

Figure 63. Unprocessed OR45 signals measured in April 21 – May 8, 2011 for Anita Near site, Edgewood, MD. Precipitation data source: www.wunderground.com.

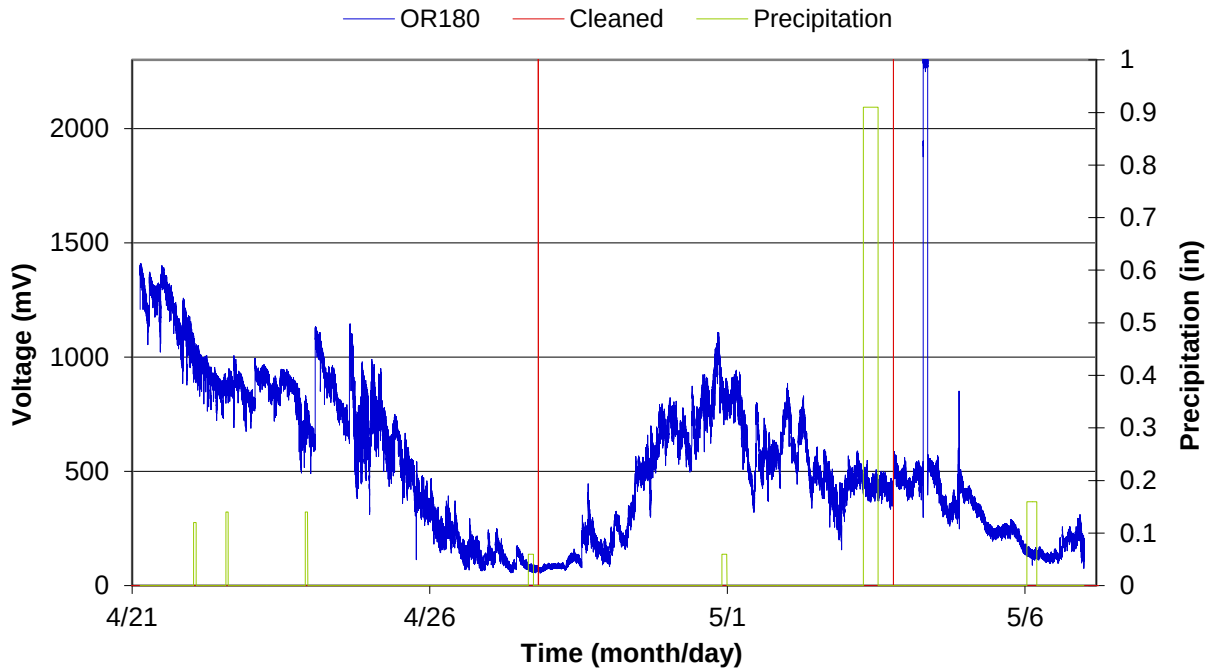

Figure 64. Unprocessed OR180 signals measured in April 21 – May 8, 2011 for Anita Near site, Edgewood, MD. Precipitation data source: www.wunderground.com.

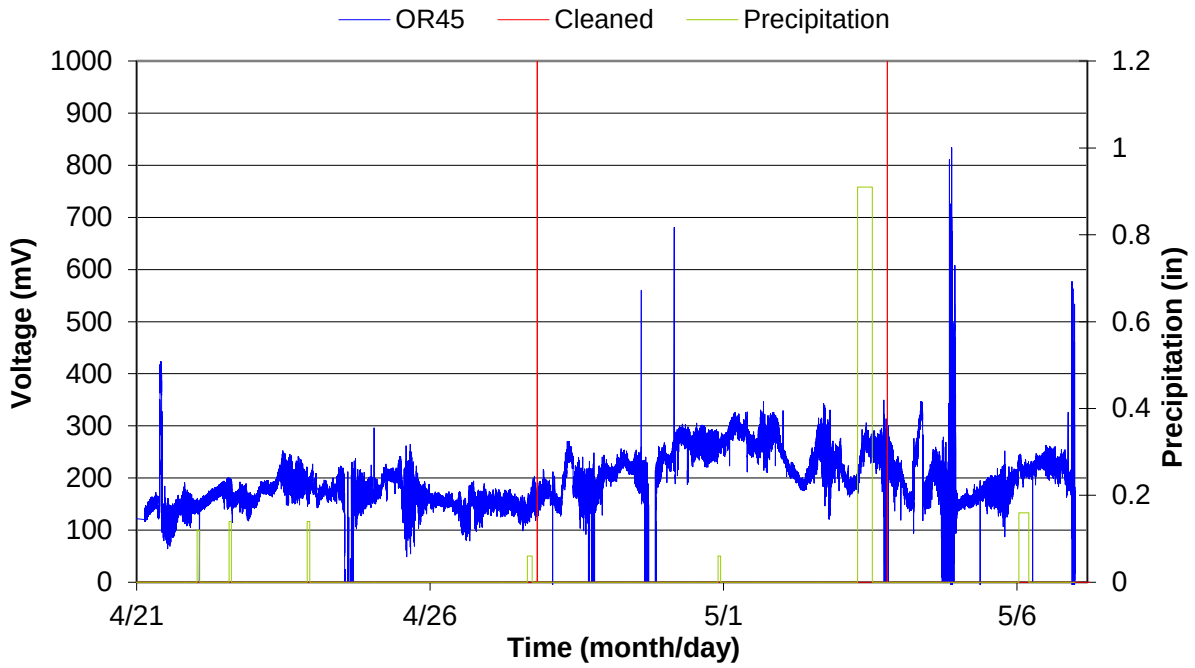

Figure 65. Unprocessed OR45 signals measured in April 21 – May 8, 2011 for Anita Far site, Edgewood, MD. Precipitation data source: www.wunderground.com.

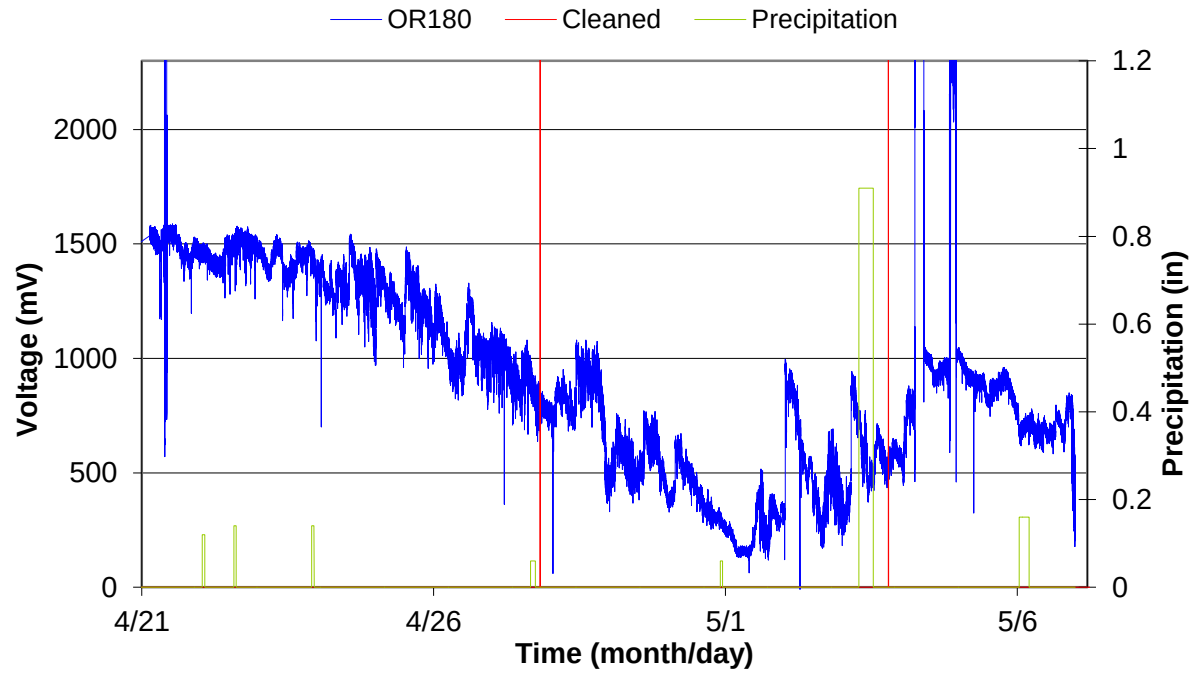

Figure 66. Unprocessed OR180 signals measured in April 21 – May 8, 2011 for Anita Far site, Edgewood, MD. Precipitation data source: www.wunderground.com.

9.2 Data Correction to Reduce Fouling Effects

The unprocessed sensor data was processed using a MATLAB program (Appendix I). The first step in the program was to filter the signal to reduce the noise. Figures 67-70 display the unfiltered and filtered signals. The filter used a moving average method that replaces each reading with the average of 11 measurements taken before and after the reading within a 5 minute period.

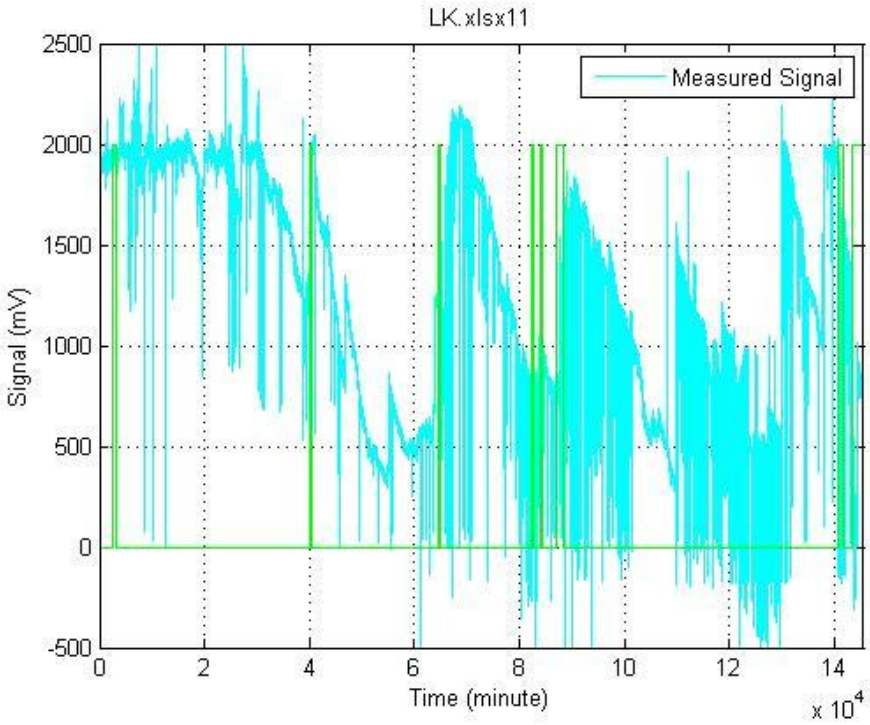

Figure 67. Measured signal OR180 signal for Little Kitten Creek. Data taken from August 15 - Oct. 10 2011. Precipitation data source: www.wunderground.com

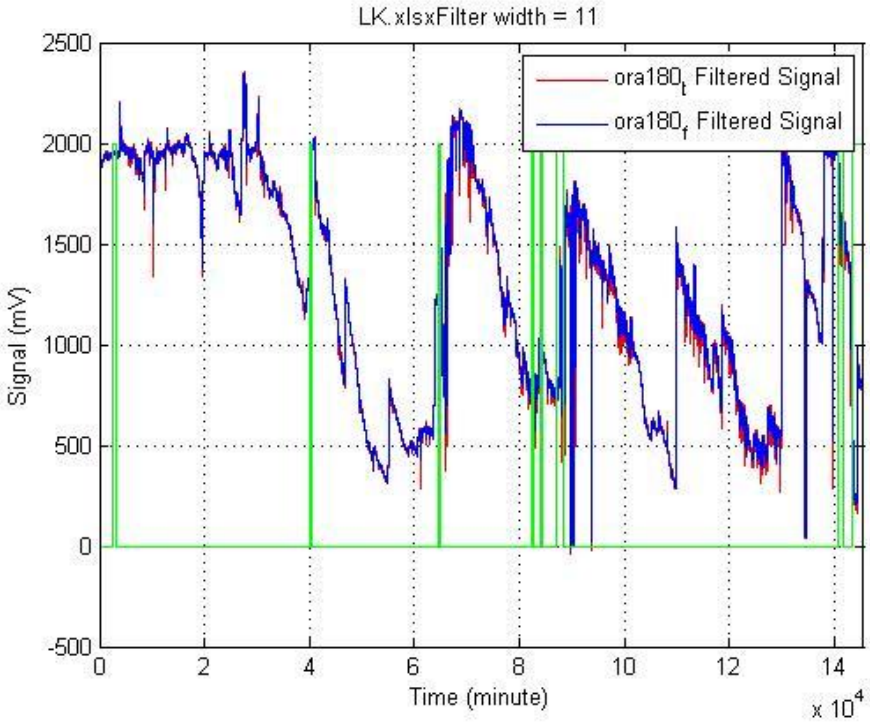

Figure 68. Filtered signal OR180 signal for Little Kitten Creek. Data taken from August 15 - Oct. 10 2011. Precipitation data source: www.wunderground.com

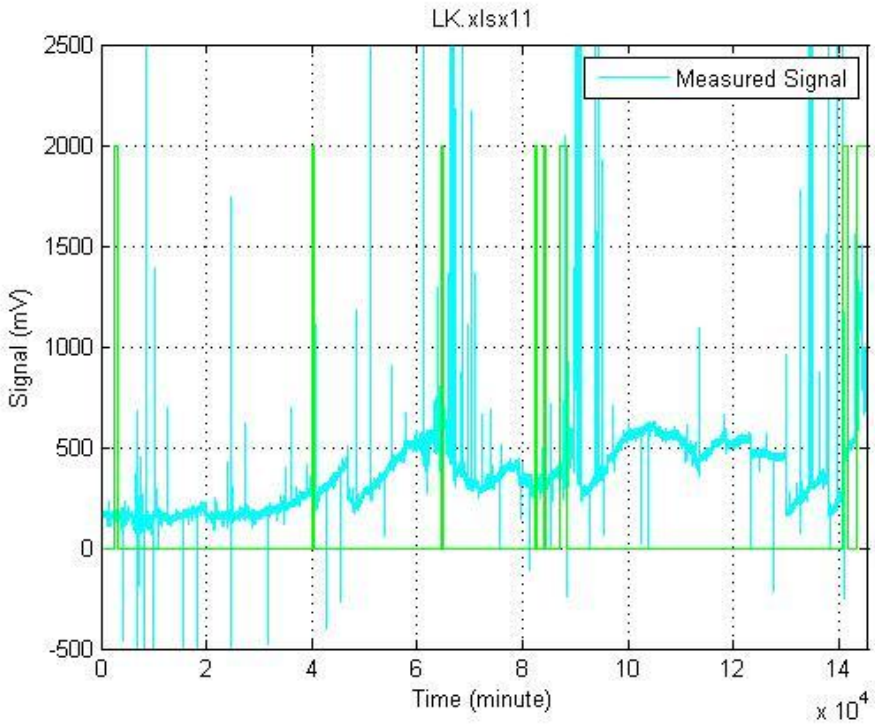

Figure 69. Measured IR45 signal for Little Kitten Creek. Data taken from August 15 - Oct. 10 2011. Precipitation data source: www.wunderground.com

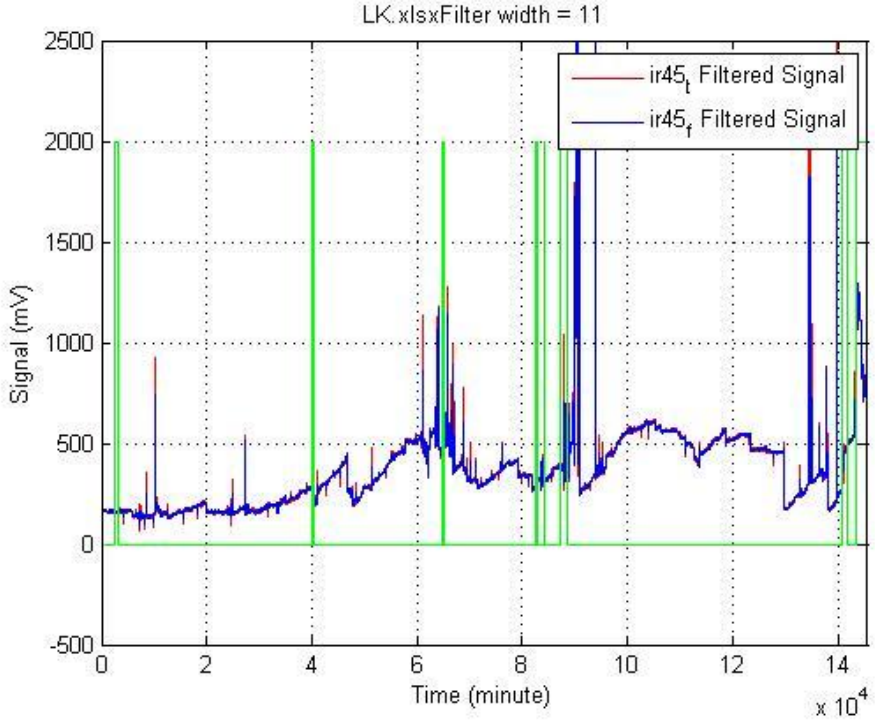

Figure 70. Filtered IR45 signal for Little Kitten Creek. Data taken from August 15 - Oct. 10 2011. Precipitation data source: www.wunderground.com

The next step in data processing removes the fouling trend seen over time in the optical sensor signals. The algorithm for fouling correction is to determine the fouling trend through a regression analysis on peak/valley signal values measured during no-rain periods. This trend is then removed from all measured data to restore the sensor signals. For the OR180 signals fouling causes a falling trend in the signals and peak values are used to determine the trend. For the IR45 and OR45 signals, fouling causes a rising trend in the signals over time, and the valleys in the data are used to determine the trend.

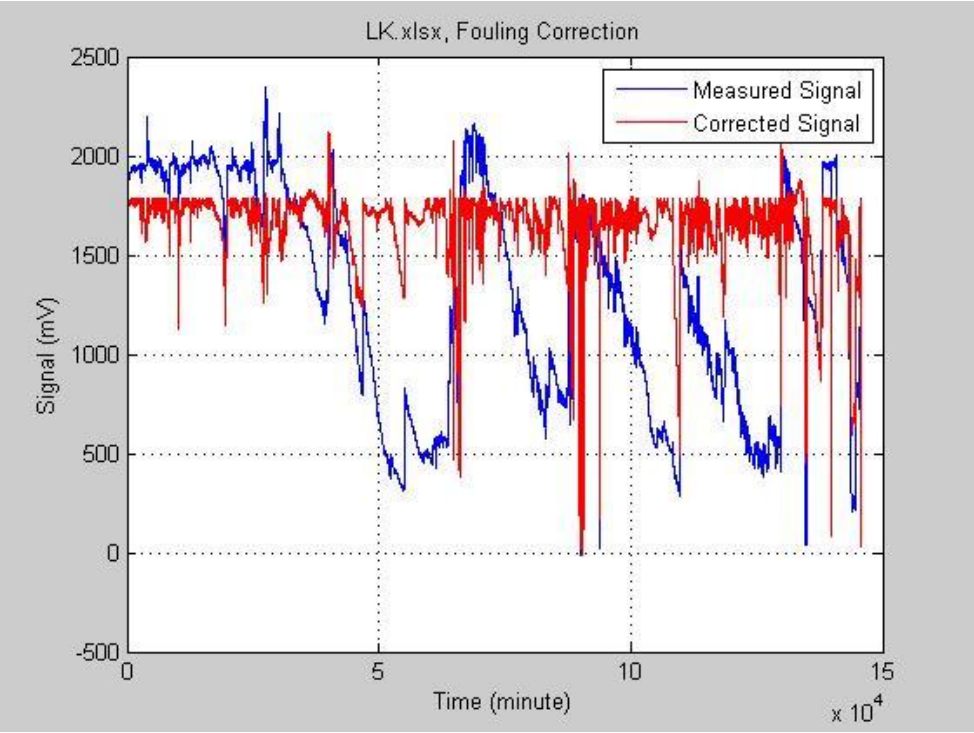

Figure 71. Sensor signals before and after fouling correction for OR180 at Little Kitten Creek. Data taken from Aug. 5 - Oct. 10 2011. Precipitation data source:www.wunderground.com

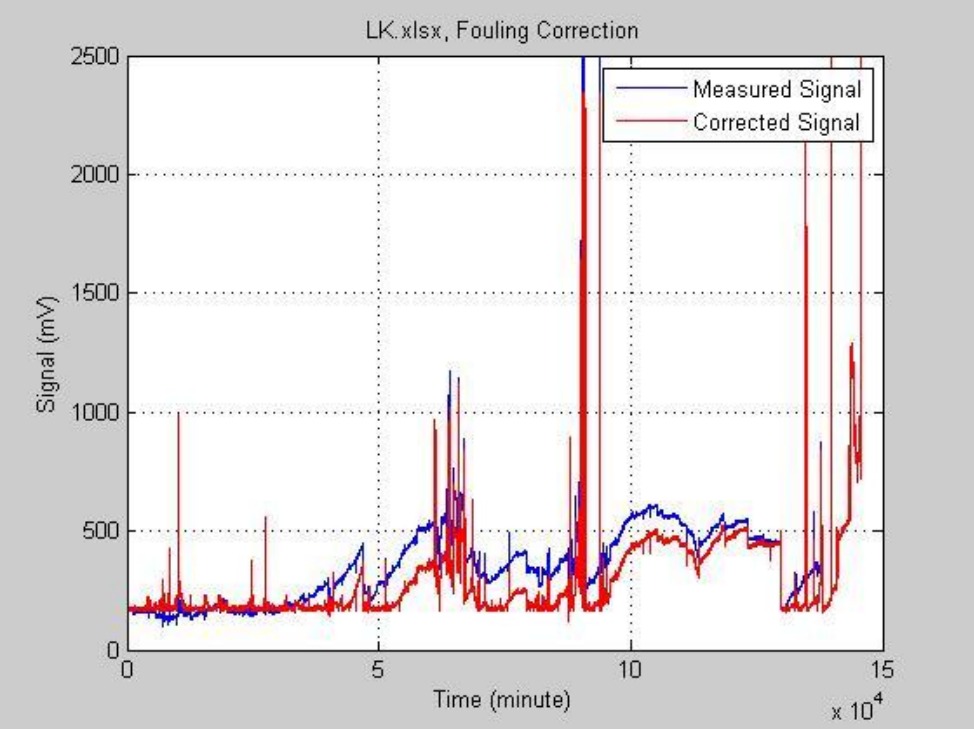

Figure 72. Sensor signals before and after fouling correction for IR45 at Little Kitten Creek. Data taken from August 5 - Oct. 10 2011. Precipitation data source: www.wunderground.com

After filtering and fouling correction, the SSC values were calculated using the prediction models. Figures 73-76 give several examples of predicted SSC measured at the Little Kitten sensor site.

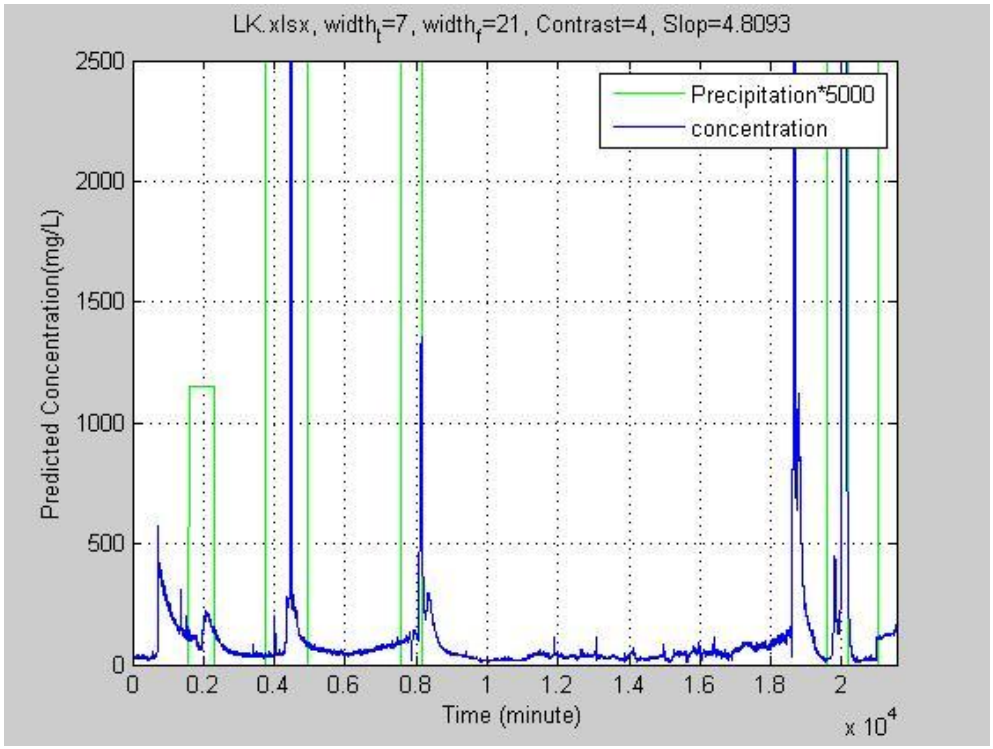

Figure 73. SSC prediction based on a polynomial model for Little Kitten Creek. Data taken from May 17-25 2011. Precipitation data source: www.wunderground.com

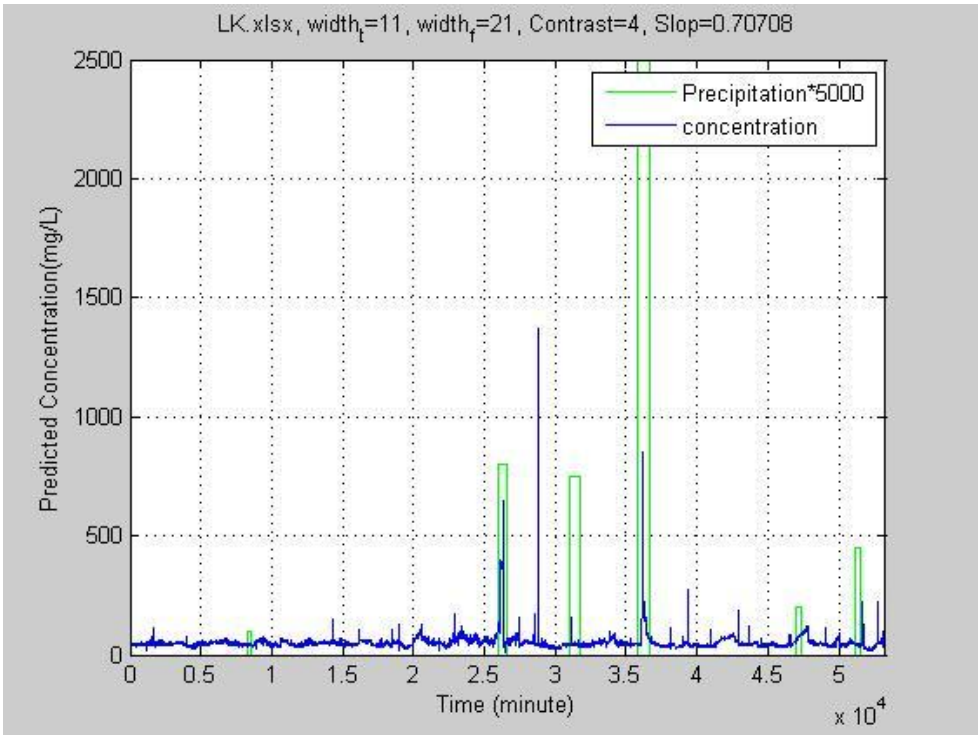

Figure 74. SSC prediction based on a polynomial model for Little Kitten Creek. Data taken from June 23 - July 13 2011. Precipitation data source: www.wunderground.com

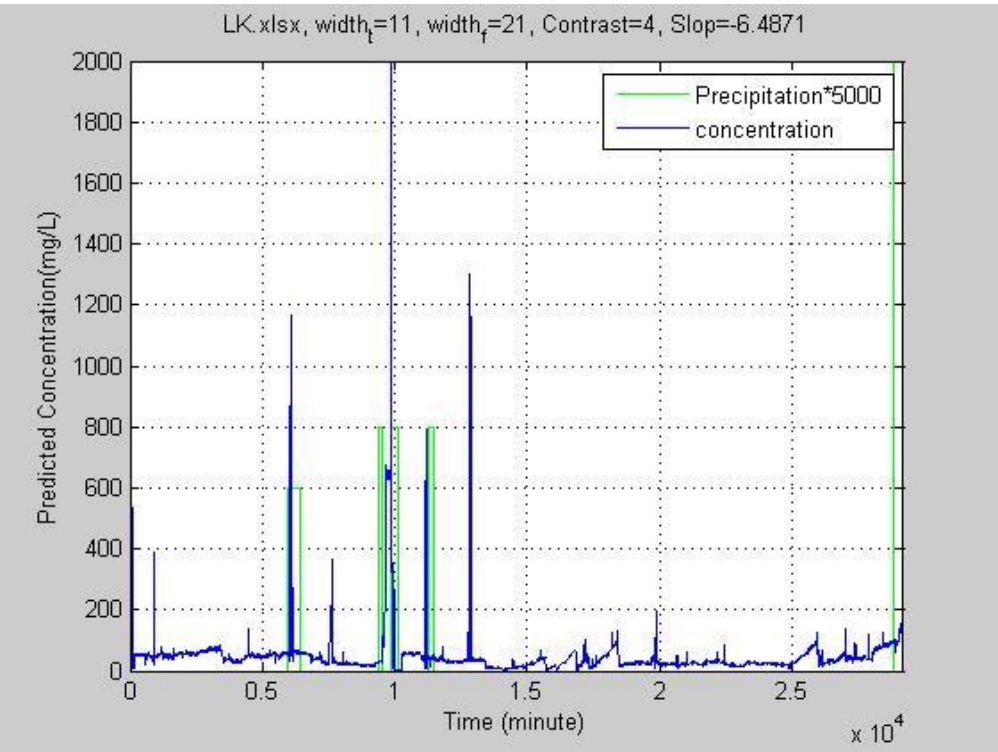

Figure 75. SSC prediction based on a polynomial model for Little Kitten Creek. Data taken from July 25 - August 5 2011. Precipitation data source: www.wunderground.com

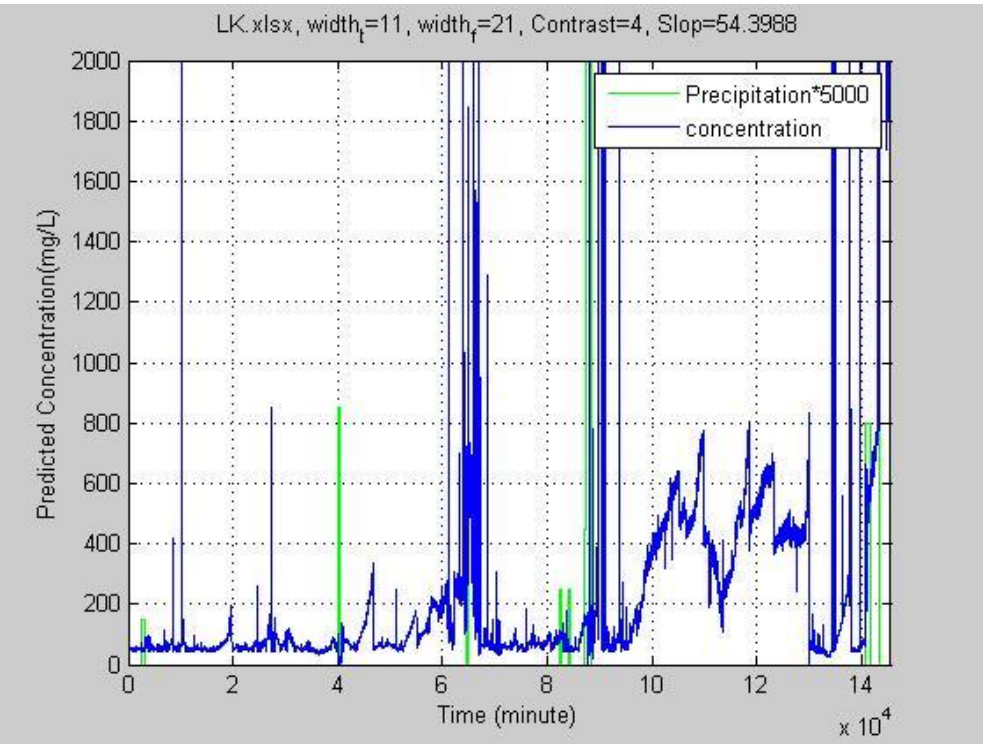

Figure 76. SSC prediction based on a polynomial model for Little Kitten Creek. Data taken from August 15 – Oct. 10 2011. Precipitation data source: www.wunderground.com

Little Kitten Creek is a small stream, in which changes in SSC during a rain event can flux very rapidly. Figures 77-80 displays the predicted SSC for several other sensor sites, which are either larger creeks or lake-like tidal water bodies Changes in SSC measured by these sensors were slower and less steep.

A large spike in predicted SSC shown in Figure 77 can be attributed to sensor clogging. This type of clogging can occur from leaves, sticks, animals, and other objects that block the sensor. The duration of clogging can vary.

Soil type, stream size, and rain events all have strong effects on changes in SSC. In general, soil at Fort Benning is more sandy than that at other installations. As a result, less change in SSC were observed in sensor data from the Fort Benning sites. This can be observed in Figures 78-80.

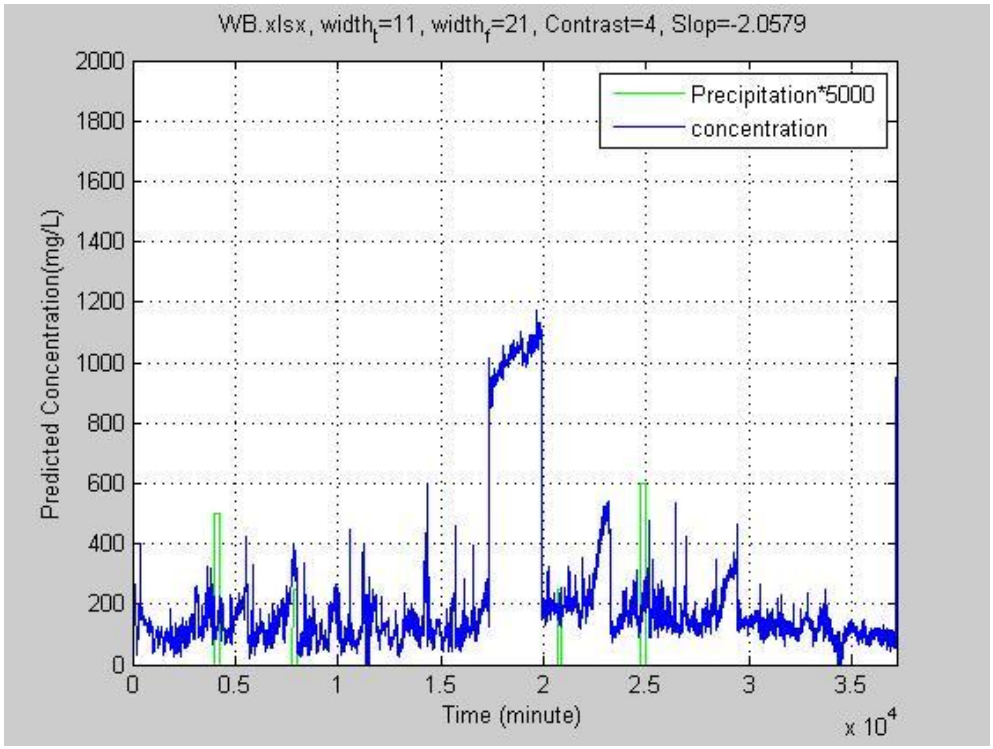

Figure 77. SSC prediction based on a linear model for Wildcat Bridge. Data taken in May 2011. Precipitation data source: www.wunderground.com

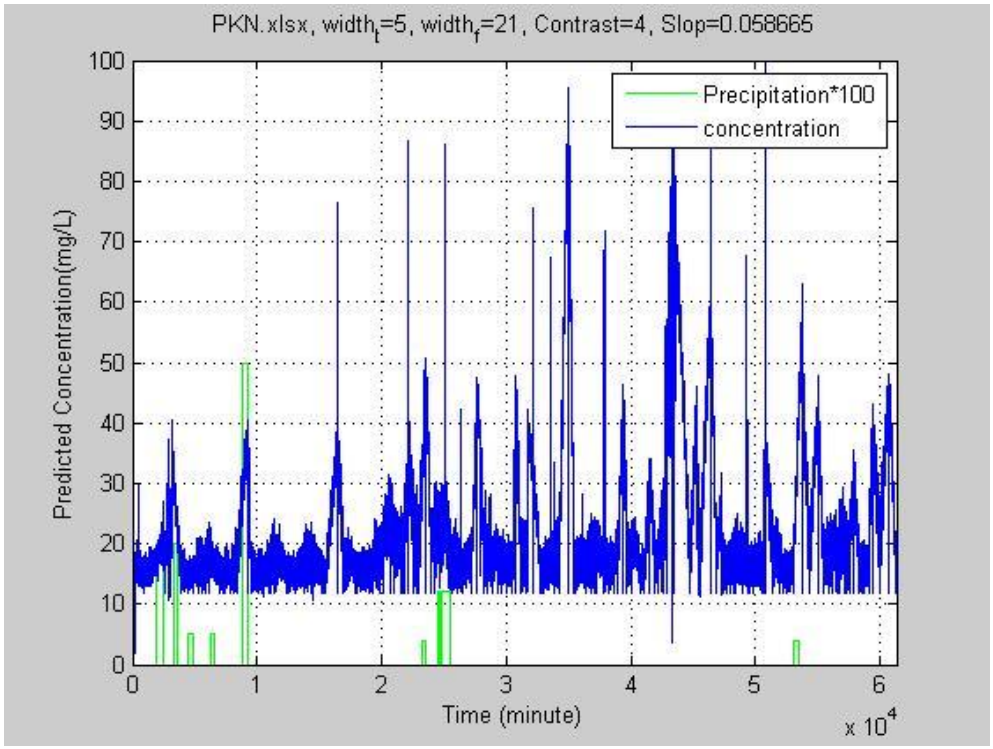

Figure 78. SSC prediction based on a linear model for Pine Knot North. Data taken in October 2011. Precipitation data source: www.wunderground.com

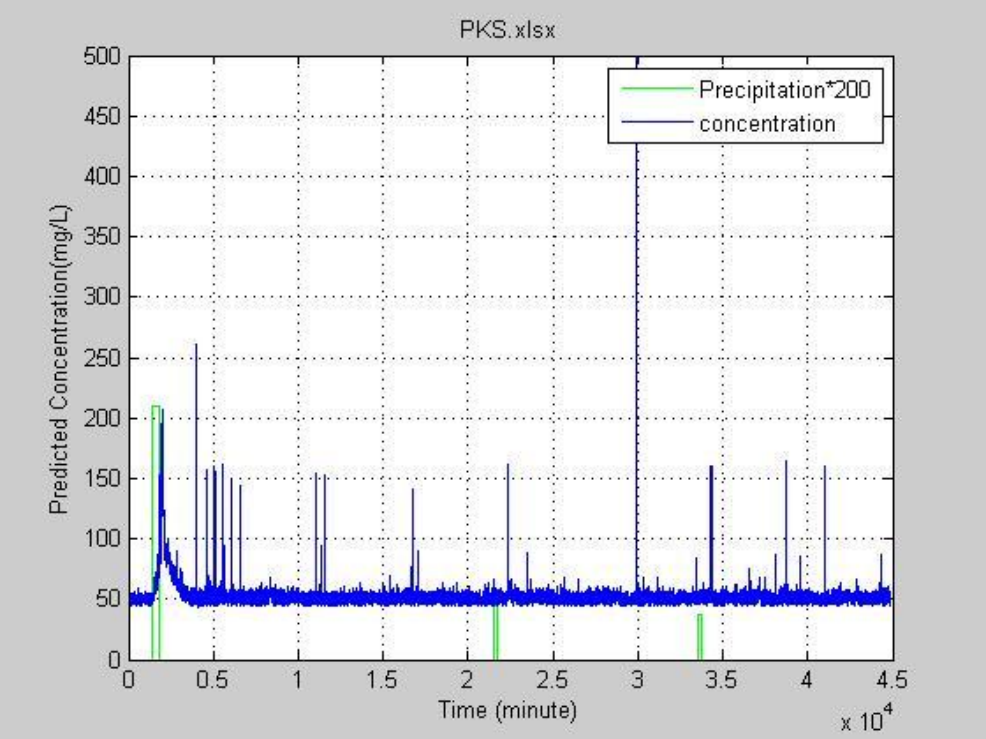

Figure 79. SSC prediction based on a linear model for Pine Knot South. Data taken in April 2011. Precipitation data source: www.wunderground.com

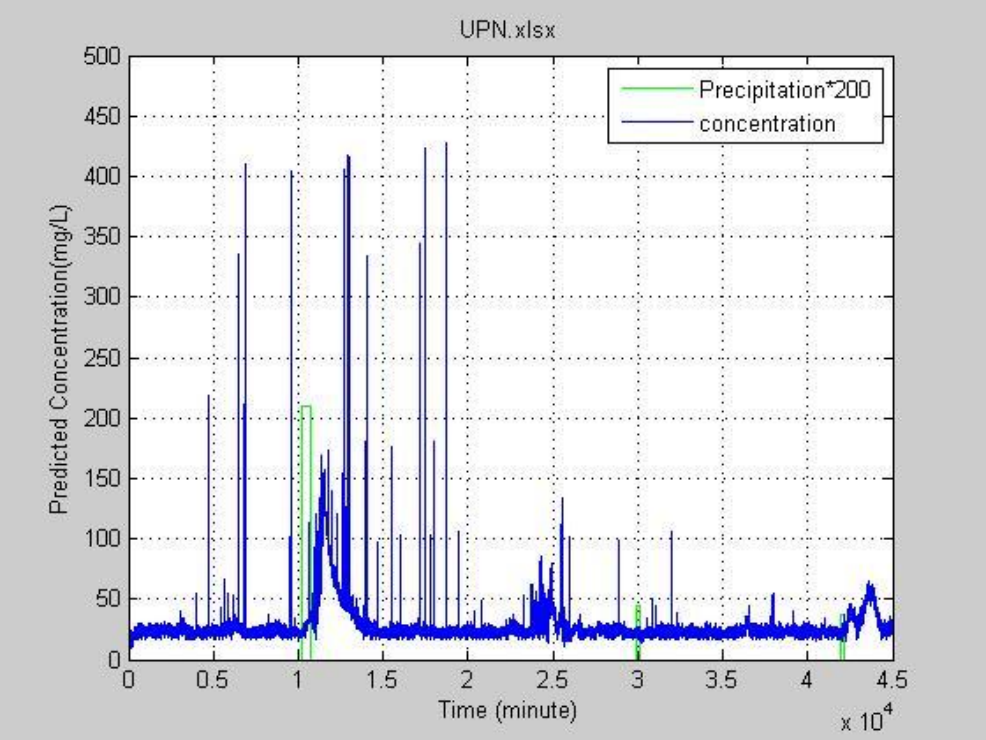

Figure 80. SSC prediction based on a linear model for Upatoi North. Data taken in April 2011. Precipitation data source: www.wunderground.com

The Anita sensor site is located in a tidal river, where tidal movement is the only cause for water flow. This allows the sediment to settle, resulting in low SSC (Figures 81-82).

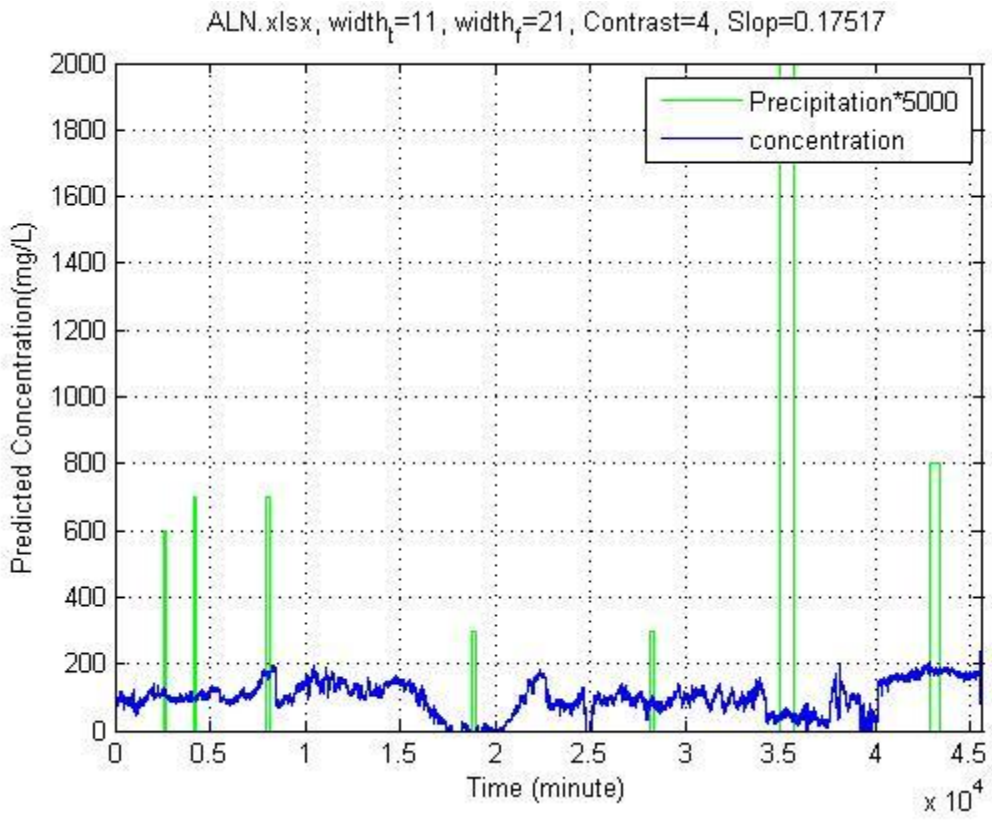

Figure 81. SSC prediction based on a polynomial model for Anita Near. Data taken in April 21 – May 8, 2011. Precipitation data source: www.wunderground.com

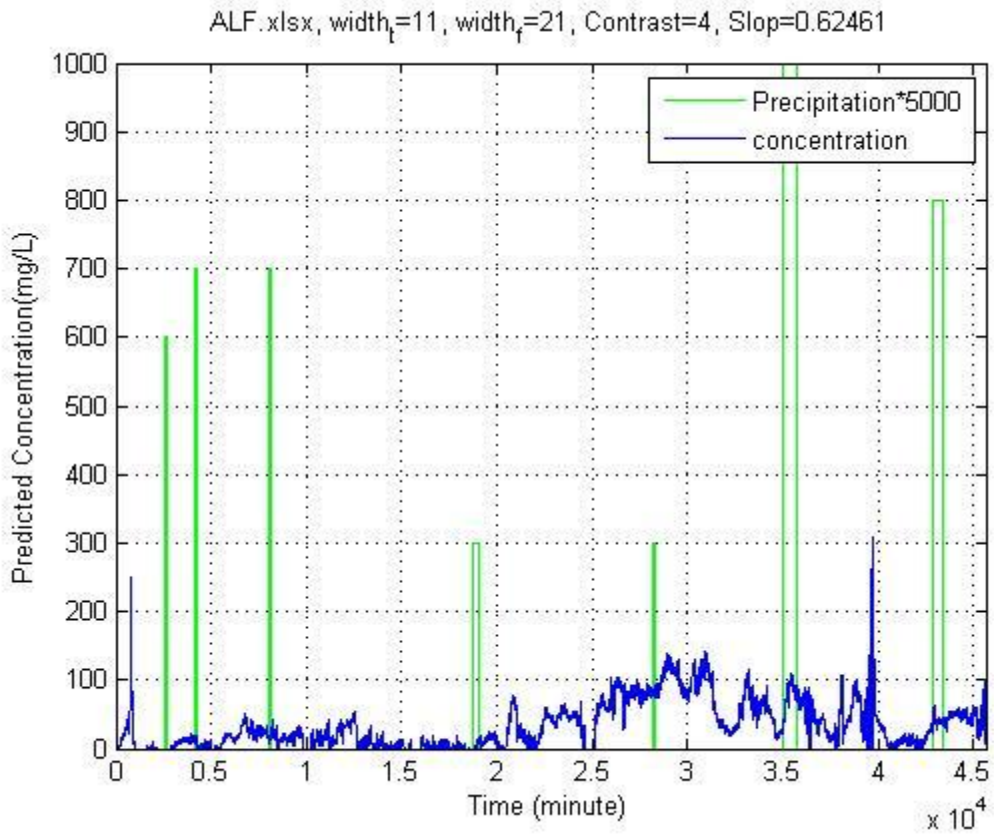

Figure 82. SSC prediction based off polynomial model for Anita Far. Data taken in April 2011. Precipitation data source: www.wunderground.com

9.3 Data Correction to Reduce Both Fouling and Clogging Effects

In situations where clogging takes place frequently, an additional algorithm can be added to the data processing program to correct for the clogging effect. This algorithm detects sudden jumps in the signal, classifies the "jumps" as natural variation on the signal or variation caused by clogging and removes the jump if it is deemed as clogging. Figure 83 displays the output of the clogging program, which can be compared to Figure 77 to see the effect of clogging correction on sediment prediction. As can be noted in the figure, the jump from the clogging was not completely removed but was brought back to normal trend over time instead of remaining clogged.

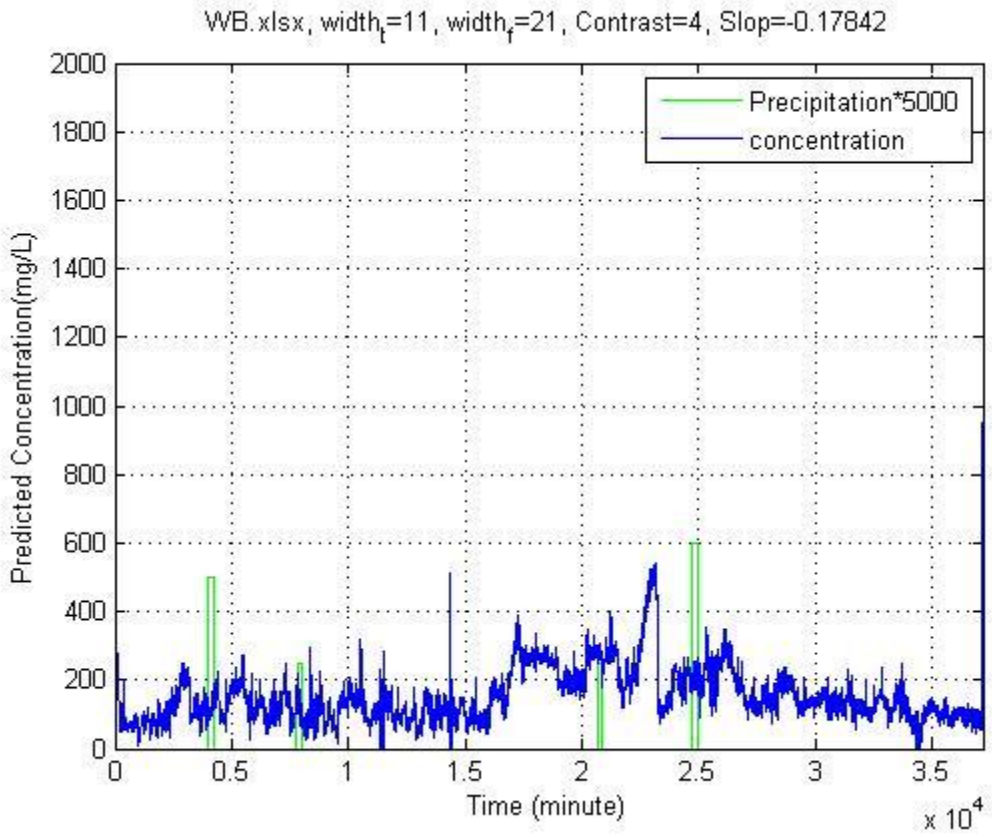

Figure 83. SSC prediction based on polynomial model with clogging correction for Wildcat Bridge. Data taken from May 1 - 17 2011. Precipitation data source: www.wunderground.com

10. **Conclusions and Future Work**

The research performed and results gathered for this sensor study in various locations around the United States further help to prove the viability of using real-time, wireless, optical sediment sensors in remote locations for the monitoring of SSC in various water bodies. This type of sediment monitoring can be useful in the quantification and measurement of stream sediment concentration, in order to further improve the understanding of stream processes and sediment flow in fluvial settings. This data can then be used to create management practices and design considerations that help to decrease sediment and other types of pollution in water bodies.

The sensor was calibrated and tested in multiple types of watersheds, soil types and ecosystems, helping to prove its versatility. Further implementation across various other watersheds and ecological regions would only further improve its feasibility and reliability. The effect of fouling can be reduced using an air-blast cleaning system and removed during data post-processing, helping to improve the viability of installing this type of sensor in remote locations where periodic manual cleaning would not be a feasible option.

Through this research it was determined that each sensor-signal processing board assembly should be independently calibrated and tested at the specific site where the sensor is deployed due to the non-uniformity in the properties of the optical components used in the sensors and the differences in the soil and water properties and biological factors among different watersheds.

Through this study, a two-stage sensor calibration procedure was demonstrated. The first stage was sensor pre-calibration in the laboratory to adjust the sensitivities of the sensors to a uniform level. The primary goal was to address the non-uniformity issue among optical components. The goal of the second stage of calibration was to establish an accurate calibration model for each sensor using a large number of water samples taken from its deployment site. The best-fit model may use one to three signals as the predictors. For some sensors, adding quadratic terms in the model improved the prediction accuracy.

The ability for this type of sensor to be implemented in-situ as an accurate and reliable method for SSC estimation is not yet feasible. But the research previously performed, coupled with future work should further improve its viability and implementation potential.

Future work for this system would include possible redesigning of the PCB control board as many problems with the sensor signal or malfunction of sensor were attributed to the PCB board. If this system can become more robust it would further improve the reliability of this type of sensor for various applications.

Another aspect that could be improved for this system is to allow both water and sediment samples to be taken from the site where the sensor will be deployed and complete both stages of calibration in the laboratory. This would allow the sensor to read SSC values within the desirable range without having to wait for large rain events to gather samples, which can be dangerous during periods of high flow and inclement weather.

Once installed in the field grab sampling could be performed to further improve the calibration model. This procedure would also be helpful during periods of drought when high sediment flows would not be common, causing a very lengthy calibration period. This method would also help with areas that are not easy to access or are expensive to travel to.

11. **Bibliography**

Agrawal, Y. C., & Pottsmith, H. C. (2000). Instruments for particle size and settling velocity observations in sediment transport. *Marine Geology, 168*(1), 89-114.

Agrawal, Y. C., & Pottsmith, H. C. (n.d.). *Laser diffraction sensors measure concentration and size distribution of suspended sediment.* Redmond, Washington: Sequoia Scientific, Inc.

Bourne, S. G., & Graves, M. R. (2001). *Classification of land-cover types for the Fort Benning ecoregion using enhanced thematic mapper data.* Strategic Environmental Research and Development Program.

Bunt, J. C., Larcombea, P., & Jagob, C. F. (1999). Quantifying the response of optical backscatter devices & transmissometers to variations in suspended particulate matter. *Continental Shelf Research, 19*(9), 1199-1220.

Campbell Scientific. (2008). *Effects of fouling on the lens of optical backscatter (OBS) sensors.* Retrieved October 2011, from http://www.campbellsci.ca/Download/LitNote_fouling.pdf

Campbell Scientific, Inc. (2008, April). *Comparison of suspended solids concentration (SSC) and turbidity*. Retrieved October 2011, from http://www.campbellsci.com/documents/technical-papers/obs_ssc-turbidity.pdf

Castle, E. E. (2007). *Geodatabases in design: a floodplain analysis of Little Kitten Creek.* Master's Thesis, Kansas State University, Department of Landscape Architecture/Regional and Community Planning, Manhattan, KS.

Christensen, V. G., Rasmussen, P. P., & Ziegler, A. C. (2000). *Real-time water-quality monitoring and regression analysis to estimate nutrient and bacteria concentrations in Kansas streams.* Reston, VA: USGS.

Davies-Colley, R. J., & Smith, D. G. (2001). Turbidity, suspended sediment, and water clarity: a review. *Journal of the American Water Resources Association, 37*, 1085-1101.

Doe III, W. W., Shaw, R. B., Bailey, R. G., Jones, D. S., & Marcia, T. E. (1999). Location and environments of U.S. Army training and testing lands: an ecoregional framework for assessment. *Federal Facilities Environmental Journal, 10*(3), 9-26.

Downing, J. (2006, November). Twenty-five years with OBS sensors: The good, the bad, and the ugly. *Continental Shelf Research, 26*(17-18), pp. 2299-2318.

EPA. (1999). EPA guidance manual: Turbidity provisions. Retrieved Sep. 2011, from http://www.epa.gov/ogwdw/mdbp/pdf/turbidity/chap_07.pdf

Gartner, J. W. (2002). Estimation of suspended solids concentrations based on acoustic backscatter intensity: theoretical background. *Turbidity and Other Sediment Surrogates Workshop.* Reno, NV.

Gippel, C. J. (1995). Potential of turbidity monitoring for measuring the transport of suspended solids in streams. *Hydrological Processes*, 83-97.

Glysson, G. D., & Gray, J. R. (2002, May 2). *Total suspended solids data for use in sediment studies.* Retrieved October 2011, from http://water.usgs.gov/osw/techniques/TSS/glysson.pdf

Gordon, N. D., McMahon, T. A., Finlayson, B. L., Gippel, C. J., & Nathan, R. J. (2004). Stream hydrology: an introduction for ecologists.

Gray, J. R., & Gartner, J. W. (2010). Overview of selected surrogate technologies for high-temporal resolution suspended-sediment monitoring. *2nd Joint Federal Interagency Conference.* Las Vegas, NV.

Gray, J. R., & Glysson, G. D. (n.d.). *Collection and use of total suspended solids data.* Retrieved October 2011, from http://www.swrcb.ca.gov/water_issues/programs/swamp/docs/cwt/guidance/3157a.pdf

Gustafson, D. L. (1999, Sept 11). *Named places in Upper Kansas HUC 10270101*. Retrieved December 2011, from Montana.edu: http://www.esg.montana.edu/gl//huc/gnis/10270101.html

Hoitink, A. F., & Hoekstra, P. (2005, February). Observations of suspended sediment from ADCP and OBS measurements in a mud-dominated environment. *Coastal Engineering, 52*(2), 103-118.

Jastram, J. D., Zipper, C. E., Zelazny, L. W., & Hyer, K. E. (2010). Increasing precision of turbidity-based suspended sediment concentration and load estimates. *Journal of Environmental Quality, 39*, 1306-1316.

Kent, C. A. (1988). Biological Fouling: Basic Science and Models. In L. F. Melo, T. R. Bott, & C. A. Bernardo, *Fouling Science and Technology* (pp. 207-221). Springer.

Kirk, J. O. (1994). *Light and photosynthesis in aquatic ecosystems.* New York, New York: Cambridge University Press.

Kuhnle, R. A., & Wren, D. G. (2005). Breakout session I, suspended-sediment measurement data needs, uncertainty, and new technologies. *Proceedings of the Federal Interagency Sediment Monitoring Instrument and Analysis Research Workshop.*

Marquis, P. (2005, Fall). Turbidity and suspended sediment as measures of water quality. *Streamline: Water Management Bulletin, 9*(1), 21-23.

McNab, W. H., & Peter, E. A. (1994). *Ecological Subregions of the United States.*

Meral, R., Smerdon, A., Merdun, H., & Demirkiran, A. R. (2010, January 11). Estimation of suspended sediment concentration by acoustic equations for soil sediment. *African Journal of Biotechnology, 9*(2), 170-177.

Pavelsky, T. M., & Smith, L. C. (2009). Remote sensing of suspended sediment concentration, flow velocity, and lake recharge in the Peace-Athabasca Delta, Canada. *Water Resources Research, 45*(W11417).

Perkey, D., Pratt, T., & Ganesh, N. (2010). Comparison of SSC measurements with acoustic backscatter data: West Bay sediment diversion, Mississippi River. *2nd Joint Federal Interagency Conference.* Las Vegas, NV.

Pimentel, D., Harvey, C., Resosudarmo, P., Sinclair, K., Kurz, D., McNair, M., et al. (1995). Environmental and economic costs of soil erosion and conservation benefits. *Science, 267*, 1117-1123.

Pratt, T., & Parchure, T. (2003). *OBS calibration and field measurements.* Retrieved October 2011, from http://water.usgs.gov/osw/techniques/sediment/sedsurrogate2003workshop/pratt.pdf

Quan, N. T. (1988, October). The prediction sum of squares as a general measure of regression diagnostics. *Journal of Business & Economic Statistics, 6*(4), 501-504.

Sadar, M. (2002, May 2). *Turbidity instrumentation - an overview of today's available technology.* Retrieved Sep. 2011, from http://water.usgs.gov/osw/techniques/TSS/sadar.pdf

Stoll, Q. (2004). *Design of a real-time, optical sediment concentration sensor.* Thesis, Kansas State University.

Stutterheim, K. M. (1972). *The rural-urban water quality interface of Wildcat Creek.* Thesis, Kansas State University, Manhattan, KS.

Sutherland, T. F., Lane, P. M., Amos, C. L., & Downing, J. (2000). The calibration of optical backscatter sensors for suspended sediment of varying darkness levels. *Marine Geology*, 587-597.

Tessier, A. (1992). Sorption of trace elements on natural particles in oxic environments. In *Environmental Particles* (pp. 425-453). Boca Raton, Florida: Lewis Publishing.

U.S. Climate Data. (2011). *Climate Columbus Ft. Benning, Georgia - Climate Graph*. Retrieved Dec 2011, from U.S. Climate Data: http://www.usclimatedata.com/climate.php?location=USGA0133

USGS. (2011, December). *GNIS Detail - Upatoi Creek*. Retrieved December 2011, from United States Geological Survey: http://geonames.usgs.gov/pls/gnispublic/f?p=gnispq:3:147470942345739::NO::P3_FID:356608

Vousdoukas, M. I., Aleksiadis, S., Grenz, C., & Verney, R. (2011). Comparisons of acoustic and optical sensors for suspended sediment concentration measurements under non-homogeneous solutions. *Journal of Coastal Research*, 160-164.

Wolman, M. G., & Miller, J. P. (1960). Magnitude and fequency of forces in geomorphic processes. *Journal of Geology, 68*, 54-74.

Wren, D. G., & Kuhnle, R. A. (2002). Surrogate techniques for suspended-sediment measurement. *Turbidity and Other Sediment Surrogates Workshop.* Reno, NV.

Zhang, Y. (2009). *An optical sensor for in-stream monitoring of suspended sediment concentration.* Dissertation, Kansas State University.

Ziegler, A. C. (2002, May 2). *Issues related to use of turbidity measurements as a surrogate for suspended sediment.* Retrieved Sep. 2011, from http://water.usgs.gov/osw/techniques/TSS/ZieglerT.pdf

Appendix A - Little Kitten Statistical Analysis, Minitab Output

Regression Analysis: Concentration (mg/L) versus IR45 (mV)

```
The regression equation is
Concentration (mg/L) = - 360 + 2.01 IR45 LED On-Off(mV)

Predictor              Coef  SE Coef      T      P
Constant           -359.69    52.53  -6.85  0.000
IR45 LED On-Off(mV)  2.0068   0.1767  11.35  0.000


S = 96.7324   R-Sq = 85.4%   R-Sq(adj) = 84.8%

PRESS = 261767   R-Sq(pred) = 81.46%

Analysis of Variance

Source          DF       SS       MS       F      P
Regression       1  1206362  1206362  128.92  0.000
Residual Error  22   205857     9357
Total           23  1412219


Unusual Observations

      IR45 LED  Concentration
Obs  On-Off(mV)         (mg/L)    Fit  SE Fit  Residual  St Resid
 17        488          815.6  619.6    42.4     196.0      2.25R

R denotes an observation with a large standardized residual.
```

Residual Plots for Concentration (mg/L)

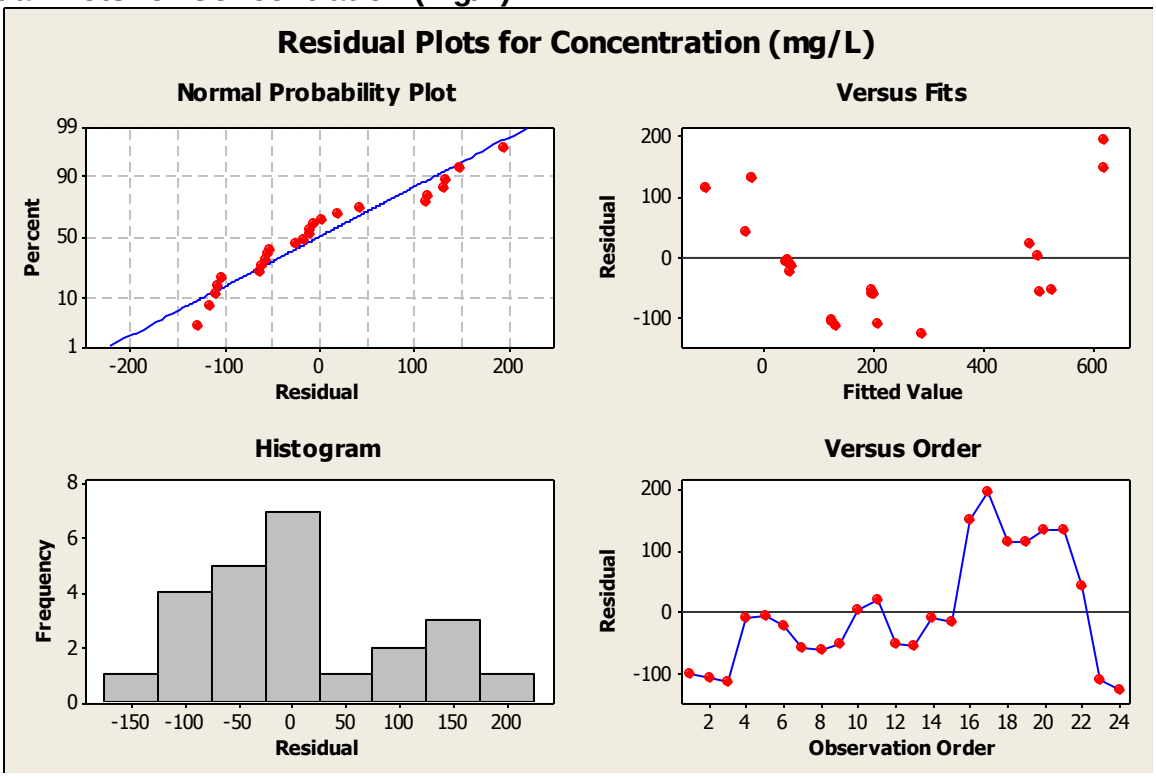

Regression Analysis: Concentration (mg/L) versus OR45 (mV)

The regression equation is
Concentration (mg/L) = - 155 + 2.04 OR45 LED On-Off (mV)

Predictor	Coef	SE Coef	T	P
Constant	-154.78	57.95	-2.67	0.014
OR45 LED On-Off (mV)	2.0417	0.2946	6.93	0.000

S = 142.004 R-Sq = 68.6% R-Sq(adj) = 67.2%

PRESS = 543920 R-Sq(pred) = 61.48%

Analysis of Variance

Source	DF	SS	MS	F	P
Regression	1	968588	968588	48.03	0.000
Residual Error	22	443632	20165		
Total	23	1412219			

Unusual Observations

Obs	OR45 LED On-Off	Concentration (mV) (mg/L)	Fit	SE Fit	Residual	St Resid
16	293	767.7	443.4	46.3	324.2	2.42R
17	291	815.6	438.9	45.8	376.7	2.80R
23	276	98.0	408.7	42.5	-310.7	-2.29R

R denotes an observation with a large standardized residual.

Residual Plots for Concentration (mg/L)

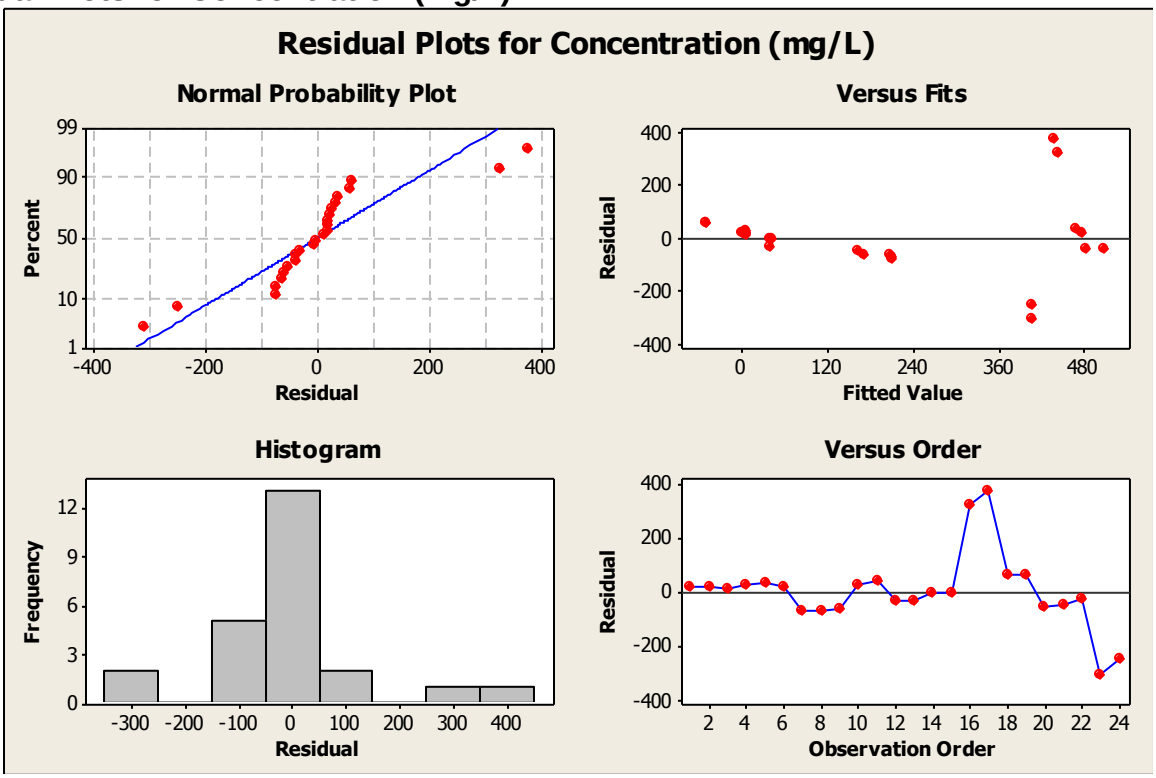

Regression Analysis: Concentration (mg/L) versus OR180 (mV)

The regression equation is
Concentration (mg/L) = 1325 - 0.701 OR180 LED On-Off (mV)

Predictor	Coef	SE Coef	T	P
Constant	1325.49	71.44	18.55	0.000
OR180 LED On-Off (mV)	-0.70084	0.04330	-16.18	0.000

S = 70.5268 R-Sq = 92.3% R-Sq(adj) = 91.9%

PRESS = 129101 R-Sq(pred) = 90.86%

Analysis of Variance

Source	DF	SS	MS	F	P
Regression	1	1302791	1302791	261.92	0.000
Residual Error	22	109429	4974		
Total	23	1412219			

Unusual Observations

Obs	OR180 LED On-Off (mV)	Concentration (mg/L)	Fit	SE Fit	Residual	St Resid
14	1603	34.7	201.9	14.4	-167.2	-2.42R
15	1601	33.8	203.8	14.4	-169.9	-2.46R
16	856	767.7	725.8	35.9	41.9	0.69 X
17	852	815.6	728.4	36.1	87.3	1.44 X

R denotes an observation with a large standardized residual.
X denotes an observation whose X value gives it large leverage.

Residual Plots for Concentration (mg/L)

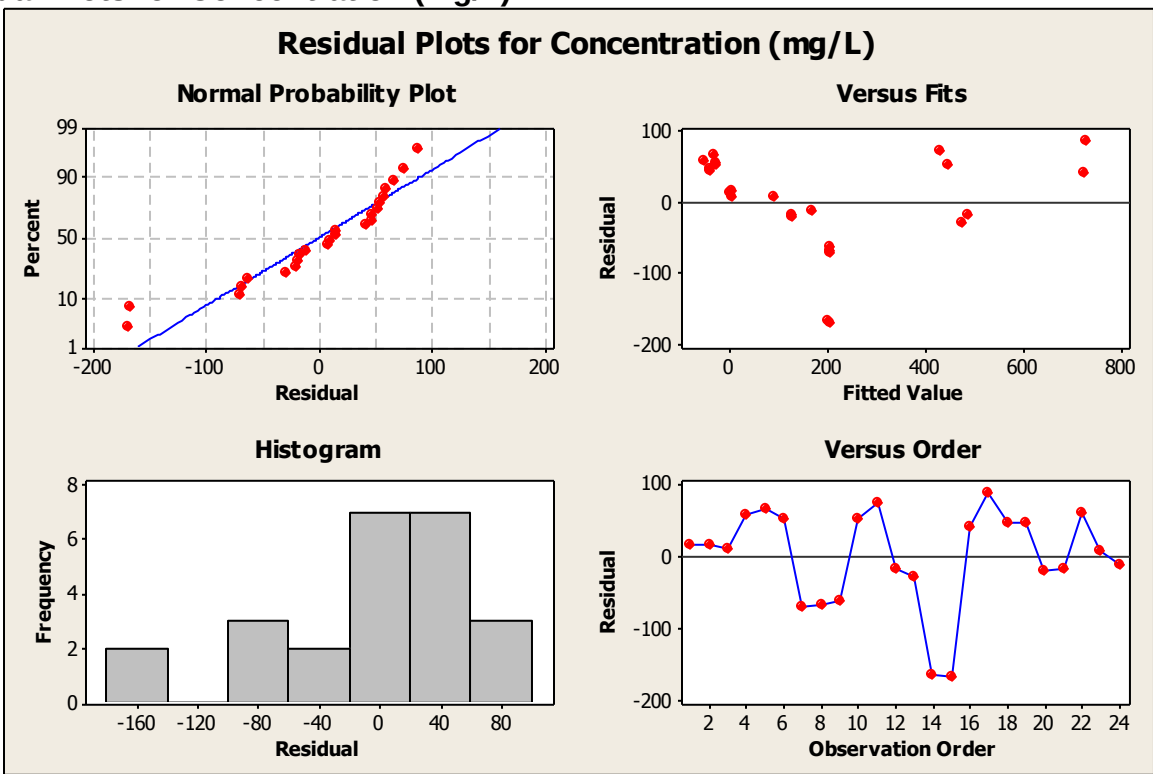

Linear Stepwise Output

Stepwise Regression: Concentration (mg/L) versus IR45 (mV), OR45 (mV), OR180 (mV)

```
  Alpha-to-Enter: 0.15  Alpha-to-Remove: 0.15

Response is Concentration (mg/L) on 3 predictors, with N = 24


Step                         1       2
Constant                1325.5   844.2

OR180 LED On-Off (mV)   -0.701  -0.509
T-Value                 -16.18   -5.21
P-Value                  0.000   0.000

IR45 LED On-Off(mV)                0.62
T-Value                            2.15
P-Value                           0.044
```

Regression Analysis: Concentration versus IR45 (mV), OR180 (mV)

```
The regression equation is
Concentration (mg/L) = 844 + 0.625 IR45 LED On-Off(mV)
                       - 0.509 OR180 LED On-Off (mV)
```

```
Predictor                 Coef  SE Coef      T      P
Constant                844.2    233.6   3.61  0.002
IR45 LED On-Off(mV)    0.6246   0.2908   2.15  0.044
OR180 LED On-Off (mV) -0.50947  0.09771  -5.21  0.000

S = 65.3615   R-Sq = 93.6%   R-Sq(adj) = 93.0%

PRESS = 124326   R-Sq(pred) = 91.20%

Analysis of Variance

Source          DF       SS      MS       F      P
Regression       2  1322505  661252  154.78  0.000
Residual Error  21    89715    4272
Total           23  1412219

Source                DF   Seq SS
IR45 LED On-Off(mV)    1  1206362
OR180 LED On-Off (mV)  1   116143

Unusual Observations

      IR45 LED  Concentration
Obs  On-Off(mV)         (mg/L)    Fit  SE Fit  Residual  St Resid
 15        204           33.8  156.1    25.9    -122.2     -2.04R

R denotes an observation with a large standardized residual.
```

Residual Plots for Concentration (mg/L)

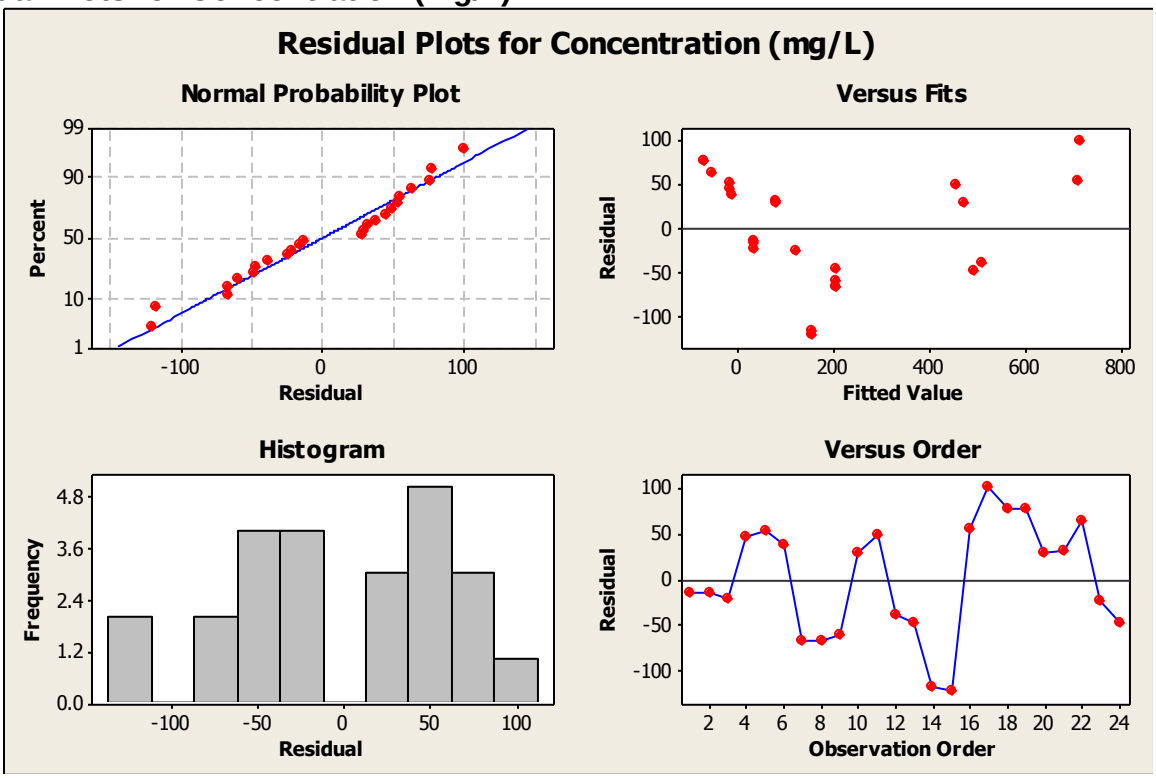

Polynomial Regression Analysis: Concentration (mg/L) versus IR45 (mV), IR45^2 (mV)

```
The regression equation is
Concentration (mg/L) = 283.5 - 2.819 IR45 LED On-Off(mV)
                       + 0.007765 IR45 LED On-Off(mV)**2

S = 44.9292   R-Sq = 97.0%   R-Sq(adj) = 96.7%

PRESS = 58572.0   R-Sq(pred) = 95.85%

Analysis of Variance

Source       DF       SS      MS       F      P
Regression    2  1369828  684914  339.30  0.000
Error        21    42391    2019
Total        23  1412219


Sequential Analysis of Variance

Source      DF       SS       F      P
Linear       1  1206362  128.92  0.000
Quadratic    1   163466   80.98  0.000
```

Residual Plots for Concentration (mg/L)

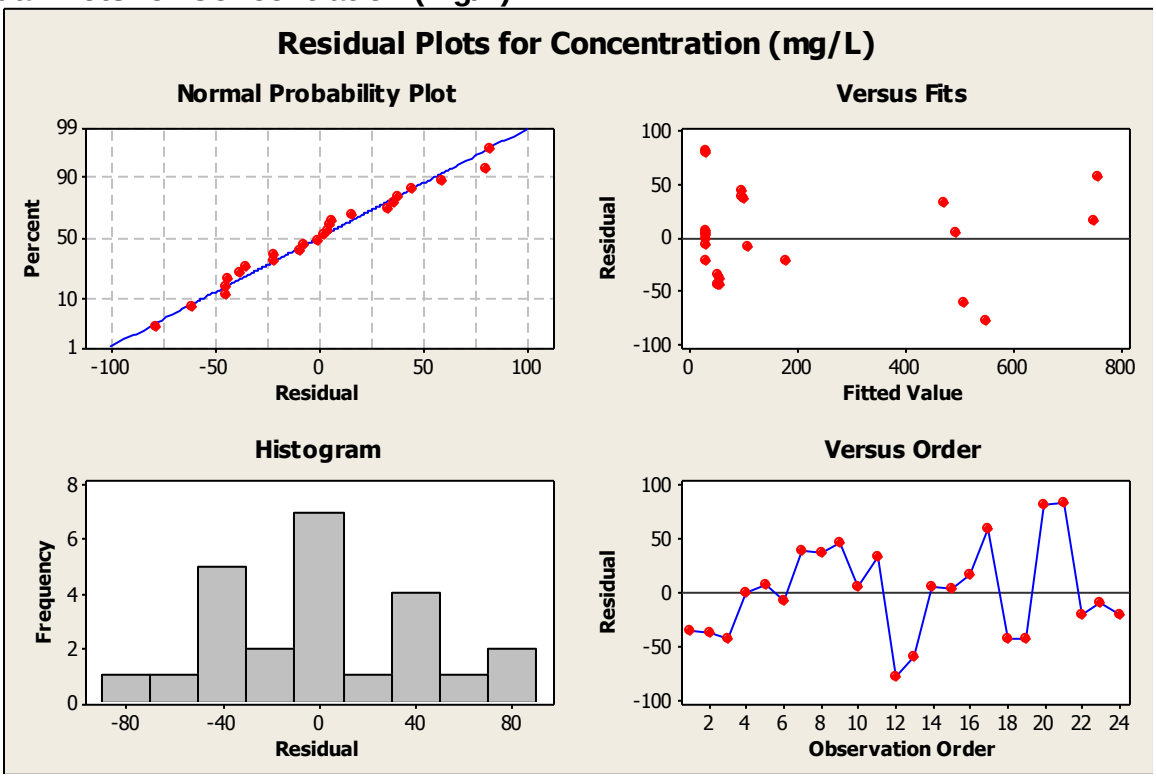

Polynomial Regression Analysis: Concentration (mg/L) versus OR180 (mV), OR180^2 (mV)

```
The regression equation is
Concentration (mg/L) = 2153 - 1.913 OR180 LED On-Off (mV)
                       + 0.000416 OR180 LED On-Off (mV)**2


S = 53.0543   R-Sq = 95.8%   R-Sq(adj) = 95.4%

PRESS = 78614.0   R-Sq(pred) = 94.43%

Analysis of Variance

Source       DF       SS      MS       F      P
Regression    2  1353110  676555  240.36  0.000
Error        21    59110    2815
Total        23  1412219


Sequential Analysis of Variance

Source      DF       SS       F      P
Linear       1  1302791  261.92  0.000
Quadratic    1    50319   17.88  0.000
```

Residual Plots for Concentration (mg/L)

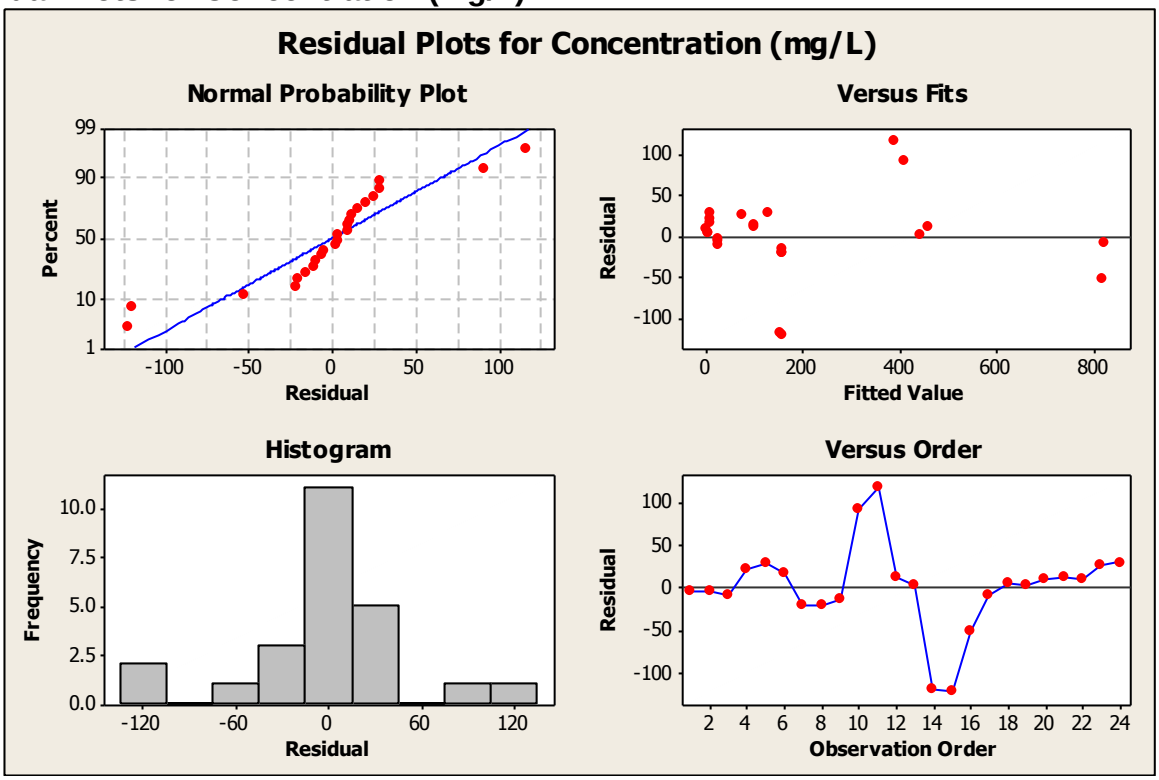

Polynomial Stepwise Output

Stepwise Regression: Concentration (mg/L) versus IR45 (mV), OR45 (mV), OR180 (mV), IR45^2 (mV), OR180^2 (mV)

```
  Alpha-to-Enter: 0.15  Alpha-to-Remove: 0.15

Response is Concentration (mg/L) on 5 predictors, with N = 24


Step                        1        2        3
Constant                -101.4    283.5    701.6

IR45^2                 0.00333  0.00776  0.00598
T-Value                  17.28     9.00     7.12
P-Value                  0.000    0.000    0.000

IR45 LED On-Off(mV)                -2.82    -2.36
T-Value                            -5.20    -5.27
P-Value                            0.000    0.000

OR180 LED On-Off (mV)                      -0.239
T-Value                                     -3.66
P-Value                                     0.002

S                          66.4     44.9     35.6
R-Sq                      93.14    97.00    98.20
R-Sq(adj)                 92.83    96.71    97.93
Mallows Cp                68.6     20.8      7.2
```

Regression Analysis: Concentration (mg/L) versus IR45^2 (mV), IR45 (mV), OR180 (mV)

The regression equation is
Concentration (mg/L) = 702 + 0.00598 IR45^2 - 2.36 IR45 LED On-Off(V)
- 0.239 OR180 LED On-Off (V)

Predictor	Coef	SE Coef	T	P
Constant	701.6	128.8	5.45	0.000
IR45^2	0.0059804	0.0008395	7.12	0.000
IR45 LED On-Off(mV)	-2.3597	0.4479	-5.27	0.000
OR180 LED On-Off (mV)	-0.23948	0.06535	-3.66	0.002

S = 35.6095 R-Sq = 98.2% R-Sq(adj) = 97.9%

PRESS = 38615.7 R-Sq(pred) = 97.27%

Analysis of Variance

Source	DF	SS	MS	F	P
Regression	3	1386859	462286	364.57	0.000
Residual Error	20	25361	1268		
Total	23	1412219			

Source	DF	Seq SS
IR45^2	1	1315328
IR45 LED On-Off(mV)	1	54500
OR180 LED On-Off (mV)	1	17031

Unusual Observations

Obs	IR45^2	Concentration (mg/L)	Fit	SE Fit	Residual	St Resid
12	194305	471.08	537.31	13.59	-66.23	-2.01R

R denotes an observation with a large standardized residual.

Residual Plots for Concentration (mg/L)

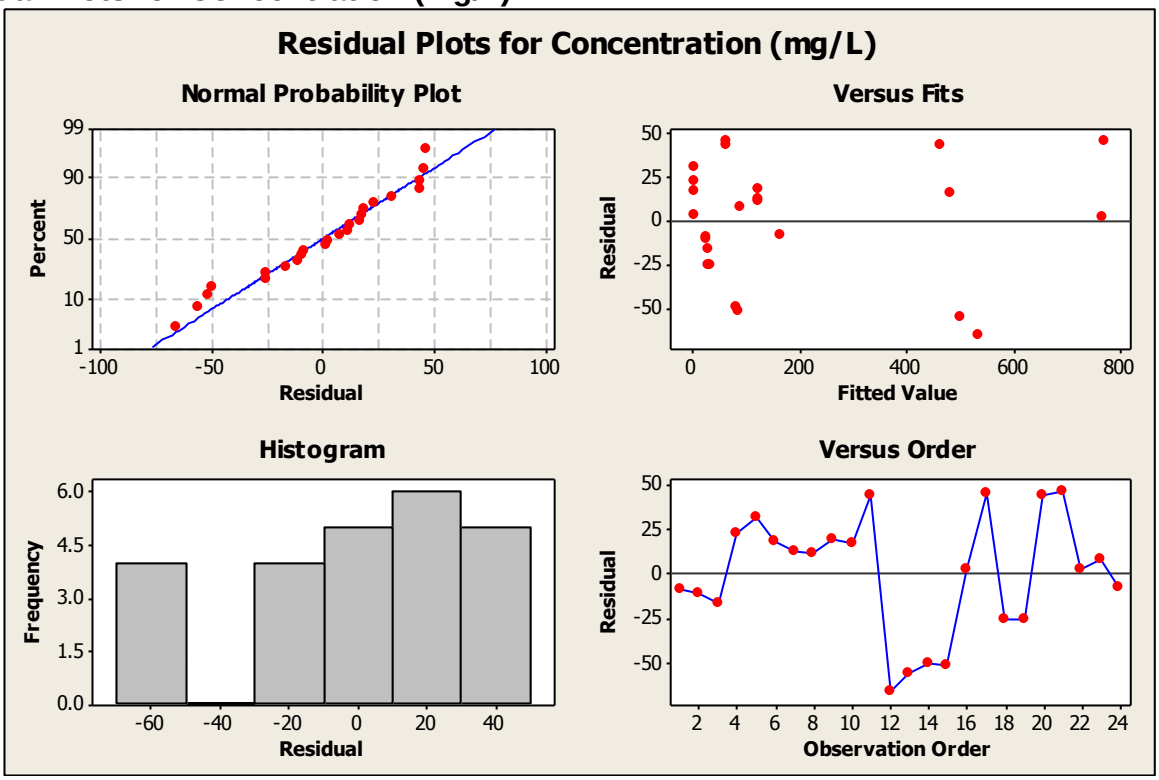

Appendix B – Wildcat Bridge Statistical Analysis, Minitab Output

Regression Analysis: Concentration (mg/L) versus (mV)

```
The regression equation is
Concentration (mg/L) = - 271 + 3.58 IR45 LED On-Off(mV)

Predictor              Coef  SE Coef       T      P
Constant            -271.37    16.05  -16.91  0.000
IR45 LED On-Off(mV)  3.58183  0.03427  104.52  0.000


S = 55.9911   R-Sq = 99.9%   R-Sq(adj) = 99.9%

PRESS = 59656.4   R-Sq(pred) = 99.83

Analysis of Variance

Source          DF        SS        MS         F      P
Regression       1  34250773  34250773  10925.26  0.000
Residual Error  15     47025      3135
Total           16  34297799

Unusual Observations

       IR45 LED  Concentration
Obs  On-Off(mV)         (mg/L)     Fit  SE Fit  Residual  St Resid
  6         141          374.8   235.1    14.1     139.7      2.58R
 10        1280         4346.7  4314.4    37.8      32.2      0.78 X
 11        1384         4654.3  4685.2    41.2     -30.9     -0.81 X
 17          83          148.5    25.6    14.7     123.0      2.28R

R denotes an observation with a large standardized residual.
X denotes an observation whose X value gives it large leverage.
```

Residual Plots for Concentration (mg/L)

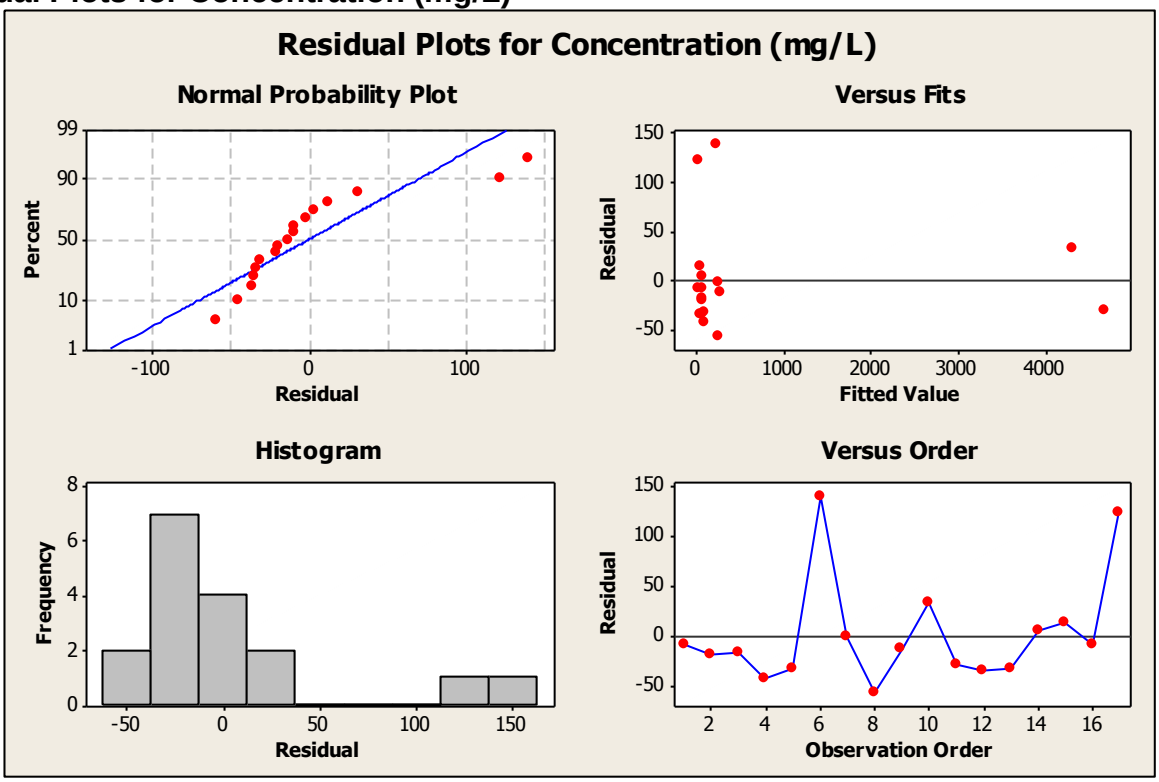

Regression Analysis: Concentration (mg/L) versus OR45 (mV)

The regression equation is
Concentration (mg/L) = - 639 + 12.4 OR45 LED On-Off (mV)

Predictor	Coef	SE Coef	T	P
Constant	-639.02	28.85	-22.15	0.000
OR45 LED On-Off (mV)	12.4185	0.1888	65.79	0.000

S = 88.8688 R-Sq = 99.7% R-Sq(adj) = 99.6%

PRESS = 154042 R-Sq(pred) = 99.55%

Analysis of Variance

Source	DF	SS	MS	F	P
Regression	1	34179334	34179334	4327.78	0.000
Residual Error	15	118465	7898		
Total	16	34297799			

Unusual Observations

Obs	OR45 LED On-Off (mV)	Concentration (mg/L)	Fit	SE Fit	Residual	St Resid
10	405	4346.7	4385.5	61.1	-38.8	-0.60 X
11	421	4654.3	4586.7	64.0	67.6	1.10 X

X denotes an observation whose X value gives it large leverage.

Residual Plots for Concentration (mg/L)

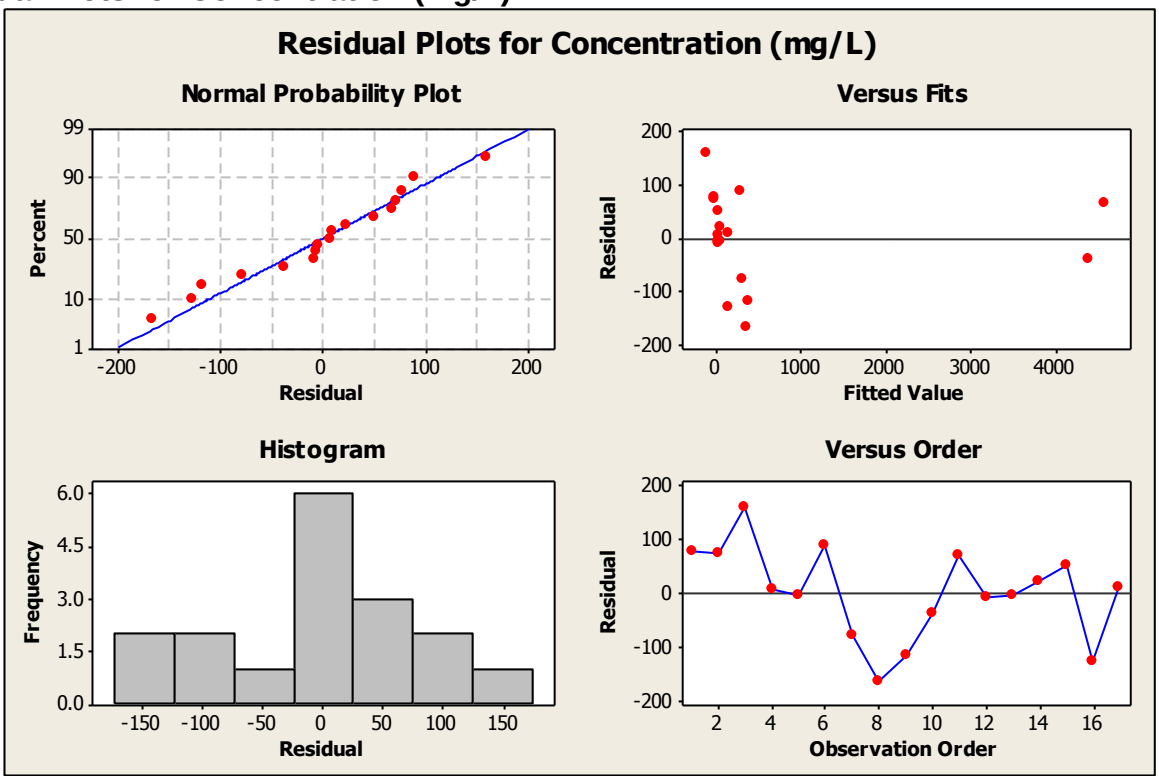

Regression Analysis: Concentration (mg/L) versus OR180 (mV)

```
The regression equation is
Concentration (mg/L) = 4757 - 2.66 OR180 LED On-Off (mV)

Predictor                  Coef  SE Coef       T      P
Constant                4757.28    68.74   69.20  0.000
OR180 LED On-Off (mV)  -2.65744  0.04180  -63.58  0.000

S = 91.9380   R-Sq = 99.6%   R-Sq(adj) = 99.6%

PRESS = 233303   R-Sq(pred) = 99.32%

Analysis of Variance

Source           DF        SS        MS        F      P
Regression        1  34171010  34171010  4042.66  0.000
Residual Error   15    126789      8453
Total            16  34297799

Unusual Observations

  OR180 LED
     On-Off  Concentration
Obs    (mV)         (mg/L)     Fit  SE Fit  Residual  St Resid
 10     112         4346.7  4458.9    64.3    -112.2     -1.71 X
 11      90         4654.3  4518.1    65.2     136.2      2.10RX

R denotes an observation with a large standardized residual.
X denotes an observation whose X value gives it large leverage.
```

Residual Plots for Concentration (mg/L)

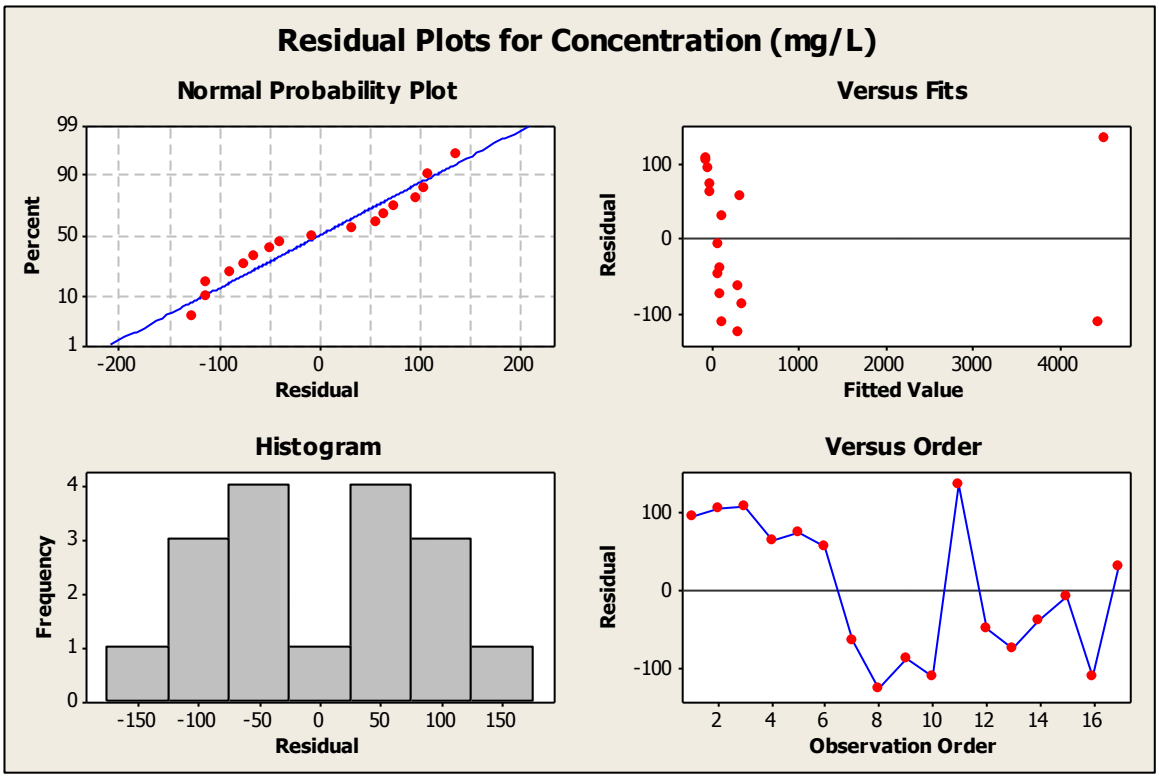
Residual Plots for Concentration (mg/L)
Normal Probability Plot
Percent
99
90
50
10
1
-200
-100
0
100
200
Residual
Versus Fits
Residual
100
0
-100
0
1000
2000
3000
4000
Fitted Value
Histogram
Frequency
4
3
2
1
0
-150
-100
-50
0
50
100
150
Residual
Versus Order
Residual
100
0
-100
2
4
6
8
10
12
14
16
Observation Order

Linear Stepwise Analysis

Best Subsets Regression: Concentration (mg/L) versus IR45 (mV), OR45 (mV), OR180 (mV)

Response is Concentration (mg/L)

Vars	R-Sq	R-Sq(adj)	Mallows Cp	S	IR45 LED On-Off (mV)	OR45 LED On-Off (mV)	OR180 LED On-Off (mV)
1	99.9	99.9	3.5	55.991	X		
1	99.7	99.6	28.7	88.869		X	
2	99.9	99.9	2.1	51.496	X		X
2	99.9	99.9	3.3	53.968	X	X	
3	99.9	99.9	4.0	53.323	X	X	X

Regression Analysis: Concentration (mg/L) versus OR180 (mV), IR45 (mV)

The regression equation is
Concentration (mg/L) = 984 - 0.664 OR180 LED On-Off (mV)
+ 2.69 IR45 LED On-Off(mV)

Predictor	Coef	SE Coef	T	P
Constant	984.2	650.0	1.51	0.152
OR180 LED On-Off (mV)	-0.6639	0.3436	-1.93	0.074
IR45 LED On-Off(mV)	2.6900	0.4626	5.81	0.000

S = 51.4955 R-Sq = 99.9% R-Sq(adj) = 99.9%

PRESS = 47198.0 R-Sq(pred) = 99.86%

Analysis of Variance

Source	DF	SS	MS	F	P
Regression	2	34260673	17130337	6459.92	0.000
Residual Error	14	37125	2652		
Total	16	34297799			

```
Source                   DF     Seq SS
OR180 LED On-Off (mV)     1   34171010
IR45 LED On-Off(mV)       1      89664


Unusual Observations

      OR180
        LED
     On-Off  Concentration
Obs     (mV)          (mg/L)      Fit  SE Fit  Residual  St Resid
  6    1671          374.8    255.5   16.7     119.4      2.45R
 10     112         4346.7   4353.7   40.3      -7.1     -0.22 X
 11      90         4654.3   4647.0   42.7       7.3      0.25 X
 17    1746          148.5     47.8   17.8     100.7      2.08R

R denotes an observation with a large standardized residual.
X denotes an observation whose X value gives it large leverage.
```

Residual Plots for Concentration (mg/L)

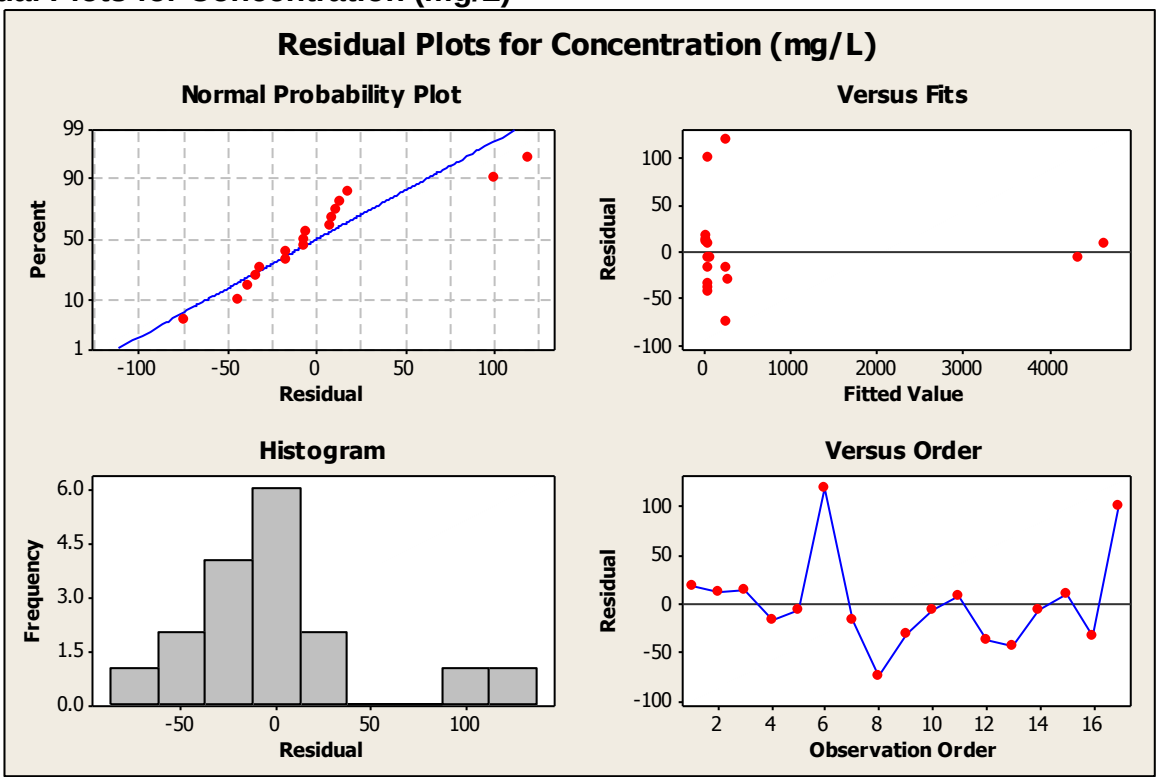

Appendix C – Pine Knot North Statistical Analysis, Minitab Output

Regression Analysis: Concentration (mg/L) versus IR45 (mV)

```
The regression equation is
Concentration (mg/L) = - 79.8 + 0.197 IR45 LED On-Off(mV)

Predictor              Coef  SE Coef      T      P
Constant            -79.79    13.55  -5.89  0.001
IR45 LED On-Off(mV) 0.19664  0.02803   7.01  0.000

S = 3.90085   R-Sq = 87.5%   R-Sq(adj) = 85.8%

PRESS = 161.746   R-Sq(pred) = 81.09%

Analysis of Variance

Source          DF      SS      MS      F      P
Regression       1  748.67  748.67  49.20  0.000
Residual Error   7  106.52   15.22
Total            8  855.19

Unusual Observations

      IR45 LED  Concentration
Obs  On-Off(mV)        (mg/L)   Fit  SE Fit  Residual  St Resid
  3        444          15.85  7.48    1.67      8.37      2.37R

R denotes an observation with a large standardized residual.
```

Residual Plots for Concentration (mg/L)

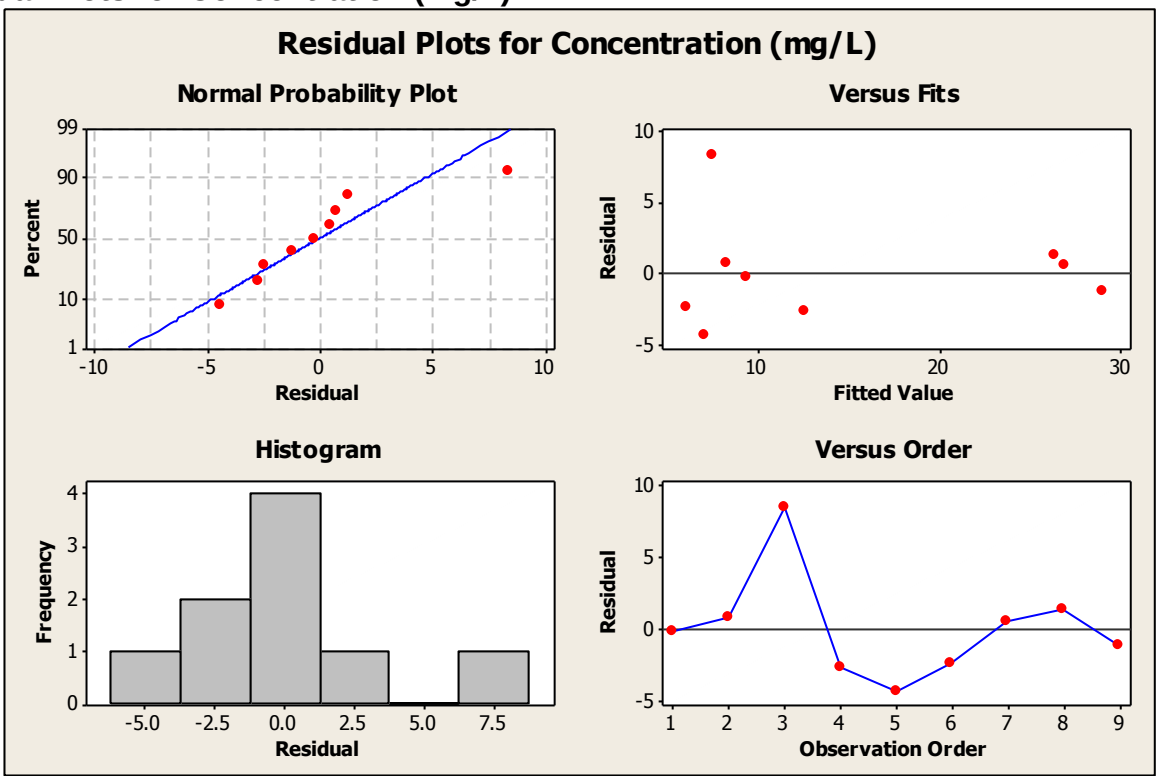

Regression Analysis: Concentration (mg/L) versus OR45 (mV)

The regression equation is
Concentration (mg/L) = - 20.6 + 0.338 OR45 LED On-Off (mV)

Predictor	Coef	SE Coef	T	P
Constant	-20.58	18.17	-1.13	0.295
OR45 LED On-Off (mV)	0.3378	0.1710	1.98	0.089

S = 8.85724 R-Sq = 35.8% R-Sq(adj) = 26.6%

PRESS = 977.309 R-Sq(pred) = 0.00%

Analysis of Variance

Source	DF	SS	MS	F	P
Regression	1	306.03	306.03	3.90	0.089
Residual Error	7	549.15	78.45		
Total	8	855.19			

Residual Plots for Concentration (mg/L)

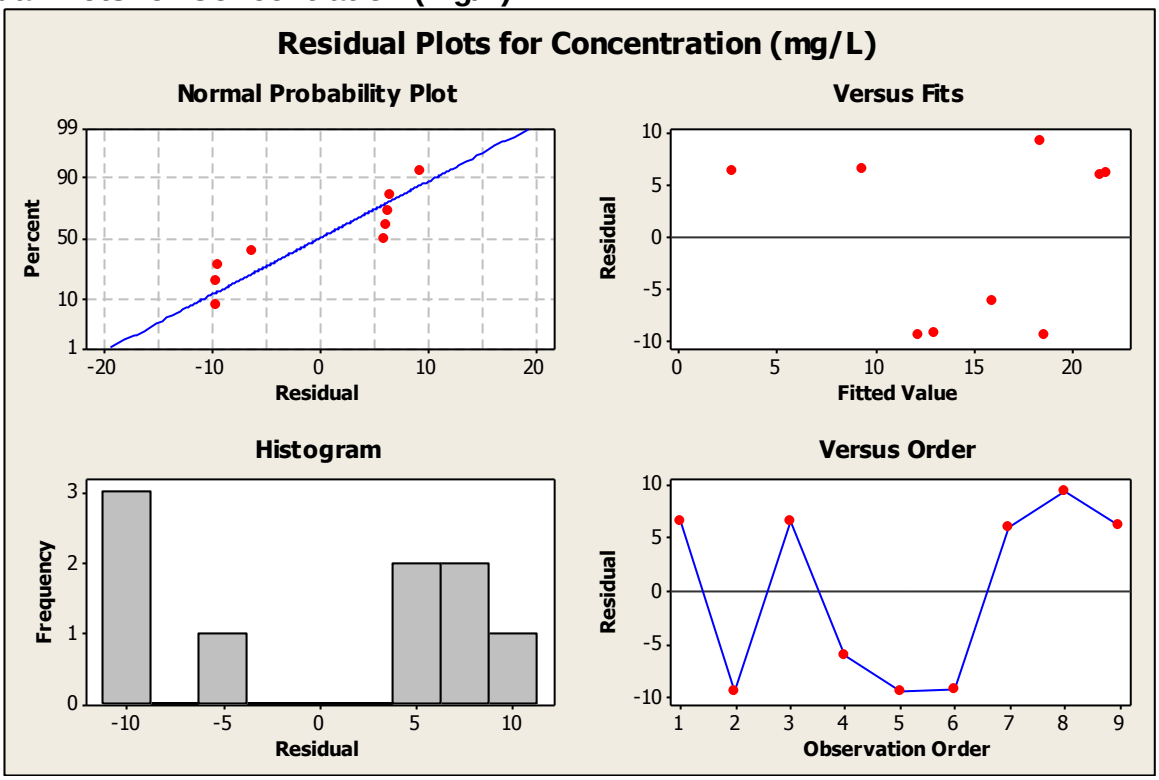

Regression Analysis: Concentration (mg/L) versus OR180 (mV)

The regression equation is
Concentration (mg/L) = - 157 + 0.0895 OR180 LED On-Off (mV)

Predictor	Coef	SE Coef	T	P
Constant	-157.12	43.44	-3.62	0.009
OR180 LED On-Off (mV)	0.08954	0.02260	3.96	0.005

S = 6.13808 R-Sq = 69.2% R-Sq(adj) = 64.8%

PRESS = 383.015 R-Sq(pred) = 55.21%

Analysis of Variance

Source	DF	SS	MS	F	P
Regression	1	591.46	591.46	15.70	0.005
Residual Error	7	263.73	37.68		
Total	8	855.19			

Residual Plots for Concentration (mg/L)

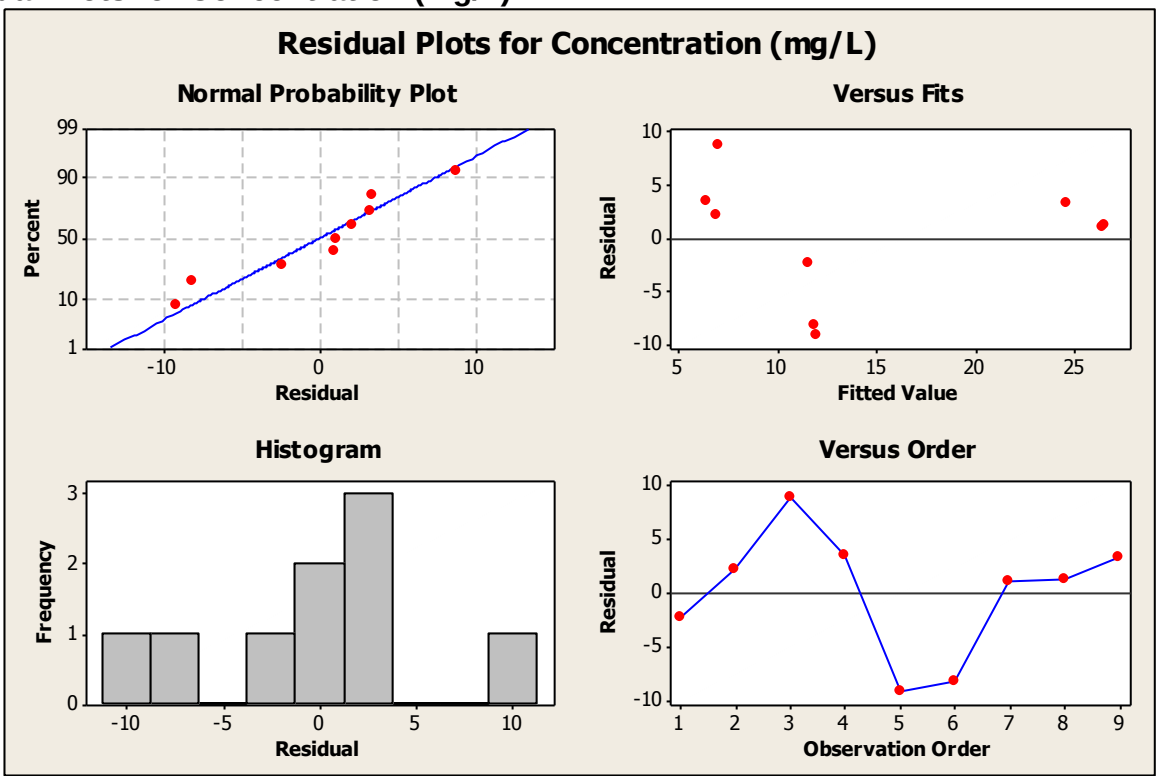

Linear Stepwise Function Output

Stepwise Regression: Concentration (mg/L) versus IR45 (mV), OR45 (mV), OR180 (mV)

```
  Alpha-to-Enter: 0.15  Alpha-to-Remove: 0.15

Response is Concentration (mg/L) on 3 predictors, with N = 9


Step                     1
Constant           -79.79

IR45 LED On-Off(mV)  0.197
T-Value               7.01
P-Value              0.000

S                     3.90
R-Sq                 87.54
R-Sq(adj)            85.77
Mallows Cp             0.6
```

Polynomial Regression Analysis: Concentration (mg/L) versus OR45 (mV), OR45^2 (mV)

```
The regression equation is
Concentration (mg/L) = 127.7 - 2.770 OR45 LED On-Off (mV)
                       + 0.01573 OR45 LED On-Off (mV)**2


S = 7.43423   R-Sq = 61.2%   R-Sq(adj) = 48.3%

PRESS = 1832.82   R-Sq(pred) = 0.00%

Analysis of Variance

Source       DF       SS       MS     F      P
Regression    2  523.582  261.791  4.74  0.058
Error         6  331.607   55.268
Total         8  855.188


Sequential Analysis of Variance

Source      DF       SS     F      P
Linear       1  306.033  3.90  0.089
Quadratic    1  217.548  3.94  0.094
```

Residual Plots for Concentration (mg/L)

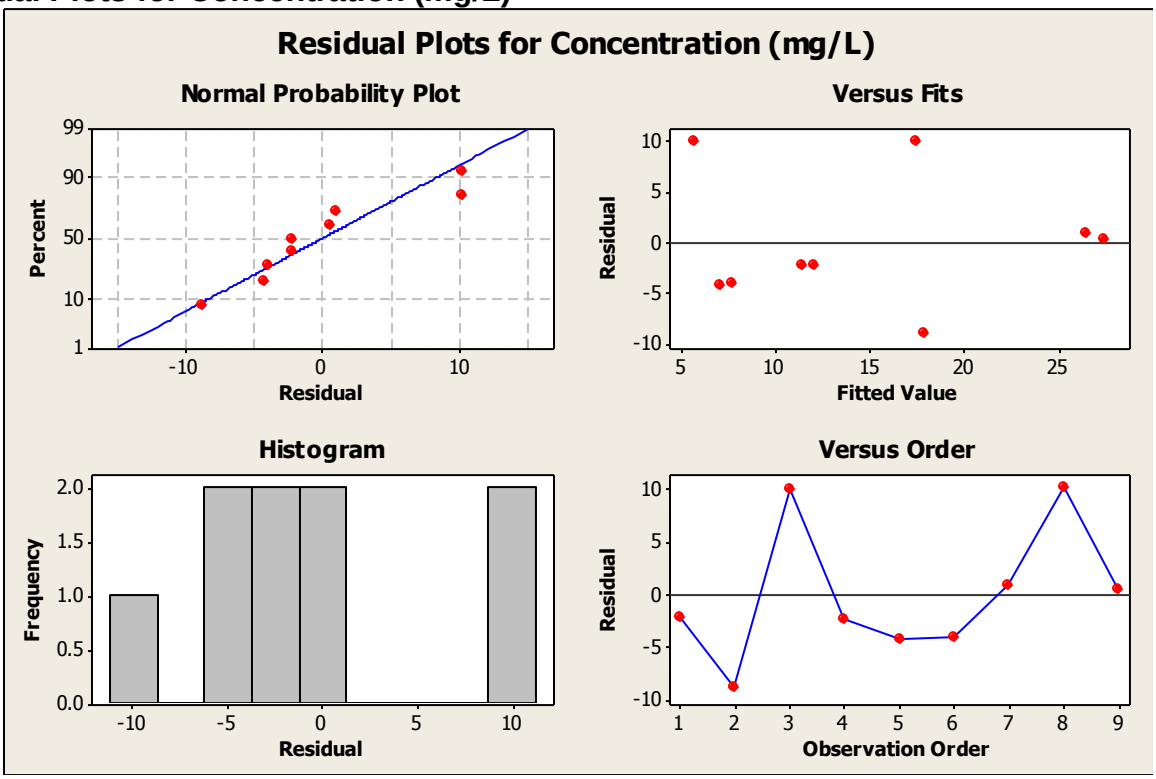

Polynomial Regression Analysis: Concentration (mg/L) versus OR180 (mV), OR180^2 (mV)

```
The regression equation is
Concentration (mg/L) = 3810 - 4.002 OR180 LED On-Off (mV)
                       + 0.001052 OR180 LED On-Off (mV)**2


S = 3.82314   R-Sq = 89.7%   R-Sq(adj) = 86.3%

PRESS = 184.156   R-Sq(pred) = 78.47%

Analysis of Variance

Source       DF       SS       MS      F      P
Regression    2  767.490  383.745  26.25  0.001
Error         6   87.698   14.616
Total         8  855.188


Sequential Analysis of Variance

Source      DF       SS      F      P
Linear       1  591.457  15.70  0.005
Quadratic    1  176.033  12.04  0.013
```

Residual Plots for Concentration (mg/L)

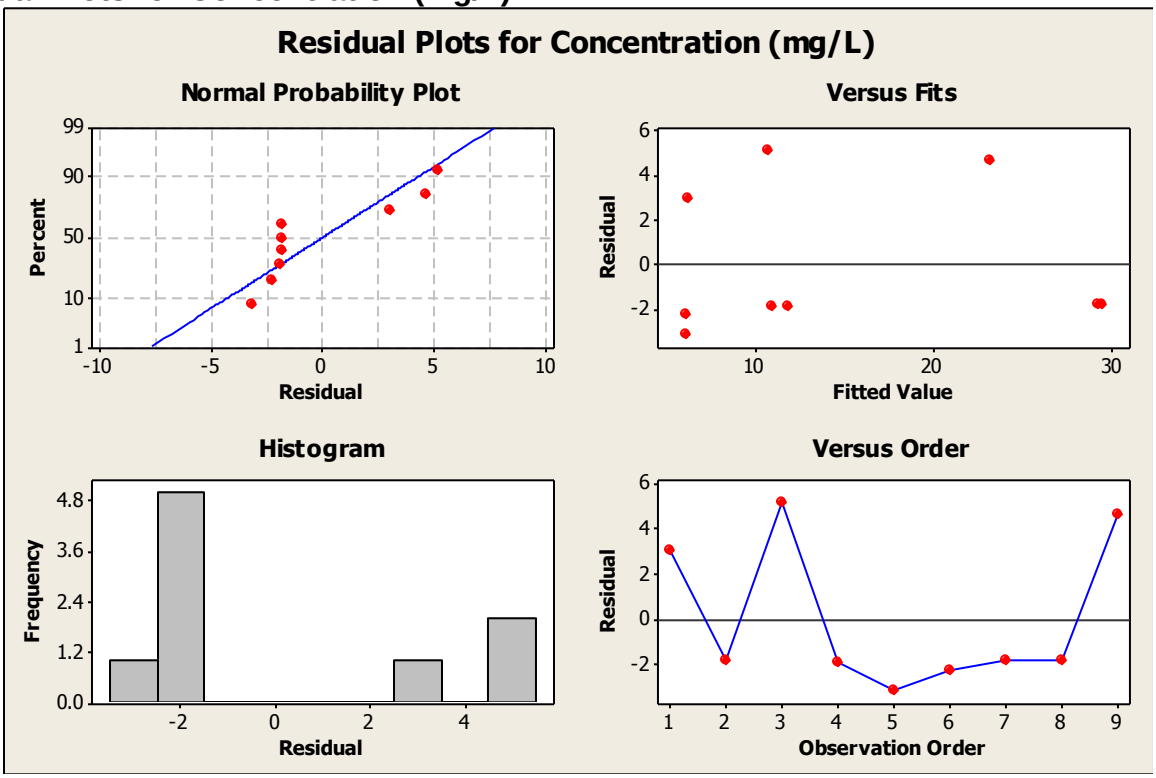

Polynomial Stepwise Function Output

Stepwise Regression: Concentration (mg/L) versus IR45 (mV), OR45 (mV), OR180 (mV), OR45^2 (mV), OR180^2 (mV)

Alpha-to-Enter: 0.15 Alpha-to-Remove: 0.15

Response is Concentration (mg/L) on 5 predictors, with N = 9

Step	1
Constant	-79.79
IR45 LED On-Off(mV)	0.197
T-Value	7.01
P-Value	0.000
S	3.90
R-Sq	87.54
R-Sq(adj)	85.77

Appendix D – Pine Knot South Statistical Analysis, Minitab Output

Regression Analysis: Concentration (mg/L) versus IR45 (mV)

```
The regression equation is
Concentration (mg/L) = 118 - 0.240 IR45 LED On-Off(mV)

Predictor               Coef  SE Coef      T      P
Constant              117.71    24.40   4.82  0.003
IR45 LED On-Off(mV) -0.24019  0.06485  -3.70  0.010

S = 16.7244   R-Sq = 69.6%   R-Sq(adj) = 64.5%

PRESS = 256284   R-Sq(pred) = 0.00%

Analysis of Variance

Source          DF      SS      MS      F      P
Regression       1  3837.3  3837.3  13.72  0.010
Residual Error   6  1678.2   279.7
Total            7  5515.6

Unusual Observations

      IR45 LED  Concentration
Obs  On-Off(mV)        (mg/L)     Fit  SE Fit  Residual  St Resid
  1        125          90.16   87.81   16.69      2.35      2.06RX

R denotes an observation with a large standardized residual.
X denotes an observation whose X value gives it large leverage.
```

Residual Plots for Concentration (mg/L)

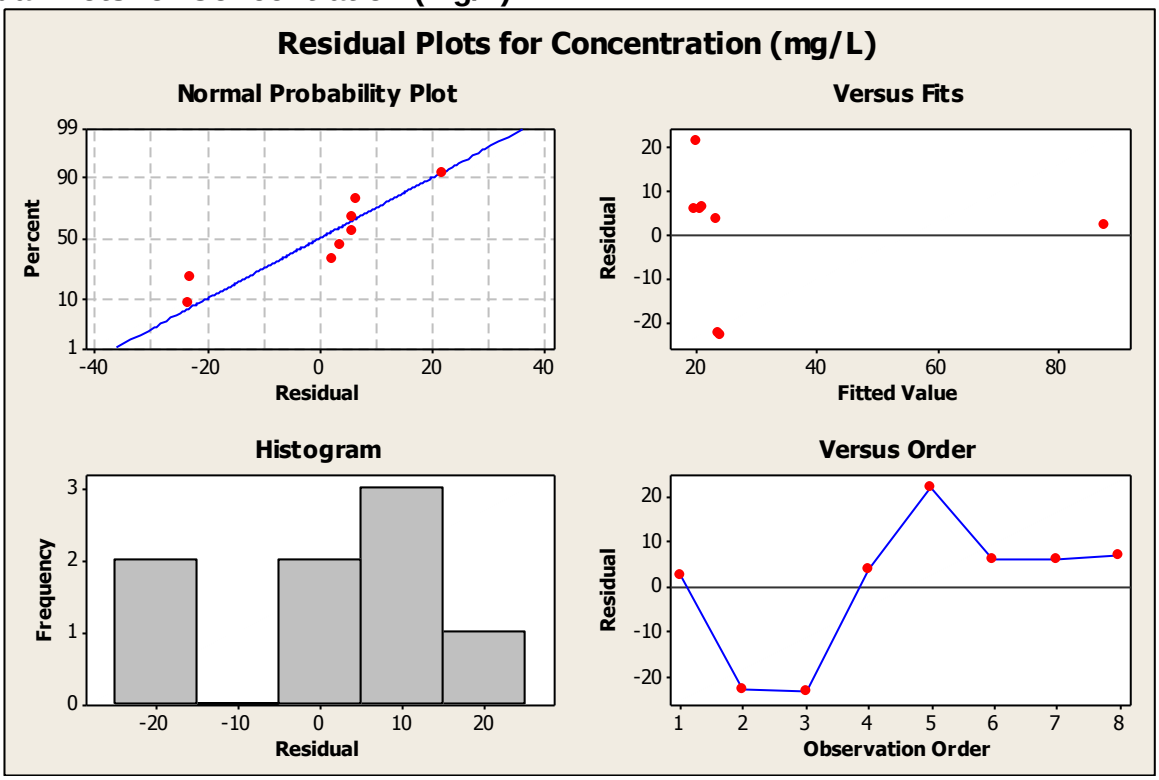

Regression Analysis: Concentration (mg/L) versus OR45 (mV)

The regression equation is
Concentration (mg/L) = 228 - 1.95 OR45 LED On-Off (mV)

Predictor	Coef	SE Coef	T	P
Constant	227.63	51.48	4.42	0.004
OR45 LED On-Off (mV)	-1.9545	0.5060	-3.86	0.008

S = 16.2378 R-Sq = 71.3% R-Sq(adj) = 66.5%

PRESS = 4126.29 R-Sq(pred) = 25.19%

Analysis of Variance

Source	DF	SS	MS	F	P
Regression	1	3933.6	3933.6	14.92	0.008
Residual Error	6	1582.0	263.7		
Total	7	5515.6			

Unusual Observations

Obs	OR45 LED On-Off (mV)	Concentration (mg/L)	Fit	SE Fit	Residual	St Resid
1	75	90.16	82.02	14.64	8.14	1.16 X

X denotes an observation whose X value gives it large leverage.

Residual Plots for Concentration (mg/L)

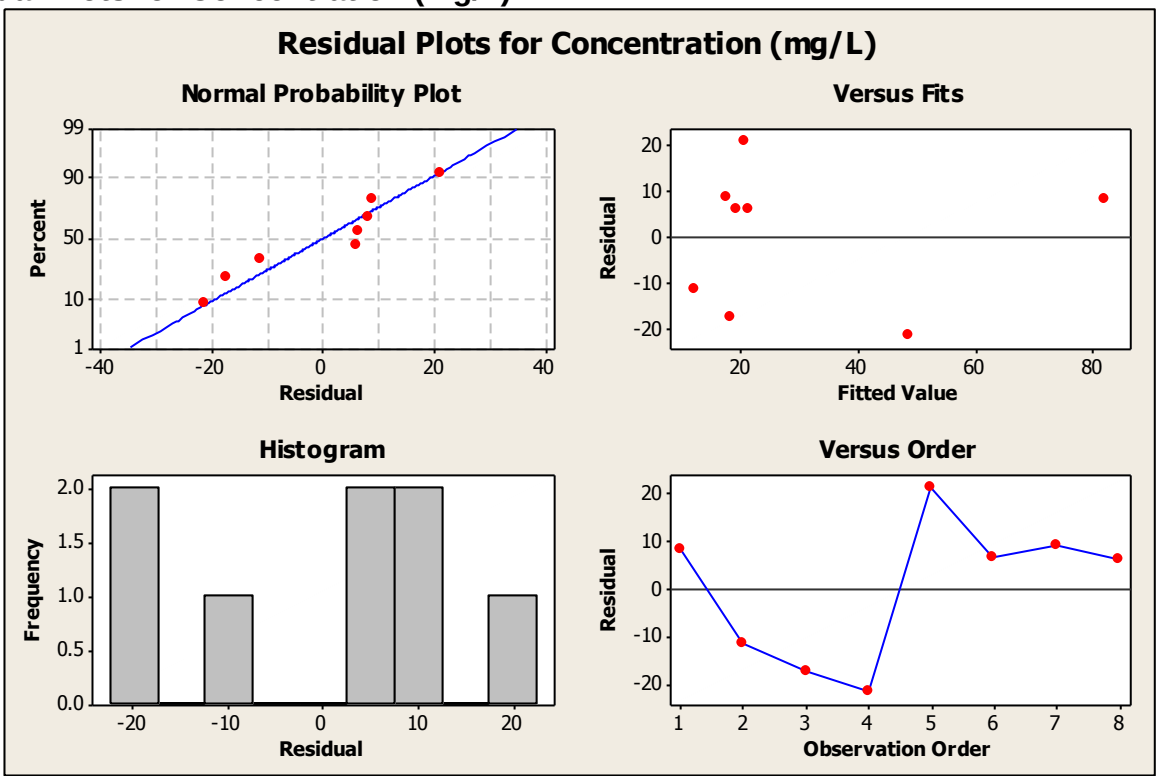

Regression Analysis: Concentration (mg/L) versus OR180 (mV)

```
The regression equation is
Concentration (mg/L) = 548 - 0.249 OR180 LED On-Off (mV)

Predictor                 Coef  SE Coef      T      P
Constant                548.07    59.74   9.17  0.000
OR180 LED On-Off (mV) -0.24898  0.02868  -8.68  0.000

S = 8.23238   R-Sq = 92.6%   R-Sq(adj) = 91.4%

PRESS = 1084.56   R-Sq(pred) = 80.34%

Analysis of Variance

Source           DF      SS      MS      F      P
Regression        1  5109.0  5109.0  75.38  0.000
Residual Error    6   406.6    67.8
Total             7  5515.6

Unusual Observations

  OR180 LED
     On-Off  Concentration
Obs      (mV)         (mg/L)    Fit  SE Fit  Residual  St Resid
  1     1829          90.16  92.64    7.78     -2.47     -0.92 X
  5     2105          41.79  23.96    2.99     17.84      2.33R

R denotes an observation with a large standardized residual.
X denotes an observation whose X value gives it large leverage.
```

Residual Plots for Concentration (mg/L)

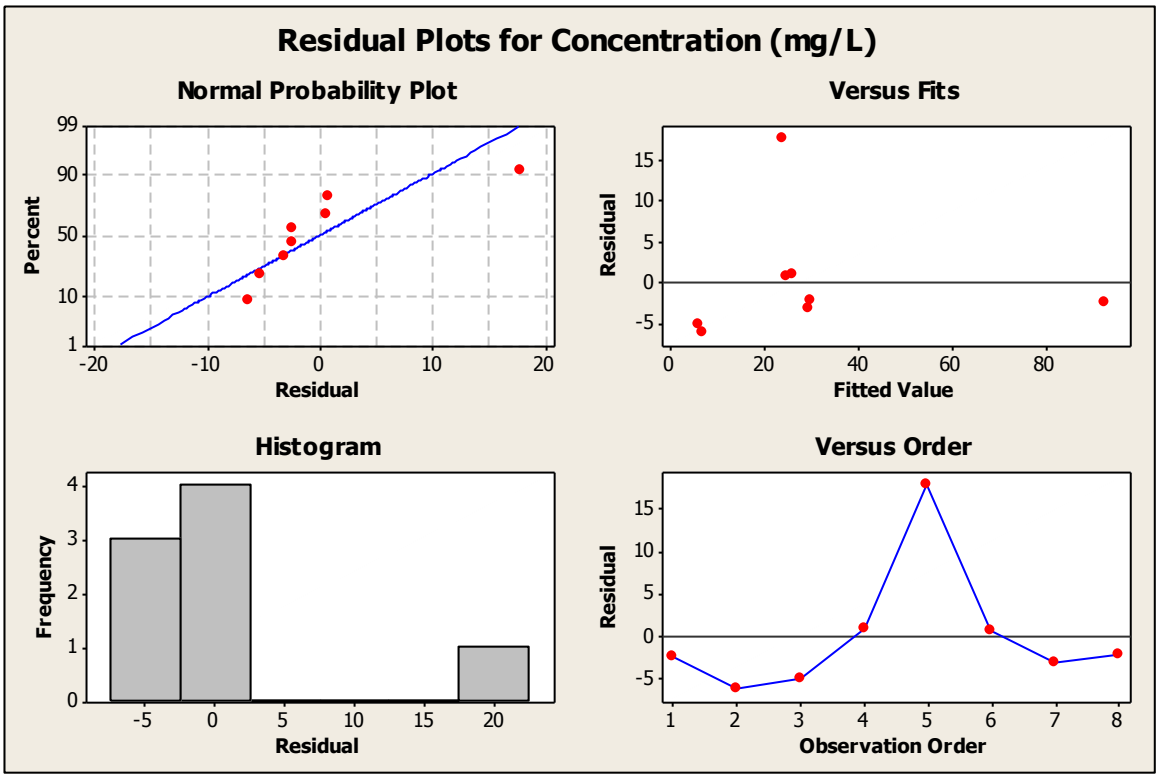

Linear Stepwise Output

Stepwise Regression: Concentration (mg/L) versus IR45 (mV), OR45 LED (mV), OR180 (mV)

```
  Alpha-to-Enter: 0.15  Alpha-to-Remove: 0.15

Response is Concentration (mg/L) on 3 predictors, with N = 8


Step                        1
Constant                548.1

OR180 LED On-Off (mV)  -0.249
T-Value                -8.68
P-Value                0.000

S                       8.23
R-Sq                   92.63
R-Sq(adj)              91.40
Mallows Cp               0.9
```

Polynomial Regression Analysis: Concentration (mg/L) versus IR45 (mV), IR45^2 (mV)

```
The regression equation is
Concentration (mg/L) = 453.9 - 3.754 IR45 LED On-Off(mV)
                       + 0.006685 IR45 LED On-Off(mV)**2


S = 10.0017   R-Sq = 90.9%   R-Sq(adj) = 87.3%

PRESS = 99860346   R-Sq(pred) = 0.00%

Analysis of Variance

Source       DF       SS       MS      F      P
Regression    2  5015.41  2507.71  25.07  0.002
Error         5   500.17   100.03
Total         7  5515.59


Sequential Analysis of Variance

Source      DF       SS      F      P
Linear       1  3837.35  13.72  0.010
Quadratic    1  1178.07  11.78  0.019
```

Residual Plots for Concentration (mg/L)

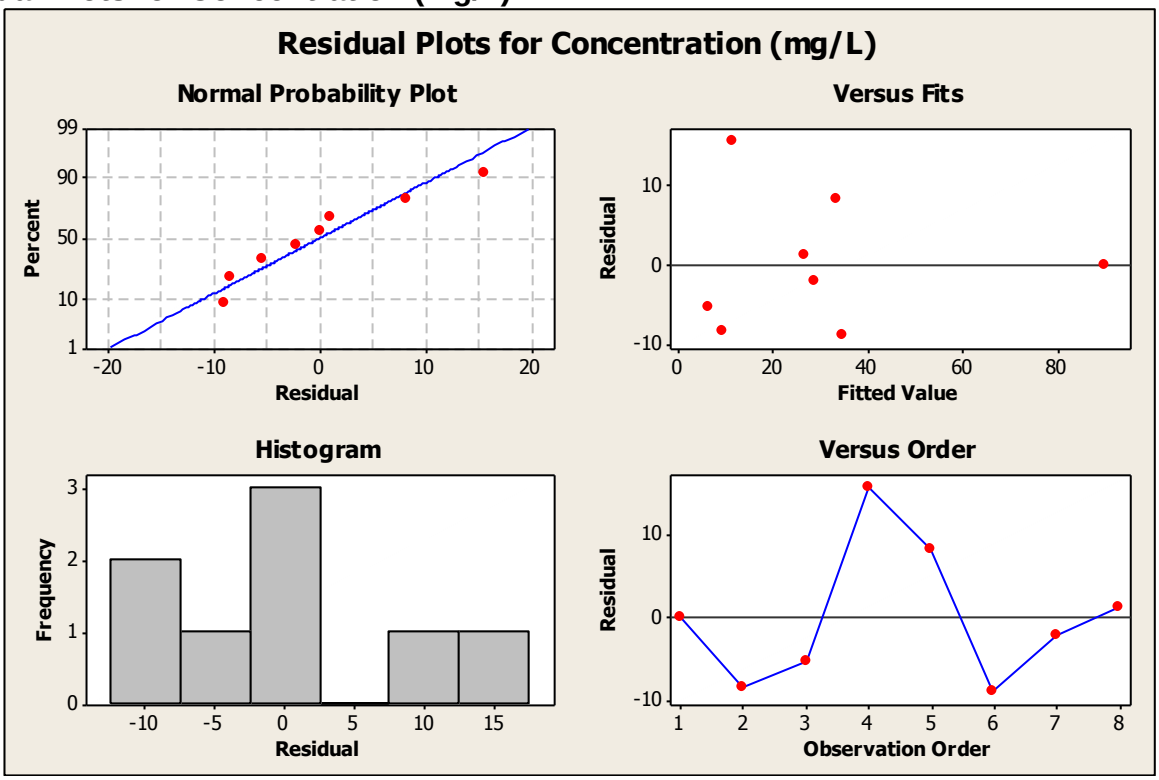

Polynomial Stepwise Output

Stepwise Regression: Concentration (mg/L) versus IR45 (mV), OR45 (mV), OR180 (mV)

```
  Alpha-to-Enter: 0.15  Alpha-to-Remove: 0.15

Response is Concentration (mg/L) on 4 predictors, with N = 8


Step                        1
Constant                548.1

OR180 LED On-Off (mV) -0.249
T-Value                -8.68
P-Value                0.000

S                       8.23
R-Sq                   92.63
R-Sq(adj)              91.40
Mallows Cp               5.0
```

Appendix E – Upatoi North Statistical Analysis, Minitab Output

Regression Analysis: Concentration (mg/L) versus IR45 (mV)

```
The regression equation is
Concentration (mg/L) = 14.6 + 0.0498 IR45 LED On-Off(mV)

Predictor              Coef  SE Coef     T      P
Constant             14.621    9.234  1.58  0.164
IR45 LED On-Off(mV) 0.04977  0.03289  1.51  0.181

S = 6.34587   R-Sq = 27.6%   R-Sq(adj) = 15.6%

PRESS = 2146.00   R-Sq(pred) = 0.00%

Analysis of Variance

Source          DF      SS     MS     F      P
Regression       1   92.18  92.18  2.29  0.181
Residual Error   6  241.62  40.27
Total            7  333.80

Unusual Observations

      IR45 LED  Concentration
Obs  On-Off(mV)        (mg/L)    Fit  SE Fit  Residual  St Resid
  1        105          25.30  19.86    5.93      5.44      2.41RX

R denotes an observation with a large standardized residual.
X denotes an observation whose X value gives it large leverage.
```

Residual Plots for Concentration (mg/L)

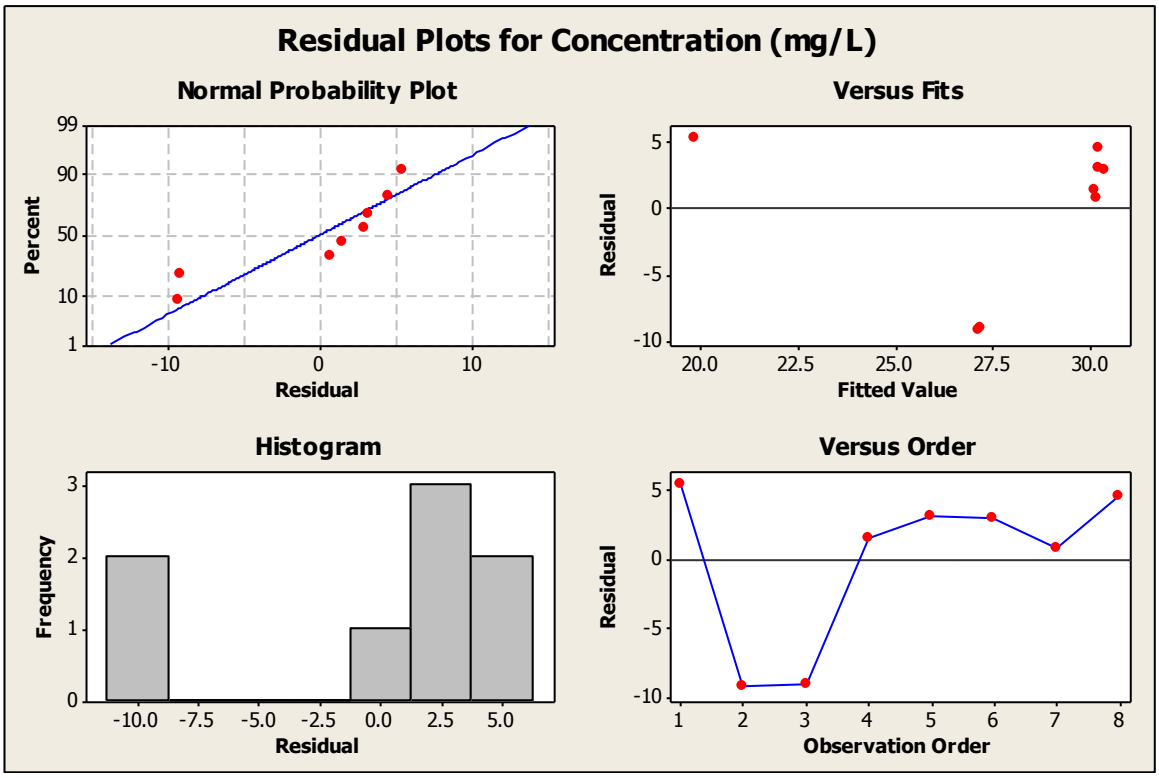

Regression Analysis: Concentration (mg/L) versus OR45 (mV)

```
The regression equation is
Concentration (mg/L) = 19.6 + 0.0497 OR45 LED On-Off (mV)

Predictor               Coef  SE Coef     T      P
Constant               19.60    10.30  1.90  0.106
OR45 LED On-Off (mV) 0.04968  0.05787  0.86  0.424


S = 7.03890   R-Sq = 10.9%   R-Sq(adj) = 0.0%

PRESS = 5278.92   R-Sq(pred) = 0.00%

Analysis of Variance

Source          DF      SS     MS     F      P
Regression       1   36.52  36.52  0.74  0.424
Residual Error   6  297.28  49.55
Total            7  333.80


Unusual Observations

       OR45 LED  Concentration
Obs   On-Off (mV)        (mg/L)     Fit  SE Fit  Residual  St Resid
  1           61          25.30   22.64    6.90      2.66      1.94 X

X denotes an observation whose X value gives it large leverage.
```

Residual Plots for Concentration (mg/L)

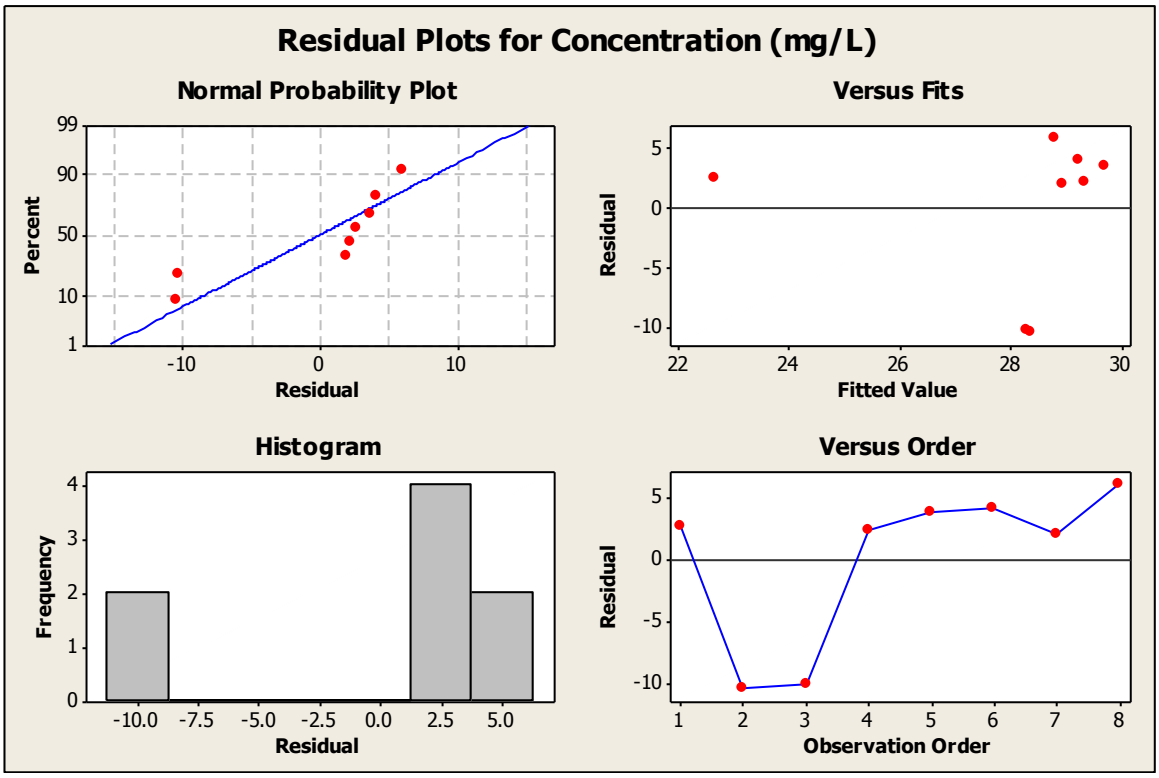

Regression Analysis: Concentration (mg/L) versus OR180 (mV)

The regression equation is
Concentration (mg/L) = 423 - 0.225 OR180 LED On-Off (mV)

Predictor	Coef	SE Coef	T	P
Constant	422.8	105.6	4.00	0.007
OR180 LED On-Off (mV)	-0.22451	0.06007	-3.74	0.010

S = 4.08864 R-Sq = 70.0% R-Sq(adj) = 64.9%

PRESS = 207.903 R-Sq(pred) = 37.72%

Analysis of Variance

Source	DF	SS	MS	F	P
Regression	1	233.49	233.49	13.97	0.010
Residual Error	6	100.30	16.72		
Total	7	333.80			

Residual Plots for Concentration (mg/L)

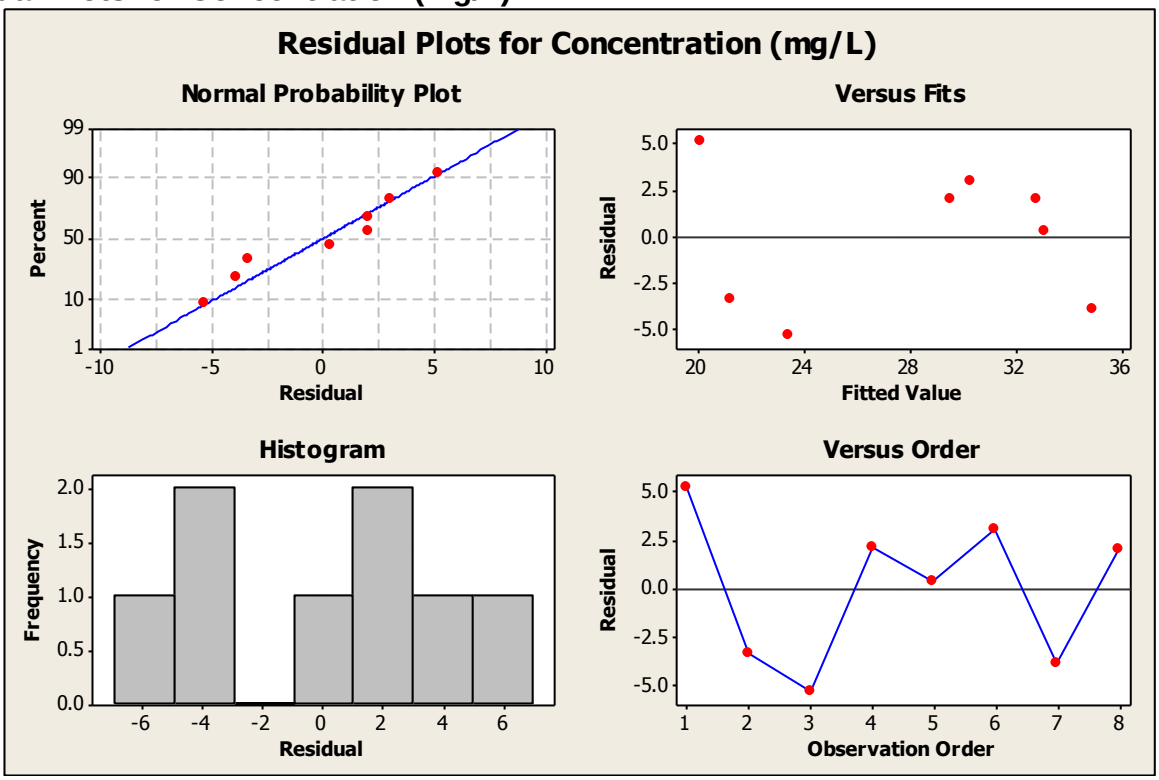

Linear Stepwise Output

Stepwise Regression: Concentration versus IR45 (mV), OR45 (mV), OR180 (mV)

```
  Alpha-to-Enter: 0.15  Alpha-to-Remove: 0.15

Response is Concentration (mg/L) on 3 predictors, with N = 8


Step                          1
Constant                  422.8

OR180 LED On-Off (mV)  -0.225
T-Value                   -3.74
P-Value                   0.010

S                          4.09
R-Sq                      69.95
R-Sq(adj)                 64.94
Mallows Cp                  4.4
```

Polynomial Regression Analysis: Concentration (mg/L) versus IR45 (mV), IR45^2 (mV)

```
The regression equation is
Concentration (mg/L) = 67.98 - 0.5533 IR45 LED On-Off(mV)
                       + 0.001407 IR45 LED On-Off(mV)**2


S = 1.17135   R-Sq = 97.9%   R-Sq(adj) = 97.1%

PRESS = 5957.21   R-Sq(pred) = 0.00%

Analysis of Variance

Source       DF       SS       MS       F      P
Regression    2  326.935  163.468  119.14  0.000
Error         5    6.860    1.372
Total         7  333.796


Sequential Analysis of Variance

Source      DF       SS       F      P
Linear       1   92.176    2.29  0.181
Quadratic    1  234.760  171.10  0.000
```

Residual Plots for Concentration (mg/L)

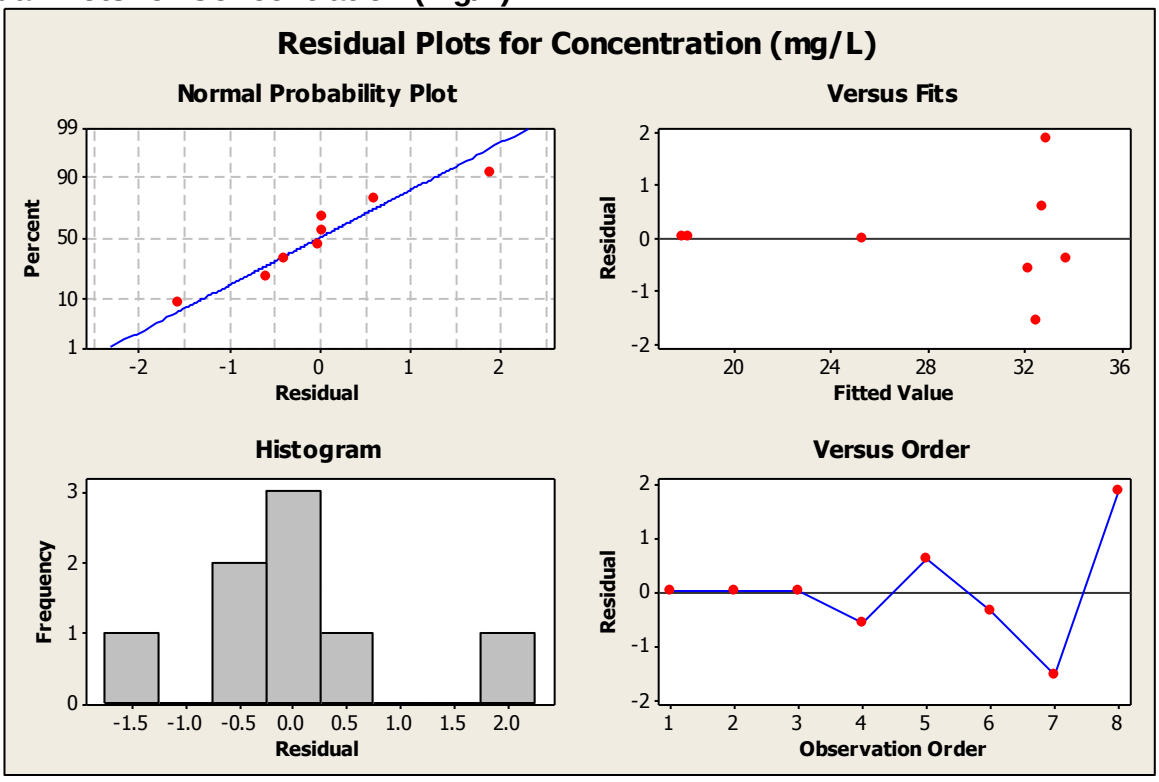

Polynomial Regression Analysis: Concentration (mg/L) versus OR45 (mV), OR45^2 (mV)

```
The regression equation is
Concentration (mg/L) = 71.57 - 1.010 OR45 LED On-Off (mV)
                       + 0.004138 OR45 LED On-Off (mV)**2


S = 5.06385   R-Sq = 61.6%   R-Sq(adj) = 46.2%

PRESS = 498091   R-Sq(pred) = 0.00%

Analysis of Variance

Source       DF       SS       MS     F      P
Regression    2  205.583  102.791  4.01  0.091
Error         5  128.213   25.643
Total         7  333.796


Sequential Analysis of Variance

Source      DF       SS     F      P
Linear       1   36.519  0.74  0.424
Quadratic    1  169.064  6.59  0.050
```

Residual Plots for Concentration (mg/L)

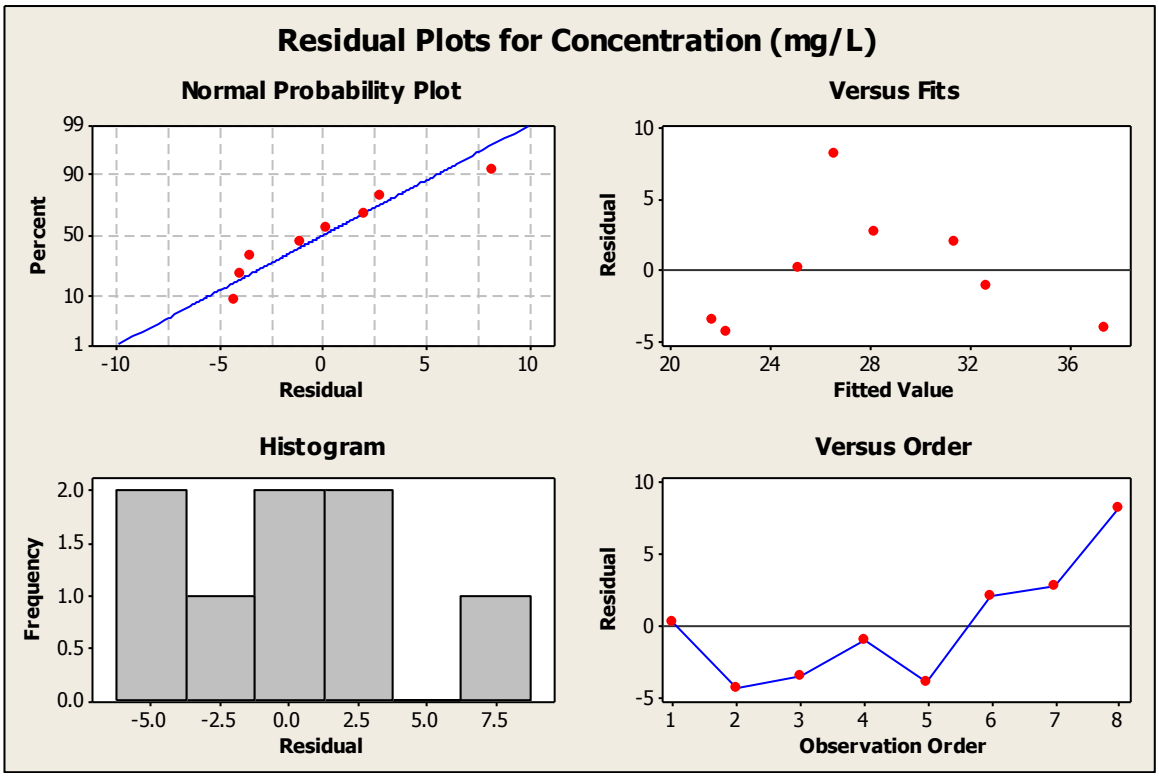

Stepwise Regression: Concentration (mg/L) versus IR45 (mV), OR45 (mV), OR180 (mV), IR45^2 (mV), OR45^2 (mV)

Alpha-to-Enter: 0.15 Alpha-to-Remove: 0.15

Response is Concentration (mg/L) on 5 predictors, with N = 8

Step	1
Constant	422.8
OR180 LED On-Off (mV)	-0.225
T-Value	-3.74
P-Value	0.010
S	4.09
R-Sq	69.95
R-Sq(adj)	64.94

Appendix F – Upatoi South Statistical Analysis, Minitab Output

Regression Analysis: Concentration (mg/L) versus IR45 (mV)

```
The regression equation is
Concentration (mg/L) = 17.7 + 0.0205 IR45 LED On-Off(mV)


Predictor              Coef  SE Coef      T      P
Constant             17.731    9.054   1.96  0.072
IR45 LED On-Off(mV) 0.02050  0.05755   0.36  0.727


S = 11.5375   R-Sq = 1.0%   R-Sq(adj) = 0.0%

PRESS = 2326.08   R-Sq(pred) = 0.00%

Analysis of Variance

Source           DF      SS     MS     F      P
Regression        1    16.9   16.9  0.13  0.727
Residual Error   13  1730.5  133.1
Total            14  1747.4
```

Residual Plots for Concentration (mg/L)

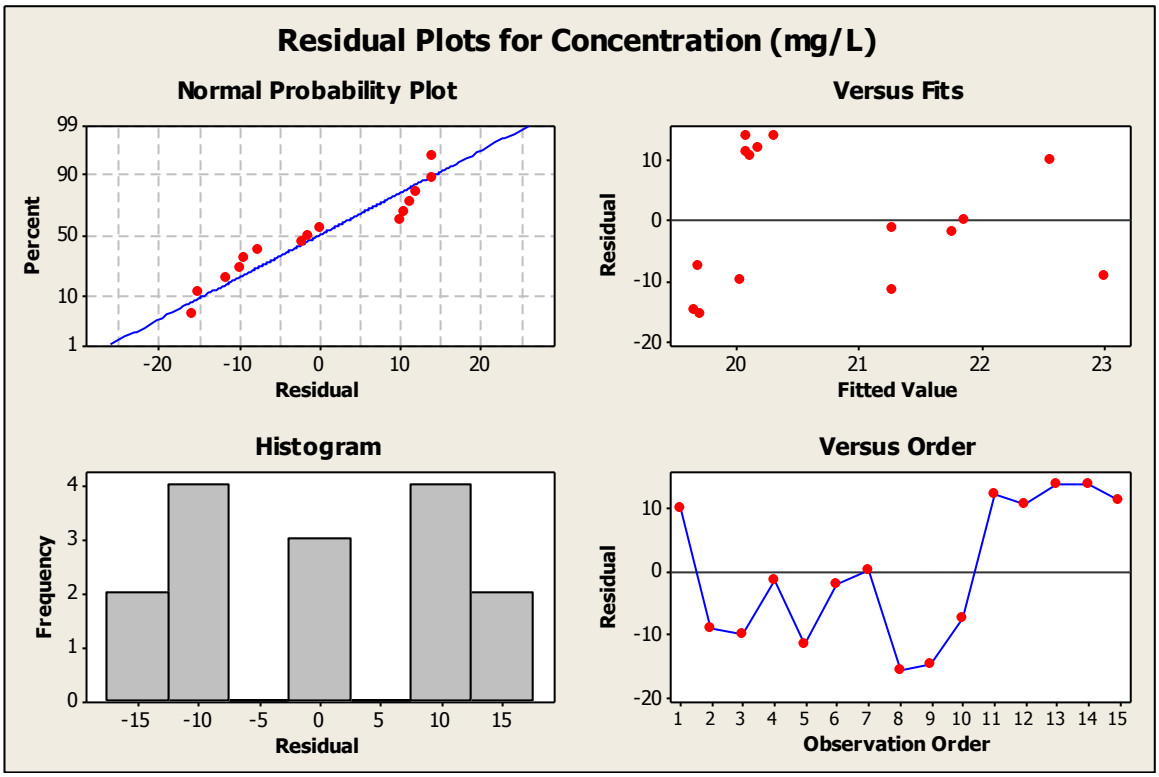

Regression Analysis: Concentration (mg/L) versus OR45 (mV)

```
The regression equation is
Concentration (mg/L) = 11.7 + 0.536 OR45 LED On-Off (V)


Predictor              Coef  SE Coef     T      P
Constant             11.682    7.119  1.64  0.125
OR45 LED On-Off (mV) 0.5356   0.3856  1.39  0.188


S = 10.8187   R-Sq = 12.9%   R-Sq(adj) = 6.2%

PRESS = 1873.95   R-Sq(pred) = 0.00%

Analysis of Variance

Source           DF      SS     MS     F      P
Regression        1   225.8  225.8  1.93  0.188
Residual Error   13  1521.6  117.0
Total            14  1747.4


Unusual Observations

       OR45 LED  Concentration
Obs   On-Off (mV)        (mg/L)     Fit  SE Fit  Residual  St Resid
  2          0.0          13.79   11.68    7.12      2.11      0.26 X

X denotes an observation whose X value gives it large leverage.
```

Residual Plots for Concentration (mg/L)

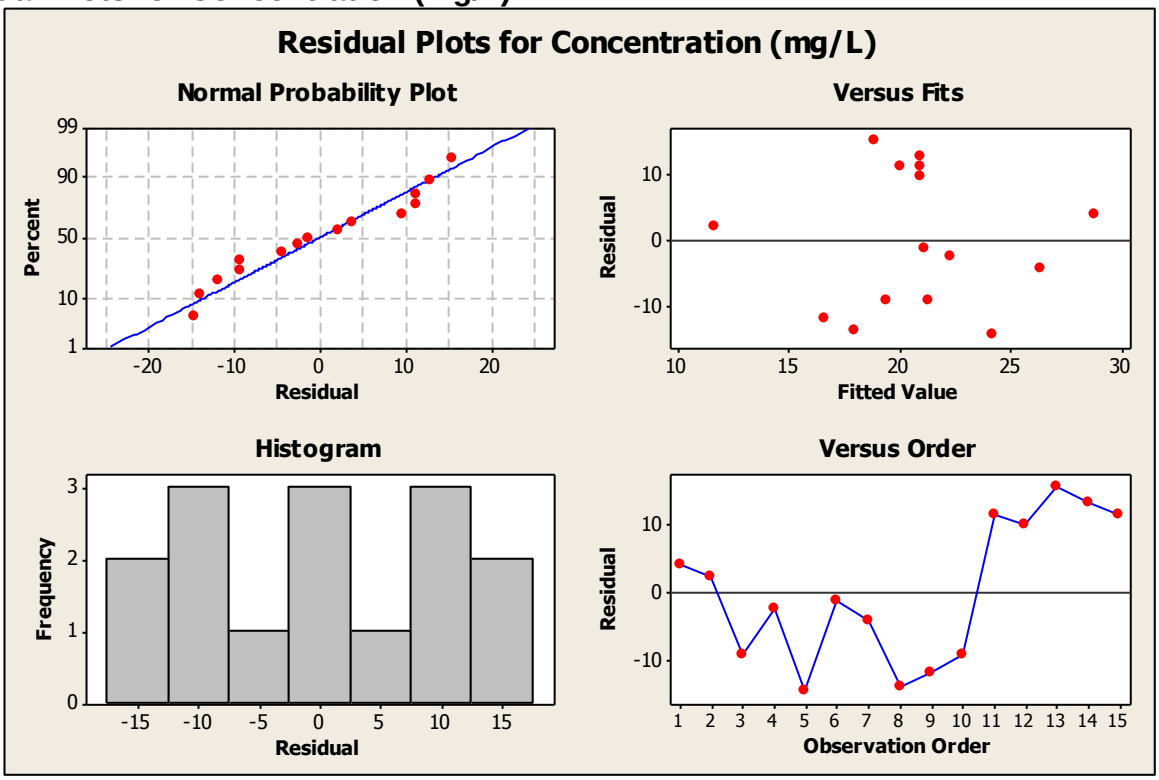

Regression Analysis: Concentration (mg/L) versus OR180 (mV)

```
The regression equation is
Concentration (mg/L) = 36.0 - 0.0133 OR180 LED On-Off (mV)


Predictor                 Coef  SE Coef      T      P
Constant                 36.00    19.64   1.83  0.090
OR180 LED On-Off (mV) -0.01331  0.01699  -0.78  0.447


S = 11.3293   R-Sq = 4.5%   R-Sq(adj) = 0.0%

PRESS = 2087.95   R-Sq(pred) = 0.00%

Analysis of Variance

Source           DF      SS     MS     F      P
Regression        1    78.8   78.8  0.61  0.447
Residual Error   13  1668.6  128.4
Total            14  1747.4
```

Residual Plots for Concentration (mg/L)

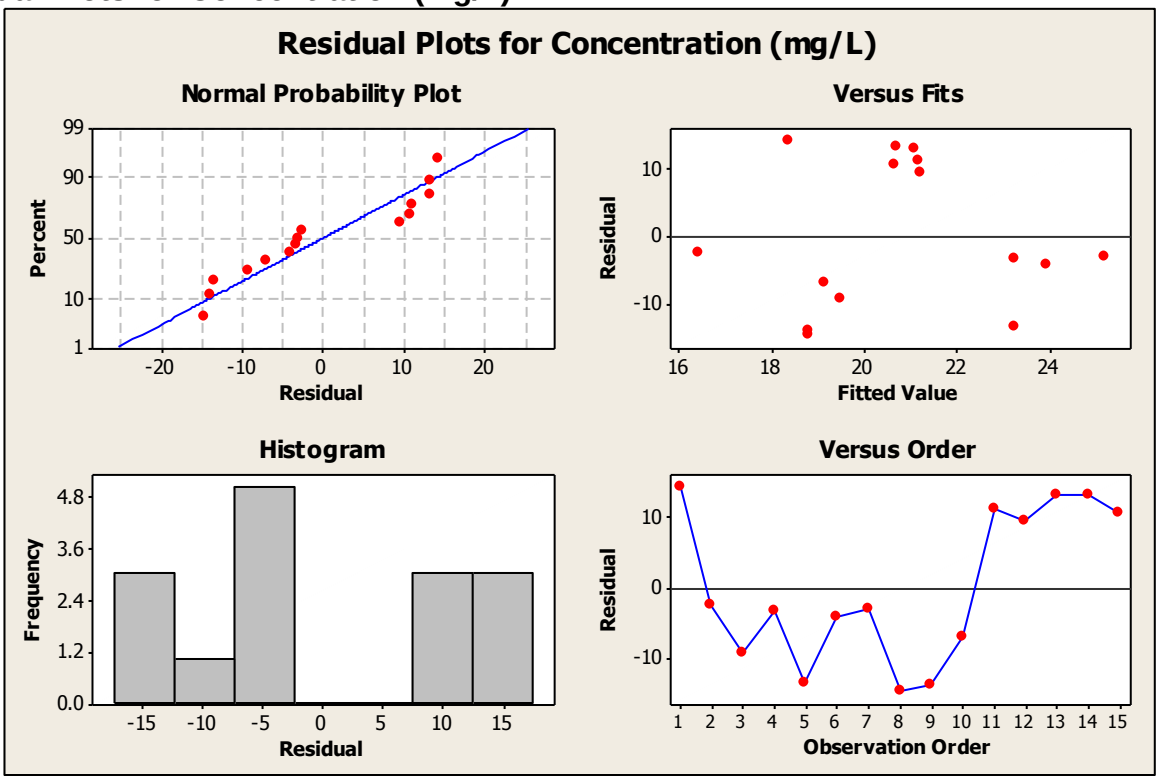

Linear Stepwise Output

Stepwise Regression: Concentration (mg/L) versus IR45 (mV), OR45 (mV), OR180 (mV)

```
  Alpha-to-Enter: 0.15  Alpha-to-Remove: 0.15

Response is Concentration (mg/L) on 3 predictors, with N = 15

No variables entered or removed
```

Appendix G – Anita Near Statistical Analysis, Minitab Output

Regression Analysis: Concentration (mg/L) versus IR45 (mV)

```
The regression equation is
Concentration (mg/L) = 70.4 - 0.0477 IR45 LED On-Off (mV)


Predictor                 Coef  SE Coef      T      P
Constant                 70.41    20.61   3.42  0.009
IR45 LED On-Off (mV)  -0.04771  0.06578  -0.73  0.489


S = 32.9692   R-Sq = 6.2%   R-Sq(adj) = 0.0%

PRESS = 11467.0   R-Sq(pred) = 0.00%

Analysis of Variance

Source           DF    SS    MS     F      P
Regression        1   572   572  0.53  0.489
Residual Error    8  8696  1087
Total             9  9267
```

Residual Plots for Concentration (mg/L)

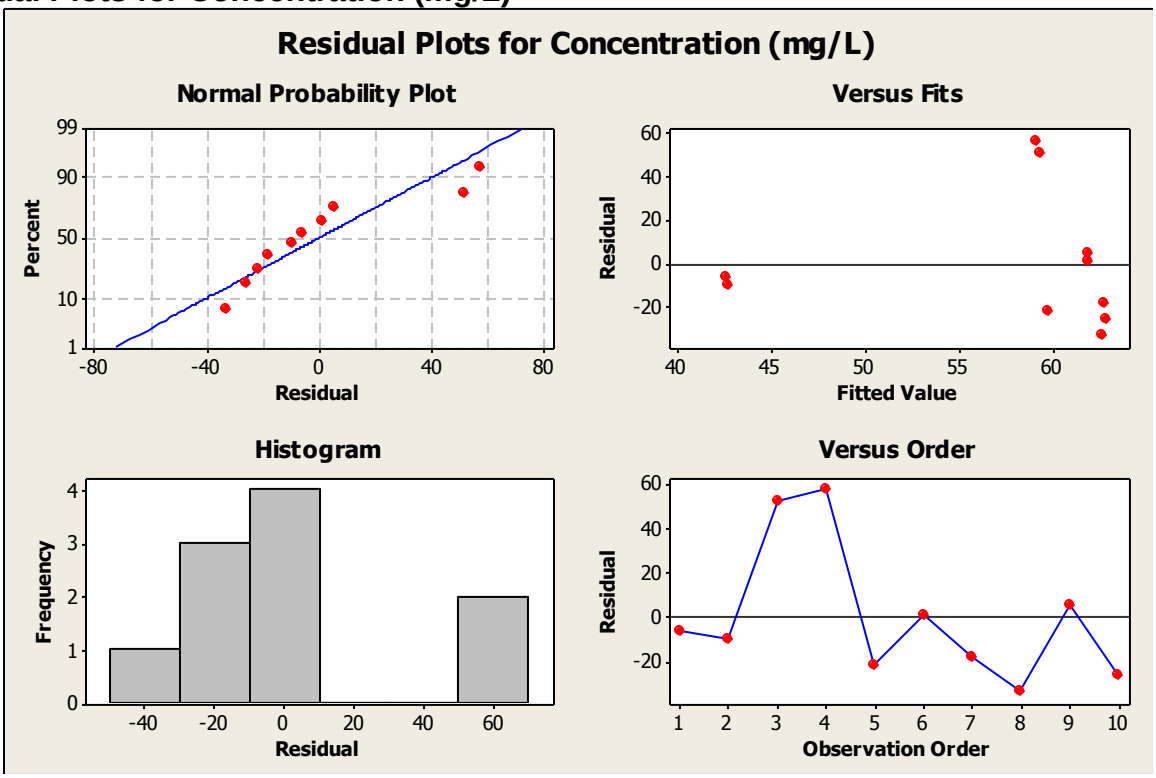

Regression Analysis: Concentration (mg/L) versus OR45 (mV)

```
The regression equation is
Concentration (mg/L) = - 46.0 + 1.29 OR45 LED On-Off (mV)


Predictor               Coef  SE Coef      T      P
Constant             -46.01    19.73  -2.33  0.048
OR45 LED On-Off (mV)  1.2867   0.2373   5.42  0.001


S = 15.7424   R-Sq = 78.6%   R-Sq(adj) = 75.9%

PRESS = 3061.55   R-Sq(pred) = 66.96%

Analysis of Variance

Source           DF      SS      MS      F      P
Regression        1  7284.9  7284.9  29.40  0.001
Residual Error    8  1982.6   247.8
Total             9  9267.4

Unusual Observations

     OR45 LED
       On-Off  Concentration
Obs       (mV)          (mg/L)     Fit  SE Fit  Residual  St Resid
  5        93           38.09   73.53    5.79    -35.44     -2.42R

R denotes an observation with a large standardized residual.
```

Residual Plots for Concentration (mg/L)

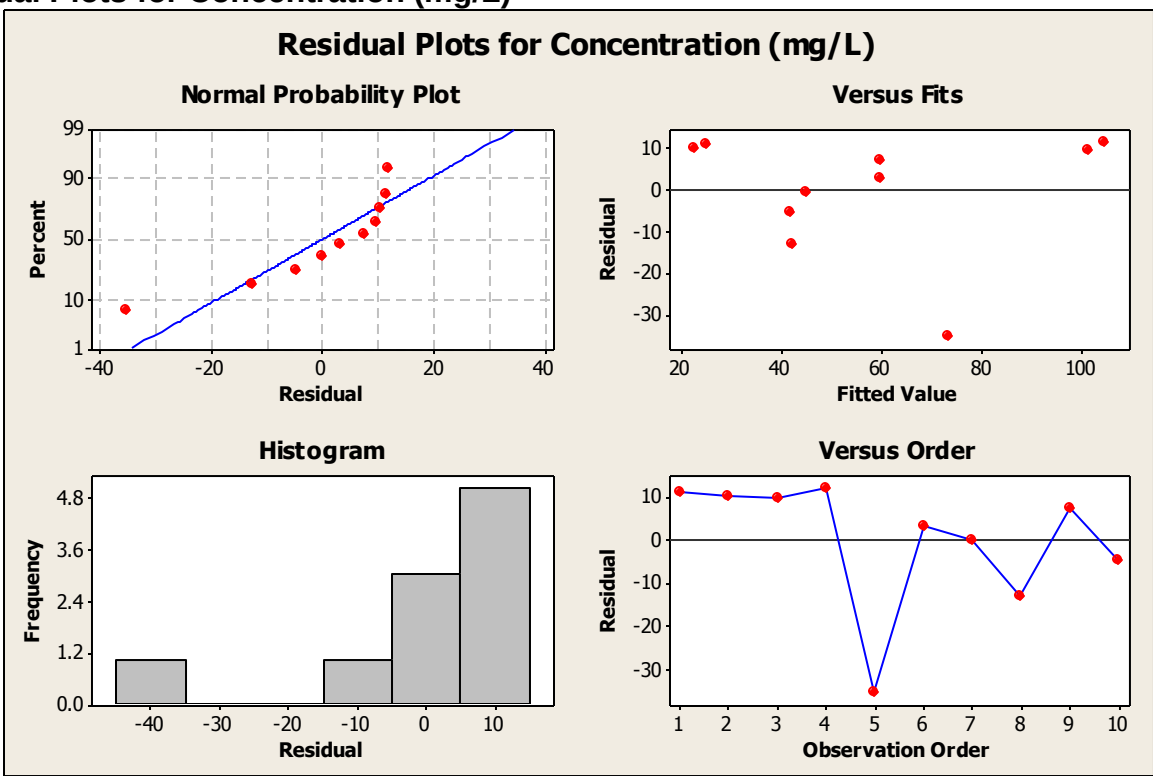

Regression Analysis: Concentration (mg/L) versus OR180 (mV)

```
The regression equation is
Concentration (mg/L) = 47.6 + 0.0392 OR180 LED On-Off (mV)

Predictor                 Coef  SE Coef      T      P
Constant                 47.59    13.22   3.60  0.007
OR180 LED On-Off (mV)  0.03917  0.03423   1.14  0.285


S = 31.5505   R-Sq = 14.1%   R-Sq(adj) = 3.3%

PRESS = 27654.2   R-Sq(pred) = 0.00%

Analysis of Variance

Source           DF      SS      MS     F      P
Regression        1  1303.9  1303.9  1.31  0.285
Residual Error    8  7963.5   995.4
Total             9  9267.4

Unusual Observations

      OR180
        LED
     On-Off  Concentration
Obs     (mV)         (mg/L)     Fit  SE Fit  Residual  St Resid
  5     946          38.09   84.63   25.70    -46.54     -2.54RX

R denotes an observation with a large standardized residual.
X denotes an observation whose X value gives it large leverage.
```

Residual Plots for Concentration (mg/L)

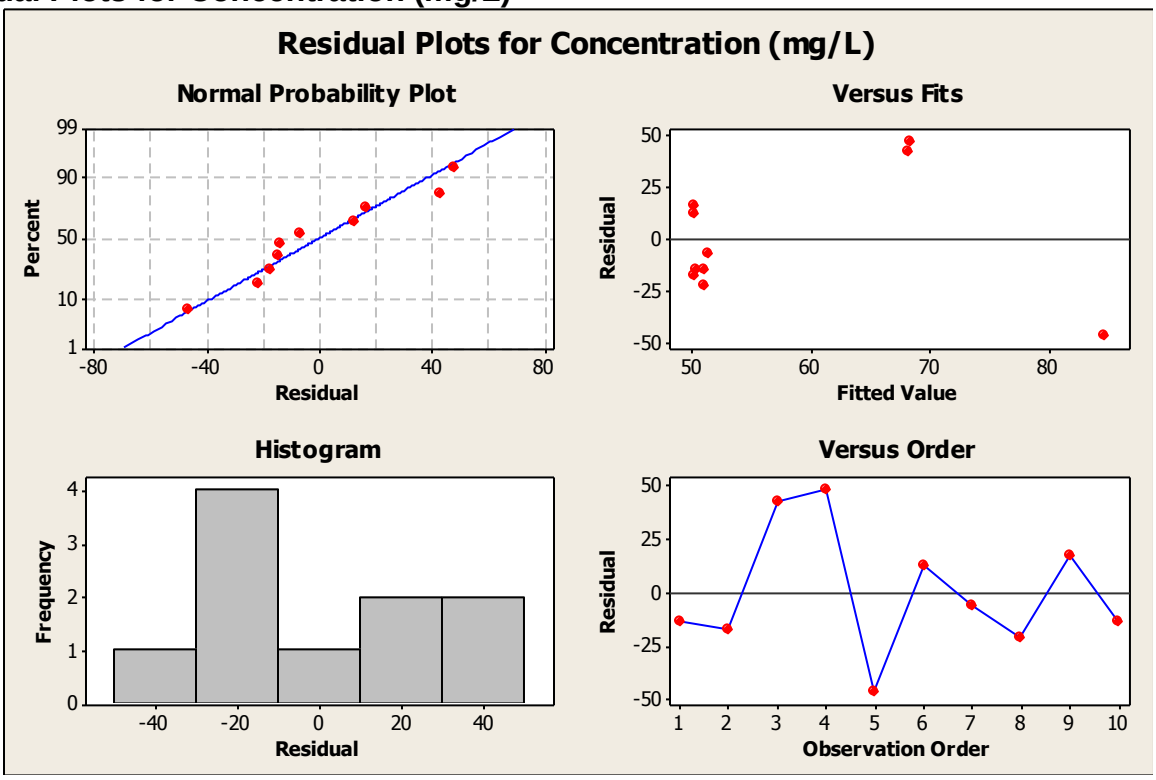

Linear Stepwise Output

Stepwise Regression: Concentration (mg/L) versus IR45 (mV), OR45 (mV), OR180 (mV)

Alpha-to-Enter: 0.15 Alpha-to-Remove: 0.15

Response is Concentration (mg/L) on 3 predictors, with N = 10

Step	1	2	3
Constant	-46.01	-71.91	-116.32
OR45 LED On-Off (mV)	1.287	1.764	2.124
T-Value	5.42	7.32	22.90
P-Value	0.001	0.000	0.000
OR180 LED On-Off (mV)		-0.0493	-0.0610
T-Value		-2.84	-10.27
P-Value		0.025	0.000
IR45 LED On-Off (mV)			0.0680
T-Value			7.61
P-Value			0.000

Regression Analysis: Concentration (mg/L) versus IR45 (mV), OR45 (mV), OR180 (mV)

```
The regression equation is
Concentration (mg/L) = - 116 + 0.0680 IR45 LED On-Off (mV)
                       + 2.12 OR45 LED On-Off (mV)
                       - 0.0610 OR180 LED On-Off (mV)


Predictor                  Coef   SE Coef       T      P
Constant                -116.320     8.111  -14.34  0.000
IR45 LED On-Off (mV)    0.068026  0.008938    7.61  0.000
OR45 LED On-Off (mV)     2.12438   0.09277   22.90  0.000
OR180 LED On-Off (mV)  -0.061025  0.005944  -10.27  0.000

S = 3.79537   R-Sq = 99.1%   R-Sq(adj) = 98.6%

PRESS = 219.806   R-Sq(pred) = 97.63%

Analysis of Variance

Source          DF      SS      MS       F      P
Regression       3  9181.0  3060.3  212.45  0.000
Residual Error   6    86.4    14.4
Total            9  9267.4


Source                 DF  Seq SS
IR45 LED On-Off (mV)    1   571.7
OR45 LED On-Off (mV)    1  7091.2
OR180 LED On-Off (mV)   1  1518.1
```

Residual Plots for Concentration (mg/L)

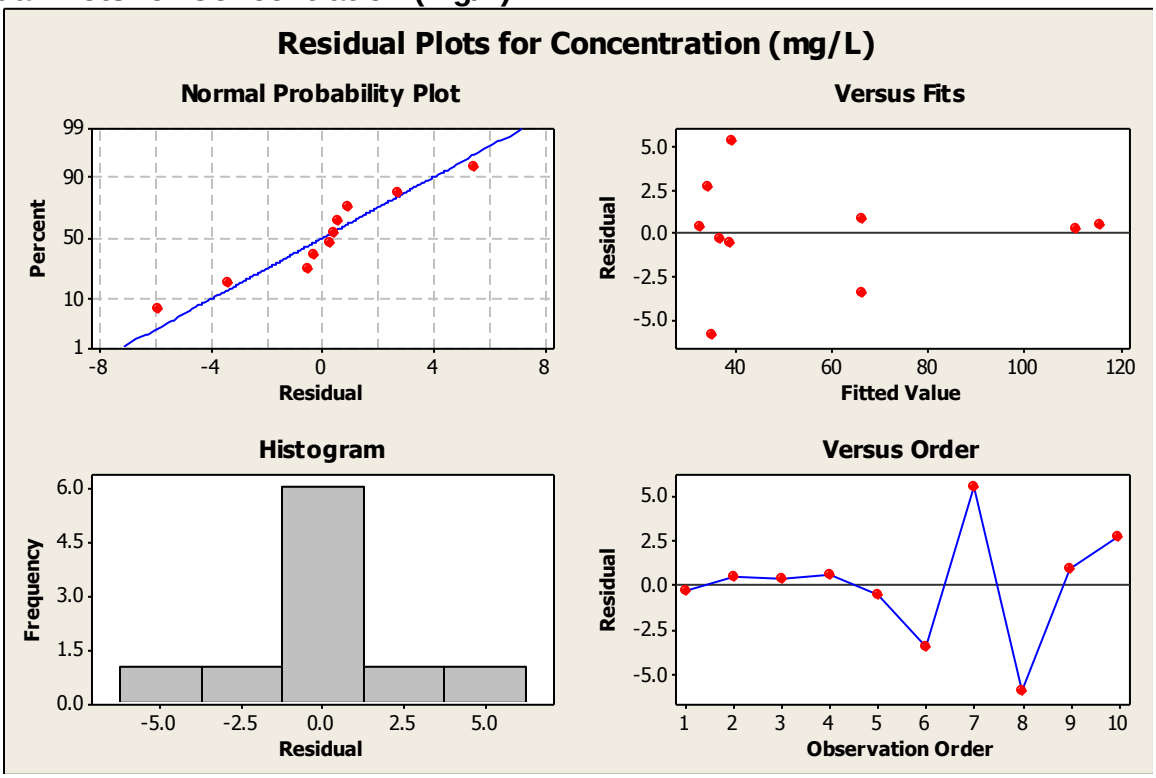

Polynomial Regression Analysis: Concentration (mg/L) versus IR45 (mV), IR45^2 (mV)

```
The regression equation is
Concentration (mg/L) = - 163.0 + 1.606 IR45 LED On-Off (mV)
                       - 0.002174 IR45 LED On-Off (mV)**2


S = 22.8333   R-Sq = 60.6%   R-Sq(adj) = 49.4%

PRESS = 7107.88   R-Sq(pred) = 23.30%

Analysis of Variance

Source       DF       SS       MS     F      P
Regression    2  5617.91  2808.95  5.39  0.038
Error         7  3649.52   521.36
Total         9  9267.43


Sequential Analysis of Variance

Source      DF       SS     F      P
Linear       1   571.70  0.53  0.489
Quadratic    1  5046.20  9.68  0.017
```

Residual Plots for Concentration (mg/L)

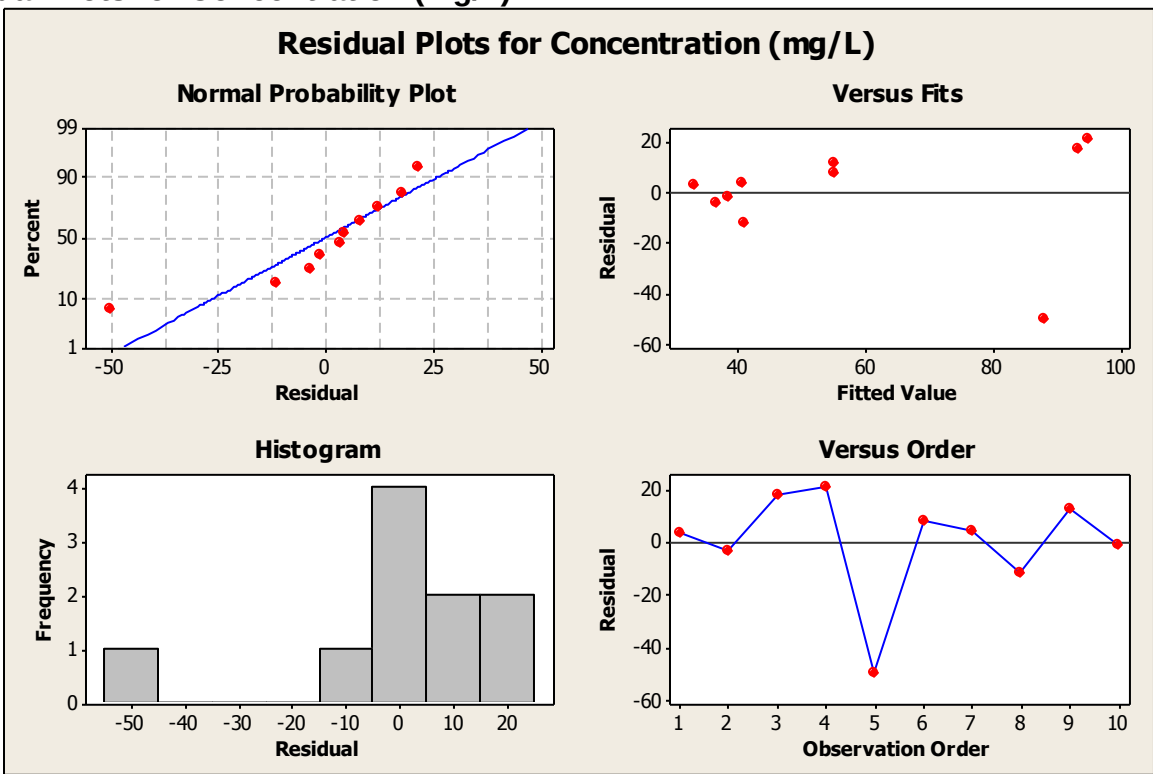

Polynomial Regression Analysis: Concentration (mg/L) versus OR45 (mV), OR45^2 (mV)

```
The regression equation is
Concentration (mg/L) = 97.39 - 2.271 OR45 LED On-Off (mV)
                       + 0.02066 OR45 LED On-Off (mV)**2


S = 13.5700   R-Sq = 86.1%   R-Sq(adj) = 82.1%


PRESS = 2224.80   R-Sq(pred) = 75.99%

Analysis of Variance

Source       DF       SS       MS      F      P
Regression    2  7978.41  3989.20  21.66  0.001
Error         7  1289.02   184.15
Total         9  9267.43


Sequential Analysis of Variance

Source      DF       SS      F      P
Linear       1  7284.85  29.40  0.001
Quadratic    1   693.55   3.77  0.093
```

Residual Plots for Concentration (mg/L)

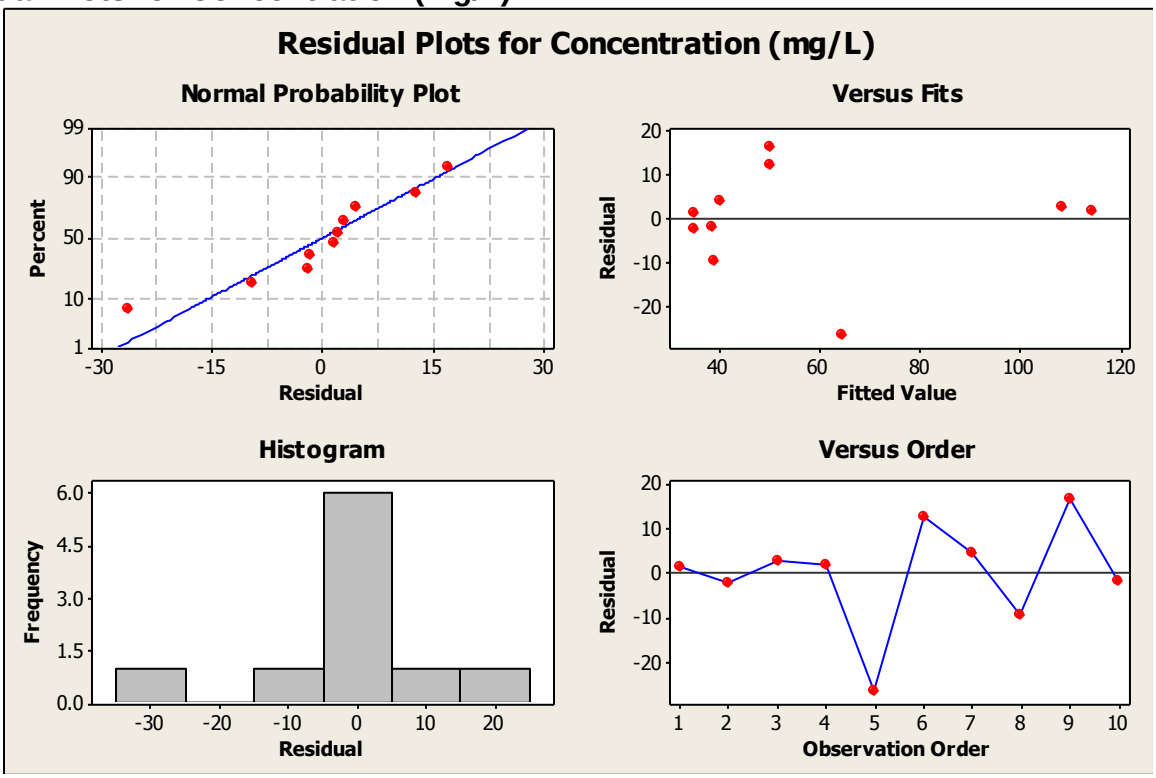

Polynomial Regression Analysis: Concentration (mg/L) versus OR180 (mV)

```
The regression equation is
Concentration (mg/L) = 18.31 + 0.3735 OR180 LED On-Off (mV)
                       - 0.000372 OR180 LED On-Off (mV)**2


S = 15.8914   R-Sq = 80.9%   R-Sq(adj) = 75.5%

PRESS = 548499   R-Sq(pred) = 0.00%

Analysis of Variance

Source       DF       SS       MS      F      P
Regression    2  7499.68  3749.84  14.85  0.003
Error         7  1767.75   252.54
Total         9  9267.43


Sequential Analysis of Variance

Source      DF       SS      F      P
Linear       1  1303.95   1.31  0.285
Quadratic    1  6195.73  24.53  0.002
```

Residual Plots for Concentration (mg/L)

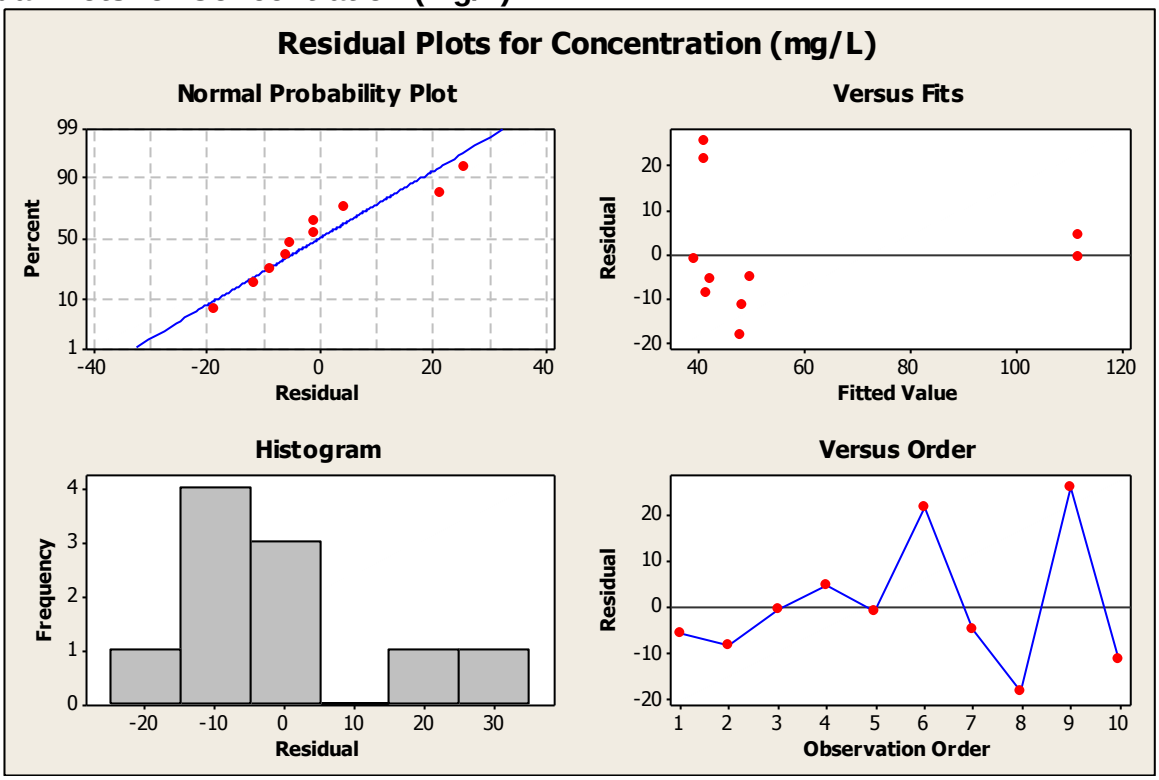

Polynomial Stepwise Output

Stepwise Regression: Concentration (mg/L) versus IR45 (mV), OR45 (mV), OR180 (mV), IR45^2 (mV), OR45^2 (mV), OR180^2 (mV)

Alpha-to-Enter: 0.15 Alpha-to-Remove: 0.15

Response is Concentration (mg/L) on 6 predictors, with N = 10

Step	1	2	3	4	5
Constant	4.7321	-0.6808	-13.1687	-153.0083	-100.5366
OR45^2	0.00764	0.00943	0.01004	-0.00611	
T-Value	6.27	12.64	17.25	-0.90	
P-Value	0.000	0.000	0.000	0.410	
OR180^2		-0.00005	-0.00005	-0.00006	-0.00005
T-Value		-4.69	-6.69	-8.67	-9.94
P-Value		0.002	0.001	0.000	0.000
IR45 LED On-Off (mV)			0.0316	0.0735	0.0579
T-Value			2.73	3.75	6.43
P-Value			0.034	0.013	0.001
OR45 LED On-Off (mV)				3.001	1.871
T-Value				2.38	23.49
P-Value				0.063	0.000
S	14.0	7.36	5.31	3.98	3.91
R-Sq	83.08	95.91	98.18	99.15	99.01
R-Sq(adj)	80.96	94.74	97.27	98.46	98.51

Regression Analysis: Concentration (mg/L) versus IR45 (mV), OR45 (mV), OR45^2 (mV), OR180^2 (mV)

The regression equation is
Concentration (mg/L) = - 153 - 0.00611 OR45^2 - 0.000058 OR180^2
+ 0.0735 IR45 LED On-Off (mV) + 3.00 OR45 LED On-Off (mV)

Predictor	Coef	SE Coef	T	P
Constant	-153.01	58.87	-2.60	0.048
OR45^2	-0.006105	0.006791	-0.90	0.410
OR180^2	-0.00005766	0.00000665	-8.67	0.000
IR45 LED On-Off (mV)	0.07354	0.01963	3.75	0.013
OR45 LED On-Off (mV)	3.001	1.260	2.38	0.063

S = 3.97819   R-Sq = 99.1%   R-Sq(adj) = 98.5%

PRESS = 494.731   R-Sq(pred) = 94.66%

Analysis of Variance

Source	DF	SS	MS	F	P
Regression	4	9188.3	2297.1	145.15	0.000
Residual Error	5	79.1	15.8		
Total	9	9267.4			

Source	DF	Seq SS
OR45^2	1	7699.3
OR180^2	1	1189.0
IR45 LED On-Off (mV)	1	210.2
OR45 LED On-Off (mV)	1	89.8

Unusual Observations

Obs	OR45^2	Concentration (mg/L)	Fit	SE Fit	Residual	St Resid
5	8630	38.09	38.07	3.98	0.01	0.12 X
8	4706	29.26	35.69	2.36	-6.43	-2.01R

R denotes an observation with a large standardized residual.
X denotes an observation whose X value gives it large leverage.

Residual Plots for Concentration (mg/L)

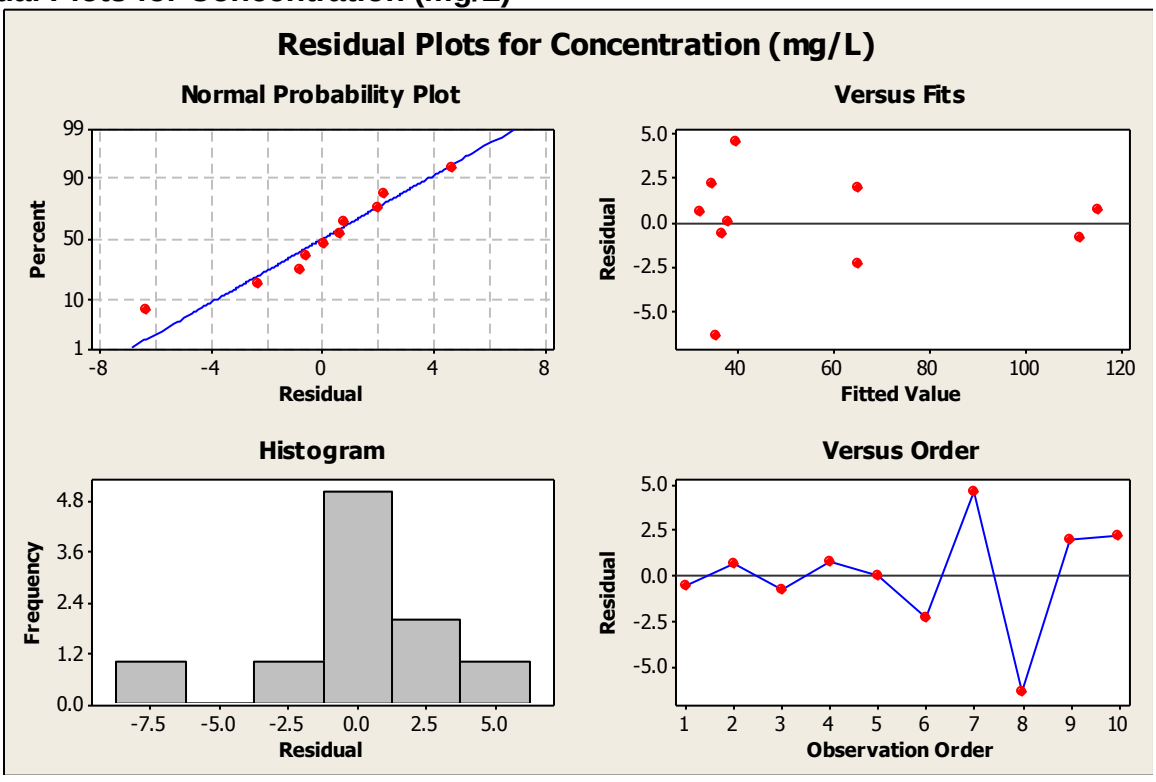

Appendix H – Anita Far Statistical Analysis, Minitab Output

Regression Analysis: Concentration (mg/L) versus IR45 (mV)

```
The regression equation is
Concentration (mg/L) = 171 - 0.381 IR45 (mV)


Predictor     Coef  SE Coef      T      P
Constant     171.2    108.5   1.58  0.149
IR45 (mV)  -0.3810   0.3266  -1.17  0.273


S = 42.2443   R-Sq = 13.1%   R-Sq(adj) = 3.5%

PRESS = 29613.4   R-Sq(pred) = 0.00%

Analysis of Variance

Source          DF     SS    MS     F      P
Regression       1   2429  2429  1.36  0.273
Residual Error   9  16061  1785
Total           10  18490


Unusual Observations

     IR45  Concentration
Obs  (mV)         (mg/L)   Fit  SE Fit  Residual  St Resid
  4   292          137.9  59.8    17.7      78.1      2.04R
  5   429           37.0   7.8    34.7      29.2      1.21 X

R denotes an observation with a large standardized residual.
X denotes an observation whose X value gives it large leverage.
```

Residual Plots for Concentration (mg/L)

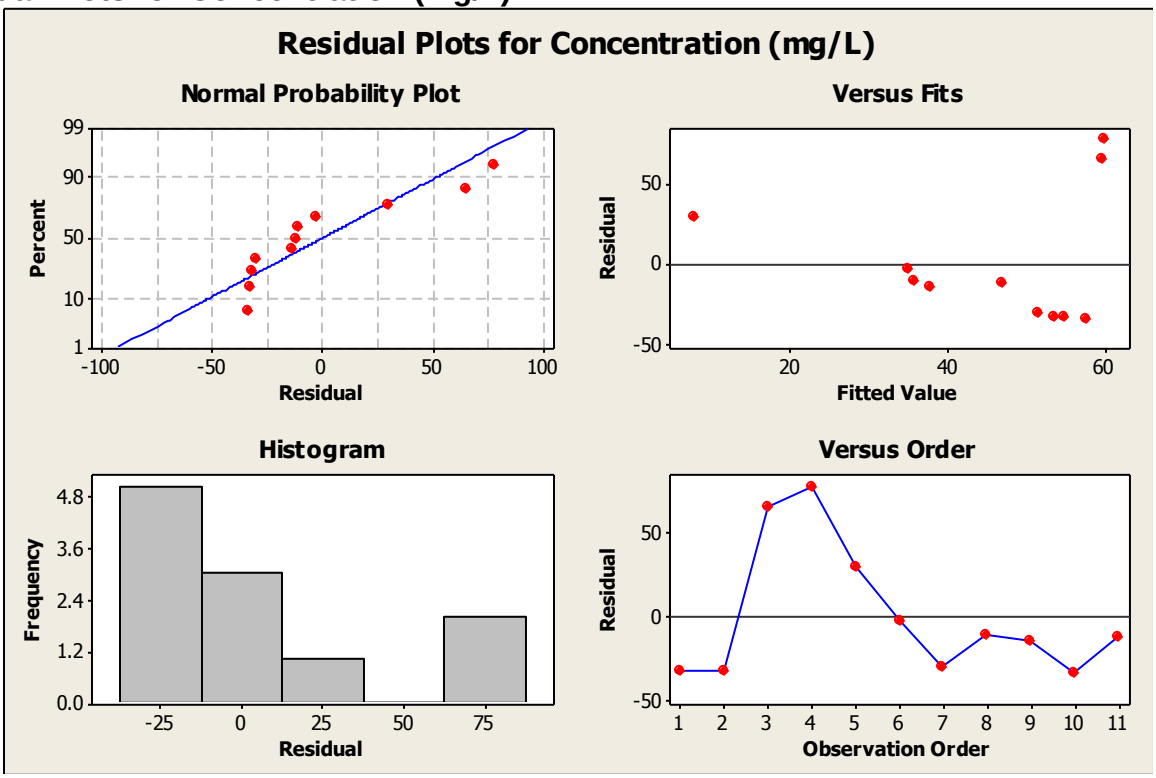

Regression Analysis: Concentration (mg/L) versus OR45 (mV)

The regression equation is
Concentration (mg/L) = - 110 + 0.767 OR45 (mV)

Predictor	Coef	SE Coef	T	P
Constant	-110.28	46.09	-2.39	0.040
OR45 (mV)	0.7671	0.2226	3.45	0.007

S = 29.7634 R-Sq = 56.9% R-Sq(adj) = 52.1%

PRESS = 13490.4 R-Sq(pred) = 27.04%

Analysis of Variance

Source	DF	SS	MS	F	P
Regression	1	10518	10518	11.87	0.007
Residual Error	9	7973	886		
Total	10	18490			

Residual Plots for Concentration (mg/L)

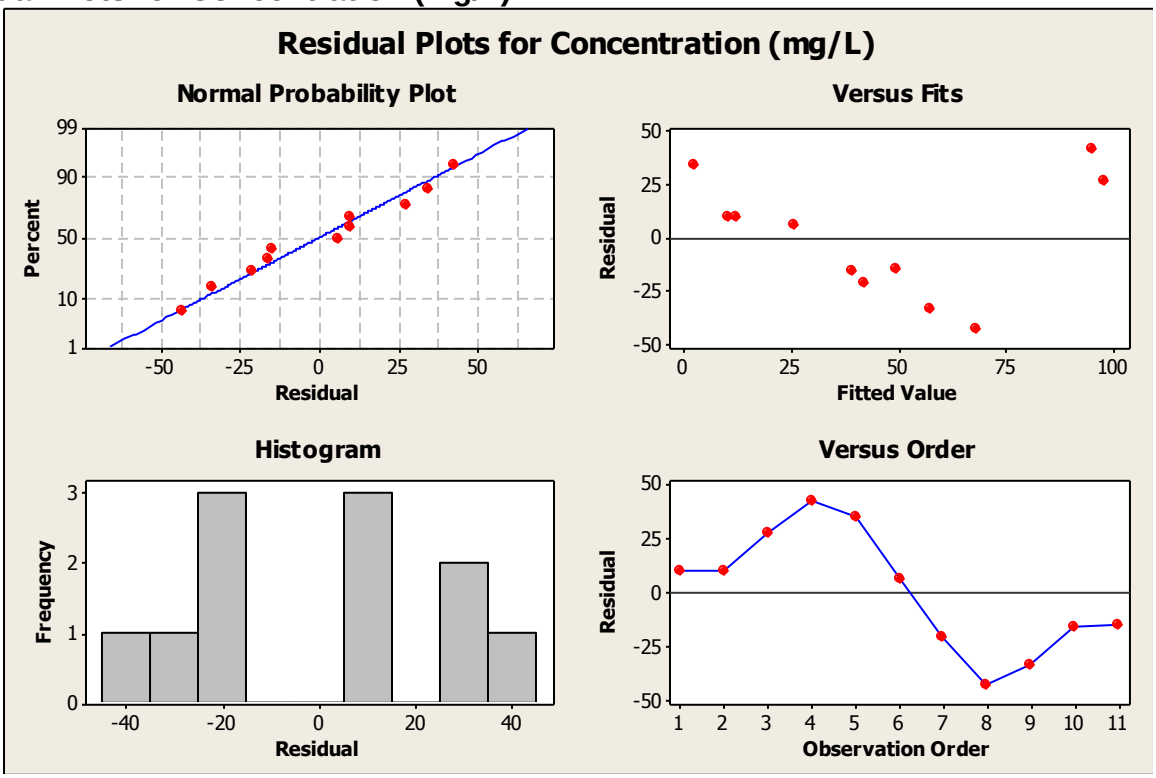

Regression Analysis: Concentration (mg/L) versus OR180 (mV)

The regression equation is
Concentration (mg/L) = 111 - 0.0536 OR180 (mV)

Predictor	Coef	SE Coef	T	P
Constant	111.38	26.62	4.18	0.002
OR180 (mV)	-0.05363	0.02002	-2.68	0.025

S = 33.8077 R-Sq = 44.4% R-Sq(adj) = 38.2%

PRESS = 16639.8 R-Sq(pred) = 10.01%

Analysis of Variance

Source	DF	SS	MS	F	P
Regression	1	8204	8204	7.18	0.025
Residual Error	9	10287	1143		
Total	10	18490			

Residual Plots for Concentration (mg/L)

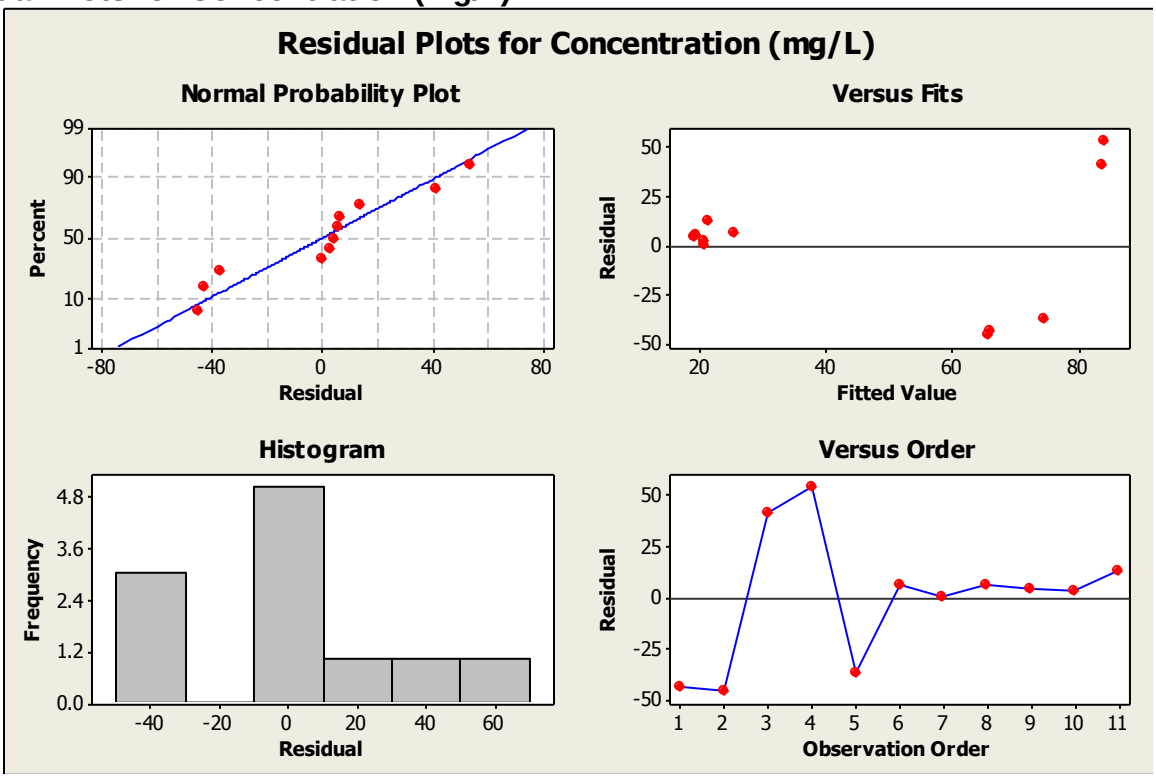

Linear Stepwise Output

Stepwise Regression: Concentration (mg/L) versus IR45 (mV), OR45 (mV), OR180 (mV)

```
  Alpha-to-Enter: 0.15  Alpha-to-Remove: 0.15

Response is Concentration (mg/L) on 3 predictors, with N = 11


Step              1        2
Constant    -110.28   -39.03

OR45 (mV)      0.77     0.71
T-Value        3.45     7.05
P-Value       0.007    0.000

OR180 (mV)           -0.0481
T-Value                -6.06
P-Value                0.000

S              29.8     13.4
R-Sq          56.88    92.28
R-Sq(adj)     52.09    90.35
Mallows Cp     32.5      2.1
```

Regression Analysis: Concentration (mg/L) versus OR45 (mV), OR180 (mV)

```
The regression equation is
Concentration (mg/L) = - 39.0 + 0.707 OR45 (mV) - 0.0481 OR180 (mV)


Predictor         Coef    SE Coef      T      P
Constant       -39.03      23.80  -1.64  0.140
OR45 (mV)      0.7075     0.1004   7.05  0.000
OR180 (mV)  -0.048131   0.007947  -6.06  0.000


S = 13.3584   R-Sq = 92.3%   R-Sq(adj) = 90.3%

PRESS = 2632.36   R-Sq(pred) = 85.76%

Analysis of Variance

Source           DF       SS      MS      F      P
Regression        2  17062.9  8531.5  47.81  0.000
Residual Error    8   1427.6   178.4
Total            10  18490.5


Source       DF   Seq SS
OR45 (mV)     1  10517.7
OR180 (mV)    1   6545.2
```

Residual Plots for Concentration (mg/L)

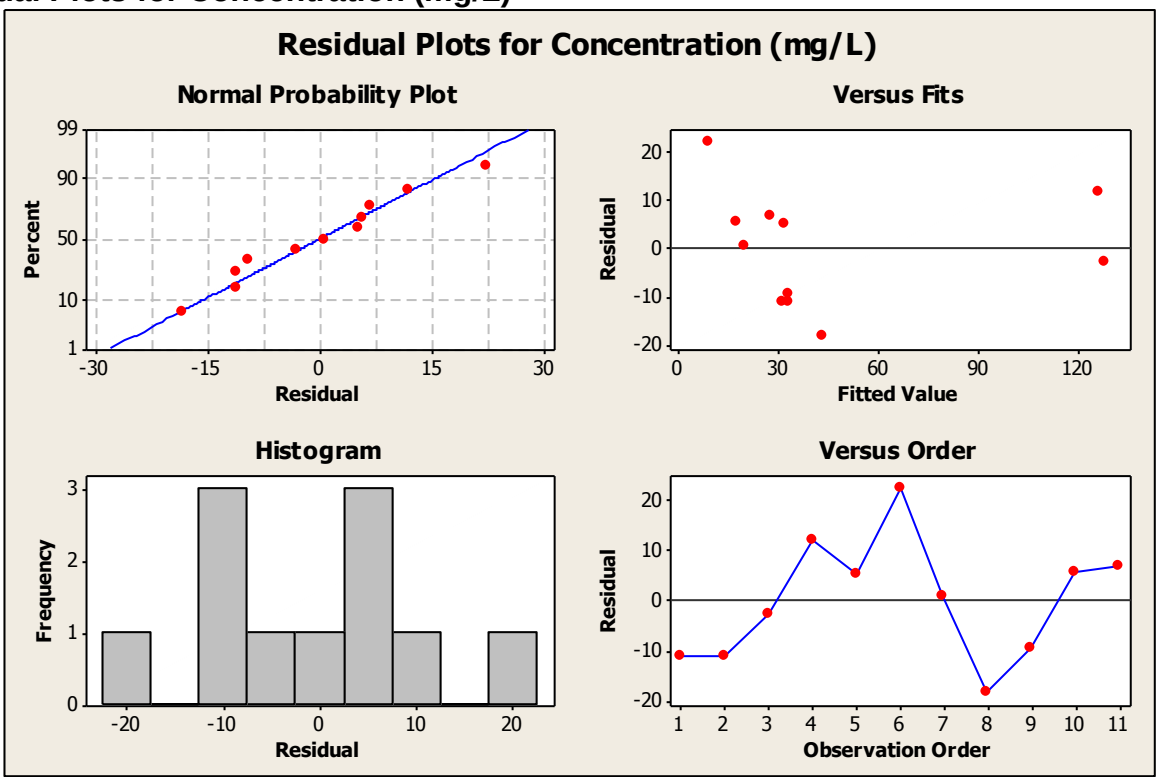

Polynomial Regression Analysis: Concentration (mg/L) versus OR45 (mV)

```
The regression equation is
Concentration (mg/L) = 561.5 - 5.881 OR45 (mV) + 0.01582 OR45 (mV)**2


S = 13.6929   R-Sq = 91.9%   R-Sq(adj) = 89.9%

PRESS = 2793.35   R-Sq(pred) = 84.89%

Analysis of Variance

Source       DF       SS       MS      F      P
Regression    2  16990.5  8495.27  45.31  0.000
Error         8   1500.0   187.50
Total        10  18490.5


Sequential Analysis of Variance

Source      DF       SS      F      P
Linear       1  10517.7  11.87  0.007
Quadratic    1   6472.8  34.52  0.000
```

Residual Plots for Concentration (mg/L)

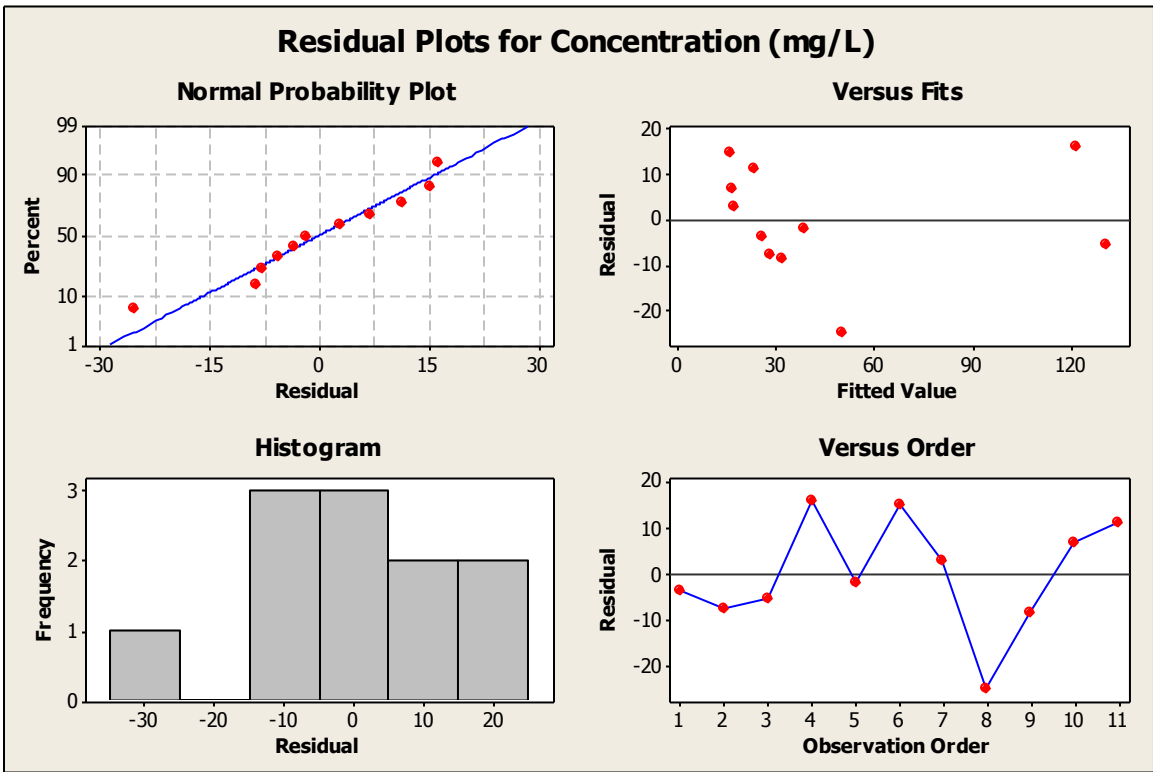

Polynomial Regression Analysis: Concentration (mg/L) versus OR180 (mV)

```
The regression equation is
Concentration (mg/L) = 403.2 - 0.6844 OR180 (mV) + 0.000273 OR180 (mV)**2


S = 14.6637   R-Sq = 90.7%   R-Sq(adj) = 88.4%

PRESS = 3007.73   R-Sq(pred) = 83.73%

Analysis of Variance

Source       DF       SS       MS      F      P
Regression    2  16770.3  8385.15  39.00  0.000
Error         8   1720.2   215.02
Total        10  18490.5


Sequential Analysis of Variance

Source      DF       SS      F      P
Linear       1  8203.86   7.18  0.025
Quadratic    1  8566.44  39.84  0.000
```

Residual Plots for Concentration (mg/L)

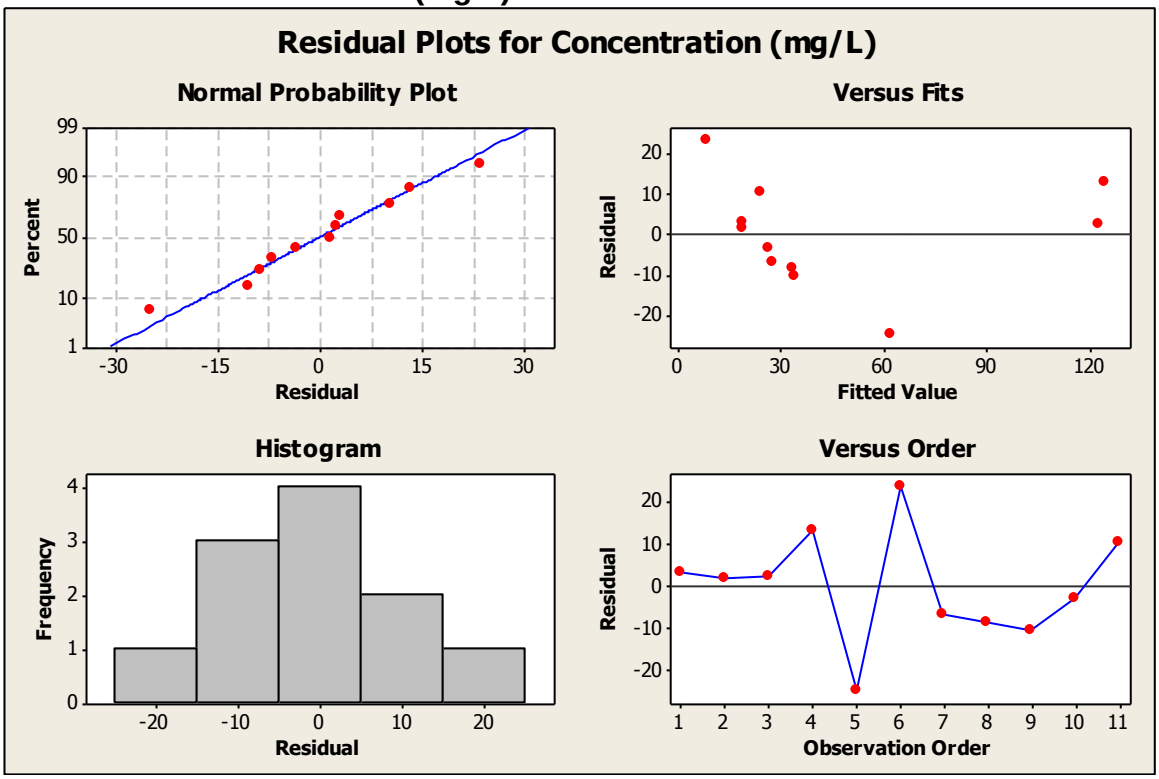

Polynomial Stepwise Output

Stepwise Regression: Concentration (mg/L) versus IR45 (mV), OR45 (mV), OR180 (mV), OR45^2 (mV), OR180^2 (mV)

```
  Alpha-to-Enter: 0.15  Alpha-to-Remove: 0.15

Response is Concentration (mg/L) on 5 predictors, with N = 11


Step              1        2
Constant     -37.64    25.56

OR45^2      0.00194  0.00170
T-Value        4.06     7.10
P-Value       0.003    0.000

OR180 (mV)           -0.0431
T-Value                -5.39
P-Value                0.001

S              26.9     13.3
R-Sq          64.72    92.38
R-Sq(adj)     60.80    90.47
Mallows Cp     23.8      1.6
```

Regression Analysis: Concentration (mg/L) versus OR45^2, OR180 (mV)

```
The regression equation is
Concentration (mg/L) = 25.6 + 0.00170 OR45^2 - 0.0431 OR180 (mV)


Predictor        Coef    SE Coef      T      P
Constant        25.56      15.98   1.60  0.148
OR45^2      0.0017002  0.0002395   7.10  0.000
OR180 (mV)  -0.043090   0.007998  -5.39  0.001


S = 13.2740   R-Sq = 92.4%   R-Sq(adj) = 90.5%

PRESS = 2614.48   R-Sq(pred) = 85.86%

Analysis of Variance

Source          DF       SS      MS      F      P
Regression       2  17080.9  8540.5  48.47  0.000
Residual Error   8   1409.6   176.2
Total           10  18490.5

Source      DF   Seq SS
OR45^2       1  11966.5
OR180 (mV)   1   5114.4
```

Residual Plots for Concentration (mg/L)

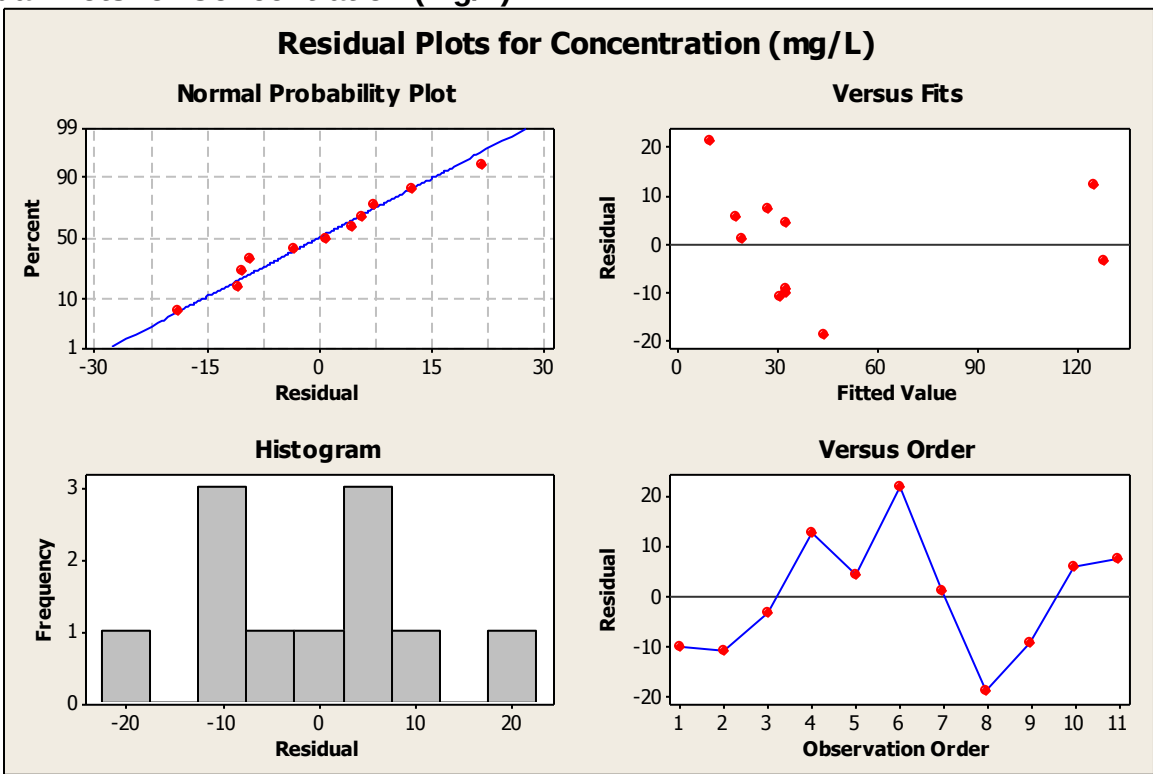

Appendix I – Fouling/Clogging Correction Algorithm, Two Signals

```
% Written for For Sensor Data Correction;
% Naiqian Zhang;
% January 28, 2007;

clear all;

filename = 'LK.xlsx';
ora180_m=xlsread(filename,'May','g3:g46155');
ir45_m=xlsread(filename,'May','e3:e46155');
time=xlsread(filename,'May','d3:d46155');
weather=xlsread(filename,'May','c3:c46155');
precipitation=xlsread(filename,'May','b3:b46155');
L=length(time);
%L = 20500;
%Sclear=ora180_m(L+1);
Sclear = ora180_m(2);
Sclear_ir45 = ir45_m(2);
%Added 11/13/11, assuming the data segment starts at lens cleaning

threshold = 0;
ripple = 0;
minilift = 10;
contrast = 4;
mean_upslope = 0;
mean_downslope = 0;
seg = L;
width_t = 11;
width_s = 11;
width_f = 21;



ora180_t=ora180_m(1:L);

for i = (width_t+1)/2:L-(width_t-1)/2
   if(width_t ~= 1)
      ora180_t(i) = mean(ora180_m(i-(width_t-1)/2:1:i+(width_t-1)/2));
   end;
end;

ora180_f = ora180_t(1:L);

for i = (width_f+1)/2:L-(width_f-1)/2
   if(width_f ~= 1)
      ora180_f(i) = mean(ora180_m(i-(width_f-1)/2:1:i+(width_f-1)/2));
   end;
end;

cv_t=std(ora180_t)/mean(ora180_t)
```

```
cv_f=std(ora180_f)/mean(ora180_f)

% cutoff = 0.1;
% [b,a] = ellip(6,5,50,cutoff);
% ora180_f(1:L) = filter(b,a,ora180_m(1:L));
% ora180_t(1:L) = filter(b,a,ora180_m(1:L));

figure
plot(time(1:L),ora180_m(1:L),'c-',time(1:L),ora180_t(1:L),'r-
',time(1:L),ora180_f(1:L),'b',time(1:L),weather(1:L)*2000,'g')
xlabel('Time (minute)');
ylabel('Signal (mV)');
axis ([0 L -500 2500]);
title ([filename, 'Filter width = ', num2str(width_t)]);
legend('Measured Signal','ora180_t Filtered Signal','ora180_f Filtered Signal');
grid on;

%start of second variable
ir45_t=ir45_m(1:L);

for i = (width_t+1)/2:L-(width_t-1)/2
   if(width_t ~= 1)
      ir45_t(i) = mean(ir45_m(i-(width_t-1)/2:1:i+(width_t-1)/2));
   end;
end;

ir45_f = ir45_t(1:L);

for i = (width_f+1)/2:L-(width_f-1)/2
   if(width_f ~= 1)
      ir45_f(i) = mean(ir45_m(i-(width_f-1)/2:1:i+(width_f-1)/2));
   end;
end;

cv_t_ir45=std(ir45_t)/mean(ir45_t)
cv_f_ir45=std(ir45_f)/mean(ir45_f)

% cutoff = 0.1;
% [b,a] = ellip(6,5,50,cutoff);
% ir45_f(1:L) = filter(b,a,ir45_m(1:L));
% ir45_t(1:L) = filter(b,a,ir45_m(1:L));

figure
plot(time(1:L),ir45_m(1:L),'c-',time(1:L),ir45_t(1:L),'r-
',time(1:L),ir45_f(1:L),'b',time(1:L),weather(1:L)*2000,'g')
xlabel('Time (minute)');
ylabel('Signal (mV)');
axis ([0 L -500 2500]);
title ([filename, 'Filter width = ', num2str(width_t)]);
legend('Measured Signal','ir45_t Filtered Signal','ir45_f Filtered Signal');
grid on;
%end of second variable segment
```

```
%start of clogging segment
for i=1:L-1
   slope(i)=ora180_f(i+1)-ora180_f(i);
end;
slope(L) = 0;

for i = (width_s+1)/2:L-(width_s-1)/2
   if(width_s ~= 1)
      slope(i) = mean(slope(i-(width_s-1)/2:1:i+(width_s-1)/2));
   end;
end;

for i = 1:(width_s-1)/2
   slope(i) = 0;
end;

for i = L-(width_s-1)/2: L
   slope(i) = 0;
end;
%slopet = slope';

% for i=1:L-1
%    slope(i)=ora180_f(i+1)-ora180_f(i);
% end;
% slope(L) = 0;
% slopet = slope';

figure
plot(time(1:L),slope(1:L),'b-',time(1:L), ora180_f(1:L)/50,'r-')
xlabel('Time (minute)');
ylabel('Slope(mV/min)');
axis([0 L 0 40]);
title ([filename, 'Slope filter width = ', num2str(width_s)]);
legend('Slope', 'Filtered signal/50');
grid on;

% converge = 0;
% limit = 3;
% iteration = 0;
% while (converge ~= 1)

%t0 = 1;
   %converge = 1;
   %converge1 = converge;
   %iteration = iteration + 1;

peak = 1;
valley = 1;
peak_all=[];
valley_all=[];

for i=1:seg-1
   if slope(i) < ripple
```

```
      if(slope(i+1)) >= 0
        valley = i+1;
        mean_downslope = mean(slope(peak:valley-1));
      end;
    else
      if slope(i+1) < 0
        peak = i+1;
        mean_upslope = mean(slope(valley:peak-1));
        lift = ora180_f(peak) - ora180_f(valley);
        if(mean_upslope >= threshold && mean_upslope>contrast*abs(mean_downslope) && lift>minilift)
%             i = i
%             mean_upslope = mean_upslope
%             mean_downslope = mean_downslope
%             lift = lift

          Pstart=ora180_f(1);
          Pend=ora180_f(valley);

          Sini0=ora180_f(1);
          Sini1=ora180_f(peak);

          if (valley ~= 1)
            [a1, a0] = coeffcom(1,valley,Pstart,Pend,Sini0,Sini1);
            %Correction;
            for j=1:valley
              E(j)=a1*time(j)+a0;
              ora180_t(j)=ora180_t(j)-E(j);
            end;
          else
            ora180_t(valley) = ora180_t(peak);
          end;

          for j = valley+1:peak-1
            ora180_t(j) = ora180_t(peak);
          end;

          peak_all=[peak_all;peak];
          valley_all=[valley_all;valley];

          figure;
          plot(time(1:seg), precipitation(1:seg)*1500,'g-',time(1:seg), ora180_f(1:seg),'b-', time(1:seg),
ora180_t(1:seg),'r-')
          xlabel('Time (minute)');
          ylabel('Signal (mV)');
          axis([0 seg 0 3000]);
          title ([filename, ', Filter width=',num2str(width_t),', Slope filter width=',num2str(width_s),',
Minilift=',num2str(minilift), ', Contrast=',num2str(contrast), ', Time=', num2str(i)]);
          legend('Percipitation', 'ora180_f Filtered signal', 'ora180_t clogging-corrected signal');
          grid on;
          hold on;
          plot(valley, ora180_t(valley), 'x', peak, ora180_t(peak), 'o');

        end;
```

```
      end;
   end;
end;
ora180_tt = [ora180_f slope'];
 %End of clogging segment

figure
plot(time(1:L),ora180_t(1:L),'-');
grid on;
hold on;

%peak=[peak_all ora180_f(peak_all(:,1))];
peak=fpeak(time(1:L),ora180_t(1:L),200,[0,L+1,400,5000]);
plot(peak(:,1),peak(:,2),'o');
title('Peak Detection');

peak=[1 ora180_t(1);peak];
New_peak = [];
Num_peak = length(peak(:,1))
for i = 1:Num_peak
   if weather(peak(i,1)) == 0
      New_peak = [New_peak; peak(i,1) peak(i,2)];
   end;
end;

Num_new_peak = length(New_peak(:,1));
ora180_n=ora180_t;
for i=1:Num_new_peak-1
   [a1, a0] = coeffcom(New_peak(i,1),New_peak(i+1,1),New_peak(i,2),New_peak(i+1,2),Sclear,Sclear);
   %Correction;
   for j=New_peak(i,1):1:New_peak(i+1,1)
      E(j)=a1*time(j)+a0;
      ora180_n(j)=ora180_t(j)-E(j);
   end;
end;

ora180_t=ora180_n;
L_new = L;

% ora180_t=ora180_t(1:New_peak(Num_new_peak));
% ora180_n=ora180_n(1:New_peak(Num_new_peak));
% L_new=length(ora180_t);

figure
plot(time(1:L_new),ora180_f,'b-',time(1:L_new),ora180_n,'r-')
xlabel('Time (minute)');
ylabel('Signal (mV)');
%axis([0 50000 -500 2500]);
title ([filename, ', Fouling Correction']);
legend('Measured Signal','Corrected Signal');
grid on;

% figure
```

```
% plot(time(1:L), precipitation(1:L)*1500,'g-',time(1:L), ora180_f(1:L),'b-', time(1:L), ora180_n(1:L),'r-')
% xlabel('Time (minute)');
% ylabel('Signal (mV)');
% axis([0 L 0 1500]);
% title ([filename, ', Filter width=',num2str(width_t),', Step threshold=',num2str(threshold)]);
% legend('Percipitation', 'Filtered signal', 'clogging/fouling-corrected signal');
% grid on;

%start of 2nd variable
figure
plot(time(1:L),ir45_t(1:L),'-');
grid on;
hold on;

mean_ir45_t = mean(ir45_t);
ir45_inv = 2*mean_ir45_t-ir45_t;

%peak=[peak_all ora180_f(peak_all(:,1))];
peak_ir45=fpeak(time(1:L),ir45_inv(1:L),200,[0,L+1,400,5000]);
peak_ir45(:,2) = 2*mean_ir45_t - peak_ir45(:,2);
plot(peak_ir45(:,1),peak_ir45(:,2),'o');
title('Peak Detection');

peak_ir45=[1 ir45_t(1);peak_ir45];
New_peak_ir45 = [];
Num_peak_ir45 = length(peak_ir45(:,1))
for i = 1:Num_peak_ir45
   if weather(peak_ir45(i,1)) == 0
      New_peak_ir45 = [New_peak_ir45; peak_ir45(i,1) peak_ir45(i,2)];
   end;
end;

Num_new_peak_ir45 = length(New_peak_ir45(:,1));
ir45_n=ir45_t;
for i=1:Num_new_peak_ir45-1
   [a1, a0] =
coeffcom(New_peak_ir45(i,1),New_peak_ir45(i+1,1),New_peak_ir45(i,2),New_peak_ir45(i+1,2),Sclear_ir45,Sc
lear_ir45);
   %Correction;
   for j=New_peak_ir45(i,1):1:New_peak_ir45(i+1,1)
      E(j)=a1*time(j)+a0;
      ir45_n(j)=ir45_t(j)-E(j);
   end;
end;

ir45_t=ir45_n;
L_new_ir45=L;

% ir45_t=ir45_t(1:New_peak_ir45(Num_new_peak_ir45));
% ir45_n=ir45_n(1:New_peak_ir45(Num_new_peak_ir45));
% L_new_ir45=length(ir45_t);

figure
```

```
plot(time(1:L_new_ir45),ir45_f,'b-',time(1:L_new_ir45),ir45_n,'r-')
xlabel('Time (minute)');
ylabel('Signal (mV)');
%axis([0 50000 -500 2500]);
title ([filename, ', Fouling Correction']);
legend('Measured Signal','Corrected Signal');
grid on;

% figure
% plot(time(1:L), precipitation(1:L)*1500,'g-',time(1:L), ir45_f(1:L),'b-', time(1:L), ir45_m(1:L),'r-')
% xlabel('Time (minute)');
% ylabel('Signal (mV)');
% axis([0 L 0 1500]);
% title ([filename, ', Filter width=',num2str(width_t),', Step threshold=',num2str(threshold)]);
% legend('Percipitation', 'Filtered signal', 'clogging/fouling-corrected signal');
% grid on;
%end of 2nd variable

% Part IV: Calculating accumulated concentration using integral;

% Read slope rate and intercept of the concentration regression;
ora180_slope=xlsread(filename,'May','K2');
ora180_intercept=xlsread(filename,'May','J6');
ir45_slope=xlsread(filename,'May','K4');
ir452_slope=xlsread(filename,'May','I6');

% Calculating concentration;
for i = 1:L_new
   conc_ora180(i)=ora180_n(i)*ora180_slope+ora180_intercept + ir45_n(i)*ir45_slope
+ir452_slope*(ir45_n(i))^2;
   if(conc_ora180(i) < 0)
      conc_ora180(i) = 0;
   end;
end;

% Initialize parameters;
% sednew - cummulative area
% sed -
sednew=0;
precinew=0;
sed=[];
preci=[];

%Calculate integral;

for i=1:L_new-1
     if precipitation(i) ~= 0
        sednew=sednew+conc_ora180(i);
        if precipitation(i+1) == 0
           sed=[sed;sednew];
           preci=[preci;precipitation(i)];
           sednew=0;
        end;
```

```
    end;
end;

% Accumulated sediment concentration vs. precipitation linear regression;
% The first value is the slope rate of the linear line;
sediment=polyfit(preci,sed,1);

figure
plot(time(1:L_new), precipitation(1:L_new)*5000,'g-',time(1:L_new), conc_ora180(1:L_new),'b-')
title([filename,', width_t=',num2str(width_t),', width_f=',num2str(width_f),', Contrast=',num2str(contrast),',
Slop=',num2str(sediment(1)/100000)]);
xlabel('Time (minute)');
ylabel('Predicted Concentration(mg/L)');
axis([0 seg 0 2000]);
legend('Precipitation*5000','concentration');
%axis([0 50000 -500 2500]);
grid on;

figure
plot(preci, sed, 'o', preci,polyval(sediment,preci), '-')
title([filename,', Accumulated Concentration vs. Precipitation']);
xlabel('precipitation (inch)');
ylabel('Accumulated Concentration (mg)');
legend('Concentration','Regressing Line');
%axis([0 50000 -500 2500]);
grid on;
```